AN ASSESSMENT OF EDDY CORRELATION TECHNIQUE IN MARINE HABITATS

PONLACHART CHOTIKARN

B.SC. & M.SC. (PHYSICS)

JUNE 2015

A THESIS SUBMITTED IN FULFILMENT OF THE REQUIREMENTS FOR THE DEGREE OF DOCTOR OF PHILOSOPHY IN SCIENCE

PLANT FUNCTIONAL BIOLOGY AND CLIMATE CHANGE CLUSTER
SCHOOL OF LIFE SCIENCES
UNIVERSITY OF TECHNOLOGY SYDNEY

CERTIFICATE OF AUTHORSHIP / ORIGINALITY

I certify that the work in this thesis has not previously been submitted for a degree nor has it been submitted as part of requirements for a degree except as fully acknowledged within the text.

I also certify that the thesis has been written by me. Any help that I have received in my research work and the preparation of the thesis itself has been acknowledged. In addition, I certify that all information sources and literature used are indicated in the thesis.

Ponlachart Chotikarn

30 June 2015

ACKNOWLEDGEMENTS

First, I would like to thank to my supervisors Professor Peter Ralph, Dr Andy Steven and Dr Mark Baird for their guidance, advice and support and all the opportunities they have provided during my candidature. I would like to thank Professor Peter Ralph for inspiring me and assisting me throughout my PhD.

I would like to thank Geoffrey Carlin, Dr Mikkel Holmen Andersen, Dr Daniel Nielsen, Dr Peter Macreadie, Professor Anthony Larkum and Dr Paul York and for their guidance and assistance during the completion of this research.

Thank you to all laboratory, technical, and administrative staffs at UTS and Heron Island Research Station. Special thanks to Greg Dalsanto, Greg Evans, Dr Vinod Kumar, Paul Brook, Stacey Ong Benyamin, Louisa Norman, Gemma Armstrong, John Moore, Shannon Hawkins and Carolyn Carter for their assistance.

Thank you to all members of the Plant Functional Biology and Climate Change Cluster (C3). I have thoroughly enjoyed working with you all. Special thanks to Stacey Trevathan-Tackett and Alex Thomson.

Thank you to Professor Tony Moon for his kind support and special thanks to Dr Sirinut Sawatdeenarunat, Dr Supitcha Supansomboon, Dr Auppatham Nakaruk, Bhanupong Dhechanunt, Pojwaree Lertsutthichawan Weenaththa Likitkom and friends for their friendship and support.

I have received financial support from a number of sources. These include the Faculty of Science, School of the Environment, Plant Functional Biology and Climate Change Cluster at UTS and CSIRO. Without these financial contributions,

this research would not have been possible.

I would also like to acknowledge the Department of Primary Industries, NSW Government for approving the research permit (GP12/0020-1.2).

Finally, this thesis is dedicated to my family; Dad, Mum, brother, and twin sisters; and my lovely wife, Dr Sutinee Sinutok, for their support, inspiration and love. Especially the wife, I realised how much she scarified for me. I love you all.

PUBLICATIONS

Chapter 1:

Chotikarn P, Chipman L, Macreadie P, Petrou K, Sinutok S, Carvalho M, Oakes J, Cyronak T, Eyre B, Ralph PJ. 2014. Literature review on gross and net ecosystem production and respiration values for estuaries and coral reefs. In: Duarte C, Ralph PJ, Doblin MA, Phinn S. 2014. Marine and Coastal Carbon Biogeochemistry Cluster Milestone 2 Report. CSIRO Wealth from Oceans Flagship. pp 56-77.

TABLE OF CONTENTS

LIST OF FIGURES

LIST OF TABLES

ABSTRACT

Oxygen production and oxygen flux play an important role in marine habitats and ecosystems. The eddy correlation (EC) technique is a key aquatic flux measurement technique to measure and calculate vertical turbulent fluxes within aquatic boundary layers without disturbing environmental hydrodynamics. This method is based on the simultaneous measurement of two parameters at the same point; the turbulent velocity fluctuations and oxygen concentration. This thesis explores the reliability of the Eddy Correlation Microelectrode system (ECE) and Eddy Correlation Optode system (ECO) for O_2 flux measurement in seagrass meadows and benthic organisms in the laboratory and field. Although EC has been used in aquatic system for over a decade, this system is still under development to gain robust results. According to its complexity, the EC and software used to analyse and calculate flux have been significantly enhanced over past three years. The method development and preliminary investigations were provided in **Chapter 2**.

Generally, the oxygen concentration data from Eddy Correlation optode system (ECO) are converted from the raw oxygen signal based on the optode phase-shifted signal using Stern-Volmer-equation. **Chapter 2** also showed a new oxygen conversion method based on the raw O_2 intensity signal using Stern-Volmer-equation. Seagrass sediment O_2 uptake was investigated in a laboratory flume under controlled flow and temperature. The calculations of sediment O_2 uptake using two oxygen conversion methods were compared. The result showed that the new oxygen conversion method can be used for EC O_2 flux measurements. Although this method has lower fluctuation in O_2 concentration which leads to better flux calculation, it

needs to be considered whether the ECO is deployed under strong light or sunlight that may interfere with the O_2 intensity signal.

The reliability and limitations of Eddy Correlation Optode system (ECO) were investigated by measuring seagrass sediment O_2 uptake in a laboratory flume under controlled flow and temperature (**Chapter 3**). The seagrass sediment was treated with temperature varying from 18°C to 28°C and flow velocity from 17 cm s^{-1} to 51 cm s^{-1}. The EC data were validated by O_2 microprofiling technique, which can measure fluctuating O_2 concentrations at micro-scales. The results showed that O_2 microprofile and eddy correlation system provided the same range of O_2 flux where the O_2 consumption was observed due to microbial activities (respirations). It clearly showed that the eddy correlation systems using O_2 optode could be used for measuring O_2 flux in the marine system. Although the results of the ECO and O_2 microprofile were similar, the ECO results were not robust. This study provided verification for using eddy correlation system as a routine measurement for O_2 flux *in situ*.

Temperature and light are important controls of seagrass metabolism (photosynthesis, enzyme activity and maintenance of the carbon balance in seagrass) which in turn governs their growth, survival, reproduction and distribution. Optimal temperature and light requirements for photosynthesis and respiration in the temperate seagrass *Zostera muelleri* were examined using the non-invasive Eddy Correlation microelectrode system (ECE) and Chlorophyll *a* fluorescence using PAM under control-flow environment (**Chapter 3**). The results showed that the ECE has a potential to quantify O_2 flux and O_2 production in seagrass meadows at

different light and temperature conditions within a control-flow environment. Temperature and light have an effect on production, photosynthetic efficiency, photoinhibition and capacity for photoprotection in *Z. muelleri*. Optimal temperature and light for photosynthesis for this temperate seagrass is 25°C and 150-250 μmol photons m^{-2} s^{-1}, respectively.

The Eddy Correlation microelectrode system (ECE), Eddy Correlation optode system (ECO) and MiniProfiler MP4 system, an *in situ* microprofiler using a microelectrode, were deployed in Tweed River (New South Wales), Moreton Bay (Queensland) and Heron Island (Queensland) to determine the O_2 flux of marine and estuarine benthic systems composed of seagrasses, benthic microalgae, and microbes (**Chapter 4**). There were some situations in which the EC was unable to measure O_2 flux correctly. However, the EC system can be used to measure O_2 flux in the non-complex environment (steady environmental condition, homogeneous habitat and flat terrain). After the deployments and a series of detailed investigation of ECE and ECO along with consulting with the manufacturer, the first generation of Eddy Correlation optode system (ECO1) was replaced with the second generation of Eddy Correlation optode system (ECO2) in order to improve the O_2 flux measurement.

Experimental results throughout the thesis provided a better understanding of the limitations and reliability of Eddy Correlation system for O_2 flux on seagrass meadows and benthic organisms in both laboratory flume and field. Although the EC has been developed with four major changes (from the first generation of the Eddy Correlation microelectrode system to the second generation of Eddy Correlation

optode system), their stability and robustness still needs to be improved. Further investigation on the limitations and reliability of this new generation of the EC are needed.

ACRONYM

Term	Description
w'	Fluctuation of vertical velocity
ø	Phase angle
C'	Fluctuation of concentration
$\overline{w}$	Mean vertical velocity
τ	Luminescence decay time
ADV	Acoustic doppler velocimeter
AZAs	Auto-zero amplifiers
BMA	Benthic microalgae assemblage
C	Solute concentration
D_0	Molecular diffusivity of solute
DBL	Diffusive boundary layer
dC/dz	Linear slope of the O_2 concentration profile in the DBL
DIC	Dissolved inorganic carbon
DO	Dissolved oxygen
DPHI	Different phase angle (phase shift)
DWN	Dunwich, Queensland
EC	Eddy covariance or Eddy Correlation
ECE1	First generation of Eddy Correlation microelectrode system
ECE2	Second generation of Eddy Correlation microelectrode system
ECO1	First generation of Eddy Correlation optode system
ECO2	Second generation of Eddy Correlation optode system
F	Total flux

Term	Description
FFT	Fast fourier transform
F_V/F_M	Maximum quantum yield
GPP	Gross primary production
H	Water depth
h	Measurement height
H_2S	Hydrogen sulphide
h_{light}	Amount of light hours
h_{dark}	Amount of dark hours
I	Luminescence intensity
I_k	Minimum saturating irradiance
IT-LD	Intensity-Linear detrending
IT-RM	Intensity-Running mean
J	Flux
k	Decay rate
l	Footprint length
LAI	Leaf area index
MB	Moreton Bay
MP	Microprofiler
NEE	Net ecosystem exchange
NEM	Net ecosystem metabolism
NPP	Net primary production
OEM	Original equipment manufacturer
PAM	Pulse-Amplitude Modulated

Term	Description
PAR	Photosynthetically active radiation
PIER	Post-illumination enhanced respiration
POC	Particulate organic compound
PSII	Photosystem II
PS-LD	Phase-shifted-Linear detrending
PS-RM	Phase-shifted-Running mean
PWM	Pulse-width modulation
R	Respiration
RC	Reef crest
Re	Ecosystem respiration
rETR	Relative electron transport rate
$rETR_{max}$	Maximum relative electron transport rate
ROM	Read only memory
RS	Reef slope
SG	Seagrass beds
SSLCs	Steady state light curves
SWI	Sediment-water interface
TWD	Tweed River
VPM	Vegetation photosynthesis model
x_{max}	Upstream location of the strongest flux
Y(II)	Effective quantum yield
Y(NO)	Non-regulated
Y(NPQ)	Non-photochemical quenching yield

Term	Description
z_0	Sediment surface roughness
α	Light utilisation efficiency
$\Delta F/F_M'$	Effective quantum yield

CHAPTER 1:

GENERAL INTRODUCTION

1. GENERAL INTRODUCTION

1.1 RESEARCH OBJECTIVES AND THESIS OUTLINE

The major objectives of this research include:

1. Determine the reliability and limitations of the eddy correlation (EC) system for O_2 flux measurement in marine and estuarine habitats as well as under laboratory conditions.
2. Determine O_2 flux of marine and estuarine benthic organisms such as seagrass, benthic microalgae and microbes.

The criteria for assessing the reliability and limitations of EC include:

1. **Accuracy and precision**: Can the EC accurately measure O_2 flux throughout the range of conditions experienced?
2. **Ranges of environmental conditions**: Over what ranges of environmental conditions would the EC need to operate?
3. **Sensor technology requirements**: What are the sensor technology requirements and sensor resolution?
4. **Data processing and data interpretation**: Are the derived data relatively simple and straightforward? Can it be used as computational routine for processing data?
5. **Ease of operation**: Are the methods sufficiently simple so as to be deployed and operated in both the lab and field environments?
6. **Replication**: Is the EC suitable for O_2 flux measurement with a number of replications?

In meeting these objectives this thesis is structured as follows:

Chapter 1 presents a literature review of net ecosystem production and respiration of the various components of estuarine (including seagrass, microphytobenthos, mangrove, and saltmarsh communities) and coral reef communities (e.g., coral dominated sand turf macroalgae, microphytobenthos and sponges). Various methodologies for O_2 flux measurement (e.g., eddy correlation, O_2 chamber) are considered.

Chapter 2 presents a detailed examination of method development and describes the preliminary investigations used in this thesis. Two O_2 conversion methods from the eddy correlation optode system (ECO), which led to O_2 flux measurement in sediment within the laboratory flume, were investigated. The O_2 flux results using these two methods were compared.

Chapter 3 examines on the limitations and reliability of EC technique used in the laboratory flume. O_2 consumption in seagrass sediment under controlled physical parameters (e.g., temperature, flow and light) was measured in a laboratory racetrack flume using the EC technique and the O_2 microprofiling technique. The optimal temperature and light requirements for photosynthesis in the temperate seagrass *Zostera mulleri* was measured using the EC technique and chlorophyll fluorescence. A Pulse Amplitude Modulated fluorometer (Diving-PAM) was also used to determine the photosynthetic efficiency of the seagrass across a range of light and temperature treatments.

Chapter 4 presents field deployments of EC in three benthic ecosystems: an estuarine system (Tweed River, New South Wales), a subtropical coastal embayment (Moreton Bay, Queensland) and a coral reef (Heron Island, Queensland). The eddy correlation and microsensor techniques were used to evaluate the O_2 flux of marine and estuarine benthic organisms such as seagrass and benthic microalgae.

Chapter 5 summarizes the key findings of this thesis, discusses the O_2 flux of marine and estuarine benthic organisms such as seagrass, benthic microalgae and microbes, and the reliability and limitations of the eddy correlation system for O_2 flux measurement in marine and estuarine habitats and laboratory flumes. As a final point, it suggests avenues for future research.

This section of this chapter was contributed to the CSIRO Marine and Coastal Carbon Biogeochemistry Cluster Milestone 2 Report.

Chotikarn P, Chipman L, Macreadie P, Petrou K, Sinutok S, Carvalho M, Oakes J, Cyronak T, Eyre B, Ralph PJ. 2014. Literature review on gross and net ecosystem production and respiration values for estuaries and coral reefs. In: Duarte C, Ralph PJ, Doblin MA, Phinn S. 2014. Marine and Coastal Carbon Biogeochemistry Cluster Milestone 2 Report. CSIRO Wealth from Oceans Flagship. pp 56-77.

1.2 GROSS AND NET ECOSYSTEM PRODUCTION AND RESPIRATION VALUE FOR ESTUARIES AND CORAL REEFS.

Coastal habitats (seagrass, mangrove, macroalgae and reef) form critical marine ecosystems that are characterized by high biodiversity and productivity (Wilkinson 2002; Harrison and Booth 2007). Coastal vegetation is supported by photosynthesis,

during which carbon dioxide is converted into biomass. Through this process, CO_2 is removed from the atmosphere and stored as organic materials that are stable over time scales of minutes to millions of years (Atwell et al. 1999). These coastal habitats have been affected by global climate changes and human activities such as overfishing, intensive agricultural activities, and industrialization (Hughes 2008). Measurement of primary production is essential to understanding these threatened, yet globally significant habitats.

Comprehending the total carbon budget of an ecosystem requires measurements of both the stock and flux of carbon (Law et al. 2004). Stock estimates only describe how much carbon is present at the time of sampling; they do not indicate how quickly the stock accumulates or the rate of its release back into the atmosphere. Generally, carbon (C) accumulates slowly via growth of living biomass and burial, whilst C loss can be a much more rapid process as a habitat declines in area (degradation of habitat) or is physically removed. Stocks can be measured using a diverse range of coring, isotope and geochemical methods (Watson et al. 2000; Fourqurean et al. 2012; Greiner et al. 2013; Lavery et al. 2013); however, flux measurements are more complex. Flux is the amount of a compound moving through a unit area over a unit of time. In the case of C flux, it is the integration of biosequestration and ecosystem respiration. These processes are non-linear and driven by the complex interaction of light, water flow, plant community, microbial community, infauna, temperature, sediment type, and redox conditions. Flux can be measured by the relatively simple "difference in stock" method, yet this requires long-term accumulation to be able to detect any changes. In contrast, real time flux

provides more rapid information, but is technically more complex and subject to a range of assumptions.

C moves between sediment, water, and air in both liquid and gas phases. To estimate the flux of C it must be measured across two interfaces (providing a rate of change), the sediment-water interface and/or the water-atmosphere interface. Therefore, a detailed understanding of C flux will allow predictive models to describe the extent of C stock into the future, as well as examine how coastal wetlands influence atmospheric composition and climate.

Measurements of gas exchange are used as a proxy of community function. O_2 production (or CO_2 uptake) of an ecosystem is defined as net primary production (NPP), while measurements of oxygen uptake in darkness provide an estimate of respiration (R). Finally, gross primary production (GPP) is equal to NPP+R (Baird et al. 2011).

As a result of short-term changes in environmental conditions, instantaneous O_2 varies with water velocity, temperature and light intensity, and therefore these factors can affect net ecosystem metabolism (NEM) because NEM which is P+R is usually measured on a daily scale This remains a serious shortcoming of short-term chamber incubations (< daily).

A conceptual diagram of oxygen flux in seagrass beds (as a model organism) during daylight and darkness is shown in Figure 1.1. Sunlight induces plant photosynthetic activity which leads to O_2 release into the water column. The O_2 production rate is greater than the O_2 consumption rate by plants and other organisms, as well as the reoxidation rate (e.g., bacteria and bioturbators); therefore, the net daylight O_2 flux is

outward flowing (efflux) from the ecosystem. During nighttime, in contrast, there is no photosynthetic activity, thus, the net darkness O_2 flux is inward (influx) to the ecosystem.

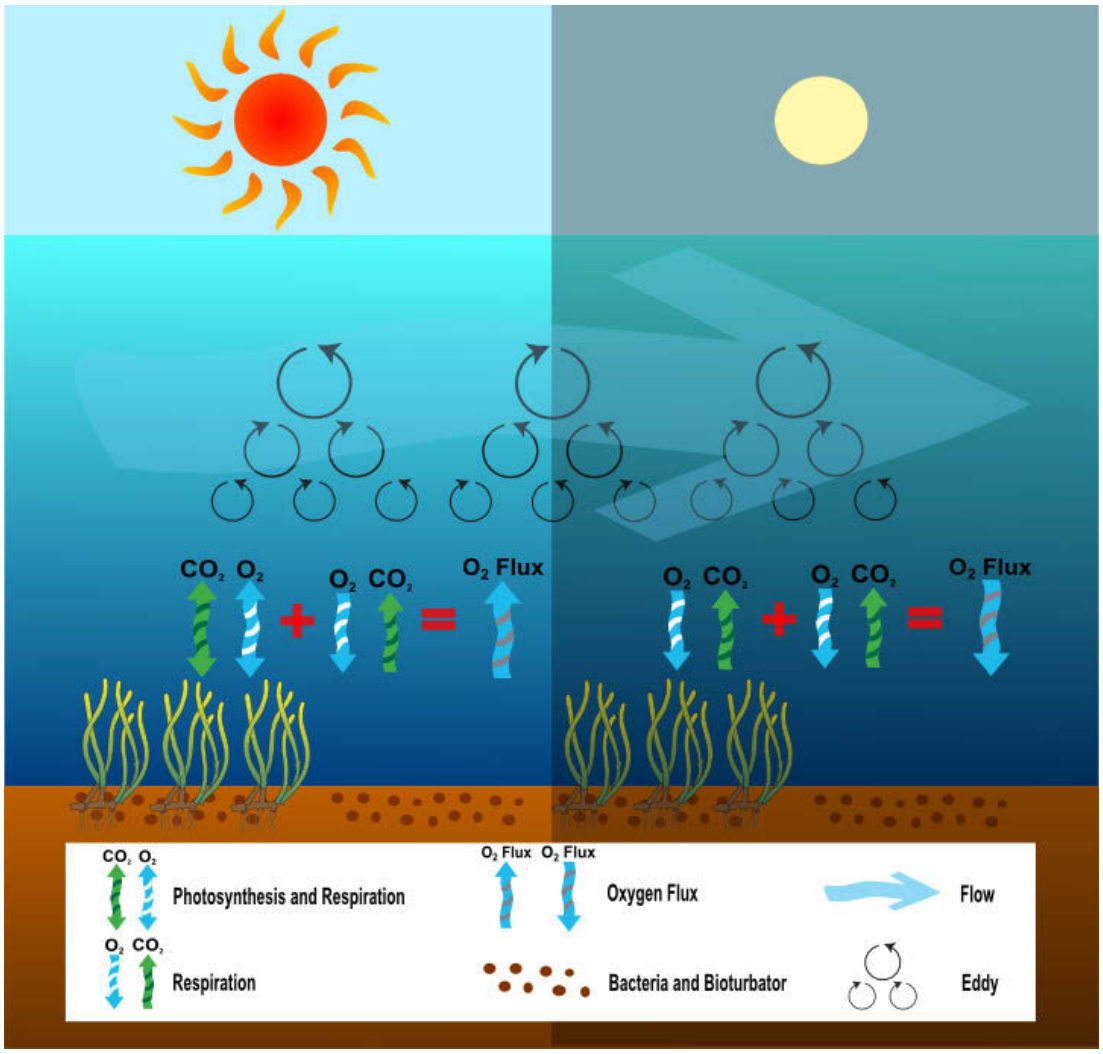

Figure 1.1: This conceptual diagram shows the O_2 flux in seagrass beds dominated by eddies during daylight and darkness.

Water motion also affects seagrass photosynthesis, gas exchange, sediment transport and epiphyte load. The thickness of the diffusive boundary layer (DBL) defines the rate of exchange between the seagrass and the bulk water. Increased water motion is beneficial to photosynthesis because it decreases the DBL thickness causing

increases in gas exchange rates and therefore potential growth (Koch 1994; Forster et al. 1996). It also increases sediment re-suspension, which reduces light and can alter sediment-based C flux (Madsen et al. 2001). Roughness of the seagrass blade (epiphytes and adhering sediment) also modifies the DBL. Therefore, estimates of gas flux that constrain or alter water motion will confound actual values (Koch 1994). Additionally, bulk water gas content alters the gas exchange and photosynthesis of seagrasses; reduced oxygen content in the bulk water will increase nighttime respiration of the plants and substantially increase net ecosystem exchange (NEE) respiration (Koch 1994).

1.3 COMPARISON OF CURRENT METHODOLOGIES FOR GROSS AND NET ECOSYSTEM PRODUCTION AND RESPIRATION MEASUREMENT IN ESTUARIES AND CORAL REEFS.

The applications, advantages and disadvantages of each methodology are discussed using the following criteria: a) conditions required for each application, b) accuracy and resolution, c) ease of use, d) data interpretation and e) limitations. A summary of applications, advantages and disadvantages of the most common methods used in seagrass and coral photosynthesis, and community metabolism studies are shown in Table 1.1 (Silva et al. 2009).

Table 1.1: Applications, advantages and disadvantages of the most common methods used in seagrass and coral photosynthesis, and community metabolism studies modified from Silva et al. (2009).

Method	Applications	Advantages	Disadvantages
Plant incubation	• Photosynthesis and dark respiration of whole plants or leaf cuts incubated in bottles (laboratory or *in situ*) • O_2 analysis of water samples from benthic chambers (field)	• High accuracy • Low price	• Intrusive (if plants are incubated in bottles) • Problems related to containment in closed chambers • Initial and final O_2 concentrations only • Cumbersome
O_2 electrode or optode coupled to small reaction chambers	• Photosynthesis and dark respiration of leaf cuts (laboratory)	• High resolution • High accuracy • Continuous O_2 measurements • Highly controlled conditions • Possibility to manipulate the incubation medium	• Intrusive • Highly artificial • Spectral quality of artificial light sources
Microprofiling using microelectrode or optode	• O_2 consumption by belowground tissues (*in situ*) • O_2 leakage into the rhizosphere (*in situ*) • O_2 production or consumption in custom-made chambers • O_2 mapping of seagrass rhizosphere (*in situ*) • Used in the eddy correlation technique (*in situ*)	• Not very intrusive (small diameter probes) • Fast response time (microeletrode is faster than optode) • Positioning possibilities • 2-dimensional measurements • Very sensitive at low O_2 Concentrations (optode only) • Does not consume O_2 (optode only) • Long-term stability	• Small spatial resolution • Fragile in field conditions (microelectrode) • Fast optode is still under development
PAM fluorescence	• *In situ* and laboratory measurements of photosynthetic efficiency at the plant level	• Non-intrusive • Portability • Autonomous underwater equipment • Possibility of continuous Measurements	• Measures light reactions only • Does not allow respiration measurements or thus production estimates
CO_2 evolution	• *In situ* measurements of community uptake and release of CO_2, in incubation chambers	• Non-intrusive • Integration of whole community metabolism • Highly reliable in air exposed Conditions	• Possibility of underestimating CO_2 uptake in underwater conditions • Problems related to containment in closed chambers
Geo-acoustics	• *In situ* large-scale estimation of community O_2 production	• Large-scale application, suitable for ecosystem level studies • Continuous measurements	• Underdeveloped technique
Eddy correlation	• *In situ* sediment–water fluxes of dissolved O_2 • Community level O_2 fluxes metabolic studies	• Non-intrusive • Autonomous underwater equipment • Good surface integrating capacity • Continuous measurements	• Underdeveloped technique

1.3.1 Difference in stock

Carbon may be lost from coastal wetlands in the form of dissolved or particulate organic compounds (POC) that move into adjacent ecosystems (mangrove-seagrass-coastal ocean) (Watson et al. 2000); this is also called leakage. Typically, the loss of dissolved organic compounds is only a small fraction of the carbon budget. Horizontal fluxes of carbon are generally missed by atmospheric measurements of flux, which explains why carbon flux estimates between the atmosphere and the sea surface may not be equivalent to changes in the coastal vegetation storage of carbon (Watson et al. 2000). For example, when POC moves down river (exported/leaks from catchment) and accumulates in a seagrass meadow; this is measured in the stock change, but not the flux measurements. Biomass growth is the same as a difference in C stock; however, increasing biomass also leads to an increase in flux measurement due to more photosynthetic active area (Watson et al. 2000).

1.3.2 Stable isotope tracers to measure production and respiration

Stable isotopes can be used to provide estimates of production and respiration for autotrophs and ecosystems based on rates of inorganic carbon fixation into biomass, respiration of CO_2 or dissolved inorganic carbon, and/or oxygen production (Beardall et al. 2009).

1.3.3 Carbon isotopes

The rare stable carbon isotope, ^{13}C, can be used to directly determine carbon fixation rates using a similar approach to the ^{14}C method which is common in oceanography (Marra 2009), whilst avoiding the hazards associated with the use and disposal of

radioactive materials. Briefly, a known quantity of inorganic carbon amended with ^{13}C is added to a culture or community of phytoplankton, and the incorporation of ^{13}C into biomass is measured after incubation for a given period. The limitations and caveats of using ^{13}C are similar to those associated with the use of ^{14}C, which have been detailed previously (Peterson 1980). However, when using ^{13}C the algal biomass at the beginning (Slawyck et al. 1977) or end (Hama et al. 1983) of the incubation must also be determined to allow calculation of total ^{13}C uptake, given that the abundance of rare stable isotopes is typically expressed as a ratio of rare to common isotope, in the form of delta notation.

Short-term incubations (4 h) with ^{13}C provide an indication of gross primary production. The incubation time will depend on the turnover rate of the autotroph or community of interest (Regaudie-de-Gioux et al. 2014). In all cases, however, the interpretation of stable isotope data becomes more complicated with longer-term incubations. Transfer of ^{13}C to heterotrophs and subsequent respiration of ^{13}C leads to fixed ^{13}C being returned to the inorganic carbon pool and potentially re-fixed again into organic carbon. Therefore, in longer-term incubations, where organic carbon and inorganic carbon approach isotopic equilibrium, the ^{13}C method estimates net productivity.

Most ^{13}C amendments used to determine production rates have focused on phytoplankton. However, it has recently been demonstrated that the ^{13}C method can be used to determine carbon fixation rates for other autotrophs including seagrass (*Zostera marina*; Mateo et al. 2001) and seaweed (kelp, *Laminaria hyperborea*; Miller and Dunton 2007). In these studies, sections of each autotroph (e.g., seagrass blades, discs of kelp lamina) were removed and incubated in closed vessels in the

presence of ^{13}C-labelled inorganic carbon. In the study by Mateo et al. (2001) this gave estimates of production comparable with those determined using the ^{14}C method, but production was underestimated when based on changes in O_2 concentration, where the interference from bubble formation under low rates of production occurred. However, given that removal of plant parts, and/or removal of autotrophs from their natural environment may alter production rates in most cases it would be preferable to apply ^{13}C to autotrophs *in situ*.

In situ application of ^{13}C has the potential to determine production by individual autotrophs and/or an entire community. The simplest example of this is the application of ^{13}C to intertidal sediments to assess production by benthic microalgae (Oakes and Eyre 2013). However, methods have also been demonstrated in the application of isotope labels *in situ* to seagrass blades (^{13}C-labelled sodium bicarbonate in water; ; Marbà et al. 2006; Kaldy et al. 2013) and mangroves (^{13}C-labelled CO_2 in air; Oakes et al. 2010), and similar methods could be used to label other coastal autotrophs. Provided that the subsequent uptake of ^{13}C is high enough to be detected in the short-term, changes in ^{13}C content of plant biomass can then be used to calculate productivity. For example, Nayar et al. (2009) enclosed subtidal seagrass sediments within benthic chambers and used ^{13}C amendment of the enclosed water to investigate seasonal variability in carbon uptake by seagrasses (*Amphibolis antarctica* and *Posidonia angustifolia*) and phytoplankton. Additions of ^{13}C can also provide insight into community-scale production rates for any community that can be contained, although this will be more expensive and complex where larger areas are involved. At the smaller scale, subtidal sediments or communities can be enclosed within benthic chambers for the period of isotope

addition (e.g., Oakes et al. 2010). At a larger scale, an enclosure may be constructed around an area of saltmarsh, seagrass, or mangrove forest for isotope labelling e.g., Gribsholt et al. 2005. In this case, the uptake of ^{13}C by the community after a short time period would indicate gross production. This could be determined by measuring the ^{13}C content of all components of the community (autotrophs and heterotrophs), taking into account their biomasses. Alternatively, for intertidal sites, uptake rates could be determined based on a mass balance of ^{13}C added to the community and ^{13}C lost on the subsequent outgoing tide.

In both *ex situ* and *in situ* amendments with ^{13}C, longer-term incubations are complicated by respiration of ^{13}C and re-fixation of ^{13}C. If the rate of respiration is known, then the gross production can be inferred. Recent advances in methods and instrumentation now make it far easier to measure ^{13}C in dissolved inorganic carbon (Osburn and St-Jean 2007) or carbon dioxide (via cavity ring-down spectroscopy; Maher et al. 2013), which should allow for respiration rates to be determined. In most cases this will be complicated by the mixing of respired ^{13}C with unincorporated ^{13}C. Flushing the system (i.e., replacing water or air) to remove unincorporated label after a given incubation period will make it easier to detect small changes in ^{13}C content due to respiration of ^{13}C-labelled organic carbon, but this is probably not feasible for incubations of phytoplankton.

For any approaches that estimate gross production by adjusting for estimated respiration rates, it is important to note that respiration rates in daylight can vary from those observed during darkness. Additions of ^{13}C can also be used to measure daylight respiration rates (Carvalho and Eyre 2012). The main difference in the previously discussed methods is that the changes in the isotopic composition of not

only the organisms, but also the water, are measured. This way, it is possible to quantify respiration in daylight and gross primary production without need of incubations in darkness. So far, this approach has been employed only preliminarily, but it has the potential to be adapted for field work if care is taken to keep the system closed to the atmosphere.

1.3.4 Oxygen isotopes

Isotopes of oxygen have been employed to measure gross primary production without the need of dark incubations, in a fashion similar to that described above (Grande et al. 1989) So far it has revealed that, in most cases, oxygen respiration in daylight is much higher (up to 1000%) than in darkness (Bender et al. 1987; Bender et al. 1999; Robinson et al. 2009), which means that oxygen gross primary production measured by the standard light and dark incubation method has been consistently underestimated. However, some exceptions have been found, suggesting that this method may lead to an underestimation of primary production in certain cases (Ostrom et al. 2005; Yacobi et al. 2007).

A second method used to measure gross oxygen primary production is the triple isotope method, which has been widely employed in the open sea (Sarma et al. 2005; Quay et al. 2010; Juranek and Quay 2013). It does not require the addition of extra compounds to the system, and also does not need closed incubations. However, it demands a series of set conditions to yield valid results, which are met in the open sea, but may be difficult to find in complex coastal ecosystems. These include absence of horizontal boundaries, low gas exchange between mixing and deeper layers and predictable gas exchange between water surface and atmosphere (Luz and

Barkan 2000; Juranek and Quay 2013). Therefore, its application in coastal systems may be limited.

1.3.5 Benthic core incubations

Benthic productivity and respiration can be measured in sediment cores; these cores typically range from 50 to 100 mm in diameter. The core is pushed into the sediment and a portion of the upper sediment containing plants and/or benthic algae and overlying water is removed. Cores are then usually transported back to a laboratory and incubated in large tanks of site water maintained at a given temperature (Sundbäck et al. 1991; Ferguson and Eyre 2010, 2013). Light is provided by photosynthetically active radiation (PAR) that is run on diel light and dark cycles and the cores are stirred to prevent the build-up of concentration gradients in X, Y and Z axis. A variation of this method incubates the cores in floating cradles in the water column near the site of core collection (Ferguson et al. 2003; Eyre and Ferguson 2005). The floating cradles expose the cores to similar *in situ* light and temperature variations to the collection site. A combination of both the laboratory and cradle techniques is to place the cores in a large tank of site water maintained at *in situ* temperature on land in the open near the site of collection so they are exposed to similar *in situ* light variations to the core collection site (Eyre et al. 2011). For both the floating cradle and on-site incubation tank techniques the cores are shaded so that they receive similar amounts of PAR to *in situ* sediments.

Benthic productivity and respiration are estimated from the change in dissolved inorganic carbon (DIC) or O_2 in the core water column over a given incubation time. Net primary productivity (NPP) is estimated from the change in O_2/ DIC during

daylight, respiration (R) is estimated from the change in O_2/ DIC during darkness, and gross primary productivity (GPP) is estimated by adding NPP and R with the assumption that light respiration equals dark respiration (see Labeled Isotope Tracers).

The three different core incubation techniques have their own advantages and disadvantages. Laboratory incubations allows control of both light and temperature so average values for the period of interest can be used, including over the diel cycle. They allow construction of functional models that can be used to predict productivity in the field. In contrast, the cradle and on-site incubations are exposed to a similar instantaneous light climate as the site of core collection, but this is only representative for the day of the incubation. A single incubation is commonly used to represent a season or a month, and as such, an average light level for that period may be more appropriate.

The advantage of cores over chambers is that they are logistically easier to use and therefore allow for far greater replication. The main disadvantage is that they cannot capture large structural complexity in the sediment such as large macrofauna burrows and macrophytes. A combined approach uses cores where there is little structural complexity such as bare sediments with microphytobenthos, and chambers where there is large structural complexity such as macrofauna burrows and macrophytes (Eyre et al. 2011; Maher and Eyre 2011). Chambers also minimise O_2 bubble formation due to their larger water volume compared to cores. Comparisons of benthic production and respiration between cores and chambers show mixed results. For example, a comparison of NPP rates between triplicate cores and chambers from a shallow site incubated in a range of temperature and light

conditions found no significant difference (Maher and Eyre 2011). Similarly, a good relationship was found between O_2-GPP and gross CO_2 fixation across a range of benthic habitats in a shallow coastal system using cores and chambers, demonstrating that there is no systematic bias in measured rates associated with using two types of incubation methods (Eyre et al. 2011). In contrast, a comparison of chamber and core measurements from a 20 m deep site showed much higher rates of respiration in the chambers than the cores (Macreadie et al. 2006). This difference in respiration was probably a disturbance effect (i.e., core compression) due to the collection of 40 cm cores (Macreadie et al. 2006). Whereas, cores used by Maher and Eyre (2011) that showed similar NPP rates to chambers were only 20 cm long and had little compression. As such, a combination of cores and chambers appears to be a suitable approach for estimating benthic respiration and productivity in shallow coastal systems that mosaic of benthic habitats.

1.3.6 Laboratory incubations of cores

Core incubation is used to determine O_2 exchange rate in the laboratory. The sediment cores are transported to the laboratory in controlled temperature containers, where they are uncapped in water which has the same temperature and air saturation as the location where the cores were collected. To ensure a good mixing and exchange between water phase of the core and the exterior seawater, a magnetic stirrer attached to the inner wall of the core should be used. The O_2 exchange rate would then be assessed by O_2 microprofiling after overnighting. During the incubation period (after microprofiling), O_2 consumption can be assessed with an O_2 sensor in darkness (Glud et al. 2010).

1.3.7 Benthic chambers

Benthic chambers can be equipped with sensors that can measure many types of fluxes i.e., O_2, CO_2, CH_4, and N_2O (Maljanen et al. 2001). O_2 and CO_2 chambers are used most commonly for measuring the photosynthesis, respiration and gas transport of isolated leaves, roots and rhizomes and whole plants. The chamber is set up to enclose a known surface area of interests. The chamber is stirred continuously to ensure good mixing of air or water without altering the surface of interests (Alongi et al. 1989). To measure net ecosystem metabolism (NEM), chambers may be used to enclose a small area (sediment, plants and leaves). Changes in the concentration of CO_2 (or other gases) within the chamber or differences between the concentrations in incoming and outgoing air/water are used to calculate flux. The advantages of this technique are that it is easy to use and inexpensive. The disadvantages, however, are that this method cannot be used to measure flux in very large areas because the flux that is measured might be an over or under estimation (Gao and Yates 1998).

There are many different chamber designs, which are all stirred to try and reproduce the benthic boundary layer, but these have mostly been designed for deep-sea measurements (Tengberg et al. 2005). Shallow water sediments typically have much larger, mostly tidal-driven (but also wind- and freshwater-driven) lateral flows compared to deep water sediments. This lateral flow can also produce passive flow through the burrows of large macrofauna (Webb and Eyre 2004b), which is an important process to replicate when measuring benthic productivity and respiration. As such, benthic chambers designed for working in shallow coastal sediments replicate this lateral flow by pumping water across the chamber floor, and hence across the community contained within the chamber (e.g., seagrass; macrofauna

burrows; Webb and Eyre 2004a; Eyre et al. 2011; Maher and Eyre 2011). It is unknown how well these lateral flow chambers replicate natural flows in shallow coastal waters and a comparison with EC would be productive research to undertake in the future.

1.3.8 Flow respirometry

The flow respirometry method has been widely used to measure primary production in rivers and streams (Odum 1956; Langdon et al. 2013) and has been adapted for the measurement of community metabolism (net community calcification, net photosynthesis and respiration) in coral reefs (Marsh and Smith 1978; Barnes 1983; Gattuso et al. 1993; 1996; 1999; Langdon et al. 2013; Shaw et al. 2014). This method measures the upstream-downstream changes of the chemical properties (O_2, dissolved inorganic carbon or total alkalinity) in a parcel of water in a unidirectional current flow using Eulerian or Lagrangian approaches (Shaw et al. 2014). The net rate at which a community alters the chemical properties is determined by dividing the changes in the chemical constituent of water by water transit time (Langdon et al. 2013). The Eulerian approach makes observations at a fixed position over time, while the Lagrangian approach makes observations with respect to the flowing parcel of water as it moves through the system of interest (Langdon et al. 2013). This method, however, is limited to environments that have a unidirectional flow of water and does not account for lateral mixing.

1.3.9 Gas flux measurement

For gases, flux measurements determine how many molecules of gases are moving up or down over a unit area per unit time. Flux can be described as a sink or a

source, corresponding to the direction of the flux. For example, seagrass beds may be a sink for CO_2 during daylight if the net flux is inward from water to seagrasses due to the photosynthesis process, while seagrass beds may be a source of CO_2 during darkness, if the net flux is away from seagrass beds due to respiration. To measure O_2 and CO_2 production and flux in coastal vegetation, various techniques have been used. These include the gas extraction technique, O_2 titration (Winkler) technique, geo-acoustic technique, microprofiling technique, eddy covariance using O_2 optode and microelectrode techniques (Borum et al. 2006; Silva et al. 2009).

1.3.10 Gas extraction

Gas extraction is a destructive technique, where tissues have to be cut or squeezed to harvest internal gases. Changes in O_2 and CO_2 concentrations in plant tissues are measured using infrared gas analysis and gas chromatography (Larkum et al. 1989; Borum et al. 2006; Silva et al. 2009). This technique has limited temporal and spatial resolution and cannot be used for recording internal gas dynamics as functions of environmental condition changes (Borum et al. 2006).

1.3.11 Plant incubations

Photosynthesis and dark respiration of whole plants or leaves can be determined by incubating them in bottles or chambers (either *in situ* or in a laboratory) and measuring the change in oxygen over the incubation period. Measuring oxygen concentrations via the Winkler technique is accurate and inexpensive compared to using O_2 electrodes and optodes (Silva et al. 2009), but the oxygen results produced are not always accurate due to user error (such as sample preservation). Nevertheless, the incubation method is invasive and destructive because of the need

to detach the plant samples. Additionally, this technique causes an increased boundary layer during incubation if not stirred, which results in an underestimation of photosynthetic rate (Koch 1994), and it can measure only initial and final O_2 concentration (Silva et al. 2009).

1.3.12 Geo-acoustic

This technique is a continuous measurement of *in situ* large-scale community O_2 production. The principle of this technique is the photosynthetic O_2 microbubbles formed on the leaf blade surface will interfere with the wave propagation of broadband acoustic transmissions and can be correlated with the photosynthetic activity of whole meadows (Hermand et al. 1998; Silva et al. 2009). Nonetheless, this technique remains under developed because validation against traditional methods has not been performed (Silva et al. 2009).

1.3.13 Microprofiling

O_2 concentration profiles can be measured across a few millimeters above the sample of interest (e.g., plant leaf, root, rhizome and sediment) using Clark-type micoroelectrodes or optodes. The diffusive O_2 flux can be calculated from O_2 profiles within the diffusive boundary layer (DBL), a layer of fluid which is not mixed with the main body of fluid, according to Fick's first law. The microelectrode and optode are not very intrusive due to their small diameter probes. The microprofiling method provides real time assessment of O_2 and CO_2 conditions in coastal vegetation (Wangpraseurt et al. 2012). This method works best in muddy, homogenous sediments where diffusion is dominant and environmental conditions are in a steady-state. Internal O_2 and CO_2 gradients and profiles can be measured at

high spatial and temporal resolutions. The O_2 optode is also not intrusive, especially if a thin, very sensitive optical sensor is used (such as a microoptode). It is capable of measuring very low O_2 concentrations and is more robust compared to a microelectrode; however, the O_2 optode has a slightly slower response than the microelectrode and new approaches are currently being tested to improve the speed of the optode (Chipman et al. 2012). The optode and microelectrode are also used for underwater eddy covariance (EC) measurements. However, it is worth noting that the microprofiling method is limited in measuring whole plant metabolism or O_2 release because it can only be used to measure flux at the microscale (Borum et al. 2006; Silva et al. 2009).

1.3.14 Eddy covariance measurements

Eddy covariance (EC) is a relatively new and non-invasive method for measuring benthic fluxes. This technique has been widely used in terrestrial systems to measure gas and heat fluxes for the last 50 years. The EC has become a popular technique to assess CO_2 flux due to four apparent avantages; scale-appropriate, CO_2 direct measurement, footprint area, and long-term CO_2 monitoring (Baldocchi 2003). The EC technique is most accurate when performed in steady conditions (e.g. wind, temperature, CO_2, humidity). In addition, the underlying vegetation is homogenous with flat terrain (Baldocchi 2003). For the aquatic environment, some issues to address would include the small-scale spatial heterogeneity of marine communities relative to many terrestrial system, impact of differences in fluid viscosity between air and water, and the impact of currents and especially ossillatory flow (Lowe et al. 2005) on vertical advection between the benthos and the water column. Finally, the control volume approach (Monismith 2007) should also be included as a potential

emerging technology that might allow EC measurement to be more effectively constrained across defined horizontal boundaries.

Berg et al. (2003) transferred the conventional terrestrial EC technology to underwater deployment in order to measure O_2 uptake in sediment. They used a similar system to measure dissolved oxygen from the sediment/water interface. The total flux across the sediment-water interface (SWI) is the sum of diffusion, bioturbation (the disturbance and overturning of sediments by burrowing organisms), porewater advection and sediment re-suspension. EC is gaining popularity due to its advantages over other methods (e.g., *in situ* chambers and DO sediment microprofiling); however, many aspects of this method need careful validation.

EC provides a wide range of technical advantages (such as allowing measurement of true flux under natural conditions) as it does not disturb hydrodynamic conditions (currents and waves), it does not alter light fields, it can be utilised in complex topographic substrates (e.g., seagrass, infauna, not just bare sediment), and it can be used *in situ* for long-term data collection. Furthermore, it allows a much larger area of habitat to be sampled (100's m^2 as opposed to a chamber with 0.5 m^2) providing a more integrated sample of the habitat. This removes sample bias towards small scale heterogeneity that can occur with smaller sample techniques (Silva et al. 2009). However, EC may not be usable in locations with rapidly varying oxygen concentrations, such as vegetated benthic communities in shallow water (Holtappels et al. 2013).

Although EC is effective in aquatic environments, it can only be used to measure O_2 flux, because the current CO_2 sensor technique is too slow for the high sampling

resolution needed for these measurements (response time of <0.3 s for O_2 sensor and >10 s for CO_2 sensor) (Köhler-Rink and Kühl 2000). Due to this slow sensor response time, the flux measured by EC is an underestimation because the sensor cannot capture changes in concentration related to small and fast eddies. Furthermore, to get information on CO_2 and O_2 flow from seagrass, wave motion pressure upon seagrass leaf blades needs to be quantified, as wave motion is a main factor influencing the direction and magnitude of CO_2 and O_2 flux.

Terrestrial eddy covariance system (mangrove/saltmarsh) - The eddy correlation technique has been used in atmospheric sciences since the mid-twentieth century to measure energy and mass transfer in agriculture, forestry, hydrology and ocean research, however initial conventional measurements were technically challenging because of the limitation in sensor response time, data collection and data processing (Burba and Anderson 2010). Recently, a novel non-invasive *in situ* system using the eddy covariance technique has been developed to measure CO_2 flux in terrestrial environments (Okimoto et al. 2007). Instantaneous vertical wind velocity, CO_2 concentration, latent and sensible heat flux, mean temperature, mean humidity and mean pressure were measured for unit conversions and other corrections (Burba and Anderson 2010).

A typical example of an eddy covariance installation includes a 3-dimensional sonic anemometer, an open-path gas analyser, a sample inlet for a closed-path gas analyser and a fine-wire thermocouple (Burba and Anderson 2010). There are a large number of EC flux towers in a wide variety of terrestrial habitats; whereas there are few in coastal wetlands (aerial mangrove and underwater systems have only recently been developed) (Polsenaere et al. 2012).

Underwater eddy correlation system (seagrass) - Underwater EC measurements are dependent upon turbulent fluctuations of the water, which are affected by fluid velocity, solute concentration, temperature, sediment roughness and flow (Berg et al. 2003). Because EC is non-invasive and integrates over a large measuring surface, it measures the net effect of all of those processes in unison. The higher the EC sampling point is above the canopy or interface, the larger the measuring area and thus, a larger area of ecosystem is integrated into the signal. Underwater EC systems currently measure O_2, temperature, conductivity, nitrate, H_2S, and CDOM, (Hume et al. 2011; Johnson et al. 2011; McGinnis et al. 2011; Berg et al. 2013; Table 1.2), although CO_2 sensors are currently not fast enough to measure turbulent parcels of water. Kuwae et al. (2006) suggested that the eddy correlation measurement could be used for investigations of photosynthesis. The application of the eddy correlation technique has also been used to investigate diurnal cycles of photosynthesis and respiration in a reservoir and turbulent oxygen transport from the stratified water column of a lake (Brand et al. 2008; McGinnis et al. 2008; Table 1.2). Other studies have used it for studying photosynthesis of seagrass and coral reef ecosystems (Hume et al. 2011; Berg et al. 2013; Long et al. 2013; Table 1.2).

The first application of eddy correlation system used in a seagrass meadow was performed in 2011 (Hume et al. 2011; Table 1.2). Hume et al. (2011) deployed the eddy correlation system to measure dissolved O_2 flux in the water column above seagrass meadows allowing the estimation of gross primary production (GPP), respiration (R) and net ecosystem metabolism (NEM).

1.4 EDDY CORRELATION: A NEW WAY TO ESTIMATE AQUATIC NET ECOSYSTEM METABOLISM

As described earlier, Eddy Correlation (also known as Eddy Covariance and Eddy flux; EC) is one of the most direct ways to measure benthic fluxes. The method is mathematically complex, requiring a great deal of care in the setting up of equipment and processing data, and is extremely vulnerable to prevailing environmental conditions. It can not only be used to measure net ecosystem metabolism (NEM), but also can be used to measure gross primary production (GPP), respiration (R) and nutrients of the ecosystem (Johnson et al. 2011).

1.4.1 General principle of eddy covariance method

Physical meaning of eddy covariance

Eddy covariance works on the principle of covariance of two components; gas concentration and vertical velocity of water where the vertical O_2 flux can be calculated as a covariance of the vertical water velocity and the concentration of O_2.

Figure 1.2 depicts a single measurement point of the underwater eddy correlation system. At $Time_1$, $Eddy_1$ moves a parcel of water (C1), containing a specific gas concentration, pressure, and temperature, downwards by vertical water velocity (w_1). At $Time_2$, $Eddy_2$ moves the water parcel C2 up by vertical water velocity (w_2). For example, if one knows how many molecules of O_2 went down with eddies at $Time_1$, and how many molecules went up with eddies at $Time_2$, at the same point, one could calculate the net vertical flux of O_2 at this point over this time ($Time_2 - Time_1$) (Burba and Anderson 2010).

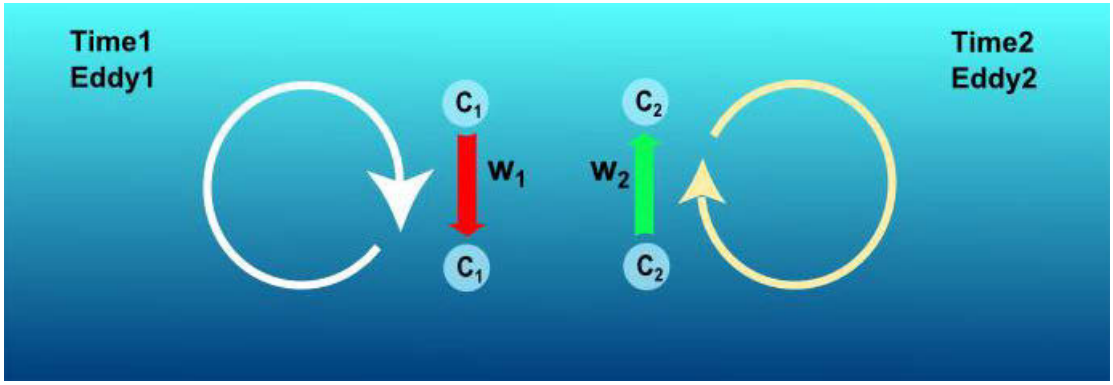

Figure 1.2**:** Diagrammatic representation of the eddy covariance method modified from Burba and Anderson (2010).

Physics of flux measurement in water

In aquatic ecosystems, total vertical diffusive flux (J) of a solute in the diffusive boundary layer and the internal boundary layer are described by the following equation:

$$J = -D\frac{\partial C}{\partial z} + wC \qquad \text{(Eqn. 1.1)}$$

where w is the vertical velocity, C is the solute concentration, and D is the molecular diffusivity of solute (Berner 1980; Boudreau 2001; Berg et al. 2003; Swett 2010). $\frac{\partial C}{\partial z}$ is the vertical gradient across the horizontal plain of the sensor.

Turbulent advection, under high flow, causes the dominant vertical transport in the water column above the DBL in most marine environments (Berg et al. 2003). For that reason, the diffusive term (Fick's first law) in Eqn. 2.1 can be neglected. Data analysis requires numerical methods to isolate the turbulent fluctuations in velocity and solute concentration from their means (Reynolds 1895; Staniši 1985; Boudreau and Paul 1997). With these assumptions, Eqn. 1.2 gives the following expression in the time domain for the vertical flux averaged over time (Berg et al. 2003; Kuwae et

al. 2006; Berg and Huettel 2008; Berg et al. 2009; McCann-Grosvenor 2010; Swett 2010; Hume et al. 2011):

$$\text{Flux} = \overline{w'C'} \qquad \text{(Eqn. 1.2)}$$

where $w'$and $C'$are turbulent velocity and gas concentration fluctuations respectively. By averaging this fluctuation product over a given time span, net turbulent fluxes can be obtained (Brand et al. 2008).

As described earlier, Hume et al. (2011) first used the EC method to measure NEM in seagrass beds. They also used the method to measure daily GPP and daily R (mmol m^{-2} d^{-1}) as described in the following equations:

$$\text{NEM} = \frac{1}{24}\left(\Sigma\text{Flux}_{\text{light}} + \Sigma\text{Flux}_{\text{dark}}\right) \qquad \text{(Eqn. 1.3)}$$

where $\text{Flux}_{\text{light}}$ is the flux where the photosynthesis active radiation (PAR) at water surface > 0.01 µmol photon m^{-2} s^{-1} and $\text{Flux}_{\text{dark}}$ is the flux where the PAR < 0.01 µmol photon m^{-2} s^{-1}.

$$\text{GPP} = \frac{1}{24}\left(\Sigma\text{Flux}_{\text{light}} + \frac{|\Sigma\text{Flux}_{\text{dark}}|}{h_{\text{dark}}} h_{\text{light}}\right) \qquad \text{(Eqn. 1.4)}$$

where h_{light} and h_{dark} are the amount of light and dark hours ($h_{\text{light}} + h_{\text{dark}} = 24$)

$$\text{R} = \frac{1}{24}\left(\Sigma\text{Flux}_{\text{dark}} + \frac{|\Sigma\text{Flux}_{\text{light}}|}{h_{\text{light}}} h_{\text{dark}}\right) \qquad \text{(Eqn. 1.5)}$$

If NEM < O, the system (i.e., sediment, seagrass beds or coral reefs) is consuming more O_2 than is being produced. In contrast, if NEM > 0, the system is producing more O_2 than is being consumed.

1.4.2 Eddy correlation system components

In aquatic EC systems, vertical velocity and oxygen concentration can be measured using an Acoustic Doppler Velocimeter (ADV; Nortek AS and SonTek/YSI) and an oxygen microsensor (electrode, e.g., Unisense, or optode, e.g., Pyroscience) (Berg et al. 2003; Berg et al. 2007; Berg and Huettel 2008; Berg et al. 2009; Chipman et al. 2012) as shown in Figure 1.3.

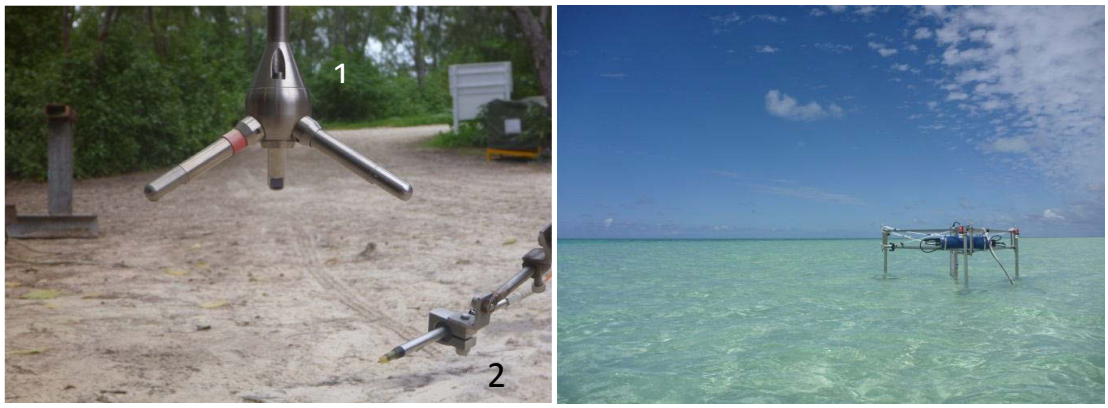

Figure 1.3: a) EC system components: ADV (a1) and oxygen optode (a2); b) EC system deployed on Heron Island.

1.5 ECOSYSTEM METABOLIC PROCESSES IN BENTHIC HABITATS AND IMPLICATIONS FOR THE APPLICATION OF EDDY CORRELATION METHODS

Several environmental parameters, such as light, temperature and water velocity, have an effect on benthic O_2 flux (Wieland and Kühl 2000; Mass et al. 2010). Light plays an important role in the photosynthesis and respiration of benthic photosynthetic organisms (Wieland and Kühl 2000). According to Arrhenius equation, increased temperature is known to enhance photosynthesis and respiration

in marine benthic autotrophs and O_2 consumption in sediment due to increasing microbial acitivity (Wieland and Kühl 2000). It is well known that increased water flow reduces diffusive boundary layer thickness and therefore enhances O_2 flux and photosynthesis in marine benthic autotrophs, such as corals, algae and seagrass (Mass et al. 2010). In permeable sea beds, water flow can increase the gas exchange process across the sediment-water interface (Berninger and Huettel 1997).

1.5.1 Sediment

Sediment O_2 consumption is a very important process in aquatic ecosystems and occurs during aerobic decomposition of organic matter, animal respiration and oxidation of reduced products of anaerobic decay including NH_4^+, Mn^{2+}, Fe^{2+}, H_2S, FeS and FeS_2 (Berg et al. 2003; Valdes-Lozano et al. 2006). Sediment O_2 consumption is important as an indicator of the decomposition rate of the sediment and the regeneration rates of nutrients from the sediment (remineralization or nutrient cycling) (Seiki et al. 1994; Valdes-Lozano et al. 2006) and provides useful information on these metabolic processes in the system (Berg et al. 2003). However, sediment O_2 consumption is difficult to measure accurately with methods available to date (e.g., *in situ* chambers) because it cannot simulate natural conditions. Sediment oxygen uptake is strongly influenced by the velocity of overlying water which transports O_2 from the overlying water down through the sediment (Berg et al. 2003). These transport processes are influenced by molecular diffusion, current- or wave-driven advection and faunal activities, for example, bioturbation (the diffusion-like transport of solutes and solids caused by movements of fauna) and bioirrigation (the transport of solutes caused by pumping activity of tube-dwelling animals) (Revsbech et al. 1980; Berg et al. 2003; Pischedda et al. 2008). Bioturbation and

bioirrigation increase sediment oxygen heterogeneity and diffusive oxygen flux due to the production of sediment-water interface available for solute exchanges between overlying water and sediments (Pischedda et al. 2008; Lagauzére et al. 2011). Water velocity determines the thickness of the oxygen boundary layer and also determines diffusive fluxes and concentration gradients of oxygen and nutrients (Cahoon 1988; Vogel 1994). Under low flow, oxygen gradients may be unstable, and oxygen transport will be more dependent on faunal activities (Revsbech et al. 1980). EC has been used to measure oxygen uptake in sediment because it does not affect active transport or the environmental conditions that influence O_2 uptake in the sediment (Berg et al. 2003). Recently, there have been many studies of O_2 consumption in sediment utilising an EC system (Berg et al. 2003; Kuwae et al. 2006; McGinnis et al. 2008; Berg and Huettel 2008; Brand et al. 2008; Berg et al. 2009; Lorrai et al. 2010; McCann-Grosvenor 2010; Johnson et al. 2011; Chipman et al. 2012; Reimers et al. 2012; Holtappels et al. 2013; Table 1.2).

1.5.2 Mangroves/saltmarsh

Barr et al. (2010) established the tower EC system method to estimate C flux in mangroves. Tower EC systems measure CO_2 concentration and vertical wind speed. These data are then converted into net ecosystem exchange (NEE); if NEE is positive the ecosystem is a source, if it is negative it is a carbon sink. It is common to use a model of NEE to fill gaps in the EC record; however, accurate nighttime ecosystem respiration (Re) and response to air temperature must be integrated. Finally, GPP = - NEE + Re and nighttime GPP = 0. For model development, tower EC systems would typically use metrological data with satellite and EC (GPP) data integrated in a vegetation photosynthesis model (VPM). MODIS-based index

(NDVI, EVI or greenness GV) is used to assess disturbance to mangrove distribution and then predict production (albedo = leaf area index (LAI)).

1.5.3 Seagrass

Due to slow O_2 diffusion in seawater (10000 times slower than in air) (Roberts et al. 2000), seagrasses may be at risk of oxygen deprivation (Borum et al. 2006). O_2 respiration supply in seagrass is derived from photosynthesis and the passive diffusion of oxygen from water column into sediment (for below ground tissue) (Borum et al. 2006). However, in the absence of photosynthetic oxygen evolution (e.g., in darkness), passive diffusion of oxygen must support both above and below ground biomass. Passive O_2 influx rate from water into leaves within boundary layer can be calculated by Fick's first law (Borum et al. 2006). The rate of passive O_2 influx is influenced by the gradient of oxygen, DBL and cuticle/cell wall thickness, and diffusion coefficients of O_2 in water and seagrasses (Binzer et al. 2005; Borum et al. 2006). However, DBL thickness depends on the flow regime (Koch 1994). If flow is reduced in darkness, then seagrass can be severely O_2 starved. When the O_2 concentration in seagrass tissue exceeds O_2 concentration in seawater, O_2 is lost to water column by passive diffusion through the DBL or formation of bubbles around the leaves (Borum et al. 2006).

Seagrass sediment characteristics are influenced by root O_2 loss, detritus accumulation and nutrient uptake (Connell et al. 1999). Under illuminated conditions, seagrasses deliver O_2 from leaves to roots for nutrient uptake and respiration and lose some of the O_2 to the surrounding sediment (Atwell et al. 1999; Connell et al. 1999; Schwarz et al. 2004) as shown in Figure 1.4. Generally,

sediments in estuaries or oceans have a low O_2 concentration (0 %) at ~1 cm below the seagrass sediment surface and can produce sulphide compounds by microbial degradation of organic materials, which are toxic to plants (Borum et al. 2006; Gruber and Kemp 2010). Photosynthesis and diffusion help increase O_2 concentration in the sediments and prevent toxicity (Gruber and Kemp 2010).

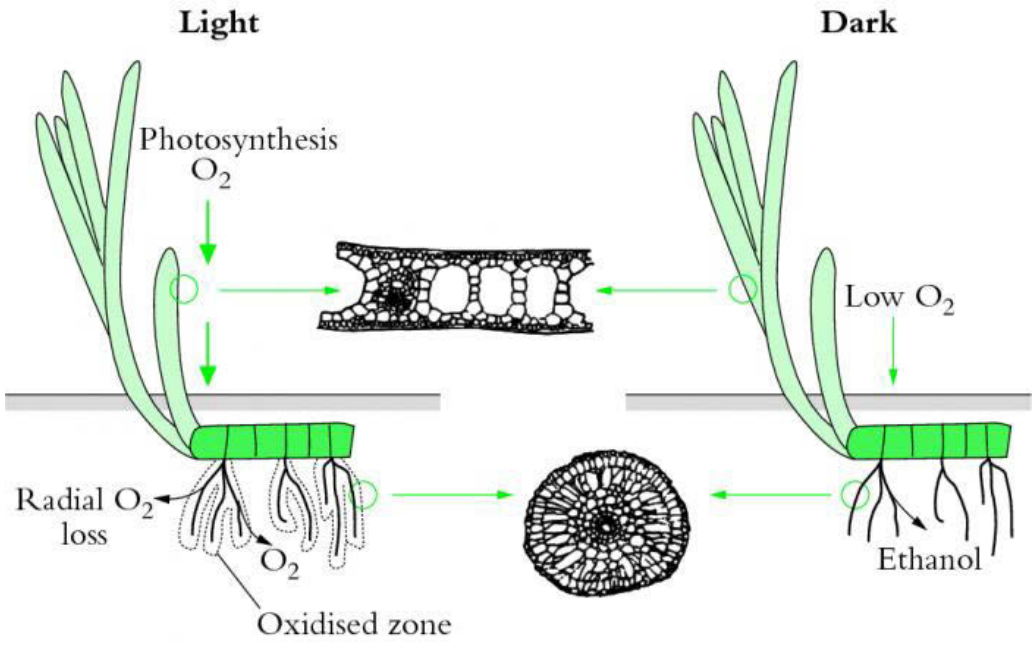

Figure 1.4**:** Under light conditions, O_2 is transported from leaves to roots and rhizomes but there is loss of O_2 into surrounding anoxic sediments. In darkness, O_2 transport ceases because the surrounding seawater is the only source of O_2 and there is an alcoholic fermentation in roots (Photos courtesy of W.C. Dennison) (Atwell et al. 1999).

Water motion affects the seagrass ecosystem in many ways, including photosynthesis (Koch 1994), gas exchange between leaves and the water column (Binzer et al. 2005), nutrient uptake and movement (Thomas et al. 2000; Cornelisen and Thomas 2002; Cornelisen and Thomas 2004), sediment transport (Paling et al.

2003) and grazer, epiphyte and seagrass biomass (Schanz et al. 2002). The thickness of the DBL and flux are influenced by water velocity and the roughness of the leaf surface (Koch 1994). Seagrass photosynthetic rates increase with cumulative flow due to higher carbon availability at the leaf blade surface, a result of a reduction in the DBL thickness (Koch 1994; Madsen et al. 2001; Sand-Jensen and Nielsen 2004). In addition, the presence of epiphytes and debris may cause a fluctuation in thickness of the DBL at higher current velocity and lead to enhanced carbon transport (Koch 1994; Sand-Jensen and Nielsen 2004; Binzer et al. 2005). Moreover, a previous study on *C. nodosa* revealed that internal oxygen increased with cumulative flow velocity reaching saturation of around 12.2 kPa (60% of air saturation) at flow velocities >7 cm s^{-1} (Binzer et al. 2005).

Water flow influences the DBL which in turn controls photosynthesis and therefore growth. Flow velocities have an effect on the internal oxygen status of seagrasses at mainstream velocities below 5 – 7 cm s^{-1} (Binzer et al. 2005). Photosynthesis and uptake of nutrients may be stimulated by increasing current flow velocities of up to 20 cm s^{-1} (Larned and Atkinson 1997), but most often saturation occurs at 2-6 cm s^{-1} (Koch 1994). Flow velocities may be much higher (50 – 150 cm s^{-1}) around and above seagrass beds (Fonseca et al. 1983; Fonseca and Kenworthy 1987; Wildish and Kristmanson 1997).

1.5.4 Microphytobenthos

Biogeochemical cycling in permeable sediments, typically colonized by benthic microalgae (and turf microalgae), is strongly affected by changes in flow (porewater flushing) and light. However, it is technically complex to measure

microphytobenthos habitat flux due to vertical migration and the shading effect on phototrophs. EC is still ideal for these environments (Berg and Huettel 2008; Hume et al. 2011; Berg et al. 2013) although no experimental EC work has been published to date.

1.5.5 Macroalgae

Macroalgae are very diverse and come in a variety of forms including crusts, foliose and filamentous thalli (a body of an alga) (Diaz-Pulido 2008). Macroalgae structures ranges from simple to complex forms with adaptations for light capture, reproduction, flotation and/or substrate attachment (Diaz-Pulido 2008). Macroalgal productivity is influenced by light, temperature, nutrient, salinity and hydrodynamism (Lobban and Harrison 1997). It has been suggested that plant density and canopy structure play important roles in macroalgal productivity due to self-shading (Binzer et al. 2006). *In situ* CO_2 and O_2 flux measurement of macroalgal NPP have been performed using incubation chambers (Plante-Cuny et al. 1998; Hubas et al. 2006; Miller et al. 2009; Tait and Schiel 2013) and continuous flow through chambers (Bottom 1981) that can measure photosynthesis and respiration. These incubation chambers may have limitations because they can only measure a small area of interest. Additionally, the chambers have an effect on the hydrodynamic regime which can in turn affect the DBL and therefore the nutrient uptake and physiology of macroalgae (Thomas and Cornelisen 2003). The depletion of nutrient or carbon dioxide and the accumulation of harmful metabolites may occur during the incubation and will affect productivity estimates (Smith et al. 2013). The EC system would be ideal for macroalgal productivity studies. However, there is no experimental EC work that exclusively studies macroalgae habitat published to date.

1.5.6 Coral reefs

Coral reefs form the most diverse ecosystems in the world, providing a wide diversity of marine organisms including coral, seagrass, macroalgae and microphytobenthos (Wilkinson 2002). Rates of reef metabolism are influenced by the variability of hydrodynamic and other marine organisms within the reef structure (Patterson et al. 1991; Atkinson et al. 1994; Lesser et al. 1994; Mass et al. 2010). The biodiversity of coral reefs is in part driven by heterogeneity in the structural complexity of the coral reef ecosystem (Harrison and Booth 2007). Extrapolation of observations in small areas or in a single organism is unlikely to represent the entirety of any reef system (Long et al. 2013). The reef structure not only impacts amounts of light received by phototrophs during the day, but also affects the direction of hydrodynamic movements - very important in gas flux measurements - due to the altering of the DBL thickness which in turn causes changes to the rate of metabolic gas exchange i.e., oxygen and carbon dioxide (Patterson et at al. 1991; Lesser et al. 1994; Mass et al. 2010).

Many studies of reef metabolism have used *in situ* techniques, i.e., chamber and microprofiling that can measure photosynthesis and respiration of a single species or a small area of interest, e.g., coral and benthic algae (Longstaff et al. 2002; Yates and Halley 2003; Levy et al. 2006; Gevaert et al. 2011; Wangpraseurt et al. 2012). These techniques nevertheless need either a controlled flow system or a unidirectional flow during measurement. Many studies use the *in situ* flow respiratory technique (Eulerian and Lagrangian approaches) for the analysis of coral reef metabolisms (McGinnis et al. 2011; Langdon et al. 2013); however, this technique requires a low energy reef with unidirectional current and shallow water. Due to these conditions,

the gas exchange rate across the air–sea interface, which is not easy to define accurately (Long et al. 2013), needs to be taken into account.

Long et al. (2013) used the EC method to assess photosynthesis and respiration of reef crest (RC) and reef slope (RS) habitats (Table 1.2). The percentage coverage of hard coral is approximately 3% for the RC sites and 1% for the RS sites. The results showed that gross primary production (GPP) was 4 times greater in the RC habitat, dominated by softcoral, than RS which is dominated by cement. The respiration (R) was 3 times greater in the RC than the RS. The net ecosystem metabolism (NEP) was 12 times greater in the RC than the RS. Hydrodynamics also have an effect on flux measurement in RC and RS habitats because changes in current direction affect the footprint represented by O_2 flux. Greater GPP, R and NEP in RC are attributed to the greater biomass of phototrophic soft corals and algae as well as their greater hydrodynamic energy.

1.5.7 Sponges

Sponges can be found across a range of marine ecosystems. They are very diverse and have a variety of growth forms and colour (Hooper et al. 2002). Sponges feed by filtering particles from water pumped through their body and obtaining nutrients from symbionts (Koopmans et al. 2010). This food is used for supplying nutrients for biomass and supplying energy when carbon is converted to CO_2 via aerobic metabolism (Hooper et al. 2002). It has been suggested that 10% of the oxygen available in water is taken up by sponges (Jørgensen et al. 1986; Hooper et al. 2002). Sponge respiratory rates and community metabolism have been measured using *in situ* O_2 chambers (Hopkinson et al. 1991; Hooper et al. 2002); however, these

chambers only measured a small, specific area. Glud et al. (2010) used EC to quantify benthic O_2 exchange across hard-bottom substrates (including sponges) (Table 1.2). However, there is no EC work that can quantify amount of flux from sponges directly into coral reefs.

1.6 CONCLUSION

Many methodologies and technologies are used to assess the primary production and net ecosystem metabolism of coastal habitats. Each method has both advantages and disadvantages that need to be taken into account. For example, microprofiling is a good method for measuring NPP and R at very small scales (e.g., leaf plants, coral tissues and sediment), however, it cannot be used to measure large areas. Chambers are also a good method for measuring fluxes in macroscale (e.g., macroalgae in very shallow water) and they are also very robust and easy to use. In contrast, EC is a powerful tool for measuring NEM (including GPP and Ra) over a very large area (coral reefs, seagrass beds) and it could potentially be used in extreme conditions (i.e., strong current, deep water). However, EC requires a great deal of care be taken with instrument setting and data processing. To date, the validation of the EC technique used either in the field and laboratory with other techniques (e.g., O_2 chamber, O_2 microprofiling) is only partially completed and there remain many habitats where EC is yet to be applied (Table 1.2). Therefore, the reliability and limitations of the eddy correlation system for O_2 flux measurement in aquatic environments have not been fully established.

Table 1.2: Summary of eddy correlation studies and deployment characteristics for measurement of benthic flux.

Author(s)	Flux analysis	Location	Water depth (m)	Measuring height (cm) above sediment	Bottom characteristic	Measurement Time (hour:min)	Averaging Window Method	Averaging Time Window (min:sec)	Sampling Frequency (Hz)	Validation Method	Average flux (mmol m^{-2} d^{-1})
Berg et al. 2003	O_2	River Wumme, Germany	1	15, 20, 40, 55	sandy sediment	0:10	moving average	2:28	25	-	-210 ± 1
		Aarhus Bay, Denmark	12	15	fine-grained marine mud	0:10		2:28	25	O_2 microprofiling, *in situ* chambers	-38
		Limfjorden Sound, Denmark	8	40	fine-grained marine mud	0:10		2:28	25	*in situ* chambers	-46
Kuwae et al. 2006	O_2	Banzu intertidal sand flat, Tokyo, Japan	0.37-0.65	7 - 17	well-sorted fine sand	0:12 – 0:40	block average	2:00	20	core-incubation	-311 ± 122
Crusius et al. 2008	Ground-water	Salt Pond Channel, Cape Cod, USA	0.6-0.8	5 - 15	estuarine sediment	3:30	running mean	15:00	16-64	seepage meters, ^{222}Rn tracer	16.9 ± 2.9 to 20.7 ± 2.9
McGinnis et al. 2008	O_2	Lake Wohlen, Switzerland	3	15	lake sediment	18:00	multiple methods	15:00 – 60:00	32	O_2 microprofiling	-40 ± 11
Berg and Huettel 2008	O_2 (anoxia)	Apalachicola Bay, Florida	1 – 1.5	12	sandy sediment	17:00	mean removal	15:00	16-64	*in situ* chambers	1138 (daytime) 368 ± 21 (nighttime)
Brand et al. 2008	O_2	Lake Alpnach, Switzerland	27	11	lake sediment	12:00	linear detrending	15:00	8	O_2 microprofiling	-13.9 ± 6.8 to 0.3 ± 0.1
Berg et al. 2009	O_2	Sagami Bay, Japan	1450	5 - 30	fine-grained marine mud	30:00	least square linear fit	13:30	64	O_2 microprofiling, *in situ* chambers	-1.62 ± 0.23
Glud et al. 2010	O_2	Southwest Greenland, Greenland	< 20	8 - 10	hard bottom	18:00 – 22:00	least square linear fit	15:00	32 to 16 (SNR)	O_2 microprofiling, *in situ* chambers	-0.4 to -19.6

Table 1.2 (continued): Summary of eddy correlation studies and deployment characteristics for measurement of benthic flux.

Author(s)	Flux analysis	Location	Water depth (m)	Measuring height (cm) above sediment	Bottom characteristic	Measurement Time (hour:min)	Averaging Window Method	Averaging Time Window (min:sec)	Sampling Frequency (Hz)	Validation Method	Average flux (mmol m^{-2} d^{-1})
Lorrai et al. 2010	O_2	Lake Wohlen, Switzerland	1	5 - 30	lake sediment	5:30	mean removal, linear detrending, and running averaging	14:00	64	two EC systems	-15.2 ± 3.1 (EC1) -14.6 ± 3.6 (EC2)
McCann-Grosvenor 2010	O_2	Yaquina Head, Newport, OR, USA	30	8-20	sandy sediment	1:30 – 23:30	mean removal, linear detrending, and running averaging	14:30 (plus 30 sec "Sleep")	64	*in situ* microprofiling	-6.2 to -30.7
Swett 2010	Dissolved Organic Carbon	Frankfort Flats, ME, USA	2.68	35	fine-grained marine mud	1:42	linear regression and moving average	10:00	8	porewater extraction (Laboratory)	-323.3 mg m^{-2} d^{-1}
		Squamscott River, NH, USA	1.44	25	fine-grained mud	N/A		10:00			-248.9 mg m^{-2} d^{-1}
		Piscaraqua River, ME, USA	1.87	30	mud flats	5:48		30:00 and 60:00			60.4 mg m^{-2} d^{-1}
		Burton Bug, ME, USA	0.60	12	N/A	8:00		-			-
Hume et al. 2011	O_2	South Bay, Virginia, USA	1-2	15	seagrass beds	18:00 – 22:00	least square fit	14:30 (plus 30 sec "Sleep")	64	*in situ* microprofiling	154.9 ± 29.3 (GPP)
											-136 ± 32.4 (R)
Johnson et al. 2011	Nitrate	Monterey Bay on the central California coast	95	35	sandy sediment	60:00	Linear detrending, least square fit	40	1.8	*In situ* chambers	-1.3 ± 0.6 (n=7)
McGinnis et al.2011	H_2S	Eastern Gotland Basin, Baltic Sea, Latvia	192	N/A	anoxic deepwater	nearly 24	linear detrending	15:00	64	*in situ* chambers	1.9 ± 1.2
Chipman et al. 2012	O_2	Wakulla River	0.3 to 4	14	sandy sediment	12:45 to 14:45	linear detrending	15:00	64	Two EC system (microelectrode)	195 ± 20 and 152 ± 61
		St. Joseph Bay, the Gulf coast of Florida	1	14	sandy sediment	13	linear detrending	15:00	64		–70 ± 28 to –12 ± 6

Table 1.2 (continued): Summary of eddy correlation studies and deployment characteristics for measurement of benthic flux.

Author(s)	Flux analysis	Location	Water depth (m)	Measuring height (cm) above sediment	Bottom characteristic	Measurement Time (hour:min)	Averaging Window Method	Averaging Time Window (min:sec)	Sampling Frequency (Hz)	Validation Method	Average flux (mmol m^{-2} d^{-1})
Long et al. 2012	O_2	small tributary fjord near Kapisigdlit, Greenland	40-45	22-26	sea ice	24:00	linear detrending	15:00	64	optode for O_2 correction	0.69 ± 0.02 (GPP) −2.13 (R) −1.45±0.02 (NPP)
Reimers et al. 2012	O_2	Oregon continental shelf, USA	~80	10-20	sandy sediment	11:00 – 15:00	detrending	15:00 (plus 15 min between burst)	64	chamber	3.2 to 9.8
Berg et al. 2013	O_2	Cape Cod, Massachusetts	2	10	sandy sediment inhabited by microalgae	24:00	running mean	14:00 (plus 1 min "Sleep")	64	chamber	-27 to 31
		Wakulla River, Florida, USA	3		mixture of sand inhabited by microalgae and grave	4:00 – 10:00					-360 to 137
Holtappels et al. 2013	O_2	Crimean shelf, Black Sea	135	20	fine grained mud	14:00	running mean	15:00	16	analytical model, microprofiling	-6 to -12
		Loch Etive, Scotland	55	12	mud and dense of the brittle star *Amphiura filliformis*	56:00		14:00	32	numerical model, chamber	-10.2 ± 11.1
Long et al. 2013	O_2	Florida Keys National Marine Sanctuary, USA	4.5	80	reef crest dominated by coral	> 24:00	linear detrending	15:00	64	optode for O_2 correction	378 ± 76
				60	reef slope dominated by cement						-6 ± 21

CHAPTER 2:

TECHNOLOGY DEVELOPMENT AND EVALUATION

2. TECHNOLOGY DEVELOPMENT AND EVALUATION

2.1 INTRODUCTION

Eddy correlation (EC) has been used for measuring solute flux in a variety of aquatic habitats (Table 2.2; Berg et al. 2003; Kuwae et al. 2006; Brand 2007; Berg and Huettel 2008; Crusius et al. 2008; McGinnis et al. 2008; Berg et al. 2009; Glud et al. 2010; Lorrai et al. 2010; McCann-Grosvenor 2010; Swett 2010; Hume et al. 2011; Long et al. 2013). However, these studies have mainly been conducted in the field and, therefore, they did not apply EC in a controlled environment (e.g., laboratory flume). These studies have only partially described the instrument setting, data analysis and calculation, and the environmental conditions in which the instruments were deployed.

This research has applied the EC system in order to estimate O_2 flux measurements in both a laboratory flume and in field experiments. During these experiments, a series of challenges become apparent. This chapter provides a detailed examination of method development and describes the validation investigations used in this thesis. Two O_2 conversion methods from the eddy correlation optode system (ECO), which led to O_2 flux measurements in sediment within the laboratory flume, were investigated. The O_2 flux results using these two methods were compared.

2.2 EDDY CORRELATION SYSTEM

EC is a complex tool used to directly measure the O_2 flux in marine environments at community scales. EC has been used in aquatic systems for over a decade (Berg et al. 2003). There are a number of commercial EC products advertised (Unisense A/S, Denmark and Rockland Scientific, Canada), but a commercial system is still under

development, as improvements need to be made to its reliability. This research is performed using a Unisense EC system. EC technology has significantly improved over past three years (i.e., during this thesis) as has the software that is used to analyse and calculate the flux.

2.2.1 Eddy correlation assumptions and requirements

EC consists of an Acoustic Doppler Velocimeter (ADV), used to measure three-dimensional velocity in fluids, and a fast sensor, used to measured O_2 concentration in the fluids. These raw data are stored in a datalogger before being exported for data conversion and O_2 flux calculation using proprietary software. Lorrai et al. (2010) described basic assumptions and requirements for measuring the vertical fluxes. Due to the fact that the EC technique used in aquatic system is still under development, this technique is mainly used in less complex environmental conditions. Ideal conditions for EC deployment are in steady conditions, which require (i) homogenous horizontal flow and (ii) small/gradual change in background O_2 concentration (Lorrai et al. 2010). Unfortunately, this less complex condition is hardly found in natural waters (McGinnis et al. 2008); therefore, the EC, in this research, was mainly used in laboratory flume (see Chapter 3).

EC also requires a fast response sensor which can capture the smallest and fastest eddies. Due to the range of short time scales of flux-contributing eddies, which is normally from 1 s (e.g. lowland streams, ocean) to 10 s (e.g. lakes, reservoirs) (Lorrai et al. 2010), EC measurememts require a sampling rate at least twice the highest frequency of the signal (Nyquist frequency = 2 Hz), and a sensor response time should be faster than 1 s (Lorrai et al. 2010). Furthermore, the measurement duration shoud be 5 – 10 times that of the eddy time scale, and thus the time window

would be approximately 15 min (Lorrai et al. 2010). In addition, the sampling volume shoud be small enough to determine the smallest eddies contributing to the fluxes, and the DO sensor tip should be close to but outside the velocity sampling volume to maximise the covariance between vertical velocity and O_2 concentration (Lorrai et al. 2010), while preventing interferences from the probe in the flux measurement.

For EC deployment, the frame, which the EC is mounted on, needs to rigid enough to prevent frame vibrations and the distance among feets are large enough to preventsinking into the substrate. In addition, the frame legs shound not disturb the natural hydrodynamics (Lorrai et al. 2010). However, the wake turbulence caused by tripod legs is hardly identified or remove, and thus needs to avoid as much as possible during measurement.

2.2.2 Instrumentation development

Since this thesis began in 2011, EC has been rapidly developed in order to make the system more robust and reliable. We have been working closely with the manufacturer of one EC system, Unisense A/S, Denmark. In order to improve the reliably and robustness of the EC system, Unisense A/S has developed four versions (generations) of the Eddy Correlation system over the past three years of this research, fast-response O_2 microelectrode were firstly used to produce two versions of Eddy Correlation microelectrode system (ECE1 and ECE2) that differed primarily on O_2 amplifiers and datalogger. In 2013, an optode recently developed by PyroScince GmbH (Germany), was used to measure the O_2 concentration in the Eddy Correlation optode systems (ECO1 and ECO2); however, these are still not commercially available. These four systems were used in this thesis to measure the

O_2 flux in laboratory flume and field studies (see Chapter 3 and 4) and are described in more detail below.

2.2.2.1 Eddy Correlation microelectrode system – First generation (ECE1)

The main components of the first generation of the ECE1 are a datalogger manufactured by Unisense A/S (Denmark), an Acoustic Doppler Velocimeter (ADV) manufactured by Nortek A/S (Norway), an Auto-zero amplifier (AZA), and a Clark-type O_2 microelectrode (Revsbech 1980) (Figure 2.1; Table 2.1). This system has a sampling velocity of 64 Hz in order to capture the fluctuations of velocity and O_2 in small and fast eddies (Berg and Huettel 2008; Crusius et al; 2008; Berg et al. 2009). As the O_2 signal produced by the O_2 microelcetrode is very small (picovolts: 10^{-12} V), the AZA is needed to amplify the signal from picovolts to millivolts, which the datalogger is able to capture. However, amplifying such a small signal generates noise in the raw signal. This type of noise can sometimes be eliminated using data processing software which will be explained later.

Noise was a major issue for the first generation of the EC (ECE1). Apart from the AZA noise, there was an electrical noise, which resulted in significant problems in laboratory experiments. In the laboratory, electrical noise generated by equipment (e.g., as power supply, incubator, and refrigerator) had a significant effect on the O_2 signal due to the fact that the microelectrode acted like an antenna and captured extraneous electrical noise around the laboratory. This kind of noise was not eliminated by software because this noise was random. To solve this issue, an electrical grounding was performed; however, it could not remove all electrical noise in the laboratory. In addition, the ECE1 was only able to be deployed for up to 18

hours, due to the internal memory of data logger and battery capacity. Thus, the system was not suitable for use in monitoring the diurnal cycle in benthic organisms.

In field experiments, the first generation of EC was deployed in seagrass beds to capture the O_2 flux in seagrass ecosystems (see Chapter 4). There was no electrical noise issue in field experiments; however, new issues were found. The EC deployments in the field were often unsuccessful due to the fact that the microelectrode (which had a 25 μm tip-size) was very fragile. It often broke before completing the deployment due to external factors (e.g., mobile animals, re-suspended sediments). To alleviate this issue, the project focused on laboratory experiments (see Chapter 3), instead of field studies. Firmware and software became important tools to eliminate both electronic noise issues from AZAs and other electrical noises in the laboratory. However, the firmware and software developments could not remove all of the noise. The firmware and software developments will be explained in the software development section.

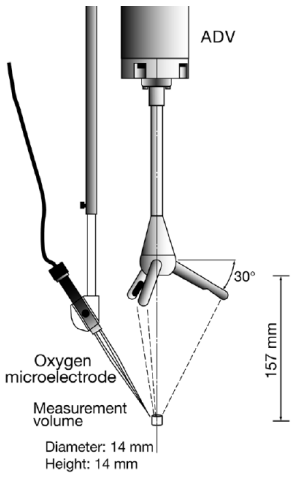

Figure 2.1: The components of the first generation of the EC (ECE1) (ADV: Acoustic Doppler Velocimeter; O_2 microelectrode) (image from Kuwae et al. (2006)).

Table 2.1: The characteristics of EC models from Unisense A/S, Denmark.

	EC model	Description	Type of O_2 sensor
1.	First generation of eddy correlation microelectrode system (ECE1)	- System components: ADV, AZAs, O_2 microlectrode and datalogger - System sampling frequency: 64 Hz	Microelectrode (Unisense A/S)
2.	Second generation of eddy correlation microelectrode system (ECE2)	- System components: ADV, O_2 amplifier (Unisense A/S), O_2 microlectrode and datalogger - System sampling frequency: 64 Hz	Microelectrode (Unisense A/S)
3.	First generation of eddy correlation optode system (ECO1)	- System components: ADV, O_2 amplifier (Unisense A/S), O_2 optode and datalogger - Optode sampling frequency: up to 16 Hz - Optode analogue output	Optode (PyroScience)
4.	Second generation of eddy correlation optode system (ECO2)	- System components: ADV, O_2 amplifier (Unisense A/S), O_2 optode and datalogger - Optode sampling frequency: up to 16 Hz - Optode digital output - Underwater optode housing with internal temperature sensor	Optode (PyroScience)

2.2.2.2 Eddy Correlation microelectrode system – Second generation (ECE2)

In mid-2012, after releasing the first generation of EC 5 years previously, Unisense A/S released the second generation EC (Figure 2.2; Table 2.1). This was due to the fact that there were a lot of technical issues that could not be eliminated by firmware and software, especially noise issues. The components of the second generation of EC were an ADV, a new EC datalogger, a new O_2 amplifier (Figure 2.2a), and a Clark-type microelectrode. The new EC datalogger had 8 GB data storage, four channels of analog inputs, and one channel of digital input which could be used to run another optode to monitor the background O_2. The new O_2 amplifier was a replacement of the AZAs. The manufacturer claimed that the new amplifier produced no noise in the O_2 signal amplification process (Unisense A/S, Denmark).

Figure 2.2: The second generation of the EC: a) A new O_2 amplifier.

Unfortunately, electrical noise remained a major issue in the laboratory due to the fact that the same microelctrode had been previously used in the laboratory

experiments. Although many firmware updates were released in order to remove this issue, the noise remained (Figure 2.3). The outcome from the second generation of EC was a modest improvement, due to improvement in the hardware. However, a great many things needed to be fixed in order to generate publishable results (e.g., a robust microelectrode and a noise-free system).

Figure 2.3: Two examples of electrical noise randomly appearing in the O_2 raw signal measured by ECE during laboratory experiments.

The second generation of the EC was deployed in a seagrass meadow, as well as mud flats in Moreton Bay, Queensland (see Chapter 4). However, the microelectrode kept breaking during deployments, mostly due to jellyfish. The broken microelectrode led to no results from these field experiments where the probe started to break since the start of deployment as shown by the O_2 concentration signal at

2000 µM and were completely broken at 6 pm where the O2 concentration signal reached 15000 µM (Figure 2.4).

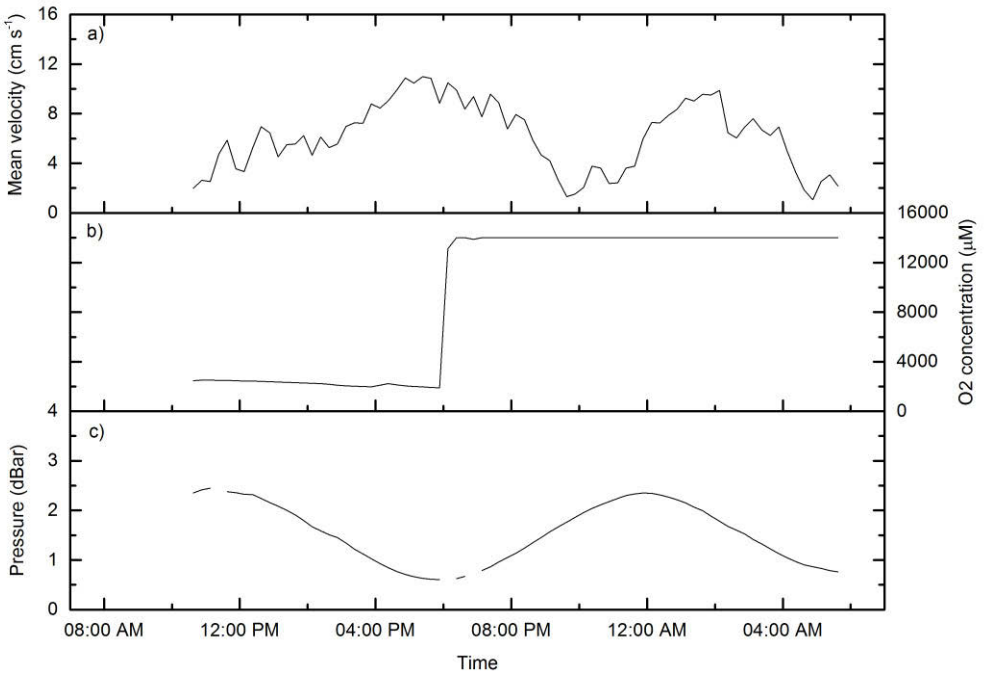

Figure 2.4: EC raw data: a) Mean velocity; b) O_2 concentration; c) Pressure.

2.2.2.3 Eddy Correlation optode system – First generation (ECO1)

In the second quarter of 2013, PyroSciece introduced FireSting OEM (PyroScience GmbH, Germany), which is a fast optode amplifier with digital and analog outputs for the O_2 signal. The ECO1 was able to read the O_2 signal from the analog output only allowing the Eddy Correlation system to use this fast micro-optode (Figure 2.5b; Table 2.1) to measure O_2 concentration, instead of using a microelectrode. The advantages of the optode over the microelectrode were low noise and a more robust construction, but the trade-offs were slower response time as the optode response time (t_{90}<0.5s) was slightly lower than the microelectrode response time (t_{90}<0.3s). Moreover, the maximum sampling rate of the optode was only up to 20 Hz, due to

the clockspeed of A/D converter, whereas the maximum sampling rate of the microelectrode system was up to 64 Hz. In order to capture fast and small eddies, high sampling frequency (64 Hz) should be applied. In addition, the microelectrode has potential artifacts including stirring sensitivity which creates an artificial flux (Holtappels et al. 2015). Although the optode had several disadvantages, it had great potential in providing a new component for use in EC O_2 flux measurements.

a) b)

Figure 2.5: a) A custom-made splash-proof housing for FireSting; b) A fast optode.

During laboratory experiments, there was no electrical noise in the O_2 signal measured by the optode system. However, the maximum sampling rate of the optode became an issue, due to an unstable sampling rate, and the fact that increasing the sampling frequency led to increased noise in the O_2 signal (Figure 2.6). Therefore, unstable A/D conversion resulting from noises had an effect on the EC data logger. A lot of firmware updates were released to try to solve this issue; however, it still remained. Although temperature correction needed to be post-processed for the optode O_2 signal, as the optode signal was temperature dependent, FireSting software did not allow the FireSting OEM to measure the temperature during high sampling rates (>10 Hz) when the fast sampling rate was enabled. Therefore, O_2

concentration might not be accurate when the optode was used in water with rapidly fluctuating temperature because a one degree temperature change would cause an error of about 1% (pers. comm. PyroScience GmbH).

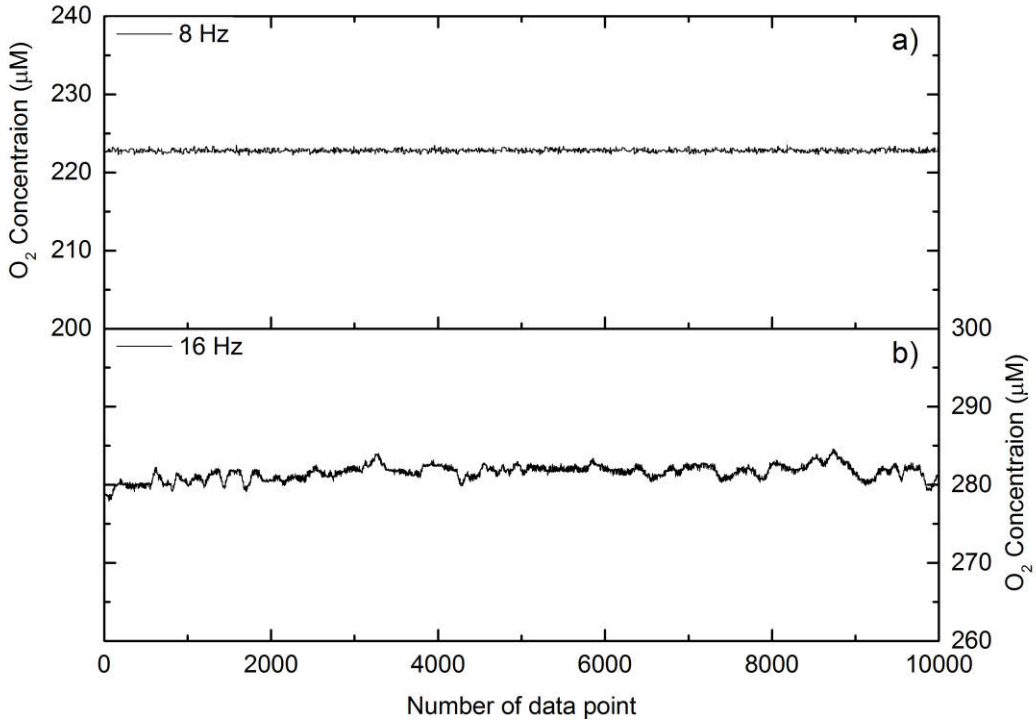

Figure 2.6: O_2 concentration sampled at a) 8 Hz and b) 16 Hz using the optode. The greater noise was found at 16Hz.

For field experiments, since there was no waterproof housing available for the FireSting OEM and its fiber needed to be used underwater; we made a custom splash-proof housing (Figure 2.5a) in order to deploy the ECO1 in seagrass beds and reef habitats including benthic microalgae habitats. Due to the limitations of the splash-proof housing and instrument cable length, the ECO1 was unable to be deployed in water that was deeper than three meters. Although impedance watching and cable shielding has been used in the system, a longer cable could be manufactured, but it would easily pick up noise in the field (pers. comm. with

Unisense A/S). The results in both laboratory and field experiments were better than the previous system even though there were some remaining issues.

2.2.2.4 Eddy Correlation optode system – Second generation

In early 2014, a prototype of an underwater optode system (Unisense A/S) was developed in order to deploy the EC in deep water. This generation came with an internal temperature sensor attached to the underwater optode housing which allowed temperature correction every 15 minutes for O_2 signal (Table 2.1). It also used the EC digital channel input connected to the underwater optode system to improve the sampling speed and signal reliability of O_2 measurements. However, the stability of sampling rate was still an issue.

In the laboratory, sampling rates was reduced from 20 Hz to 16 Hz, 14 Hz, 12 Hz, and 8 Hz in order to improve the stability and reliability of the O_2 signal. A number of firmware upgrades were released in order to solve these issues. Unfortunately, there was no way to solve the stability and reliability of the O_2 signal by using firmware due to communication (hardware) issues between the underwater optode system and the EC datalogger. Therefore, a reduction in the sampling rate and the firmware updates only led to a minor improvement in stability and reliability of the optode signal. The fast and reliable A/D converter can be used to obtain higher sampling rate; however, this could not be used in this EC system due to its cost.

In order to improve the stability and reliability of the O_2 signal, a new O_2 conversion method was developed for the ECO in order to convert the raw O_2 signal to O_2 concentration. Previously, the O_2 concentration was converted from the phase-shifted signal, because the photo bleaching of the optode tip did not alter the phase-

shifted signal. The new method used the O_2 intensity signal instead of the phase-shifted signal as the raw O_2 signal even though photo bleaching of indicator dyes (Klimant et al. 1995) might alter the O_2 intensity signal during long deployments. To solve this, the O_2 intensity signal was calibrated with the phase-shifted signal. To get robust measurements, the phase of both O_2 intensity and phase-shifted signals needed to be in phase for the entire deployment. Unfortunately, the phase of the phase-shifted signal and the intensity signal were not in phase in some parts of each deployment because communication issues between the underwater optode system and the EC datalogger still existed (Figure 2.7).

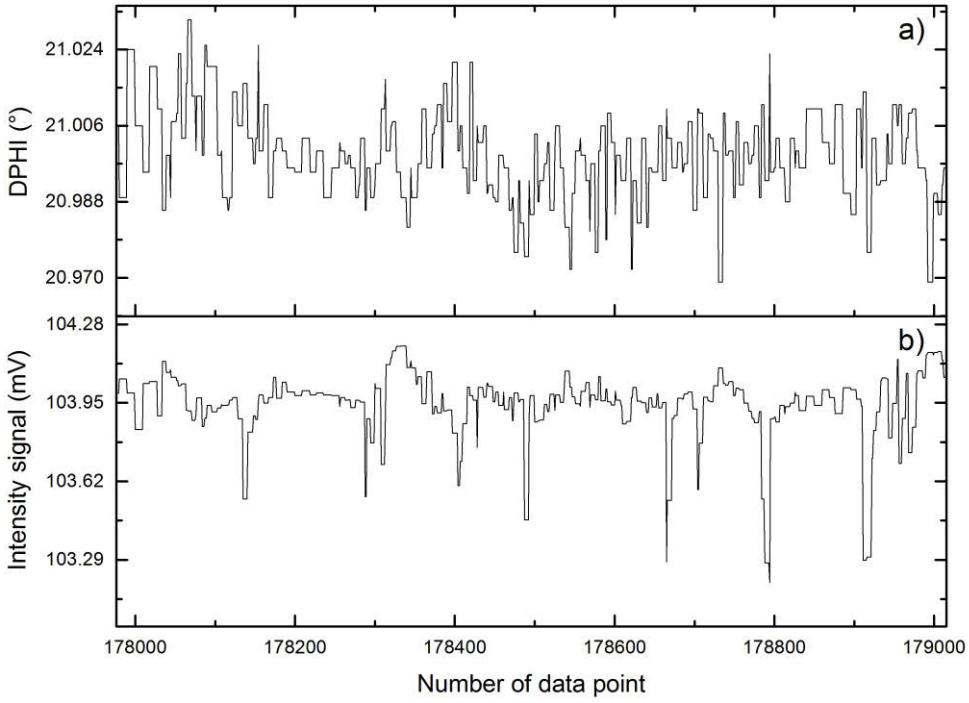

Figure 2.7: DPHI and intensity signal from ECO2.

After evaluating the new O_2 conversion method under laboratory conditions (see Section 2.5), the results showed that there was an improvement of signal stability and reliability compared to the phase-shifted method (see Section 2.5). The software

that was used for O_2 conversion will be explained further on in the software development section.

2.2.3 Software development

Software and firmware improvements are an important part of Eddy Correlation system development. The development of firmware (e.g. tweak clockspeed) is mainly used for solving some issues caused by the EC hardware itself, as well as the communication between the EC datalogger and other hardware devices, such as the underwater optode system. Although firmware is very important in keeping the system running smoothly, software plays a critical role in data conversion, data processing and data analysis. The data conversion software is used for converting raw data, normally the electrical voltage of the sensor, into a readable data format. For example, the unit of the raw O_2 signal was millivolt (mV), and the unit of the O_2 data after conversion was micromolar (μM). The data conversion software was developed by Unisense A/S in order to generate readable calibrated data.

The O_2 flux software is very important because the Eddy Correlation technique is mathematically complex and lot of care needs to be taken in order to process and calculate the flux. Prior to calculating to the O_2 flux, the raw data needs to be pre-processed to remove artifacts. For example, the despike method will be performed if there was a spike in the velocity data (Goring and Nikora 2002) or coordinate rotation is performed if the EC system is not aligned to natural hydrodynamics (mean vertical velocity = 0) (Lee et al. 2004). Time-lag correction will also be performed if there is a time lag between the velocity and O_2 signals (Lorrai et al. 2010) in order to obtain the best correlation of velocity and O_2 signal. According to Kolmogorov's theory of turbulence, the vertical velocity spectra can be used to

indicate well-developed turbulence and represent the inertial subrange where inertial forces dominate transport (Long et al. 2012).

2.2.3.1 Eddy Correlation firmware

Firmware is a software program or set of instructions programmed into an EC hardware device, such as an EC datalogger. It provides the necessary instructions for how the EC datalogger communicates with other EC hardware, such as ADV, AZAs, FireSting and computer. Firmware is typically stored in the flash ROM of a hardware device. While ROM is "read-only memory", flash ROM can be erased and rewritten because it is actually a type of flash memory.

The Firmware was developed and released by Unisense A/S as requested in order to fix the issues that have been most commonly found during this research project. The issues that needed new firmware updates are as follows:

- Communication

  There were communication problems between the EC datalogger and the ADV, as well as the FireSting OEM. For example, the EC datalogger could not receive the acknowledge signal from the ADV resulting in loss of ADV data during an experiment. In addition, the communication issues caused data pulling and data transfer problems. For instance, the EC datalogger was not able to transfer the EC data stored in the EC datalogger to the computer correctly, which led to issues with flux calculation. Furthermore, the datalogger was not able to receive all instantaneous data from the microsensor and microoptode.

- Signal reliability and stability

  There were signal reliability and stability issues caused by the hardware. These issues, which were caused by noise and signal interferences, were often solved by a firmware update. The new firmware was able to remove some noise and interference using low-pass or high-pass filters. Some noise and interference, however, were not removable from the raw signal because these noises occurred randomly in the signal.

- Time synchronization

  There was a time synchronization issue between the EC datalogger and FireSting OEM. The EC should be able to pull the data from the FireSting at 16Hz constantly. After examination of these data, we found that the EC datalogger did not receive the FireSting data at exactly 16 Hz resulting in loss of data at 0.1% to 5%. Therefore, the raw data needed to be examined before calculating the flux. Unfortunately, this issue still exists. Unisense A/S claimed that is not from the EC datalogger, but from the FireSting OEM. Therefore, it is still under investigation by Unisense A/S and PyroScience GmbH.

Some of the issues described above were mostly fixed by firmware updates; however, firmware upgrade was not likely to overcome fundamental engineering issues associated with noise pick-up, stability of the A/D conversion and sampling rate as well as external electromotive force. Therefore, the flux O_2 calculation needed to be done manually.

2.2.3.2 Flux calculation and analysis software

Data processing software was crucial to the use of the Eddy Correlation technique. The software needed to be able to handle a lot of data. For example, the EC provided at least 20 million data points from a one-day deployment. The software also needed to perform complex processing of EC data, such as coordinate rotation and time lag correction. Processing flux data was a multi-stage process.

- *Stage I: MATLAB*

  When this research project began, there was no software to calculate the flux and analyse the data. MATLAB was used in this thesis as a tool to handle all of the EC data. Suitable coding in the MATLAB environment has also been used for flux calculation. At this early stage, the software could handle all of the EC data, and perform a simple flux calculation (Figure 2.8).

```
47    %% Remove outliners of vertical velocity using Despike function
48    % Remove outliners of w using Despike function (func_despike_phasespace3d.m
49 -  save data; clear all; load data;
50 -  [w_despike] = func_despike_phasespace3d(w, 0, 2);
51 -  save data; clear all; load data;
52
53    %% Block average
54    % input blocking time
55 -  tblock = inputdlg('Block time (min)','Block Average');
56 -  tblock = str2double(tblock)*60*64;
57
58    %% Calculate w' and C' and O2 flux
59 -  h = waitbar(0,'Flux calculation in progress');
60
61 -  for count = 2:floor(end_data/tblock)                    %number of block
62 -      waitbar(count/floor(end_data/tblock));
63 -      index1 = start_data+(count-1)*tblock:start_data+count*tblock;
64          %mean removal
65          %w_mean(count) = mean(w(index1,1));               %mean w in each bl
66          %C_mean(count) = mean(C(index1,1));               %mean C in each bl
67
68          %linear detrending
69          %w_mean(count) = w(index1,1)-detrend(w(index1,1)    %mean w in each bl
70          %C_mean(count) = w(index1,1)-detrend(C(index1,1)    %mean w in each bl
71
72          %running mean
73 -        for ii=1:length(index1)                          %running 148 second
74 -            w_mean(ii) = mean(w(index1(1)+ii-64*74:index1(1)+ii+64*74));
75 -            C_mean(ii) = mean(C(index1(1)+ii-64*74:index1(1)+ii+64*74));
76 -        end
77
78 -      w_prime(index1) = w(index1,1)-w_mean';             %time series of w'
79 -      C_prime(index1) = C(index1,1)-C_mean';             %time series of C'
80 -      flux(index1) = w_prime(index1)'.*C_prime(index1)'; %time series of flu
81 -      flux1(count) = mean(flux(index1));                 %mean flux in each
82 -      tdata1(count) = mean(tdata(index1,1));             %mean time in each
83 -  end
84
85 -  close(h);
86
```

Figure 2.8: MATLAB script for flux calculation using a running mean.

- *Stage II: EddyFlux and complex data processing using MATLAB*

  The second generation of EC came with *EddyFlux* which was the EC data processing software which can perform complex processing, such as coordinate rotation and signal time lag correction. A 2D coordinate rotation was performed to force the mean vertical velocity ($\overline{w}$) to zero. This process was necessary to avoid instrument misalignment, especially the ADV to the streamline (Foken 2008). The time lag correction using cross-correlation between the fluctuation of vertical velocity (w') and O_2 (C') concentration was performed to eliminate time gaps between vertical velocity data and O_2 concentration data (Lorrai et al. 2010; Berg et al. 2013). Performing these corrections allowed us to obtain an accurate O_2 flux. This software is based on Berg et al (2003)'s software, and subsequently developed by Unisense A/S. However, this software lacked some functionality, such as data plotting. Therefore, the software based on the MATLAB environment has been developed to do the complex data processing, in the same way as the EddyFlux program (Unisense A/S, Denmark). The MATLAB scripts for coordinate rotation and time lag correction are shown in Figure 2.9 and Figure 2.10. Table 2.2 shows the flux calculation procedure.

Table 2.2: Procedure of Eddy correlation flux calculation.

	Processing step	Description	Reference
1.	Despiking flow velocity signals	Removing noise in the velocity signals	Goring and Nikora 2002
2.	Tilt correction	Aligning the ADV to the current streamline	Folken 2008
3.	Calculating fluctuation of w and c	Mean removal, linear detrending and running average: take average off raw data to extract *w'* and *c'*	Berg et al. 2003; Kuwae et al. 2006
4.	Time lag correction	Removing time delay between *w'* and *c'*	Lorrai et al 2010; Berg et al. 2013
5.	Calculating spectra and cospectra	Examining flow velocity and the frequency of eddies contributed to vertical turbulence O_2 transport	Long et al. 2012
6.	Flux calculation	Calculating $\overline{Flux} = \overline{w'c'}$	Berg et al 2003; Kuwae et al. 2006

```
%coord_rot.m:  Computes coordinate rotation of two given data vector and
%              return the new vector
%              u,v,w = 1-D data vectors of measurment
%
%              usage: [u2, v2, w2]=coord_rot(u,v,w)
%              Reference: Folken T. 2008 p109 - 110

function [u2, v2, w2]=coord_rot(u,v,w)

% Rotation of coordinate system around z-axis
    theta = atan(mean(v)/mean(u));

    u1 = u*cos(theta) + v*sin(theta);
    v1 = -u*sin(theta) + v*cos(theta);
    w1 = w;

 % Rotation of coordinate system around the new y-axis
    phi = atan(mean(w1)/mean(u1));

    u2 = u1*cos(phi) + w1*sin(phi);
    v2 = v1;
    w2 = -u1*sin(phi) + w1*cos(phi);

 end
```

```
function [u2, v2, w2]=jc_co_rot(u1,v1,w1)

eta = atan(mean(v1)/mean(u1));
theta = atan(mean(w1)/sqrt(mean(u1)^2+mean(v1)^2));

% rotate x,y plane around Z-axis

Z_eta = [cos(eta) sin(eta) 0; -sin(eta) cos(eta) 0; 0 0 1];

% rotate x,z plane around Y-axis

Y_theta = [cos(theta) 0 sin(theta); 0 1 0; -sin(theta) 0 cos(theta)];


%new u,v,w

vel_comp = Y_theta * Z_eta * [u1; v1; w1]';

u2 = vel_comp(1,1);
v2 = vel_comp(2,1);
w2 = vel_comp(3,1);

end
```

Figure 2.9: MATLAB scripts for 2D coordinate rotation.

```
function [w_prime_al,C_prime_al] = tlag(w_prime,C_prime,Fs)
%Time lag function using cross correlation

%The cross-correlation of the two measurements is maximum at a lag equal to the delay.
%Plot the cross-correlation. Express the delay as a number of samples and in seconds.

t1 = (0:length(w_prime)-1)/Fs;
t2 = (0:length(C_prime)-1)/Fs;

[acor,lag] = xcorr(C',w');

[~,I] = max(abs(acor));
lagDiff = lag(I);
timeDiff = lagDiff/Fs;

figure;
plot(lag,acor);
a3 = gca;
a3.XTick = sort([-10:1:10 lagDiff]);


%Align the two signals and replot them.

C_prime_al = C_prime(+lagDiff:end);
t2_al = (0:length(C_prime_al)-1)/Fs;
w_prime_al = w_prime;

subplot(2,1,1);
plot(t1,w_prime);
title('w_prime');

subplot(2,1,2);
plot(t2_al,C_prime_al);
title('C_prime, aligned');
xlabel('Time (s)');

```

Figure 2.10: MATLAB script for time lag correction.

- *Stage III: Software development for the integration of the EC with the analog optode system (ECO1)*

  Software based on MATLAB was slightly modified in order to pull the optode O_2 data into the MATLAB environment. At this stage, MATLAB could process and display the data and results of the microelectrode and the optode system at the same time. However, the ECO1 was not able to gather both microelectrode data and optode data at the same time, due to signal interference (Figure 2.11). This issue is still under investigation.

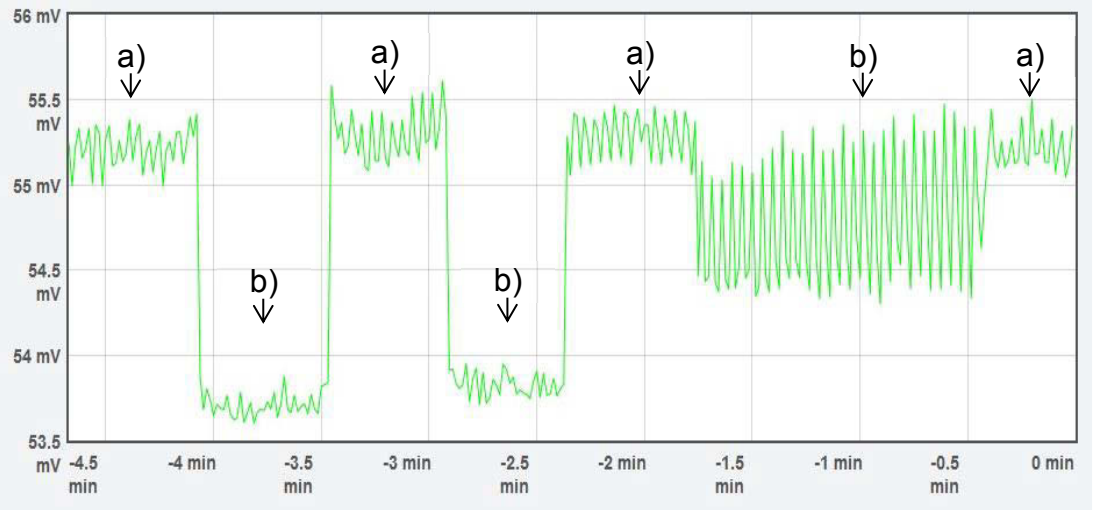

Figure 2.11: Optode signal: a) Optode connected to EC; b) Optode and microelectrode connected to EC.

- *Stage IV: Software development for the integration of the EC with digital optode system (ECO2)*

  The underwater optode system was connected to the digital channel input (serial communication port) allowing better sampling speed and signal reliability. However, there was no commercial EC software that could process the data from the EC integrated with a digital optode. Therefore, software based on MATLAB had to be developed for importing the data from the underwater optode, such as the O_2 concentration, O_2 phase-shifted signal (DPHI), O_2 intensity signal, ambient light signal and temperature signal. Only then could the software process the EC data and calculate the O_2 flux. At this stage, the spectra and co-spectra analysis functions were written (Figure 2.12) and added to the software for frequency response analysis of velocity and O_2 data. The frequency response information gave a better understanding of the hydrodynamic characteristics and instrumentation response associated with

the flux. Figure 2.13 shows that turbulence was well-developed with mean flow velocity > 10 cm s^{-1}.

```
%spec_FFT.m :     Computes the power spectrum of a 1-D data vector.
%
%        a       = 1-D data vector (must be integer power of 2)
%        wn      = Window size (e.g. 1024)
%
%        usage: y=spec_FFT(a,wn);

function [E]=spec_FFT(a,wn)

%wn=size of window;
ntemp=length(a);
n=ntemp(1);
numw=n/wn; %number of windows in file
t=[1:wn];
%create sin^2 window for tapering first and last 10% of each window
N=wn;
N1=round(0*N);
N2=round(1*N);
t1=[1:N1];
t2=[N1+1:N2];
t3=[N2+1:N];
W=zeros(1,N);
W(1:N1)=(sin(5*pi*t1./N)).^2;
W(N1+1:N2)=1;
W(N2+1:N)=(sin(5*pi*t3./N)).^2;
i=1;
E=zeros(wn/2,1);
while i <= numw
%grab a window of data
   first=(i-1)*wn+1;
   last=i*wn;
   awin=a(first:last);
%fit straight line to data
   p=polyfit(t,awin',1);
   y=polyval(p,t);
%detrend
   awin=awin-y';
%taper edges
   awin=awin.*W';
%Take FFT
   f=fft(awin,wn)./wn;
   Ew=conj(f).*f;
   Ew2=Ew(2:wn/2+1);
   E=E+Ew2;
   i=i+1;
end
```

a)

```
%xspec_FFT.m:  Computes the 1-D Fourier cospectrum spectrum,
%              quadrature spectrum, and squared coherence
%              of two given data vectors a, b.
%
%              a,b = 1-D data vectors (size must be integer power of 2)
%              wn = Window size (e.g. 1024)
%              usage: z= xspec_FFT(a,wn)

function [co, q, coh]=xspec_FFT(a,b,wn)

%wn=size of window;
ntemp=size(a);
n=ntemp(1);
numw=n/wn; %number of windows in file
t=[1:wn];
%create sin^2 window for tapering first and last 10% of each window
N=wn;
N1=round(.1*N);
N2=round(.9*N);
t1=[1:N1];
t2=[N1+1:N2];
t3=[N2+1:N];
W=zeros(1,N);
W(1:N1)=(sin(5*pi*t1./N)).^2;
W(N1+1:N2)=1;
W(N2+1:N)=(sin(5*pi*t3./N)).^2;
i=1;
%zero out arrays that will sum the spectra by window
co=zeros(wn/2,1);
q=zeros(wn/2,1);
coh=zeros(wn/2,1);
cross=zeros(wn/2,1);
Easave=zeros(wn/2,1);
Ebsave=zeros(wn/2,1);

while i <= numw;
%grab a window of data
   first=(i-1)*wn+1;
   last=i*wn;
   awin=a(first:last);
   bwin=b(first:last);

%fit straight line to data
   pa=polyfit(t,awin',1);
   ya=polyval(pa,t);
   pb=polyfit(t,bwin',1);
```

b)

Figure 2.12: MATLAB scripts: a) Spectra; b) Co-spectra.

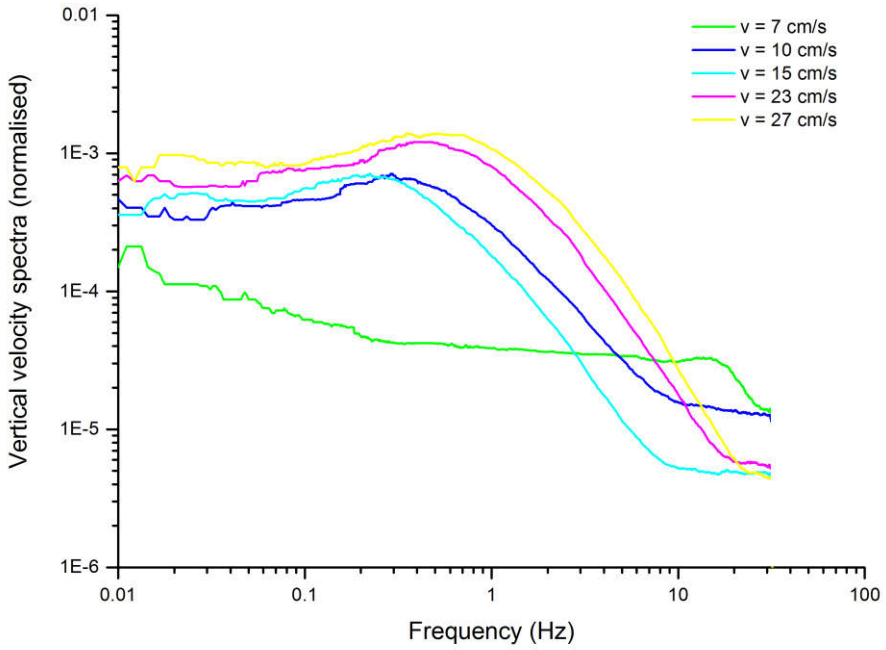

Figure 2.13: Spectra of vertical velocity in the laboratory flume under four different mean horizontal velocities.

- *Stage V: new method to conduct O_2 conversion based on O_2 intensity signal*

  During the sediment-uptake experiment, a new method for EC O_2 conversion had to be developed (see 2.5). Based on this method, the O_2 concentration was converted from an intensity signal. The results showed that the O_2 concentration had less noise compared to the previous O_2 conversion method. As there was no commercial EC software that could do this convertion, code was written into MATLAB to process this conversion. At the early stages, a simple O_2 conversion based on the intensity signal was performed (see Section 2.5). The initial results were promising, e.g., cross-correlations (time lag correction) looked good and were much better with in the new O_2 conversion (Figure 2.14). This method is still under development in order to

perform the complex O_2 flux calculation using the derivative of the slope for the scaling dDPHI/dIntens over short periods (see Section 2.5).

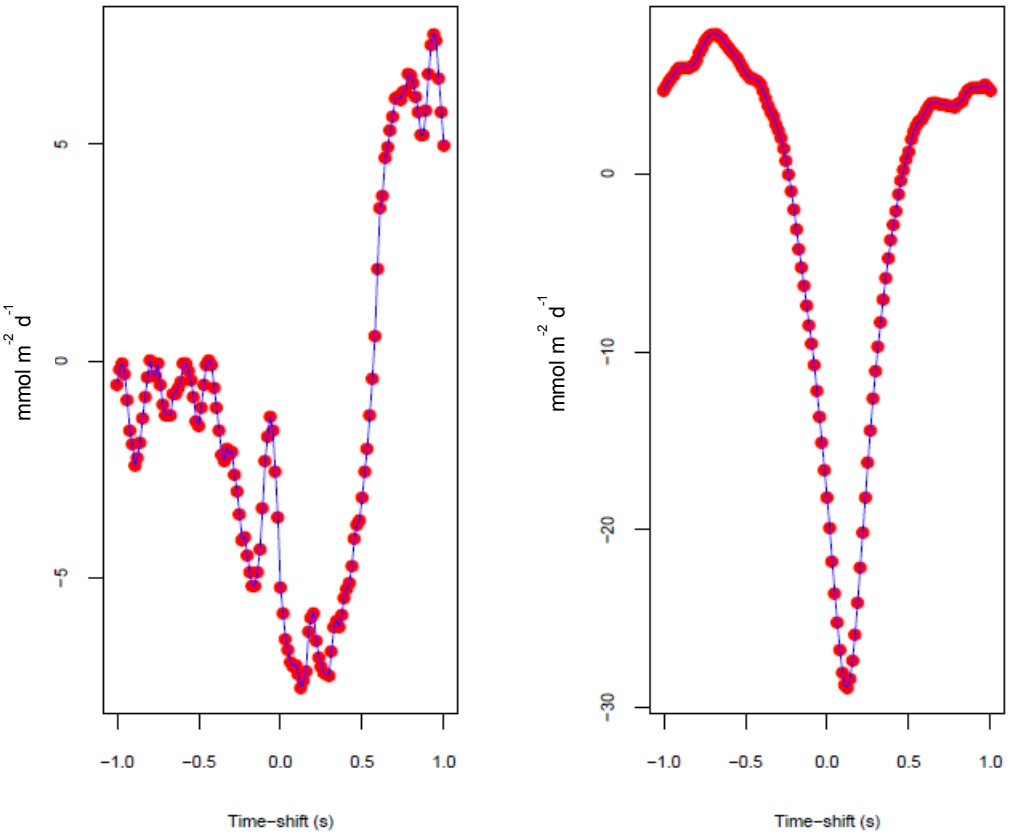

a) b)

Figure 2.14: Time lag between vertical velocity and O_2 concentration: a) Phase-shifted O_2 conversion; b) Intensity O_2 conversion.

2.3 LABORATORY EXPERIMENTAL SET-UP

EC was mainly used in a laboratory racetrack flume (Figure 2.15) in order to investigate the O_2 flux associated with mud and seagrasses. EC was deployed into the flume (Figure 2.16a). The experiments started with a simple system (seawater only), a moderately complex system (seawater and mud) and finally a complex system (seawater and seagrass bed; Figure 2.16b). In the O_2 uptake experiments (see

Chapter 4), the EC measuring height was 5 cm above the 90 cm x 40 cm of mud which was the working area in the flume (Figure 2.15). The thickness of mud was 5 cm. In this experiment, the physical conditions in the flume (e.g., flow velocity and temperature) were adjusted. In the O_2 production experiments (see Chapter 3), the EC was deployed 5 cm above the seagrass canopy. The same working area was used for the seagrass bed. The seagrass bed was treated under different physical conditions, such as altered light and temperature.

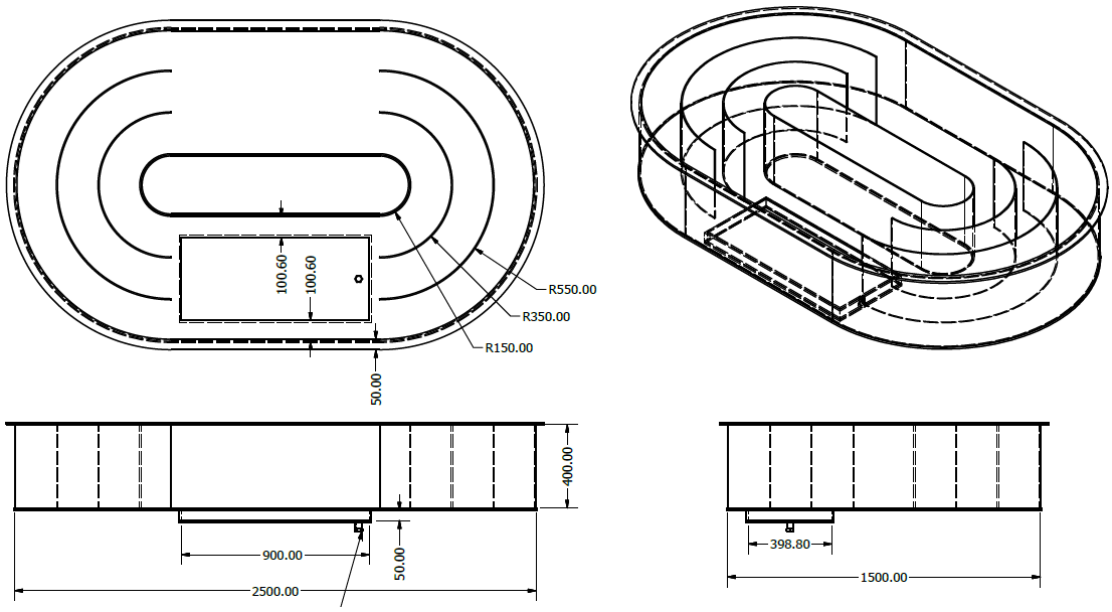

Figure 2.15: Laboratory racetrack flume. Numbers on the figure indicates size (mm).

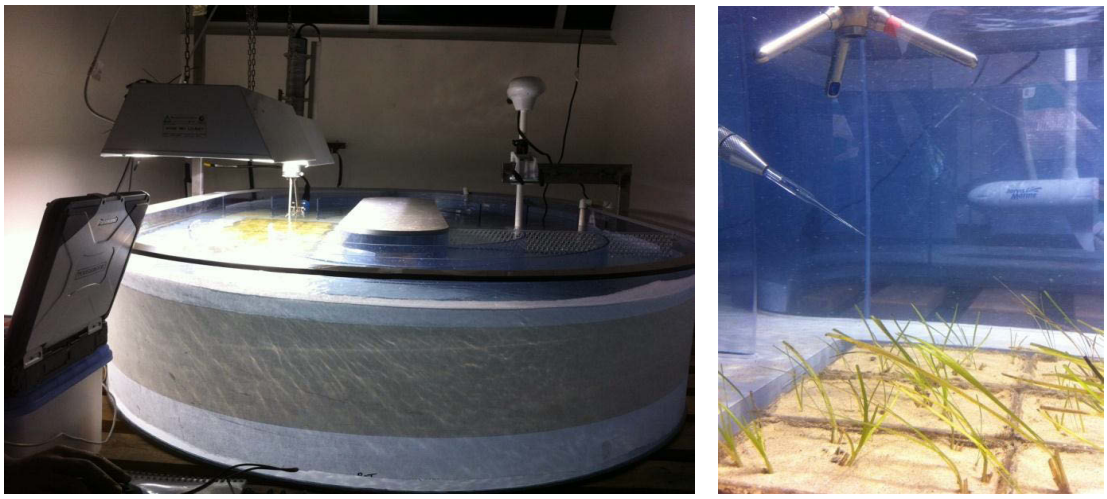

a) b)

Figure 2.16: a) The EC set-up in the laboratory racetrack flume; b) The ECE1 deployed in laboratory seagrass bed.

This research was the first attempt to use the Eddy correlation system in a laboratory flume. Due to the size of the laboratory flume, the footprint needed to be determined; the footprint is the smallest area on the sediment surface that provides 90% of the flux at the measuring point (e.g., Leclerc and Thurtell 1990; Schuepp et al. 1990; Schmid 2002; Berg et al. 2003). The flux footprint was calculated using the empirical function from Berg et al. (2007):

$$l = -2.783 - 158.7h + 159.2h^2 - 120.8h \log z_0 \qquad \text{(Eqn. 2.1)}$$

where *l, h* and z_0 are the footprint length, Eddy Correlation measurement height and the sediment surface roughness, respectively, and w is footprint width.

$$w = 6.531h \qquad \text{(Eqn. 2.2)}$$

In our laboratory racetrack flume, the water depth, measuring height and sediment surface roughness were 0.35 m, 0.05 m and 0.001 m, respectively, and thus foot-print length was 19.11 m, and the width was 0.33 m (Figure 2.17). According to these numbers, the working area of the laboratory racetrack flume was not long

enough to cover 90% of area that contributes to the flux. However, the upstream distance to the location that provides the strongest flux signal needed to be determined using the Eqn. 2.3 (Berg et al. 2007).

$$x_{max} = -0.09888 - 11.53h + 10.25h^2 - 6.650h \log z_0 \quad \text{(Eqn. 2.3)}$$

where x_{max} is the upstream location, from a measuring point, which provides the strongest flux signal

The upstream location of the strongest flux (x_{max}) in the laboratory flume was 0.34 m from the measuring point, which was in the working station area. Therefore, the Eddy correlation system was able to measure the flux in the laboratory racetack flume even though the working area was not able to cover all of the footprint area. In addition, the footprint and the upstream strongest flux distance are independent of flow velocity, according to Eqn. 2.1 – 2.4 (Berg et al. 2007).

$$factor = 1 + 8.347e^{-0.2453H/h} \quad \text{(Eqn.2.4)}$$

where H is water depth

The relationship between sediment surface roughness and footprint length (at h = 0.05 m and H = 0.35 m) is shown in Figure 2.18a. Figure 2.17b shows the relationship between sediment surface roughness and the upstream location profile from the EC measuring point at h = 0.05 m and H = 0.35 m. Both profiles were computed using the MATLAB script shown in Figure 2.18.

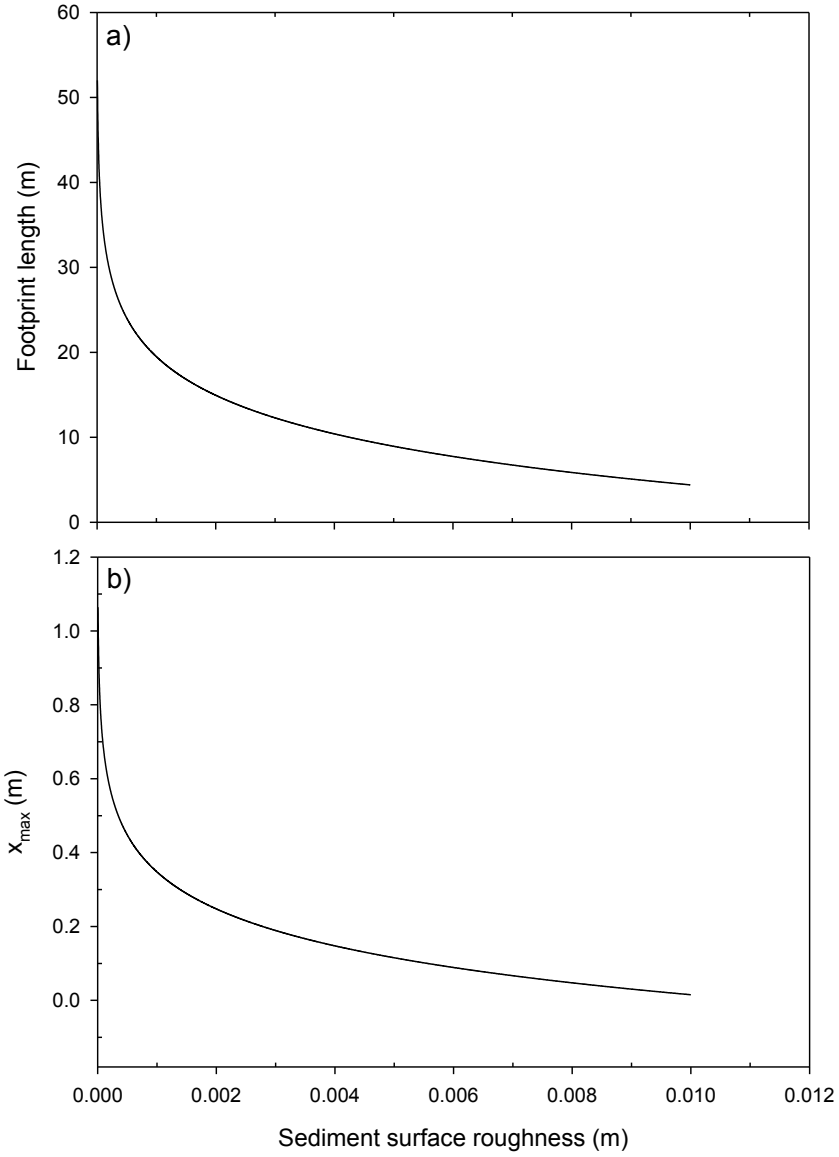

Figure 2.17: a) Footprint length profile in the laboratory flume; b) The upstream location (x_{max}) profile in the laboratory flume.

```
%% Seddiment surface foot print calculation (Berg et al 2007)
%
% Parameters
% length = footprint length (m)
% h = Eddy correlation measuring heights between 0.05 and 0.3 m
% above the sediment surface (m)
%
% z0 = sediment surface roughness parameter (z0) values between
% 7.04 x 10e-6 and 0.01 m. (m)
%
% width = footprint width (m)
%
% xmax = up stream distance (m)
%
% H = water depth (m)
%
% These expressions were developed for water depths (H) of H>27h.
% In the depth interval, 6.7h<H<27h, length can be calculated by
% multiplying the length, as given above, by the factor
% 1 + 8.347exp(-0.2453H/h), whereas xmax is independent of H. For
% H<6.7h, the tracer transfer rate over the air-water interface controls
% the size and shape of the footprint.

%% Variable values

h = 0.05;
H = 0.35;
z0 = (0.000007:0.000001:0.01);
factor = 1 + 8.347*exp(-0.2453*(H/h));
length = - 2.783 - (158.7*h) + (159.2*(h^2)) - (120.8*h*log10(z0));

%% Calculation
if H/h > 27
    length = length;
elseif H/h <= 27 && H/h >= 6.7
    length = length * factor;
else
    disp('the tracer transfer rate over the air-water interface controls th
end

width = 6.531 * h;
xmax = - 0.09888 - (11.53*h) + (10.25*(h^2)) - (6.650*h*log10(z0));


%% plot
```

Figure 2.18: MATLAB script for footprint and upstream location profile.

Due to the depth of the laboratory flume, air-water exchange flux may play an important role in flux measurement, and thus air-water exchange flux was determined using the following equation:

Net O_2 flux = Total flux – air-water exchange:

$$\frac{\partial O_2}{\partial t} = F - k(O_2 - O_{2sat}) \qquad \text{(Eqn. 2.5)}$$

Therefore, total flux is calculated by

$$F = \frac{\partial O_2}{\partial t} + k(O_2 - O_{2sat}) \qquad \text{(Eqn. 2.6)}$$

$$O_2 = O_{2int} e^{(-kt)} \quad \text{(Eqn. 2.7)}$$

where F is total flux, k is decay rate O_{2int} is initial O_2 and O_{2sat} is O_2 saturation in water which is temperature and salinity dependent.

The decay rate is velocity-dependent which means the decay rate changes when velocity changes, and thus the decay rate (k) was determined by air-sea flux experiments as shown in Table 2.3.

Table 2.3: The decay rate of O_2 in the laboratory flume under different flow velocity.

Velocity (cm s^{-1})	**k(min^{-1})**
7	0.0013732
12.5	0.0013627
13	0.0015011
19.5	0.0018028

From equations, the total O_2 flux at 12.5 cm/s is 408 µmol L^{-1} d^{-1} calculated as below:

$$F = \frac{30\ \mu mol\ L^{-1}}{2\ hr} + \left(0.078\ hr^{-1} \times (O_2\ \mu mol\ L^{-1} - O_{2sat}\ \mu mol\ \ L^{-1})\right)$$

However, in the seagrass experiment, seagrass coverage was 0.144 m^2 and the seawater volume in the flume is 0.8687 m^3. Thus, the total O_2 flux from seagrass is:

$$F = \frac{408\ \mu mol}{L \cdot d} \times \frac{L}{10^{-3}\ m^3} \times \frac{0.8687\ m^3}{0.144\ m^2} = 2.46\ mol\ m^{-2}\ d^{-1}$$

Because benthic microalgae and seagrass have an element ratio of photons to C to N to P to O_2 (photons:C:N:P:O_2) of approximately 5500:550:30:1:716, known as

Atkinson ratio (Atkinson et al. 1987; Baird et al. 2001), this ratio was used to determine the O_2 flux in seagrass experiment in order to investigate the effect of air-water gas exchange on EC flux measurements in laboratory racetrack flume. Therefore, the O_2 flux, in the seagrass experiment (see Chapter 3), which irradiance was held constant at 250 µmol photons m^{-2} s^{-1} ($2.16x10^7$ µmol photons m^{-2} d^{-1}) was:

$$O_2\ flux = \frac{716}{5500} \times 2.16 \times 10^7 = 2.81\ m^{-2}\ d^{-1}$$

The results demonstrated that there was a potential to measure O_2 flux in the flume because the air-water exchange rate was small when compared with the O_2 flux from the seagrasses themselves. Addtionally, the O_2 flux calculated from seagrasses (2.46 mol m^{-2} d^{-1}) is close to flux calculated by Atkinson ratio (2.81 mol m^{-2} d^{-1}) which denotes that O_2 can be measured in the laboratory flume.

2.4 FIELD EXPERIMENTAL SET-UP

The EC was deployed in several natural habitats, such as seagrass beds, microalgae, and coral reefs. The first generation of the Eddy Correlation microelectrode system (ECE1) was deployed in seagrass beds (Figure 2.19c) in the Tweed River, NSW (Figure 2.19b). The experiments at Tweed River produced poor results because the legs (Figure 2.19a) of the EC frame altered the natural hydrodynamics which likely had an impact on EC flux measurements. Thus, the second version of the EC frame had to be developed. The space between two legs of the new frame was wide enough to avoid disturbance to natural hydrodynamics, according to Unisense A/S EC frame specification. The second generation of the Eddy Correlation microelectrode system (ECE2) was deployed along with the new frame at Moreton Bay, Queensland. The results were also not good, due to jelly fish, and the frame was unstable which

created noise in the EC data (see Chapter 4). Thus, the third version of the EC frame was made.

a) b) c)

Figure 2.19: a) The EC mounted on the first version of the EC frame; b) The EC deployed in the Tweed River; c) The EC above the seagrass canopies.

The first generation of Eddy correlation optode system (ECO1) using the third frame design was deployed in Heron Island lagoon, Queensland over reefs and benthic microalgae (BMA) (Figure 2.20) and over seagrass beds in Moreton Bay, Queensland. The third EC frame performed well. The eddy flux result from the EC deployment over the BMA was robust (see Chapter 4). However, this result needed further discussion because the entire O_2 flux data did not meet the expectation (see Chapter 4). In Moreton Bay, the result was not good due to the complexity of the marine environment (e.g., wave and wind direction) as well as the reliability of the ECO1 (see Chapter 4).

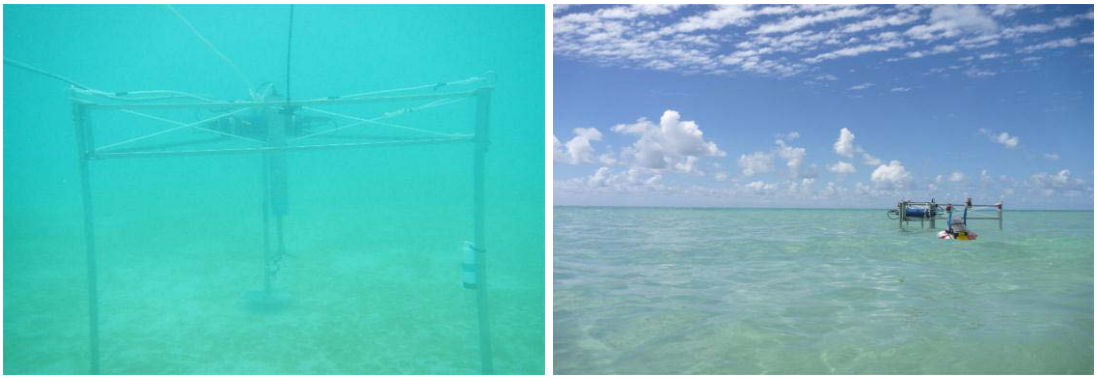

a) b)

Figure 2.20: a) The EC deployed on Heron Island; b) the EC mounted on the new EC frame deployed above the BMA in Heron Island shallow lagoon.

2.5 NEW OXYGEN CONVERSION METHOD FOR AN EDDY CORRELATION OPTODE SYSTEM (ECO2)

There are two types of underwater EC system: the Eddy Correlation Electrode system (ECE) and the Eddy Correlation Optode system (ECO). The ECE consists of an Acoustic Doppler Velocimeter (ADV), a datalogger, an O_2 amplifier and an O_2 microelectrode. The ECO uses an optode instead of the O_2 microelectrode. Although, most underwater EC studies used the ECE to measure the O_2 fluxes (Kuwae et al 2006, McGininis et al 2008, Glud et al 2010, Lorrai et al 2010, McCann-Grosvenor 2010, Holtappeis et al 2013), some studies recently used the ECO to measure the O_2 flux in sediment (Chipman et al 2012). Since 2012, the fast-responding optode has replaced the fast-responding EC O_2 microelectrode, hence many researchers have started working with the ECO due to the fact that the optode is more robust and makes less noise compared to the O_2 microelectrode (Chipman et al. 2012). These advantages of the ECO lead to the possibility of O_2 flux measurements in the laboratory flume, where it was almost impossible to measure the flux using the

microelectrode due to surrounding electrical noise. Although the EC can be used to measure the flux in the flume, the methods used to calculate the flux needed to be modified in order to obtain correct flux measurement.

In this next section, two O_2 conversion methods are described where ECO O_2 raw data are transformed into O_2 flux measurement within a laboratory flume. Then we compare the O_2 flux results using two methods.

2.5.1 Materials and Methods

2.5.1.1 Experimental design

Seagrass sediment was collected from Brisbane Water, NSW. The sediment was sieved through 3 mm mesh to remove shells, rocks, and invertebrates, and maintained in a laboratory flume with bubbled 30 (pss – practical salinity scale) seawater. The sediment was placed in the 90 cm x 40 cm x 5 cm flume working area (Figure 2.15). Before staring the experiments, the sediment was maintained under constant pH, salinity, water temperature, and water velocity for 48 hours acclimation. The 48 hours acclimation period also allowed the establishment of a constant diffusive boundary layer (DBL) thickness at the sediment-water interface, avoiding fluctuations due to the changes in the DBL thickness. The temperature, salinity, velocity, and pH were set at 28ºC, 30, 23 cm s^{-1}, and 8.1, respectively. pH was maintained by 0.1 M HCl or 0.1 M NaOH. The water velocity in the racetrack flume was maintained by a Pulse Width Modulation (PWM) motor speed controller connected to a trolling motor (Venom ETW34/26, Jarvis Marine Watersnake, Australia). Water temperature in the experiment was controlled by a water heater-chiller (TC20; Teco S.l.r., Italy). The salinity, temperature, and pH were also monitored by multimeters (WTW3430 GmbH, Germany).

The ECO (Figure 2.21) was deployed in the laboratory racetrack flume to investigate the O_2 flux associated with seagrass sediment in darkness for 2 hours. In this experiment, the EC measuring height was 5 cm above the 90 cm x 40 cm (Figure 2.21) of mud which was the area of interest in the flume (footprint). The thickness of the mud was 5 cm.

2.5.1.2 Eddy correlation optode system

The ECO consisted of the ADV (Nortek A/S, Denmark), datalogger (Unisense A/S, Denmark), O_2 amplifier (PyroScience GmbH, Germany), and 25 µm tip size fast-responding optode (t_{90}<0.3s) (PyroScience GmbH, Germany) (Figure 2.21). The ADV measured three-dimensional velocities (X, Y and Z) of the seawater. The optode connected to an O_2 amplifier and measured O_2 concentration in the seawater. The velocities and O_2 concentration were continuously recorded by datalogger at high-frequencies (64 Hz) in order to eliminate noise data using data processing. The ECO raw data (velocities and O_2 concentration) was exported to a computer and then converted to readable data using Eddy Conversion Software (Unisense A/S, Denmark) and MATLAB scripts (MathWorks, United States). After that, the data were processed and calculated into O_2 flux using scripts in MATLAB version 2012b and EddyFlux software (Unisense A/S, Denmark).

The optodes were calibrated using a two-point calibration procedure, which measured zero O_2 concentration and 100% O_2 concentration. The zero O_2 concentration solution was made by adding sodium dithionite in water, and the 100% O_2 concentration solution was made from air saturated seawater which was bubbled for 2 hours.

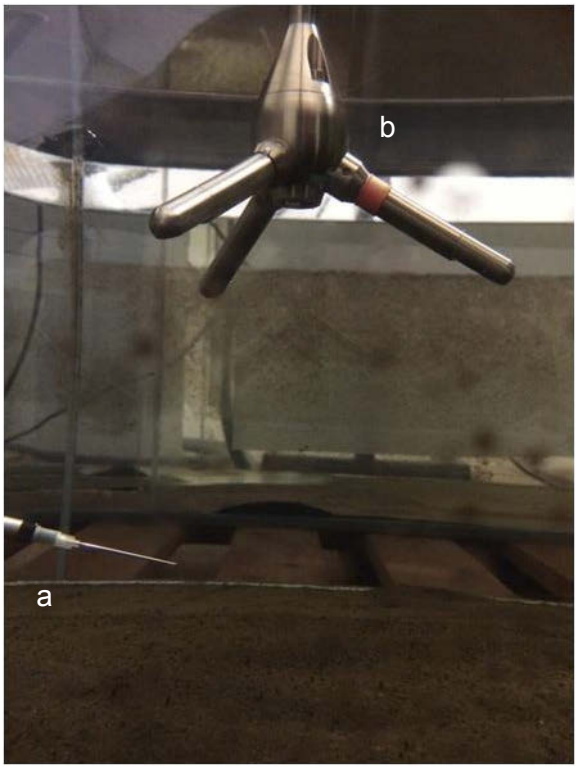

Figure 2.21: The ECO was deployed in the flume above seagrass sediment: a) O_2 optode, b) ADV.

2.5.1.3 O_2 conversion methods

Two O_2 conversion methods were developed to derive the O_2 concentration data from the O_2 raw phase-shifted signal. Normally, the O_2 concentration is converted from the raw O_2 phase-shifted signal (which in turn is based on the optode phase-shifted signal) using the Stern Volmer equation (Stern and Volmer 1919; Holst et al. 1998) as follows:

$$\frac{\tau}{\tau_0} = \frac{\tan(\emptyset)}{\tan(\emptyset_0)} = \frac{frac}{1 + K_{sv} \cdot [O_2]} + (1 - frac) \qquad \text{(Eqn. 2.8)}$$

Here $\tau_0, \emptyset_0$ are, respectively, the luminescence decay time and the phase angle in absence of oxygen, and $\tau, \emptyset$ are the luminescence decay times for measuring the

phase angle in the presence of oxygen, [O_2] the oxygen concentration, and K_{SV} is the overall quenching constant. According to eq. 2.8 the O_2 concentration was calculated by the phase-shifted method, which is the most common method used in oxygen measurements using this optode (Holst et al. 1995; Klimant et al. 1995; Rickelt et al 2013).

The phase shifted parameters can be described as following:

$$\tan(\emptyset) = 2\pi f_{mod}\tau \qquad \text{(Eqn. 2.9)}$$

where f_{mod} is modulation frequency, and $\emptyset$ is phase angle

Secondly, the O_2 concentration was also calculated based on the optode O_2 intensity signal which can be described as following (Holst et al. 1998):

$$\frac{I}{I_0} = \frac{\tan(\emptyset)}{\tan(\emptyset_0)} = \frac{frac}{1 + K_{sv} \cdot [O_2]} + (1 - frac) \qquad \text{(Eqn. 2.10)}$$

where I and I_0 are, respectively, the luminescence intensity in the presence and absence of oxygen.

However, the ECO did not provide the direct O_2 calibration method for the raw O_2 intensity signal; thus, the O_2 concentration from the raw O_2 signal intensity was calibrated against the raw O_2 phase-shifted signal using the following steps:

Step 1: Calculate the mean value of O_2 from the concentration of the serial output µM (O2_DPHI_mean) by linear detrending and running mean methods.

Step 2: Calculate the mean value of intensity in mV (Intens_mean) by linear detrending and running mean methods.

Step 3: Calculate the scale factor between µM and intensity (O2_DPHI_mean/ Intens_mean = ScaleFactor).

Step 4: Set the oxygen concentration based on the intensity (O2_µM_Intensity_mean = O2_DPHI_mean).

Step 5: Calculate the difference between the mean value of intensity and each intensity data point in mV (Diff_Intens = Intens_instantanious - Intens_mean).

Step 6: Calculate for each Intensity data point the µM concentration (Diff_Intens*ScaleFactor + O2_µM_Intensity_mean) yielding oxygen O2_µM_Intensity.

The above method inverts the intensity signal (Diff_Intens) in order to take into account that intensity falls with increasing oxygen concentration (Klimant et al. 1995)

2.5.1.4 O_2 flux calculation

After the data were converted into readable data, the raw time series data were examined. The despike technique was performed on the noisy vertical velocity data in order to remove high frequency fluctuation and spikes in the data (Goring and Nikora 2002). In each 15 min burst, the linear detrending and running mean techniques were performed on both the O_2 concentration data and vertical velocity data to remove any trend in the data, and to find the mean of data. Then, the 64 Hz raw time series of O_2 concentration (C) corresponding time series of vertical velocity (z) were computed for eddy O_2 flux every 15 min using Eqn. 2.11. Coordinate rotation technique was performed when the EC system was not aligned to horizontal

velocity ($u_z \neq 0$) during the experiment. If the vertical velocity did not correlate to the O_2 concentration, the time lag technique was performed to correct the data.

$$\overline{\text{Flux}} = \overline{u_z' C'} \qquad \text{(Eqn. 2.11)}$$

To examine the fluctuation characteristics of vertical velocity and O_2 concentration, spectra analysis of u_z and C were performed using Fast-Fourier transformation (FFT) for the time series of u_z and C, respectively. Co-spectra analysis using FFT was used to analyse O_2 flux characteristic, which frequently contributed to the O_2 flux. The spectra analysis was used to examine the effect of high and low frequencies on vertical velocity and O_2 concentration in order to investigate turbulence mixing in the water indicating that the water and O_2 concentration was well-mixed.

2.5.1.5 O_2 microprofile

O_2 microprofiles in the sediment were performed at the end of each experiment using a Clark-type O_2 microelectrode (OX-100, Unisense A/S, Denmark) connected to a microsensor multimeter, which in turn was connected to a computer running the Sensor Trace Pro software (Unisense A/S, Denmark). The O_2 microelectrode was mounted on a motorized micromanipulator (Unisense A/S, Denmark). The microelectrode had an outer tip diameter of 100 µm, a 90% response time of 8s and a stirring sensitivity of 1.5%. The microelectode was polarized for 24 h before experiment and was calibrated at flume temperature in air-saturated seawater and O_2-free seawater (made anoxic by the addition of sodium dithionite). Nine O_2 concentration profiles were performed in the sediment surface in order to cover the entire area of the sediment surface. The profiles were started at approximately 10 mm above the sediment and carried out in 100 µm steps to approximately 30 mm below sediment surface. The sediment-water interface was identified from the

produced profile as the depth where the profile first deviated from a straight line (below the boundary layer). The local diffusive O_2 flux (J; μmol O_2 m^{-2} d^{-1}), that is, the O_2 uptake rate, was calculated from the measured steady-state O_2 concentration profiles via Fick's first law (Revsbech et al. 1980): $J = -D_0(dC/dz)$ where D_0 is the molecular diffusion coefficient in seawater at experimental salinity and temperature, and dC/dz is the linear slope of the O_2 concentration profile in the diffusive boundary layer (DBL) above the sediment surface.

2.5.1.6 Statistical analysis

To determine any significant differences in O_2 flux between different conversion techniques (EC phase-shift method, EC intensity method, O_2 microprofiling) and flux calculation methods (linear detrending and running mean), one-way ANOVA tests were used (SPSS Version 17) with a significance level of 95%. Data were transformed using $\log_{10}$ or square root if the data did not meet the assumptions of normality (Kolmogorov-Smirnov test) and equal variance (Levene's test).

2.5.2 Results

Eight bursts (15 minute each) of O_2 flux calculated and based on O_2 phase-shifted conversion and intensity conversion techniques are shown in Figure 2.22. In O_2 phase-shifted conversion technique, O_2 fluxes in each burst calculated by both linear detrending (Figure 2.22a) and running mean (Figure 2.22b) methods were not constant; however, both calculation methods were not significantly different (p = 0.728) either. For example, in third burst, both the flux from the linear detrending (Figure 2.22a) and running mean (Figure 2.22b) methods changed from negative (consumption) to positive (production), while the ECO was deployed above the

sediment. The average flux of the linear detrending and running mean methods was -1.09±1.77 mmol m^{-2} d^{-1} and -1.41±1.85 mmol m^{-2} d^{-1}, respectively.

In O_2 phase-shifted conversion, the O_2 fluxes in each burst calculated by linear detrending (Figure 2.22c) and running mean (Figure 2.22d) methods were steady and not significantly different (p = 897). The average flux of the linear detrending and running mean methods was -17.21±1.35 mmol m^{-2} d^{-1} and -17.32±1.73 mmol m^{-2} d^{-1}, respectively.

The comparisons of O_2 concentration, O_2 cumulative flux, and O_2 flux results from the first 15 minute burst using phase-shifted conversion and intensity conversion techniques are shown in Figure 2.23. The first 15 minute burst of oxygen concentration converted using the phased-shifted technique (Figure 2.23a) had more noise (green line) than the intensity technique (Figure 2.23b). The cumulative O_2 flux from the phase-shifted conversion technique was fluctuating (Figure 2.23c). In comparision, the cumulative O_2 flux from the intensity conversion technique decreased linearly, demonstrating a steady sediment consumption rate during the O_2 flux measurement (Figure 2.23d). The fluctuation of cumulative O_2 flux from the phase-shifted conversion technique at t=0s to t=200s (Figure 2.23c) indicated that there was no O_2 flux captured by ECO during that period. In addition, there was an increase in cumulative O_2 flux from t=400s to t=600s which indicated that O_2 production appeared on both the linear detrending and running mean methods (Figure 2.23c). The O_2 flux over the experimental period from the phase-shifted technique (Figure 2.23e) was significantly lower than that from the intensity technique (Figure 2.23f). The O_2 flux from linear detrending and running mean methods based on raw O_2 phase-shifted signal were not significantly different (-2.51

and -3.53 mmol m^{-2} d^{-1}, respectively; Figure 2.23e). There was no significant different in O_2 flux between linear detrending and running mean methods from the raw O_2 intensity signal (-17.07 and -17.18 mmol m^{-2} d^{-1}, respectively; Figure 2.23f).

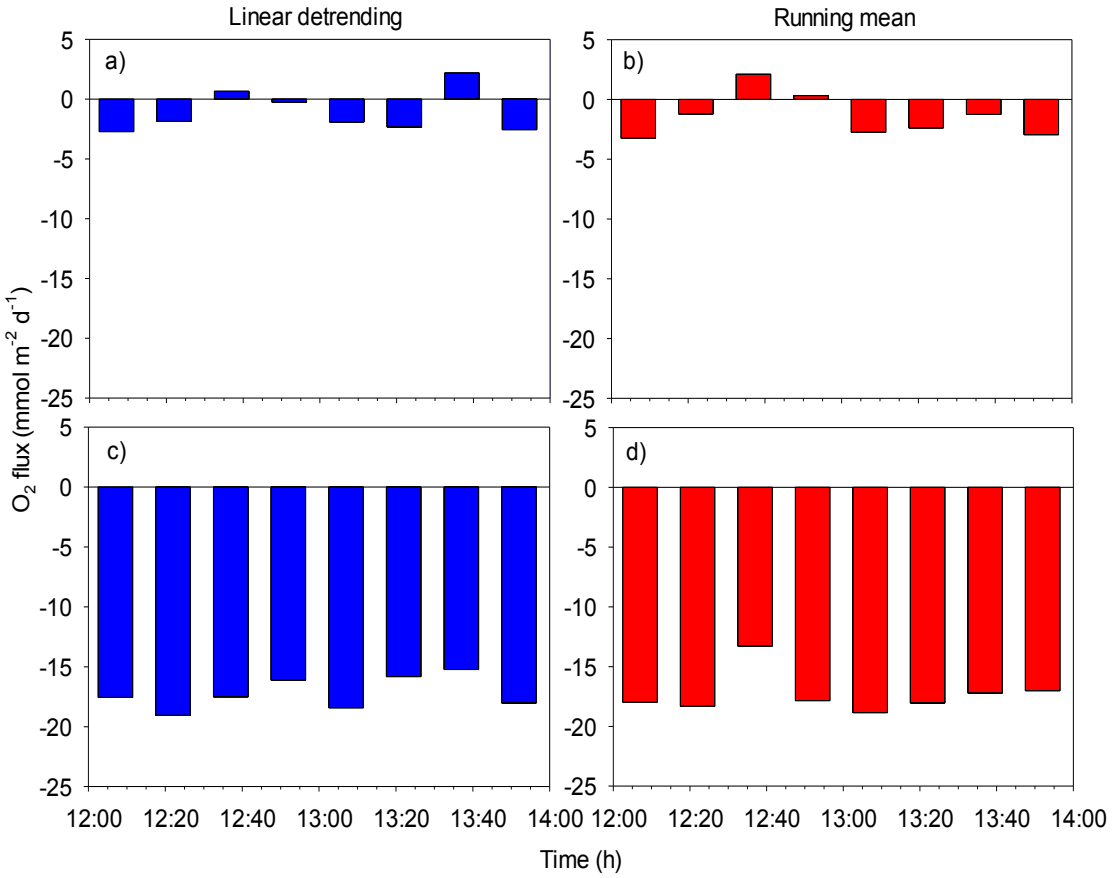

Figure 2.22: Eight bursts of O_2 flux calculated linearly using a detrending method (a, c) and a running mean method (b, d) based on phase-shifted O_2 conversion technique (a, b) and intensity O_2 conversion technique (c, d) (n = 1).

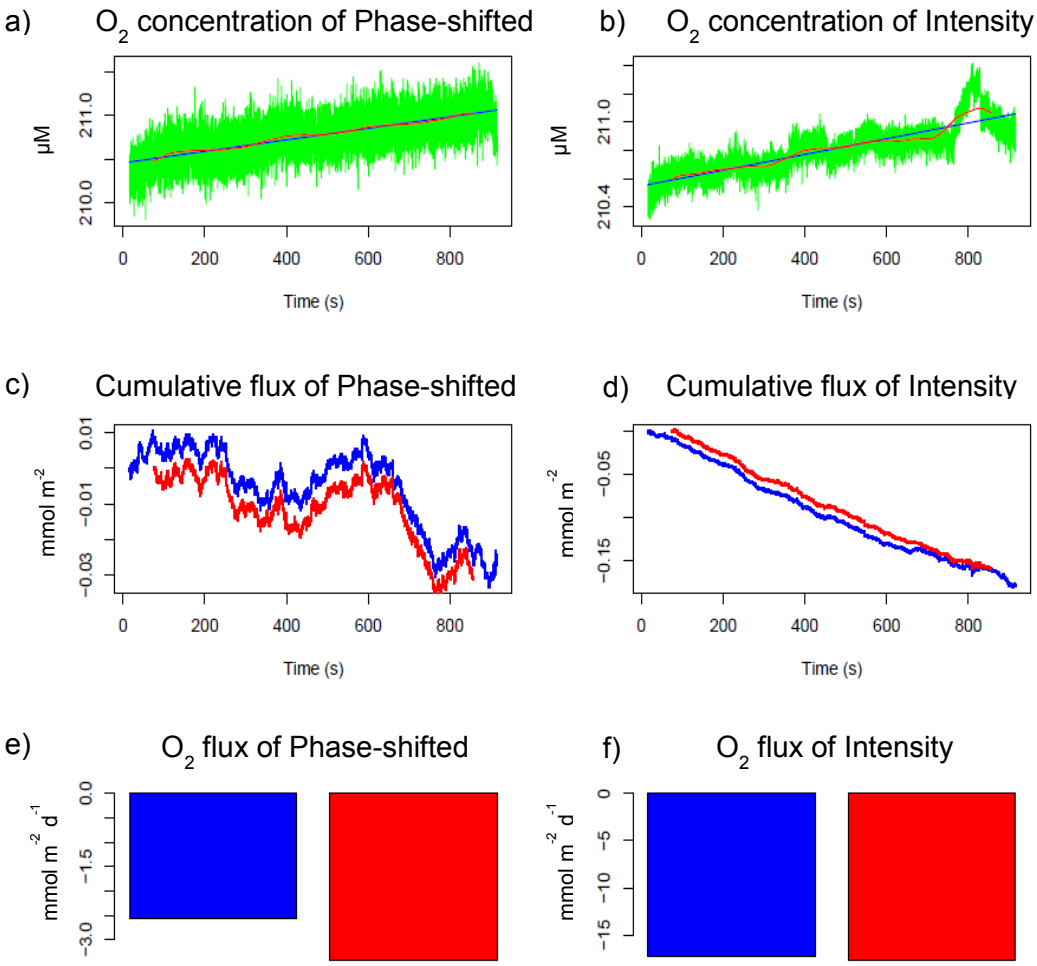

Figure 2.23: O_2 concentration (a, b), cumulative O_2 flux (c, d), and O_2 flux (e, f) using phase-shifted O_2 conversion (a, c, e) and intensity O_2 conversion (b, d, f) techniques in the first 15 minutes of 2 hour deployment. The green lines represent the raw O_2 concentration data. The blue and red lines and bars represent the mean of O_2 concentration and flux calculated by linear detrending and running mean method, respectively.

O_2 microprofiling was performed in order to validate the O_2 flux data from the ECO calculations based on O_2 phase-shifted conversion and intensity conversion techniques with linear detrending method and running mean method (Figure 2.24). There was no significant difference in average O_2 flux data among O_2 microprofiling

and intensity conversion techniques with the linear detrending method (IT-LD) and running mean method (IT-RM) (p = 0.888 and p = 0.919, respectively; Figure 2.24). However, average O_2 flux data from ECO calculated and based on O_2 phase-shifted conversion technique with linear detrending method (PS-LD) and running mean method (PS-RM) were significantly lower than that from the O_2 microprofiling and intensity conversion techniques with linear detrending method (IT-LD) and running mean method (IT-RM) (p < 0.001; Figure 2.24). Average O_2 from O_2 microprofiling was -18.30±1.42 mmol m^{-2} d^{-1}. There was no significant difference in O_2 flux between PS-LD and PS-RM (p = 0.996), and between IT-LD and IT-RM (p = 1.000; Figure 2.24).

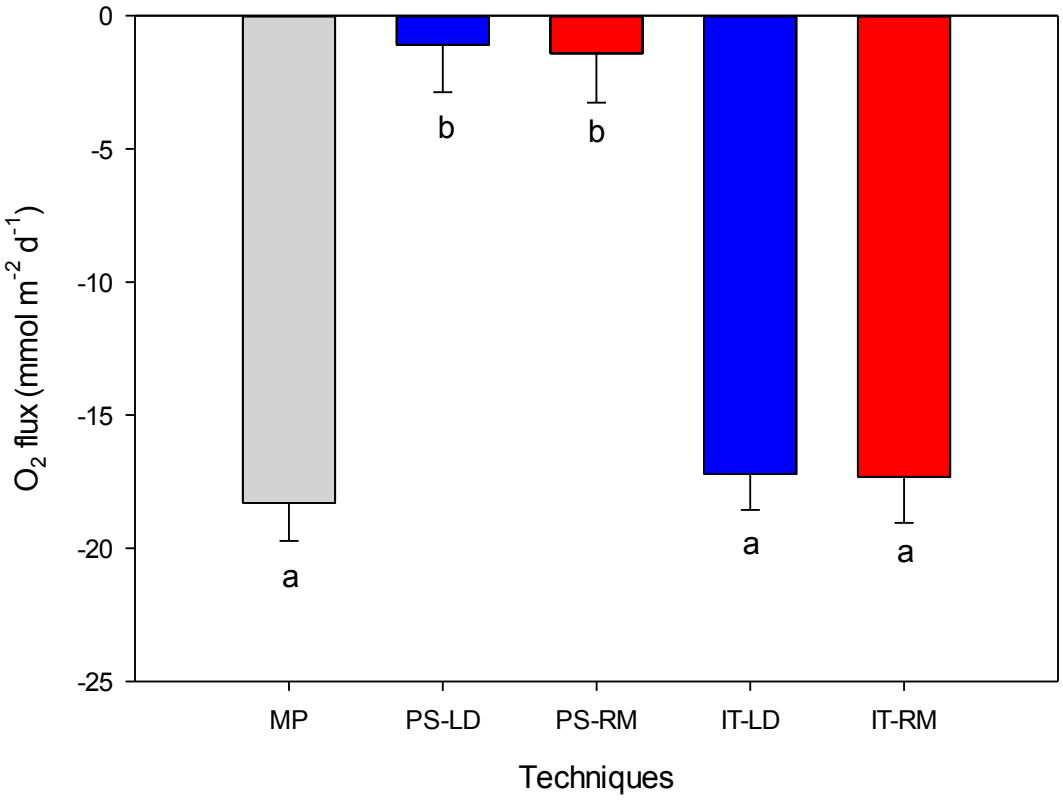

Figure 2.24: Average of 9 O_2 fluxes from O_2 microprofiling (MP), phase-shifted O_2 conversion with linear detrending method (PS-LD) and running mean method (PS-RM) and intensity O_2 conversion with linear detrending method (IT-LD) and running mean method (IT-RM) from 2 hour deployment. Data represents mean ± SE. [a, b] determine significant differences ($p < 0.05$; ANOVA).

2.5.3 Discussion

This is the first study to compare the two oxygen conversion methods used in eddy correlation systems. Optodes, optical sensors made for chemical species, have been rapidly developed in order to remove some limitations of Clark-type O_2 microelectrodes (Wolfbeis 1991; Klimant et al. 1995) because microelectrodes are very expensive, do not always have good measurement properties, and are unreliable

for long-term measurement (Klimant et al. 1995). Optodes are normally calibrated using two-point calibration (Holst et al. 1997) in order to convert the measured data. Two types of conversion methods, phase-shifted and fluorescence intensity signal, have been used for O_2 conversion (Klimant et al. 1995; Holst et al. 1997). The phase-shifted method is based on luminescence lifetime or decay (Holst et al. 1997). Since optodes show a non-linear decrease in fluorescence signal when the O_2 concentration increases, Eqn. 2.10 is applied in order to linearise the signal (Klimant et al. 1995). However, fluorescence intensity (called intensity signal) is interfered with by the fluctuation of light sources or bleaching effect of indicator dyes (Holst et al. 1995; Klimant et al. 1995). Thus, the well-known phase-modulation technique (Lakowicz 1983; Berndt and Lakowicz 1992; Wolfbeis 1991; Holst et al. 1997; Kühl 2005), which is not affected by light or photo-bleaching, is used as a calibration for the optode (Holts et al. 1995; Holst et al. 1997). The phase angle (phase-shifted), which is related to luminescence decay, is changed as a function of the O_2 concentration (Lakowicz 1983; Wolfbeis 1991; Berndt and Lakowicz 1992; Holst et al. 1997; Kühl 2005; Rickelt et al 2013).

Although the phase-shifted technique is the most common method that researchers use for O_2 conversion (Lakowicz 1983; Berndt and Lakowicz 1992; Wolfbeis 1991; Holst et al. 1997; Kühl 2005; Rickelt et al 2013), our study showed the new O_2 conversion method for the Eddy Correlation system based on the O_2 intensity signal yielded better flux results compared to the phase-shifted method. This is attributed to the fact that the intensity method provided lower fluctuations (Figure 2.23a and 2.23b) of O_2 concentration which lead to a steady consumption rate in the sediment (Figure 2.23c and 2.23d). Therefore, the fluxes were consistent over two hours

(figure 2.22c and d). The fast O_2 measurement (greater than 10 Hz) may result in a high noise level, and therefore the resolution of O_2 measurement (pers. comm. with PyroScience GmbH, Germany) which resulted in higher noise level of O_2 in Figure 2.23a. In comparison, the O_2 measurements based on intensity signal had less noise due to the fact that the intensity signal has lower sensitivity (Holst et al. 1995; Klimant 2003). Higher noise led to the instability of the cumulative O_2 data (Figure 2.23c), which resulted in unreliable flux measurements. Therefore, the EC system, which needs high frequency measurement (> 16 Hz) of O_2 (Berg et al. 2007; Chipman et al. 2012) may need the O_2 data based on intensity signal in order to obtain lower noise at high frequency. In this study, the O_2 conversion method based on intensity signal proved more suitable than O_2 conversion based on the phase-shifted method. However, the intensity method cannot be used in short-term monitoring due to photo-bleaching of indicator dyes (Holst et al. 1997; Klimant et al. 2003). In addition, light interference also needs to be considered (Klimant et al. 1995).

To validate the O_2 flux in the laboratory racetrack flume, the microprofiling system was used to measure the O_2 flux. The microprofiler has been commonly used to measure the flux in micro-scale because this method is very precise and accurate (Silva 2009). The 9 O_2 profiles were measured in 3 x 3 arrays in order to cover the entire area of sediment. Thus, we used the microprofiling technique to validate the O_2 flux measured by ECO and compared the O_2 flux measured by the microprofiling system (MP), EC O_2 flux using the intensity method (IT), and EC O_2 flux using the phase-shifted method (PS). This study showed that there was no significant difference between O_2 flux measured by MP and IT (Figure 2.24). In contrast, the

MP O_2 flux was significantly higher than the PS O_2 flux (Figure 2.24). This study suggested that IT is more reliable to use in the calculation of flux and IT has a potential to be used as an O_2 conversion of the EC system.

In EC methods, the fluctuation of vertical velocity and O_2 concentration are calculated by subtracting the mean value of the measurement from its instantaneous value (Kabat 2004; Hume et al. 2011; Reimers et al. 2012; Long et al. 2013). The mean can be calculated by various methods such as mean removal, linear detrending, or running mean. Linear detrending is commonly used for calculating the average over blocks of data (Kabat 2004). Rannik and Vesala (1999) compared to various methods, and results indicate that the use of linear detrending is favored (Kabat 2004). The weakness of the running mean method, which is definitely acceptable over the short canopy, results in an underestimation of the flux if low frequency plays a major role in the tall canopy (Kabat 2004; Moncrieff et al. 2006).

In our study, we found that there was no significant difference between O_2 flux calculated by linear detrending and running mean (Figure 6.5), indicating that both methods were acceptable for use in O_2 flux calculations. However, linear detrending was preferable due to a 15 minute block. These results are consistent with previous studies that used EC to measure the O_2 flux in sediment (Lorrai et al. 2010; Reimers et al. 2012; Berg et al. 2013; Holtappels et al. 2013; Long et al 2013).

In conclusion, the O_2 conversion method, which converted the O_2 concentration based on O_2 intensity signal, is potentially useful for Eddy Correlation O_2 flux measurements under specific conditions. The intensity method can convert the O_2, when the eddy correlation optode system is deployed in controlled environments with no light source interference, such as strong light and shallow water. In addition,

this method is not able to be used in long-term deployments due to photo-bleaching of indicator dyes. In comparison, the phase-shifted method, which converted the O_2 concentration from a phase angle signal, is able to be used under strong light conditions. However, use of the phase-shifted method for high frequency measurement needs to be conducted with care due to the inaccuracy of O_2 flux measurements.

2.6 CONCLUSION

In conclusion, there were a lot of technical, electronic and digital issues and challenges associated with eddy flux measurements for the entire research project. Most of the issues were caused by hardware malfunction, as well as software errors. Although most of hardware and software issues have been solved by software programing, some of issues still exist due to the limitations of the hardware. Some hardware has been replaced to improve these limitations and overall reliability. However, some hardware could not be replaced due to the fact that it is still under development. For those reasons, EC is still under development to deliver robust measurements which lead to better flux results. However, MATLAB scripts have been developed in this research to handle all facets of the processing of EC data from data cleaning and correction through to flux calculation. The frames for EC deployment in the field have been refined and the system and protocols have been developed for flume based applications. The comparison between conversion methods used in O_2 optode studies showed that the intensity method is more suitable for short-term deployment of the Eddy Correlation optode system in controlled environments with no light source interference (such as strong light and shallow water) due to photo-bleaching of indicator dyes. On the other hand, the phase-shifted

method is able to be used under strong light conditions. However, use of the phase-shifted method for high frequency measurements needs to be conducted with care due to the inaccuracy of O_2 flux measurement.

CHAPTER 3:

RELIABILITY AND LIMITATIONS OF EDDY CORRELATION TECHNIQUE ON OXYGEN DYNAMICS IN SEAGRASS AND SEDIMENT OXYGEN UPTAKE IN LABORATORY RACETRACK FLUME

3. RELIABILITY AND LIMITATIONS OF EDDY CORRELATION TECHNIQUE ON OXYGEN DYNAMICS IN SEAGRASS AND SEDIMENT OXYGEN UPTAKE IN LABORATORY RACETRACK FLUME

3.1 INTRODUCTION

Seagrass meadows are one of the most important ecosystems in the world providing biodiversity, productivity and ecosystem functions including a carbon sink capacity known as blue carbon (Duarte et al. 2008; Duarte 2009) with an estimated ecosystem service value of $3.8 billion annually (Costanza et al. 1997). Photosynthetic processes in seagrasses remove CO_2 from the atmosphere and convert it to organic carbon stored in seagrass leaves and roots and detritus which can remain over millennia (Duarte and Cebrian 1996; Mateo et al. 1997). However, seagrass meadows worldwide are under threat, in terms of distribution and health, from the impact of human activities and climate change (Short and Neckles 1999). An increase in atmospheric CO_2 concentration has led to an increase in air temperature through the trapping of heat by the greenhouse effect and has resulted in an increase in ocean temperature (Johnson and Marshall 2007; Houghton 2009). An increase in turbidity, epiphyte and algal blooms due to elevated nutrients and sediment loading from the catchment due to coastal development and poor agricultural practices has led to a reduction in light intensity, resulting in the progressive loss of seagrass meadows (Ralph 2000; Ralph et al. 2006).

Oxygen production, respiration and net oxygen flux play an important role in marine habitats and ecosystems. However, the production of oxygen is dependent upon physical parameters such as temperature and light (Drew 1979; Short and Neckles 1999). Temperature and light are important controls of seagrass metabolism,

photosynthesis, enzyme activity and maintenance of the carbon balance in seagrass, which in turn governs their growth, survival, reproduction and distribution (Short and Neckles 1999). It has been shown that with increasing temperature *Zostera* sp. increased respiration more rapidly than photosynthesis, resulting in a decrease in photosynthesis: respiration ratio (Moore and Short 2006). Moreover, productivity would decrease when each species reaches its thermal maximum, as observed in *Zostera noltii* and *Posidonia oceanica* (Moore and Short 2006; Massa et al. 2009; Marba and Duarte 2010). Light was found to control growth rate, shoot morphology, shoot density, photosynthetic efficiency and productivity of seagrasses (Ralph and Gademann 2005; Moore and Short 2006). A decrease in light intensity leads to a reduction in shoot density and above-ground biomass of *Zostera marina* (Backman and Barilotti 1976), *P. australis* (Backman and Barilotti 1976), and *Thallassia testudinum* (Lee and Dunton 1997) and reduction in growth rate in *P. sinuosa* (Gordon et al. 1994), *P. australis* (Fitzpatrick and Kirkman 1995), *P. oceanica* (Ruiz and Romero 2001), *Z. marina* (Short et al. 1995) and *T. Testudinum* (Lee and Dunton 1997; Ibarra-Obando et al. 2004).

Oxygen flux across the sediment-water interface has also been widely studied in order to assess benthic metabolism and organic mineralization in aquatic environments (Rasmussen and Jorgensen 1992; Berg et al. 2009). Seagrass productivity and oxygen production have also been investigated using a range of instruments and techniques such as oxygen titration (Winkler method) and oxygen chamber (Silva et al. 2009). These methods are effective; however, they are intrusive and can only measure over a small spatial scale (organism level; Silva et al. 2009). Benthic flux chambers and vertical O_2 microprofiles are common methods used to

determine O_2 flux *in situ* (Rasmussen and Jørgensen 1992). These methods, however, have a number of draw-backs, which invariably affects the measurements. For example, benthic chambers impede the natural hydrodynamic flow over the study area, affecting the flux rate over the surface, and the measured flux only represents that of a small area (<2 metres), necessitating a high level of replication (Berg et al. 2009). Microprofiling provides one-dimensional measurements of the physiochemical microenvironment of the sediment-water interface at high spatial resolution (De Beer and Larkum 2001), but is sensitive to variability at the horizontal microscale, making large scale estimates of O_2 flux unfeasible except for the most uniform sediment conditions (Berg et al. 2009).

Over the last decade, the eddy correlation (EC) technique has gained interest as a method for measuring net oxygen fluxes in aquatic systems including sediment, seagrass meadows, coral reefs, hard bottom surfaces and sea ice (Berg et al. 2003, Glud et al. 2010; Hume et al. 2011; Long et al. 2012; Long et al. 2013). Moreover, the EC technique has been used to measure fluxes of various compounds such as H_2S, dissolved organic carbon (DOC), and nitrate (Swett 2010; Johnson et al. 2011; McGinnis et al. 2011).

To obtain an eddy flux measurement, the covariance between fluctuations in both the concentration of the compound in question and its vertical velocity, measured by a high-speed sensor (e.g., microelectrode or microoptode) and a high-speed acoustic Doppler velocimeter (ADV), respectively, is computed. The advantages of this technique are that: 1) it can measure the fluxes in a very large area depending on the measurement height above the benthic surface and the horizontal current velocity (Berg et al. 2003; Berg et al. 2007; Berg et al. 2008), 2) it is a non-invasive

technique, and 3) it does not disturb or enclose the benthic surface which otherwise could lead to changes in measurement conditions (light and hydrodynamics; Kuwae et al. 2006; Brand et al. 2008; McCann-Grosvenor 2010). However, it also requires many of the same assumptions as terrestrial EC about the conditions, mass balance and data filtering-correction techniques that are used by meteorologists to discriminate between good and bad gas flux measurements in land-atmosphere interfaces (Finnigan 1999, Finnigan et al. 2003; Aubinet 2008). These assumptions must be re-evaluated in each new field situation (Reimers et al. 2012; Burba 2013) because every field site has different natural conditions such as geometry, physical parameters (e.g., wind and wave direction), and size of footprint. Due to the nature of these assumptions, the EC technique cannot be applied to a complex system which has a non-homogeneous wind and current direction, as this may lead to erroneous flux measurements (Holtappels et al 2013).

Sediment O_2 consumption is an important indicator of the rate of nutrient recycling (remineralization) in the sediment (Seiki et al. 1994; Valdes-Lozano et al. 2006) and is caused by the aerobic decomposition of organic matter, animal respiration and oxidation of reduced products including NH^{4+}, Mn^{2+}, Fe^{2+}, H_2S, FeS and FeS_2 (Berg et al. 2003; Valdes-Lozano et al. 2006). It can also provide useful information on these metabolic processes in the system (Berg et al. 2003) such as seagrass and coral reef metabolism (Hume et al. 2011; Long et al. 2013). However, sediment O_2 consumption is difficult to measure accurately with conventional methods (such as *in situ* chambers) because of how these methods invariably affect the environmental conditions over the measuring area during the measurement.

Sediment O_2 uptake is affected by a multitude of factors such as microbial activity in sediment, water velocity, water temperature, and light. In deep water, sediment O_2 uptake is strongly influenced by the velocity of the overlying water which transports O_2 from the overlying water down through the sediment (Berg et al. 2003). The diffusive boundary layer (DBL), where molecular diffusion is the dominant transport mechanism for dissolved material, plays an important role in the transport of O_2 into the sediment. Water velocity determines the thickness of the oxygen boundary layer and determines diffusive fluxes and concentration gradients of oxygen and nutrients (Cahoon 1988; Vogel 1994). O_2 transport process in the sediment is driven by current and wave and other biological activities. Under low flow, oxygen gradients may be unstable, and oxygen transport will be more dependent on faunal activities (Revsbech et al. 1980) such as bioturbation (the diffusion-like transport of solutes and solids caused by movements of fauna) and bioirrigation (the transport of solutes caused by the pumping activity of tube-dwelling animals) (Revsbech et al. 1980; Berg et al. 2003; Pischedda et al. 2008). Recent studies show that bioturbation and bioirrigation increase sediment oxygen heterogeneity and diffusive oxygen flux due to an increase in the interface area between the sediment and the overlying water (Pischedda et al. 2008; Lagauzere et al. 2011). The EC technique has been used to measure oxygen uptake in sediment because it does not affect active transport and environmental conditions that influence O_2 uptake in the sediment (Berg et al. 2003).

In this chapter, EC measurements were used for the first time in a laboratory racetrack flume to measure O_2 flux of the temperate seagrass *Zostera muelleri* under different temperature and light and O_2 consumption in seagrass sediment under controlled physical conditions (e.g., temperature, flow, and light). This flume study

was completed in order to: 1) test fundamental assumptions about the EC, and 2) control some environmental factors such as temperature and water velocity so that the effect of other factors on O_2 flux can be assessed. The optimal temperature and light requirements for photosynthesis and respiration in *Z muelleri* were examined. A Pulse Amplitude Modulated fluorometer (Diving-PAM) was used to determine the photosynthetic efficiency of the seagrass at each light and temperature treatment. In addition, O_2 microprofiles were used to assess O_2 uptake in micro-scale, and were then compared with EC O_2 flux measurements, thus assessing limitations and reliability of the EC technique in the laboratory flume.

3.2 MATERIALS AND METHODS

3.2.1 Effect of temperature and light on *Z. muelleri*

3.2.1.1 Experimental design

Specimens of *Zostera muelleri* were collected by hand from shallow sub-tidal seagrass beds at Cam Wharfs, Lake Macquarie, New South Wales (GPS location: -33.125727, 151.613467) and maintained in an outdoor 500 L aquarium tank with seawater from Sydney Harbour (changed weekly) for 3 months. Water temperature at Lake Macquarie varies from 23-33°C (mean of 26.5°C) in summer to 12-29°C in winter (York et al. 2013). *Z. muelleri* (250 shoots m^{-2}) were randomly placed in a 1000 L transparent racetrack flume (Figure 3.1a). For the temperature experiment, the seagrass samples were treated under 21, 25, 28 and 31°C for 72 hours including 48 hours for acclimation. Light intensity was set at 400 μmol photons m^{-2} s^{-1} on a 12:12 h light:dark cycle (light on: 0900 h, light off: 2100 h). For the light intensity experiment, new samples were randomly placed in the racetrack flume (Figure 3.1d and 3.1h) as previous described in temperature experiment and treated under 150,

250, 400, 600 μmol photons m^{-2} s^{-1} (12:12 h light:dark cycle; light on: 0900 h, light off: 2100 h) under 25°C for 72 hours including 48 hours for acclimation. For both single and combined temperature and light experiments, pH, salinity and turbidity were set at 8.1, 33, 1.0 NTU, respectively. The water velocity in the racetrack flume was set to 7 cm s^{-1} using a Pulse Width Modulation (PWM) motor speed controller (Figure 3.1f) connected to a trolling motor (Venom ETW34/26, Jarvis Marine Watersnake, Australia; Figure 3.1g). Water temperature in each treatment was controlled by a water heater-chiller (TC20; Teco S.l.r., Italy). Salinity and turbidity was measured using YSI multiprobe (6920 sonde and 650MDS; YSI, United States). Light was produced by 2 x 400-Watts metal halide lamp (Venture® HIT 400W/U/EURO/4K, England). Light intensity was measured using an underwater PAR sensor (Li-250A; Li-Cor, United States).

3.2.1.2 Eddy Correlation microelectrode system

Oxygen flux and oxygen production of seagrass from different temperature and light intensities were investigated using the first generation of the Eddy Correlation microelectrode system (ECE1; Unisense A/S, Denmark; Figure 3.1a, 3.1b, and 3.1c). This Eddy Correlation microelectrode system consists of an acoustic Doppler velocimeter (ADV; Nortek AS, Denmark; Figure 3.1b, 3.1c, and 3.1d), which measures three-dimensional velocity (X, Y and Z) and an oxygen microelectrode (Unisense A/S, Denmark; Figure 3.1b, 3.1c, and 3.1d), which measures oxygen concentrations at high resolution (t_{90}<0.3s). The O_2 microelectrode was connected to an amplifier (Unisense A/S, Denmark; Figure 3.1b) to increase O_2 signals. Both velocity and O_2 concentration data were continuously logged into ECE1 datalogger (Unisense A/S, Denmark; Figure 3.1b) at a high-speed sampling rate (64 Hz) in

order to eliminate noisy data using data processing. The EC raw data were exported to a computer and then converted to readable data using Eddy Conversion Software (Unisense A/S, Denmark). After that the data were processed and calculated to O_2 flux using scripts in MATLAB version 2009b (MathWorks, United States) and EddyFlux software (Unisense A/S, Denmark). MATLAB scripts were used to process the ECE1 raw data using different methods e.g., de-spiking and coordinate rotation. After that, the scripts converted the processed raw data to oxygen flux. Results from the scripts and EddyFlux software were then compared.

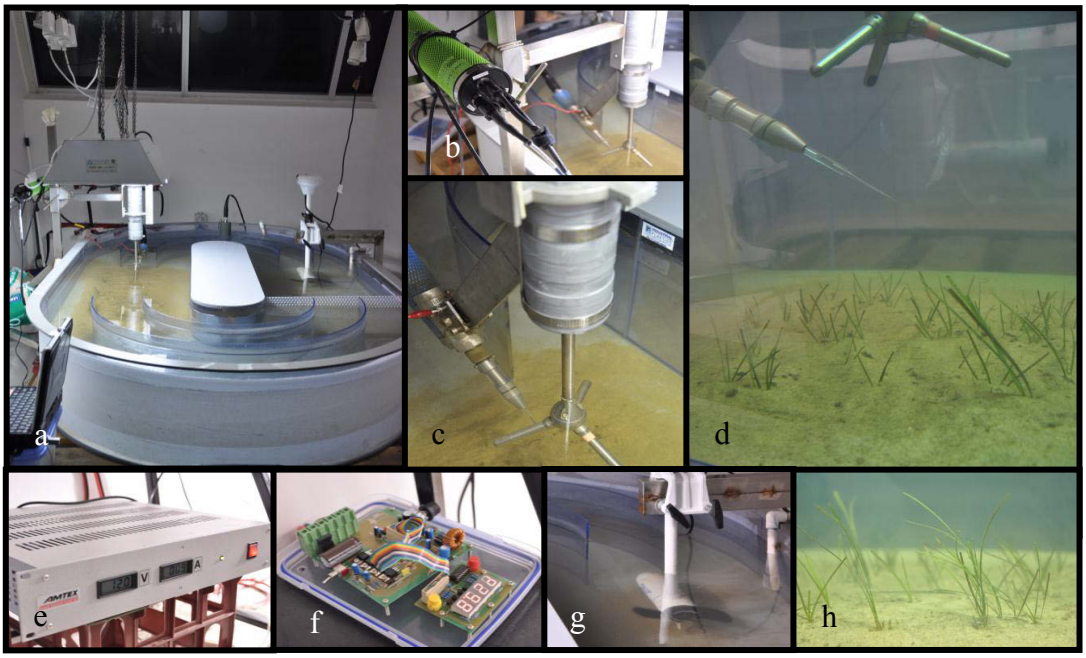

Figure 3.1: Eddy Correlation microelectrode system (ECE1) and experimental setup devices a) Laboratory racetrack flume, b) ADV, microelectrode, and ECE datalogger mounted on a frame, c) ADV and microelectrode on seagrass meadows, d) Power supply, e) Motor speed controller, f) Trolling motor, g) Seagrass meadows.

3.2.1.3 Eddy O_2 flux analysis technique

After the data were converted to readable data format, the raw time series data were examined. If noisy vertical velocity data were found, the de-spike technique was performed to remove high frequency fluctuation and spikes in the data (Goring and Nikora 2002). In each 15 min burst, linear detrending, which forces the data mean to zero and reduces overall variation in order to get a better picture of fluctuations in the data, and an averaging window (running mean) was performed on both O_2 concentration data and vertical velocity data redundant. Then, the 64 Hz raw time series of O_2 concentration (C) and the corresponding time series of vertical velocity (w) were converted to eddy O_2 flux every 15 min using Eq.1. Coordinate rotation technique was performed if the ECE1 was not aligned to horizontal velocity ($w \neq 0$) during the experiment. If the vertical velocity did not correlate to the O_2 concentration, the time lag technique was performed to correct the data. The calculated O_2 flux using linear detrending and averaging window were then compared.

To examine the fluctuation characteristics of vertical velocity and oxygen concentration, spectral analysis of u_z and C was performed using Fast-Fourier transformation (FFT). Co-spectra analysis using FFT was used to analyse the O_2 flux characteristic. These spectra and co-spectra analyses were used to examine the effect of frequency response on vertical velocity, oxygen concentration, and oxygen flux measurements in order to check the quality of the data.

3.2.1.4 Chlorophyll *a* fluorescence

Steady state light curves (SSLCs) with 6 irradiance steps (18, 51, 174, 354, 686 and 1437 μmol photons m^{-2} s^{-1}) were performed with a Diving-PAM fluorometer (Walz, Effeltrich, Germany) connected to a 6 mm diameter fibre-optic sensor 24 hours after incubation at each treatment (0900 h; Diving-PAM settings: measuring intensity < 0.15 μmol photons m^{-2} s^{-1}, saturating irradiance >4500 μmol photons m^{-2} s^{-1}, saturating width = 0.8 s, gain = 10, damping = 1). The seagrass leaf was attached to the transparent racetrack flume wall using a high powered magnet and the measurement was done through the transparent wall to avoid changes in flow velocity and direction. Photosystem II (PSII) photosynthetic efficiency was investigated using maximum quantum yield (F_V/F_M) and effective quantum yield (Y(II)). The level of photoinhibition (non-regulated heat dissipation yield (Y(NO)) and the capacity for photoprotection (non-photochemical quenching yield (Y(NPQ)) were determined through SSLCs (Kramer et al. 2004; n = 4). The sum of Y(II) + Y(NO) + Y(NPQ) = 1 (Kramer et al. 2004). In addition, there were no relationship between PAM measurement and EC flux; therefore, the PAM measurement was unable to predict the photosynthesis irradiance curve or changes in O_2 concentration generated from EC.

3.2.2 O_2 consumption in seagrass sediment

3.2.2.1 Experimental design

Sediment was collected by hand from a seagrass bed in Fagans Bay (Gosford, New South Wales, Australia; GPS location: -33.435319, 151.324730, Figure 3.2) during low tide, transported to the laboratory where it was sieved through a 3 mm mesh in order to remove shells, rocks, and any macrofauna. Until further application, the

sediment was stored in a container overlaid with aerated seawater at 18°C, pH 8.1, salinity of 28. The sediment was placed in a designated, recessed container (4 cm deep, 40 cm wide, and 90 cm long) in the bottom of a laboratory racetrack flume (Figure 2.15), after which the flume was filled with approximately 1000 L of continuously aerated seawater (Sydney Harbour), and the sediment was left to acclimate for one week. Temperature, pH and salinity of seawater were maintained at 18°C, 8.1 and 30, respectively.

Figure 3.2: Location map of Fagans Bay, Gosford, New South Wales. Australia. Source: Google Earth.

The bare sediment was treated under two scenarios. First, in a variable water velocity scenario, the sediment was exposed to three different velocity treatments (17, 34, and 51 cm s^{-1}; low, medium and high flow, respectively). Each treatment was run for 12 h under constant temperature (18ºC). Second, in a temperature scenario, the sediment was exposed to temperatures of 18, 23, and 28°C. Each temperature was run for 12 h under controlled flow velocity (17 cm s^{-1}). The 24 h acclamation periods were applied to the sediment before starting the experiments in order to stabilise the

sediment-water interface. The water temperature and water velocity was controlled as previously described. The salinity, temperature and dissolved O_2 were monitored throughout the experiment with a multimeter (Multi 3430; WTW, Germany) at a sampling frequency of 1 Hz.

An Eddy Correlation optode system (ECOS; Figure 3.4) was used to measure the O_2 concentration and three dimensional water velocities at high resolution (64 Hz), for a period of 24 hours in each treatment. In order to evaluate the validity of the measured flux rate, at the end of each treatment, 9 O_2 microprofiles, covering the entire sediment surface (3 x 3 arrays), were performed, from which the O_2 flux was calculated (Figure 3.3).

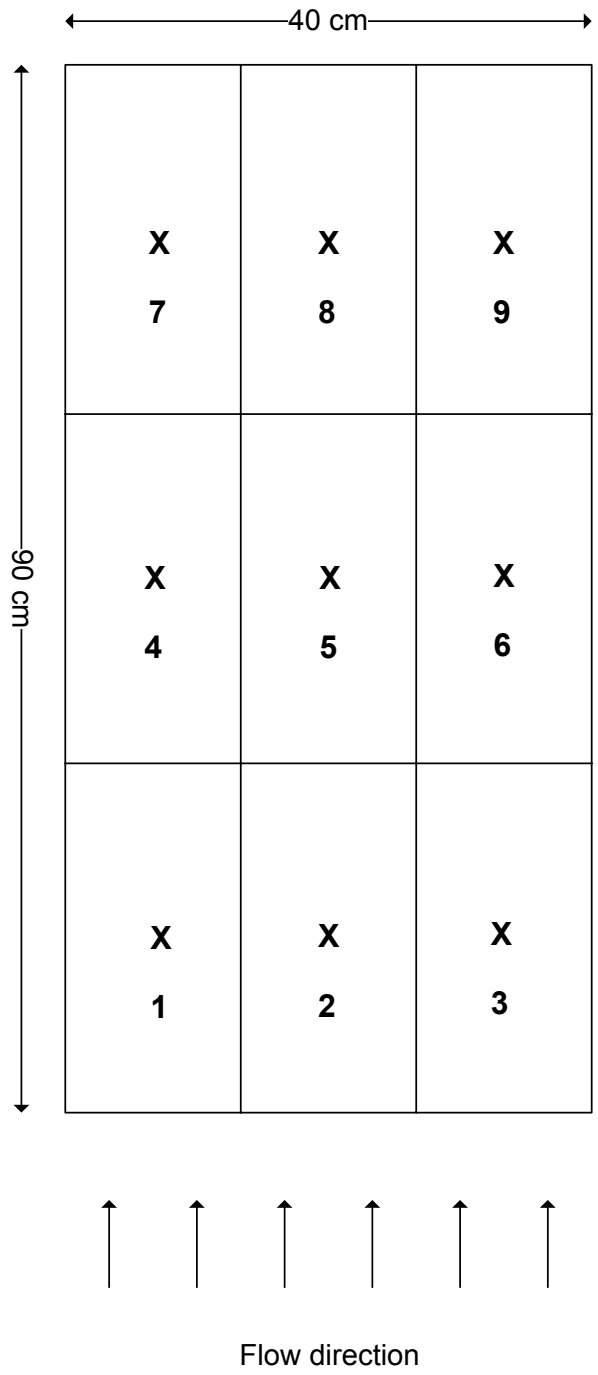

Figure 3.3: The sediment area was divided into 3 x 3 arrays in order to use the O_2 microprofiling technique to measure O_2 fluxes. X indicates the measurement point.

3.2.2.2 Eddy Correlation optode system

The first generation of the Eddy Correlation optode system (ECO1; Unisense A/S, Denmark) used for this study consisted of an acoustic Doppler velocimeter (ADV; Nortek A/S, Norway), an O_2 microoptode (PyroScience GmbH, Germany), and an ECO1 datalogger (Unisense A/S, Denmark) onto which the velocity and oxygen concentration data was recorded. The optode was located 15 cm from the ADV and 5 cm from the sediment surface (Figure 3.4). The ECO1 was programmed to collect data at 64 Hz for 12 hours during each treatment.

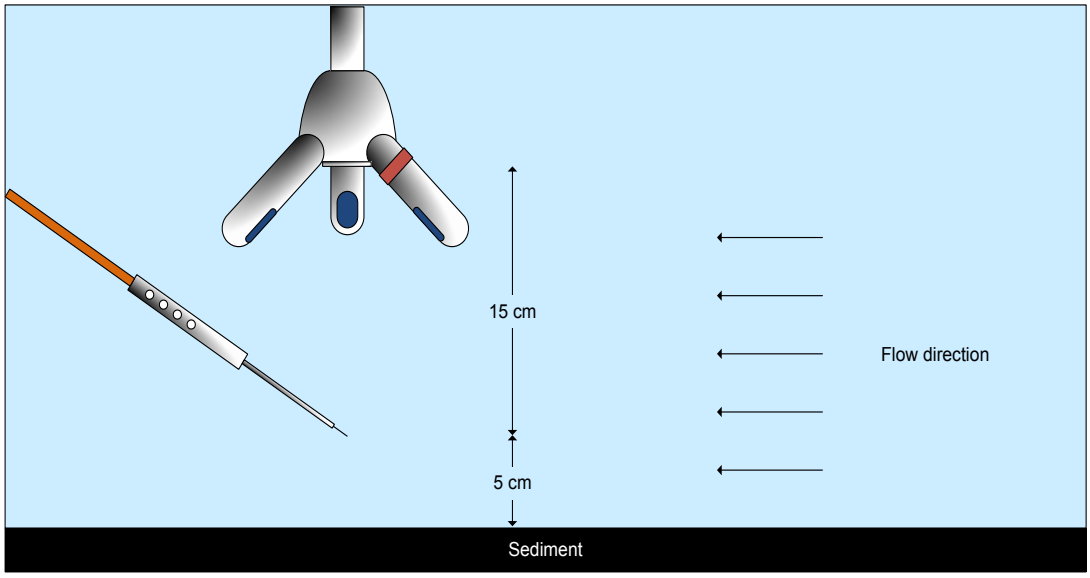

Figure 3.4: The first generation of the Eddy Correlation optode was placed in the laboratory racetrack flume.

The raw data from the ECO1 datalogger were imported into a computer, and converted to readable data using dedicated Eddy Conversion Software (Unisense, Denmark), after which the data was processed by a series of custom scripts programmed in MATLAB (v. 2009b, MathWorks, United States) as well as the EddyFlux GUI 2.6 software (Unisense A/S, Denmark). The custom scripts applied

despiking and coordinate rotation techniques to eddy correlation time series data if needed, and converted the data into eddy fluxes.

3.2.2.3 EC O_2 flux processing techniques

O_2 flux was calculated every 15 min period (burst) for 24 hours. The O_2 eddy flux for each burst is defined as $\overline{w'C'}$ where w' is the fluctuating vertical velocity away from the mean and C' is the fluctuating concentration away from the mean (Berg et al. 2003). Time lag correction in each burst was performed if the time lag (which may occurred due to sensor position) between vertical velocity and O_2 concentration was found. Coordinate rotation was performed to force the mean vertical velocity to zero ($\overline{w} = 0$) to obtain the maximum horizontal velocity.

3.2.2.4 O_2 microprofiling

Microprofiling measurements of O_2 in the sediment were performed at the end of each experiment using a Clark-type O_2 microelectrode (OX-100, Unisense A/S, Denmark) connected to a microsensor multimeter (Unisense A/S, Denmark). The microelectrode had an outer tip diameter of 100 µm, a 90% response time of 8 s and a stirring sensitivity of 1.5%. A linear calibration of the microelectrode was performed at flume temperature in air-saturated seawater and O_2-free seawater (made anoxic by the addition of sodium dithionite). The O_2 microsensor was mounted on a motorized micromanipulator (Unisense A/S, Denmark). The electrode was connected to a multimeter (pico-ampmeter), which in turn was connected to a computer running the Sensor Trace Pro software (Unisense A/S, Denmark). To cover the entire area of the sediment surface (Figure 3.3), a total of nine O_2 concentration profiles were measured for velocity and temperature treatment. The profiles were started

approximately 10 mm above the sediment and the profiles were carried out in 100 μm steps towards and approximately 30 mm into the surface of the sediment. The sediment-water interface was identified from the profile as the depth where the profile first deviated from a straight line (below the boundary layer). This point of the profile was set to 0 μm on all figures.

The local diffusive O_2 flux (J; μmol O_2 m^{-2} d^{-1}), that is, the O_2 uptake rate, was calculated from the measured steady-state O_2 concentration profiles via Fick's first law (Revsbech et al. 1980): $J = -D_0(dC/dz)$ where D_0 is the molecular diffusion coefficient in seawater at a defined experimental salinity and temperature, and dC/dz is the linear slope of the O_2 concentration profile in the diffusive boundary layer (DBL) above the seagrass sediment surface.

3.2.3 Statistical analyses

For any significant differences among treatments and irradiance steps in chlorophyll fluorescence parameters (F_V/F_M, Y(II), Y(NO), and Y(NPQ)) and among techniques (EC and O_2 microprofiling) and flow and temperature treatments in O_2 flux, a two-way ANOVA test was used (SPSS IBM, United States) with a significance level of 95%. Tukey's Honestly Significant Difference post hoc tests were used to determine the statistically distinct groups. Data were transformed using $\log_{10}$ or square root (if the data did not meet the assumptions of normality (Kolmogorov-Smirnov test)) and equal variance (Levene's test). The normality and homogeneity of variance tests were performed using the Kolmogorov-Smirnov test and Levene's test.

3.3 RESULTS

3.3.1 Effect of temperature and light on *Z. muelleri*

Average oxygen flux was greatest at 25°C and was lowest at 21°C under ambient light conditions (400 μmol photon m^{-2} s^{-1}). Oxygen flux was negative in darkness due to respiration of both the seagrass and sediment microbial consortia (Figure 3.5a). Oxygen production was highest at 28 and 31°C (Figure 3.5b); however when the light was turned off, oxygen production rapidly decreased, suggesting that post-illumination enhanced respiration (PIER) occurred, resulting in the substantial removal of oxygen and a rapid switch in microbial activity in the surface layer from aerobic to anaerobic condition (Figure 3.5a, 3.5b, and 3.5c). Moreover, Figure 3.5a showed that the positive fluxes occurred while the bulk oxygen concentration was decreased. This may either reflet low flow in the non-mixing O_2 in water column or an effect of the air-water gas exchange. Moreover, Figure 3.5b also showed that the bulk oxygen concentration began decline around 18:30, about 2 h before the transition to darkness at 20:30. This sugests that photoinhibition occurred after 18:30 (Ralph et al. 1998).

Light intensity had little effect on the oxygen flux (Figure 3.6a), while oxygen production was greatest at the 250 μmol photons m^{-2} s^{-1} treatment (Figure 3.6b). The lowest oxygen production and the highest respiration were observed at the 150 μmol photons m^{-2} s^{-1} treatment. PIER was found in all light treatments; however, levels of PIER accumulated with increasing light intensity.

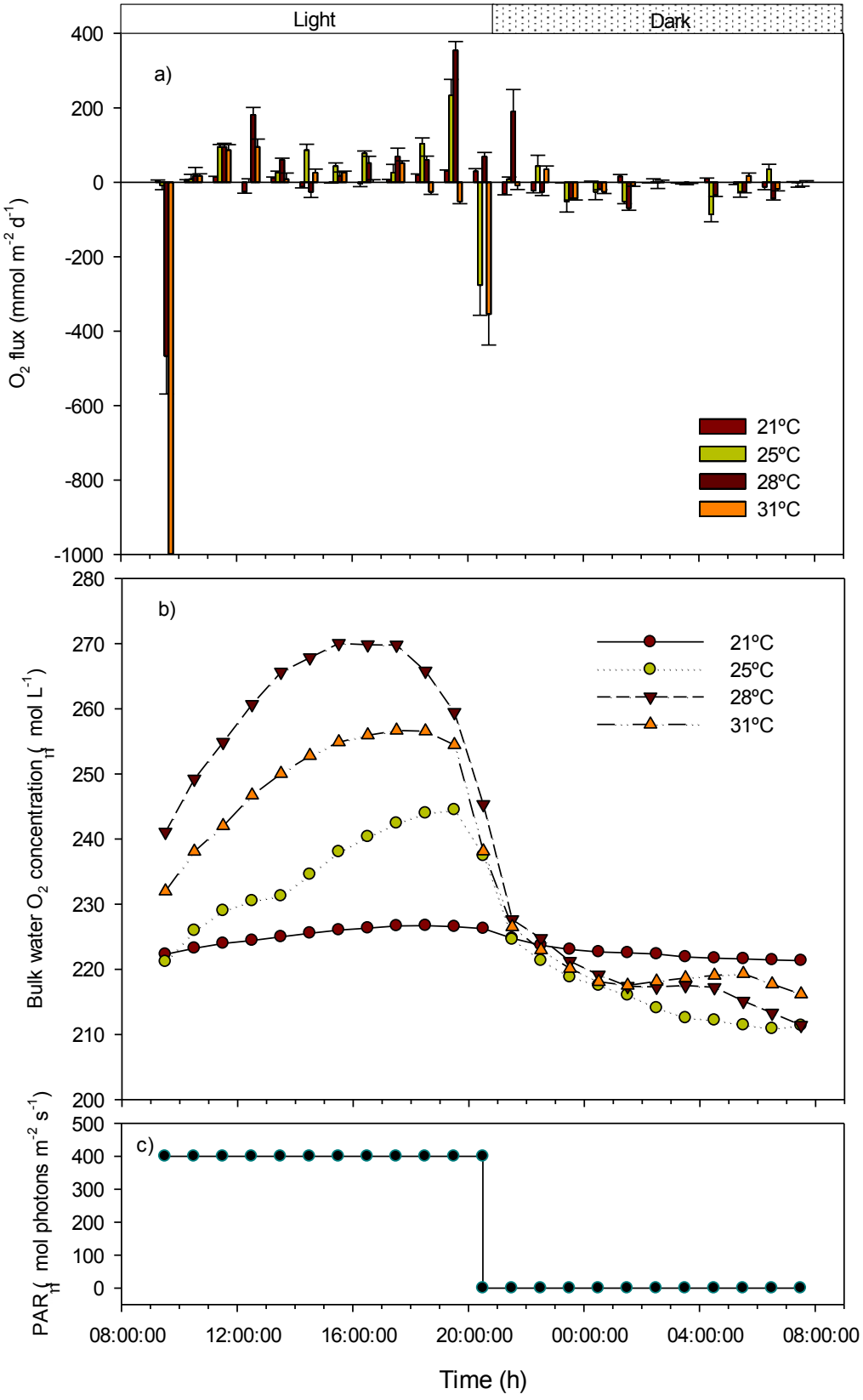

Figure 3.5: Effects of temperature on oxygen fluxes (a) and oxygen concentration (b) of *Z. muelleri* under light and dark conditions (c).

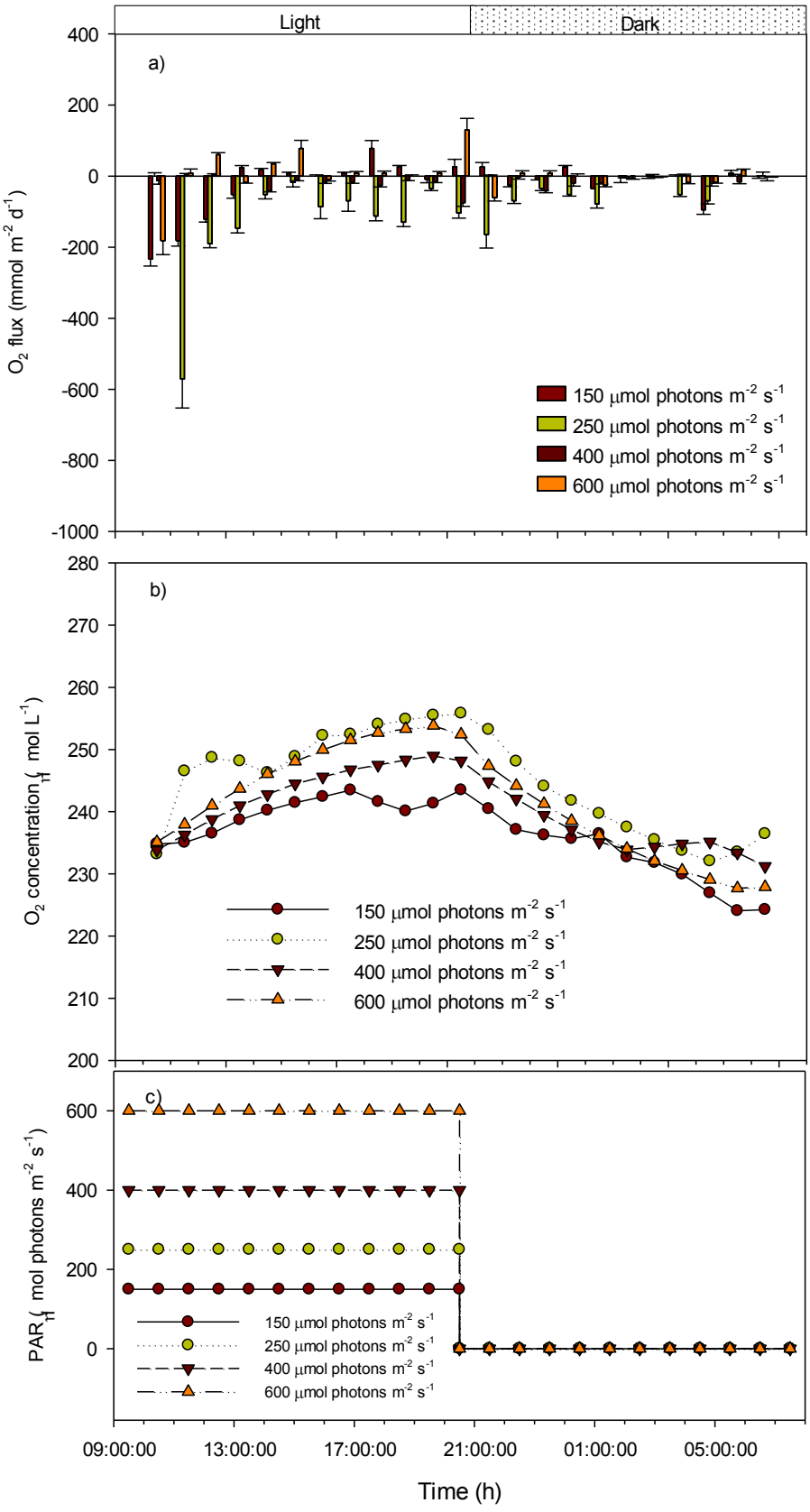

Figure 3.6: Effect of light on oxygen fluxes (a) and oxygen concentration (b) of *Z. muelleri* in light and dark conditions(c).

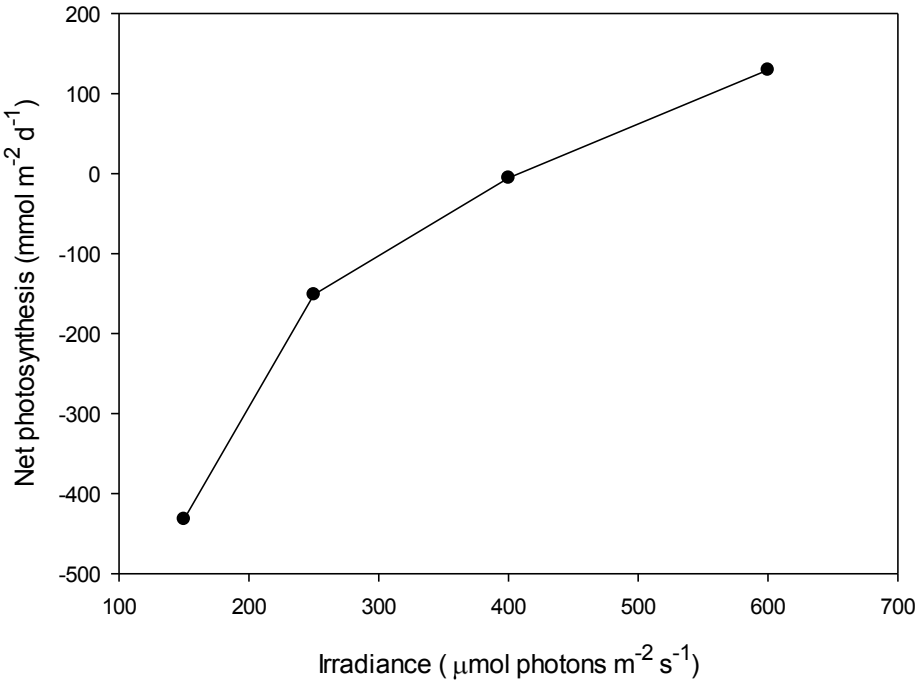

Figure 3.7 The Photosynthesis – Irradiance curve (P-I curve) generated from O_2 flux vs Irradiance data in Figure 3.6

Figure 3.7 showed that increasing the irradiance led to an increase in net photoshynthesis. However, this P-I pattern was unable to indicate the EC system reliability as there was no relationship between the P-I curve generated from EC O_2 flux and the P-I curve generated from PAM measurement.

Steady state light curves showed no significant difference in maximum quantum yield of PSII (F_V/F_M) between temperature treatments (p = 0.160; Figure 3.8a). Effective quantum yield (Y(II)) was significantly greater at 25°C than at other temperatures (p <0.001; Figure 3.8b) and Y(II) significantly decreased with increasing actinic light intensity (p < 0.001; Figure 3.8b). Non-regulated heat dissipation yield (Y(NO)) was significantly higher at 28 and 31°C (p < 0.001; Figure 3.8c). Non-photochemical quenching yield (Y(NPQ)) was highest at 25°C (p < 0.001; Figure 3.7d) and accumulated with increasing actinic light intensity in all temperature treatments (p < 0.001; Figure 3.8d).

There was no significant difference in F_V/F_M among light treatments (p = 0.171; Figure 3.9a). Y(II) was significantly higher at 150 and 250 μmol photons m^{-2} s^{-1} treatments (p < 0.001; Figure 3.9b). Y(NO) was greatest in 400 and 600 μmol photons m^{-2} s^{-1} treatments (p =0.003; Figure 3.9c). There was no significant difference in Y(NPQ) between light treatments (p = 0.172; Figure 3.9d), whereas Y(NPQ) increased with increasing PAR in all light treatments (p < 0.001; Figure 3.9d).

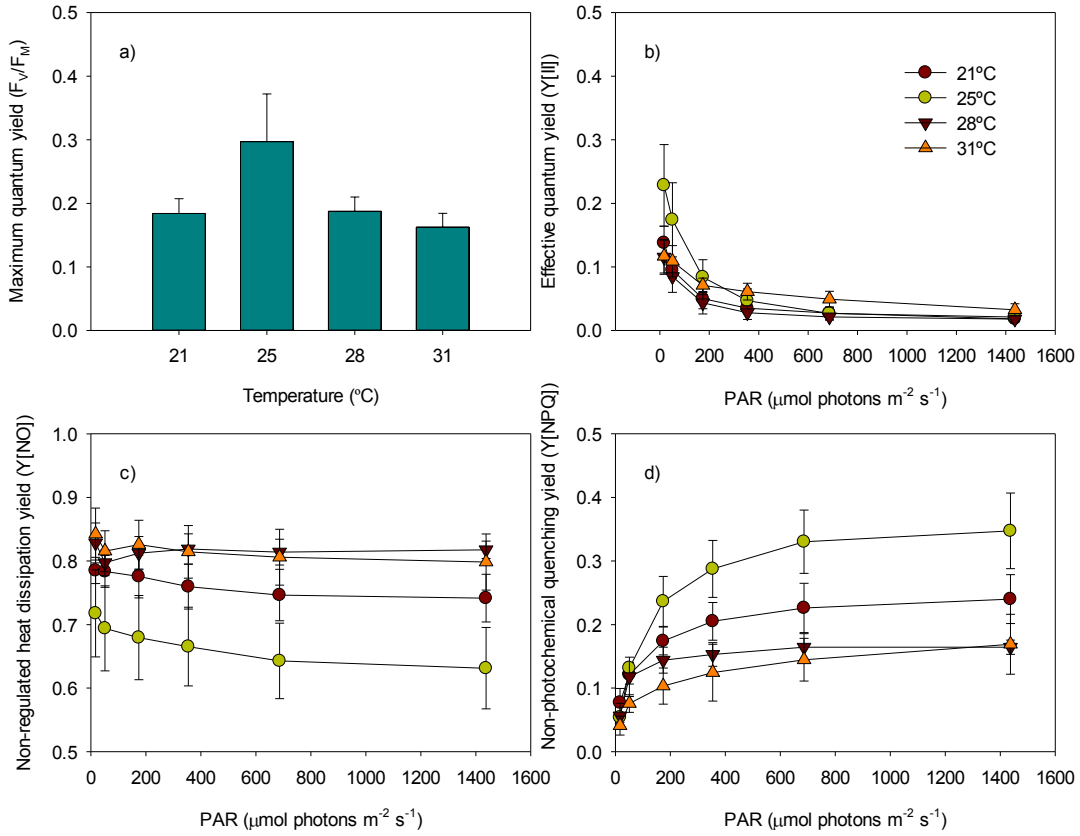

Figure 3.8: Seagrass health results according to temperature treatment; a) Maximum quantum yield ($F_V/F_{M)}$, b) Effective quantum yield (Y(II)), c) Non-regulated heat dissipation yield (Y(NO)), and d) Non-photochemical quenching yield (Y(NPQ)). Data represent mean + SE (n =4).

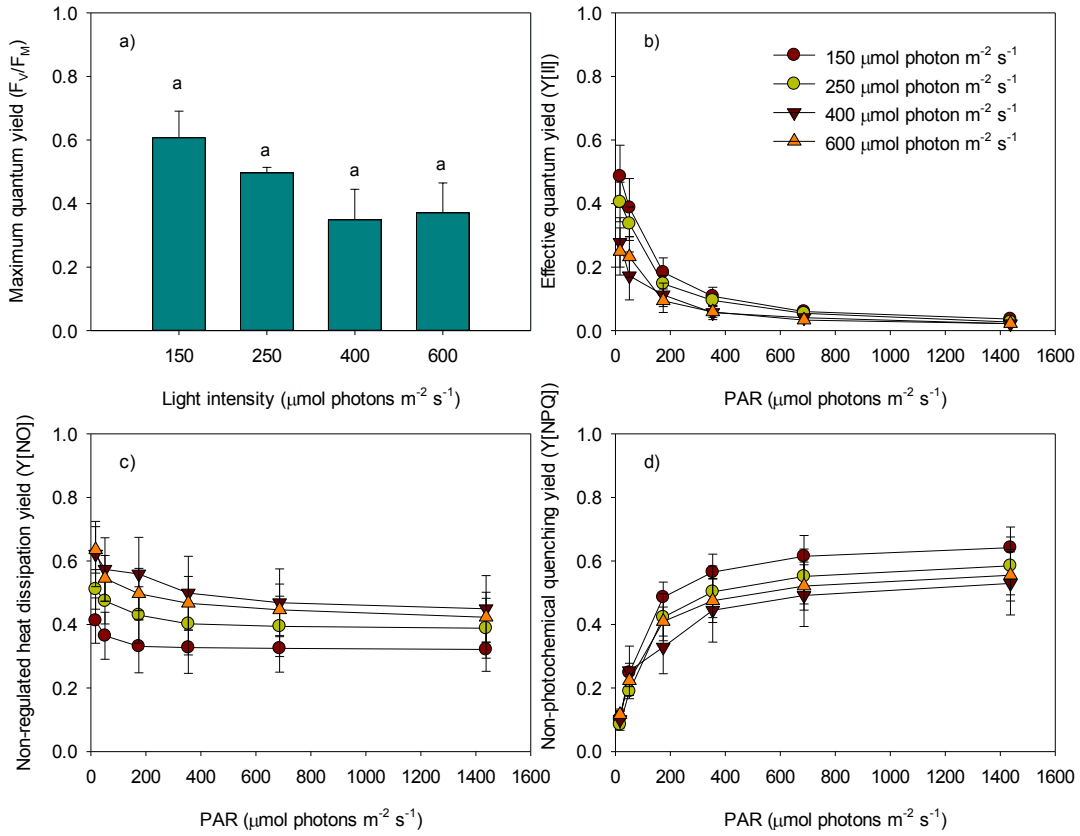

Figure 3.9: Seagrass health results according to light treatment; a) Maximum quantum yield (F_V/F_M), b) Effective quantum yield (Y(II)), c) Non-regulated heat dissipation yield (Y(NO)), and d) Non-photochemical quenching yield (Y(NPQ)). Data represent mean + SE (n =4). [a] represent significant difference.

3.3.2 O_2 consumption in seagrass sediment

The results from Eddy Correlation optode system (ECO1) showed that there was sediment O_2 consumption as shown by negative flux, and sediment respiration was greater than sediment production during the experimental period in darkness in both flow and temperature treatments (Figure 3.10 and 3.13). In different flow velocity treatments, sediment O_2 consumption measured hourly from the first generation of the Eddy Correlation optode system (ECO1) was highest at 51 cm s^{-1}, while the lowest of sediment O_2 consumption was found at 17 cm s^{-1} (Figure 3.10). Sediment

O_2 consumption for each hour was significantly higher at high flow than medium and low flow (p <0.01; Figure 3.10). There were no significant differences in sediment O_2 flux between hours of measurement at each flow treatment (p = 0.155; Figure 3.10).

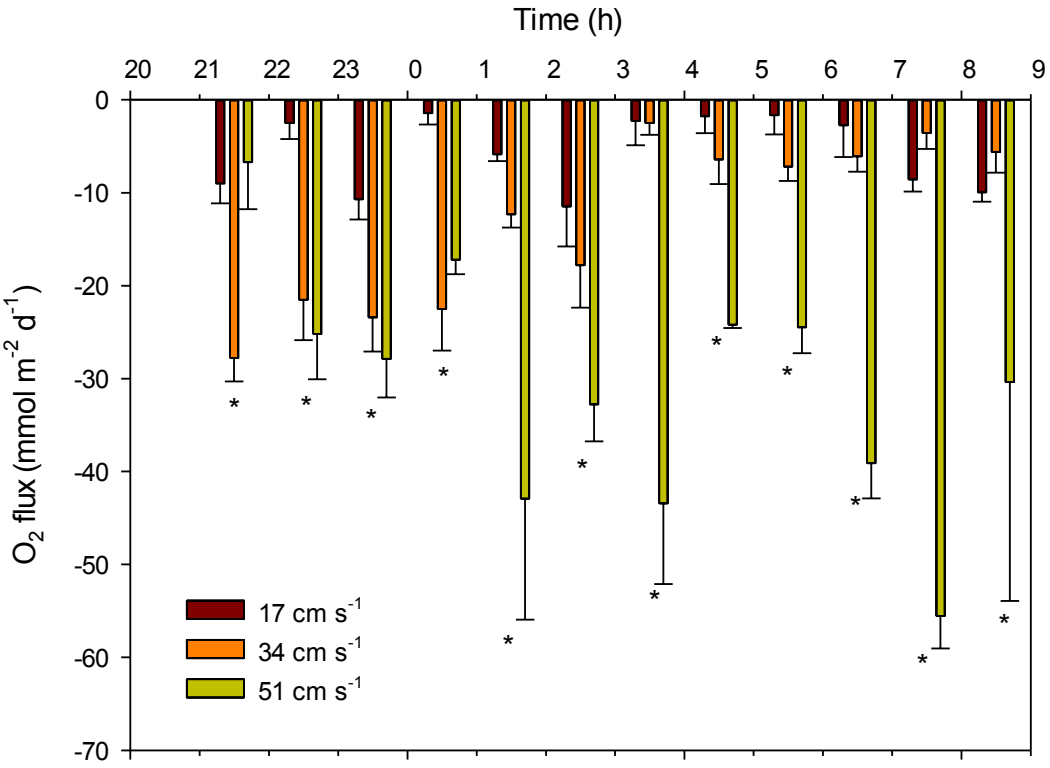

Figure 3.10: Sediment O_2 flux in darkness measured hourly using the first generation of the Eddy Correlation optode system (ECO1) at low (17 cm s^{-1}), medium (34 cm s^{-1}) and high flow (50 cm s^{-1}) from 21:00 to 09:00 under constant temperature (18°C). Data represent mean + SE (n = 4). *represent significant differences (p < 0.05).

O_2 profiles from O_2 microprofiling system in sediment at 17, 34 and 51 cm s^{-1} showed a significant decrease in O_2 concentration from 210.6 ± 7.7, 206.0 ± 7.2 and 215.0 ± 1.7 mmol m^{-2} d^{-1} at 1000 mm above the sediment surface to 0.1 ± 0.0, 1.4 ± 4.0 and -1.3 ± 1.7 at 3400 mm below sediment surface, respectively (Figure 3.11).

Average sediment O_2 consumption from 12 hour measurement using ECO1 and O_2 microprofiling system was significantly greatest at 51 cm s^{-1}, followed by 34 and 17 cm s^{-1}, respectively ($p < 0.001$ and $p < 0.001$, respectively, Figure 3.12). There were no significant differences in sediment O_2 flux between the ECO1 and O_2 microprofiling system measurements at each flow velocity ($p = 0.693$; Figure 3.12).

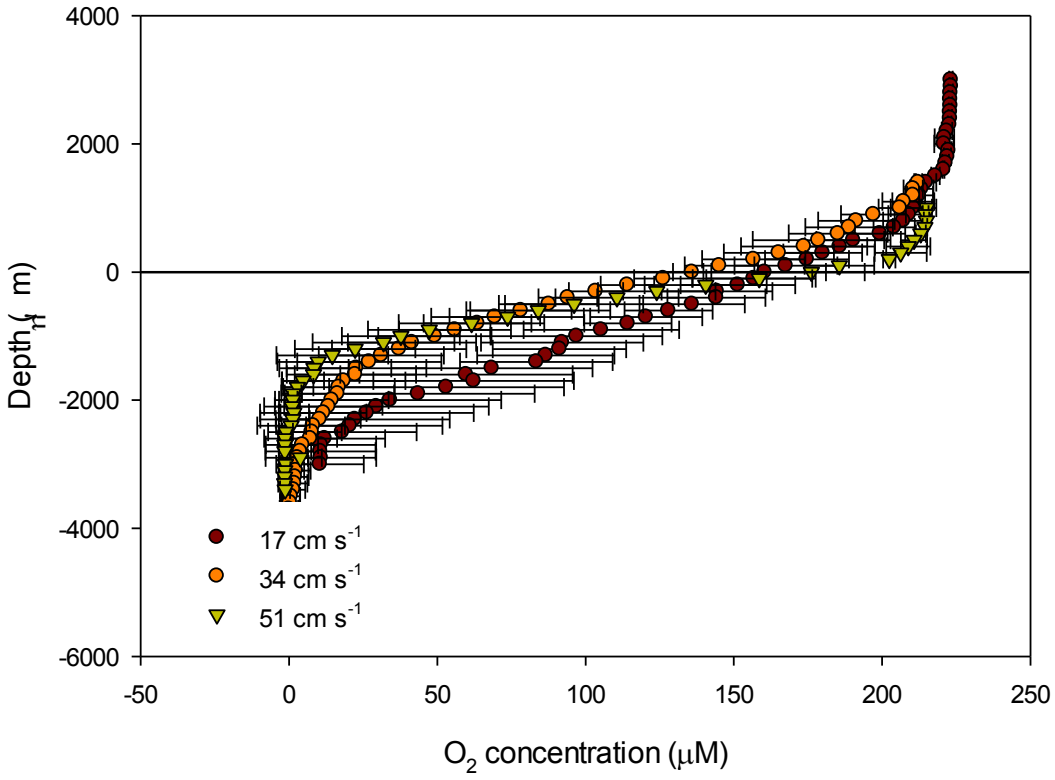

Figure 3.11: O_2 profiles at flow velocity of 17, 34 and 51 cm s^{-1} and water temperature at 18ºC. Data represent mean + SD ($n = 9$).

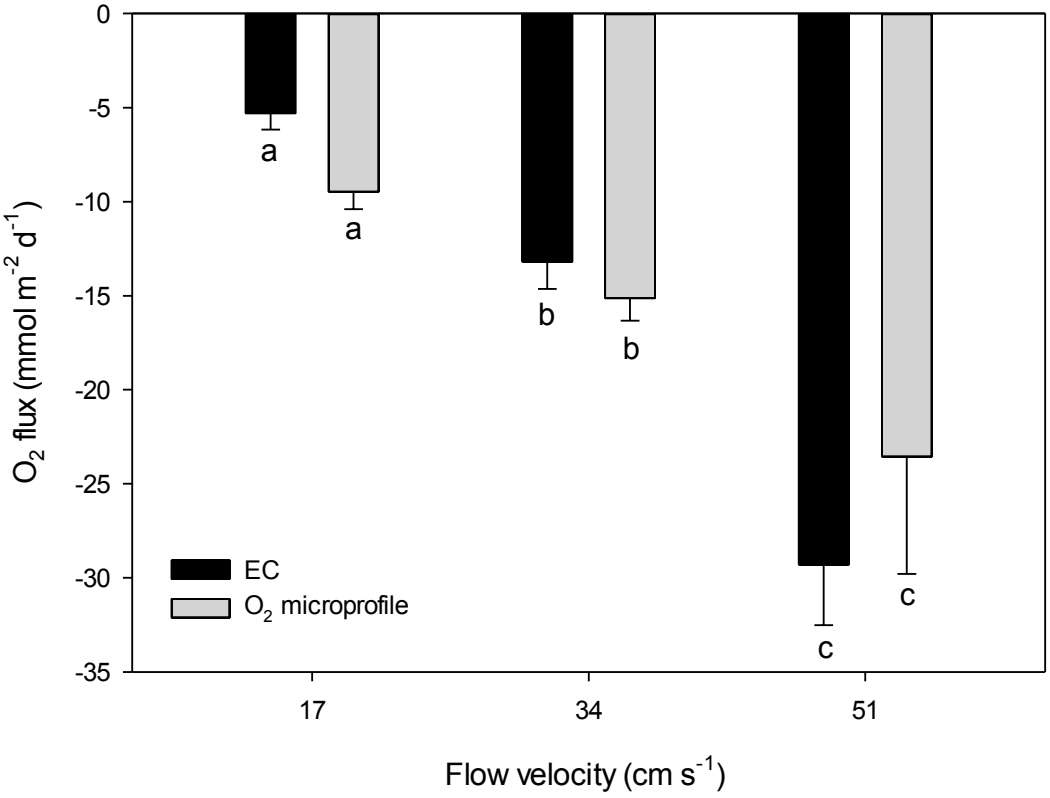

Figure 3.12: The comparison of average sediment O_2 flux from 17, 34 and 51 cm s^{-1} flow treatment measured in darkness using the first generation of Eddy Correlation optode (ECO1) system and O_2 microprofiling system over a 12 hour period. Data represent mean + SE (n =12). [a, b, c] represent significant differences ($p < 0.05$; two-way ANOVA).

In the variable temperature scenario, sediment O_2 consumption was measured hourly using the first generation of the Eddy Correlation optode system (ECO1) and was significantly higher at 28ºC than that at 23ºC and 18ºC ($p < 0.001$; Figure 3.12). There were no significant differences in sediment O_2 flux between hours of measurement at each temperature treatment ($p = 0.068$; Figure 3.13).

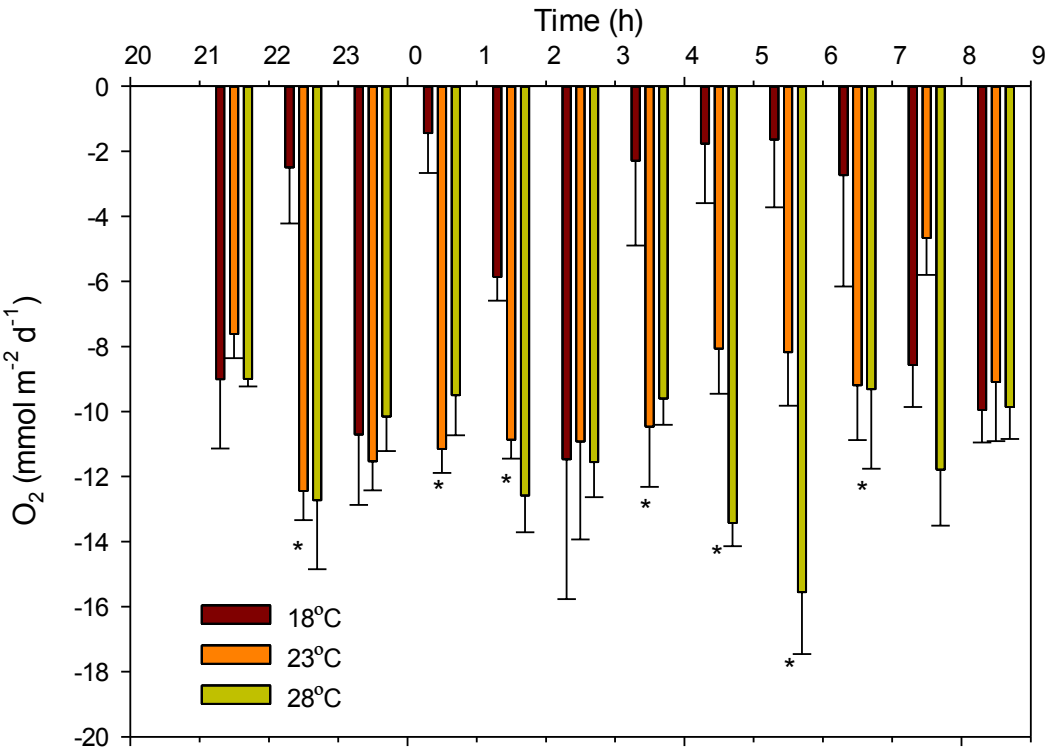

Figure 3.13: The sediment O_2 flux in darkness measured hourly using the first generation of Eddy Correlation optode system (ECO1) from 21:00 to 09:00 at 18, 23 and 28°C under constant flow velocity. Data represent mean + SE (n =4). * represent significant differences ($p < 0.05$).

O_2 profiles from the O_2 microprofiling system in sediment at 18, 23 and 28°C showed a significant decrease in O_2 concentration from 214.8 ± 3.5, 214 ± 2.0 and 214.9 ± 2.5 mmol m^{-2} d^{-1} above 1400 mm over sediment surface to 0.0 ± 0.0, -1.7 ± 0.3 and -1.5 ± 0.1 at 3500 mm depth of sediment, respectively (Figure 3.14). Average sediment O_2 consumption from 12 hour measurement using ECO1 was significantly greater at 23 and 28°C than that at 18°C, respectively ($p < 0.001$; Figure 3.14), while the O_2 consumption from the O_2 microprofiling system was significantly greater at 28°C than that at 18 and 23°C ($p < 0.001$; Figure 3.15). There were no significant differences in sediment O_2 flux between ECO1 and O_2 microprofiling

system measurement at all temperature treatments (p = 0.991), except at 18°C (p < 0.001; Figure 3.15).

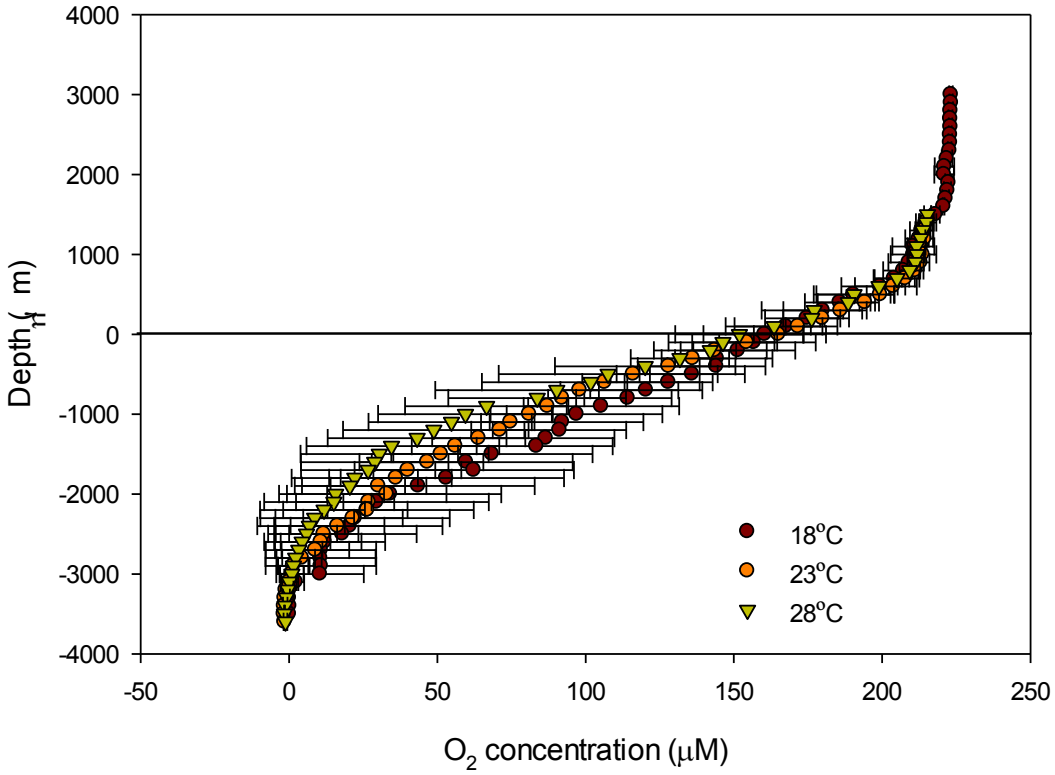

Figure 3.14: O_2 profiles at temperatures of 18, 23 and 28°C and flow velocity of 17 cm s^{-1}. Data represent mean + SD (n = 9).

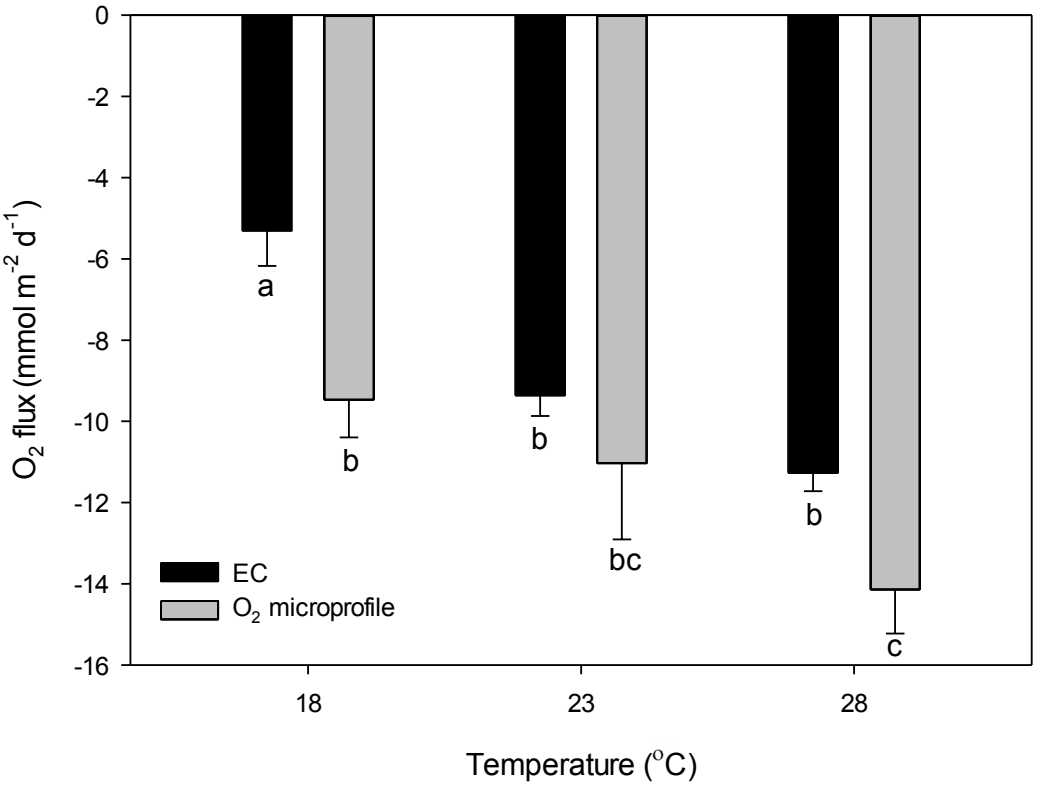

Figure 3.15: Comparison of average sediment O_2 flux in 18, 23 and 28°C temperature treatment measured in darkness using the first generation of Eddy Correlation optode (ECO1) system over a 12 hour period and O_2 microprofiling system. Data represent mean + SE (n = 12). [a, b, c] represent significant differences ($p < 0.05$; two-way ANOVA).

3.4 DISCUSSION

To our knowledge, this is first investigation on the effect of light and temperature using the Eddy Correlation technique in combination with chlorophyll *a* fluorescence in a controlled environment. This study showed, for the first time, a comparison of sediment O_2 flux measurements within a laboratory flume between the Eddy Correlation technique and O_2 microprofiling technique in order to demonstrate the reliability and limitations of the Eddy Correlation system, particularly using the first

generation of the Eddy Correlation optode system (ECO1). This study demonstrated that photosynthesis of *Z. muelleri* from Lake Macquarie is driven by light availability and temperature, and that oxygen flux and oxygen production could be monitored using the Eddy Correlation microelectrode system. It also demonstrated that the rate of O_2 consumption of sediment collected from Fagans Bay is driven by flow velocity and temperature. This study additionally proved that the sediment O_2 flux measured by ECO1 and O_2 microprofiling showed similar results.

3.4.1 Effect of temperature and light on *Z. muelleri*

Temperature and light availability are known to affect seagrass photosynthesis, abundance, growth rate, reproduction and survival of seagrasses (Short and Neckles 1999; Ralph and Gademann 2005; Moore and Short 2006). In addition, thermal tolerance and optimal temperature and light range for photosynthesis, respiration and growth vary among different species (Short and Neckle 1999). Chl *a* fluorescence results have shown that photosynthetic efficiency (Y(II)) of *Z. muelleri* increased with accumulating temperature to 25°C and gradually decreased at 28 and 31°C, suggesting that 25°C might be an optimal temperature for photosynthesis for this species from Lake Macquarie. Y(NO) was highest at 28 and 31°C indicating photoinhibition occurred (Campbell et al. 2006), while Y(NPQ) was highest at 25°C which may indicate increased photoprotection at this temperature. These results are generally consistent with other studies that show damage to seagrass photosynthetic efficiency under higher temperature (Ralph 1998; Campbell et al. 2006; York et al. 2013). Increased temperature is likely to damage PSII reaction centres, possibly by injuring the D1 protein and disrupting the thylakoid membrane stability (Allakhverdiev et al. 2008). The closure of PSII reaction centres also leads to

chloroplast dysfunction (Campbell et al. 2006). Previous studies on *Z. muelleri* from Lake Macquarie showed that long-term increases in temperature (42 days at 32°C) led to mortality and suggest that thermal threshold for Lake Macquarie seagrass survival is between 30 and 32°C (York et al. 2013).

Light generally influences photosynthesis by increasing rates of photosynthesis with increasing light until reaching saturation point (Hemminga 1998). This study, however, showed that irradiance at 150 and 250 μmol photons m^{-2} s^{-1} may be optimum for *Z. muelleri* from Lake Macquarie as indicated by the highest Y(II) and lowest Y(NO) at this irradiance. Increase Y(NO) at 400 and 600 μmol photons m^{-2} s^{-1} treatments indicates that photoinhibition and the down-regulation of photosynthesis occurred at higher irradiance (Hanelt et al. 1993), possibly due to structural change and damage to D1 proteins in the reaction centre of PSII (Aro et al. 1993; Marin-Guirao et al. 2013). This result is consistent with the other studies that show a decrease in photosynthetic efficiency and an increase in photoinhibition at higher irradiance (Ralph 1999). There were no significant changes in F_V/F_M over temperature and light treatments, while significant differences in Y(II) were found. This may be due to the reduced sensitivity to high-light or high-temperature stress of F_V/F_M (Ralph 1999).

This study showed the effect of temperature and light individually; however, it is suggested that optimal temperature for photosynthesis varies with irradiance due to the need to maintain positive carbon balance, which means seagrasses at higher temperatures need more light for photosynthesis or more time at photosynthesis-saturating irradiances than seagrasses at lower temperatures. Therefore, photosynthesis in seagrass is more efficient in low light and high temperature

conditions (Masini et al. 1995; Lee et al. 2007; Collier et al. 2011). On the other hand, seagrasses living in higher light intensities that induce photoinhibition may be less tolerant to higher temperatures due to thermal stress (Ralph 1999). Therefore, further investigation on the combined effect of light and temperature on seagrass photosynthesis should be considered.

3.4.2 Limitations and reliability of ECE

In seagrass meadows, positive fluxes, which occurred when the oxygen production is greater than respiration due to photosynthetic activity, were expected to occur during daylight conditions, whilst negative fluxes, where the respiration is greater than production, appear during darkness (Hume et al. 2011; Long et al. 2013; Rheuban et al. 2014) and oxygen metabolism is slower at night than during the day (Kemp et al. 1987). Previous studies showed that increased water temperature leads to an increase in photosynthesis (until optimum temperature) and respiration in seagrasses (Bulthuis 1983; Marsh et al. 1986; Perez and Romero 1992; Masini and Manning 1997; Moore et al. 1997). Other studies on *Z. noltii* and *P. oceanica* showed that rising temperature over optimum temperature led to a reduction in photosynthetic capacity (Massa et al. 2009; Marba and Duarte 2010). Generally, respiration rates increase more than photosynthesis rates at progressively higher temperatures, thus leading to a reduction in net photosynthesis (Lee et al. 2007). Therefore, photosynthesis and oxygen flux would be highest at the optimum temperature and irradiance. In addition, the down-regulation of photosynthesis and photoinhibition under high temperature and light can be reflected in oxygen evolution (Häder et al.1996). Our results from Chl *a* fluorescence showed that the optimal temperature and irradiance for photosynthesis for *Z. muelleri* from Lake Macquarie are 25°C and

150-250 μmol photons m^{-2} s^{-1}, respectively. Therefore, the oxygen flux and oxygen concentration results from the Eddy Correlation technique would be consistent with Chl *a* fluorescence results (Francklin and Badger 2001; Longstaff et al. 2002).

This study, however, showed random fluctuation of the oxygen fluxes during light and dark conditions in both temperature and light treatments (Figure 3.5a and 3.6a), and the results were not consistent with other studies (Marsh et al. 1986; Bulthuis 1987; Perez and Romero 1992; Lee et al. 2007; Massa et al. 2009; Marba and Duarte 2010; Hume et al. 2011). These events may be caused by the small size of the laboratory racetrack flume footprint (Berg et al. 2007) along with the density of the seagrass patch. The negative fluxes which occurred during light conditions may be a reflection of the poor seagrass health during the experiment where the F_V/F_M was 0.2 instead of 0.7 for the healthy seagrass (Figure 3.8a). The positive flux, which occurred during darkness, may be caused by the electrical noises which can contaminate the oxygen sensor measurements (McGinnis et al. 2011). Although all of electrical equipment of ECE1 was grounded in order to reduce background electrical noises which may alter eddy flux measurements, the electrical noise could randomly occur during the experiment and was not possible to remove due to the nearby electrical equipment. Also, it will be difficult to assess whether the noise events occurs over very short period of time. In addition, low mean flow (7 cm^{-1}) used in this study may lead to low turbulence in the laboratory racetrack flume. Low turbulence, when oxygen is unable to mix well into the bulk water, may lead to inaccurate oxygen flux measurements (Burba 2013). Furthermore, during experiments, there were nearby construction sites (2012-2014) which lead to significant vibrations impacting the oxygen microelectrode. These vibrations may

alter the oxygen measurement measured by the oxygen microelectrode, because the oxygen microelectrode is very sensitive (Karande 2007).

3.4.3 Flow and temperature influences on sediment O_2 uptake

Flow velocity and temperature are known to play an important role in sediment O_2 uptake (Hargrave 1969; Jørgensen and Revsbech 1985; Arnosti et al. 1998; Berg et al. 2003). Flow velocity has an effect on the thickness of diffusive boundary layers (DBL), and therefore affects the rate of sediment O_2 uptake (Jorgensen and Revsbech 1985; Jørgensen and Marais 1990). The O_2 profiles from microprofiling clearly showed that increases in flow velocity reduced the DBL thickness as shown by an increase in O_2 flux (negative flux; Figure 3.11 and 3.12) which is, in turn, due to the fact that the thickness of DBL depends on the flow velocity of fluid and surface roughness (Jorgensen and Marais 1990). Therefore, sediment O_2 uptake measured by the O_2 microprofiling system had the highest consumption rate at highest flow, as well as sediment O_2 uptake as measured by the ECO1 (Figure 3.12). This study is consistent with a previous study on the O_2 flux in deep ocean sediment that showed net consumption at increasing depths (Berg et al. 2009)

Temperature also plays an importance role in O_2 uptake of sediment (Hargrave 1969; Liang et al. 2003). Higher temperature leads to not only increased microbial metabolism in sediment, but also increases the population dynamics (e.g., composition and density) of microbes (Liang et al. 2003). Measurements using the ECO1 and O_2 microprofiling systems showed that the O_2 uptake (negative flux) increased when increasing temperature from 18°C to 23 and 28°C, resulting in higher sediment O_2 uptake (Figure 3.15). This result is consistent with previous

studies showing that temperature influences O_2 uptake in sediment (Iannotti et al. 1993; Liang et al. 2003).

This study also showed that flow had more of an effect on O_2 flux than temperature. A previous study showed that the microbial activity rapidly increased after 50 hours of incubation at 22°C (Liang et al. 2003). This may explain the non-significant difference in sediment O_2 consumption between 23 and 28°C in this experiment which were incubated for only 36 hours. Longer incubation periods (>50 hours) in this experiment may show significant differences in O_2 consumption between 23 and 28°C due to an increase in the microbial population dynamics.

3.4.4 Comparison of sediment O_2 uptake measurement using ECO1 and O_2 microprofiling system

At medium and high flow conditions, the sediment O_2 uptake measured by ECO1 and O_2 microprofiling were not significantly different (Figure 3.12), indicating that the O_2 was well-mixed (Berg et al. 2003; Burba 2013). The well-mixed O_2 in the water column allow ECO1 to be able to capture all gas flux. However at 18°C and 17 cm s^{-1} treatment (low flow, low temperature) and temperature scenario (18, 23, 28°C at 17 cm s^{-1} treatment), the average O_2 flux between ECO1 and microprofiling systems was significantly different (Figure 3.15). This may indicate that the ECO1 which measured the O_2 using eddy turbulence (advection) provided an under-estimation of O_2 at low flow velocity due to poor-mixing, indicating that there was low turbulence during deployment (Berg et al. 2003; Burba 2013). This demonstrates the limitation of ECO1 in capturing small fluxes at low flow (< 50 mmol m^{-2} d^{-1}; Berg et al. 2003; Berg et al. 2009). Our results in this controlled environment support field-studies that found no significant differences in O_2 flux measurement among EC

system, benthic chamber and microprofiler in deep-sea sediment (Berg et al. 2009). However, the EC system focuses on flux measurements at a community level, while the benthic chamber and microprofiler systems represent the flux over smaller areas (Berg et al. 2003; Berg et al. 2009).

3.5 CONCLUSION

3.5.1 Temperature and light have an effect on photosynthetic efficiency, photoinhibition and capacity for photoprotection in *Z. mulleri* which is consistent with the findings from Ralph 1998; Campbell et al. 2006 and York et al. 2013. Optimal temperature and light for photosynthesis for this temperate seagrass is 25°C and 150-250 μmol photons m^{-2} s^{-1}, respectively.

3.5.2 Flow velocity and temperature have an important role on sediment O_2 flux.

3.5.3 The eddy correlation microelectrode system (ECE) has a potential to quantify oxygen flux and oxygen production in seagrass meadows at different light and temperature conditions within a controlled-flow environment. However, this EC system is unreliable as there were random fluctuations of the oxygen fluxes during light and dark conditions in both temperature and light treatments, resulting in inconsistent with Chl *a* fluorescence data due to the fact that the EC O_2 flux measurements were affected by electrical noise, low flow velocity and the sensitivity of microelectrode.

3.5.4 This study demonstrates that the ECO1 may have limited sensitivity when deployed in low flow environments (<17 cm s^{-1}) which might result in unreliable flux estimates results.

3.5.5 The accuracy and precision of ECE depends on both the prevailing flow conditions and surrounding environment (e.g., electrical instrumentation),

while the accuracy and precision of ECO depends only on flow condition. Data processing and data interpretation for ECE and ECO are similar and both systems are unable to have a replication. Even though ECE has more sensitivity than ECO (lower sensor response time) and higher sensor resolution (64 Hz for ECE and 16 Hz for ECO), the ECO provides more robustness over ECE which will allow ECO to be used in more extreme environments with greater ease of use.

CHAPTER 4:

FIELD VALIDATION OF OXYGEN FLUX MEASUREMENTS USING ECE AND ECO IN THE TWEED RIVER, MORETON BAY AND HERON ISLAND

4. FIELD VALIDATION OF OXYGEN FLUX MEASUREMENTS USING ECE AND ECO IN THE TWEED RIVER, MORETON BAY AND HERON ISLAND

4.1 INTRODUCTION

The eddy correlation technique relies on simultaneously measuring the fluctuating vertical velocity of water and corresponding fluctuating oxygen concentration in the water column above the seafloor (5–30 cm) at a high temporal resolution (>2 Hz). From these data, the dissolved oxygen (DO) flux between a benthic community and the overlying water can be estimated (Berg et al. 2003). While eddy correlation systems are more expensive and are also technically more challenging to use than traditional flux methods, they do have several significant advantages (Kuwae et al 2006). Measurements can be made over vegetated (Hume et al. 2011) or permeable sediments (Reimers et al. 2012), as well as over hard surfaces (Glud et al. 2010) such as coral reefs (Long et al. 2013) or even mussel beds under *in situ* conditions where there is no disturbance to the natural light and hydrodynamic conditions. Further, the ‘‘footprint’’ (the area of the sediment surface that contributes to the flux) covers a relatively large area (typically >100 m^2) and more realistically integrates spatial heterogeneity inherent in benthic ecosystems than the replications from *in situ* chamber or core incubations (Berg et al. 2007). The high temporal resolution of the EC measurements allows us to capture short-term variations in benthic fluxes that are usually triggered by rapid variations in light and/or changing local hydrodynamic forcing (Berg and Huettel 2008).

Boundary layer microsensor techniques have been applied to the estimation of O_2 flux measurement at micro-scale in order to investigate O_2 changes in the diffusive

boundary layer (DBL) (Silva et al. 2009). The results of O_2 flux measurements are usually represented as the flux across sediment-water interface (SWI) in very small areas (Silva et al. 2009). This technique has very high resolution and accuracy, and can be used to measure the O_2 flux in a very small area (< 10 cm^2). However, this flux cannot be extrapolated to represent larger areas (Berg et al. 2009; Silva et al. 2009).

In this chapter, the investigations of O_2 fluxes in marine habitats have been performed using an Eddy Correation system. The results of O_2 flux measurements in the Tweed River (New South Wales), Moreton Bay (Queensland), and Heron Island (Queensland) are presented. This study will cover the application of EC in an estuarine and open water environment comprising seagrass beds, bare sediment and benthic microalgae. The eddy correlation and microsensor techniques are used to evaluate the O_2 flux of marine and estuarine benthic organisms such as seagrass, benthic microalgae, and microbes and validate the reliability of eddy correlation techniques when using in the field.

4.2 MATERIALS AND METHODS

4.2.1 Study Sites

Tweed River

The first generation of the Eddy Correlation microelectrode system (ECE1; Unisense A/S, Denmark) was deployed in the Tweed River, Coolangatta, New South Wales from 28 February 2011 – 4 March 2011 in order to investigate the O_2 flux in seagrass beds located in an estuarine environment. The ECE1 was deployed at 2 study sites comprised of seagrass patches at approximately 5 m x 20 m (TWD1, GPS location: -

28.191867º, 155.529917º) and 5 m x 60 m (TWD2, GPS location: -28.191117º, 153.522317º) (Figure 4.1, 4.2, and 4.3; Table 4.1).

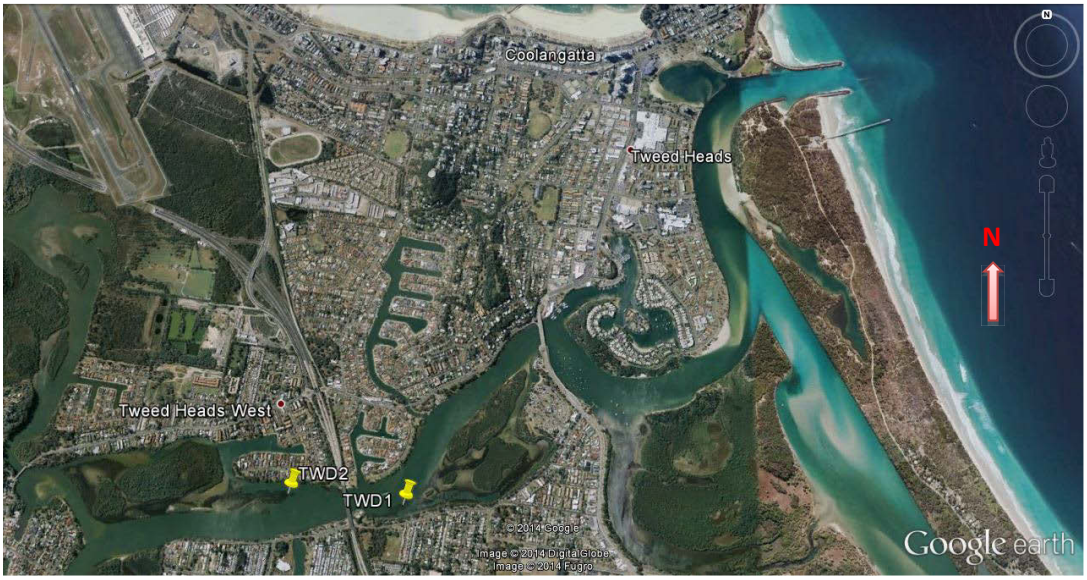

Figure 4.1: Location map of deployment sites in the Tweed River, Coolangatta, New South Wales.

Table 4.1: Summary of location, instruments, site name, GPS location and date of deployment.

Location	Instrument	Site name	GPS	Date
Tweed River, NSW	ECE1	TWD1	-28.191867º, 155.529917º	28 February – 4 March 2011
Tweed River, NSW	ECE1	TWD2	-28.191117º, 153.522317º	28 February – 4 March 2011
Moreton Bay, QLD	ECE2, MP4	MB48	-27.166615º, 153.09881º	21 October 2012 13 February 2013
Moreton Bay, QLD	ECE2, MP4	MB27	-27.22810333º, 153.1854433º	22 October 2012
Moreton Bay, QLD	ECE2, MP4	MBSG9	-27.1931 º, 153.076 º	12 February 2013
Moreton Bay, QLD	ECO1	DWN	-27.45824444º, 153.4001333	May 2013
Heron Island, QLD	ECO1	BMA	-23.6988889º, 152.1436111º	9 – 14 April, 2013

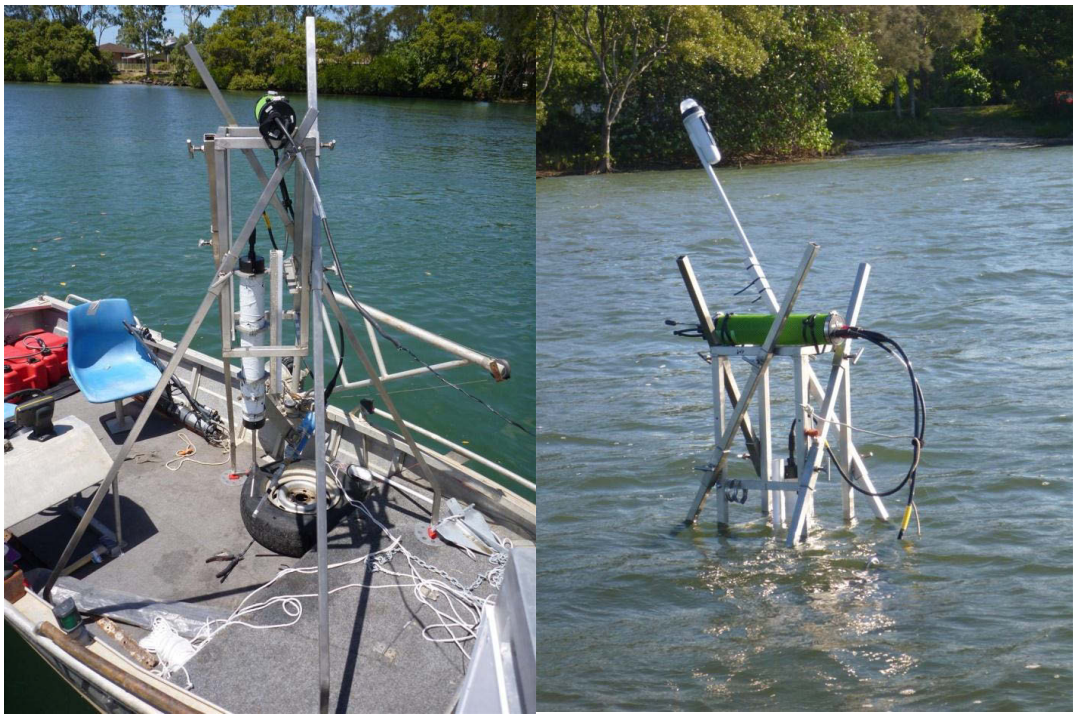

Figure 4.2: The first generation of the Eddy Correlation microelectrode system (ECE1; left) and the ECE1 during deployment in the Tweed River (right).

Figure 4.3: The deployment of the first generation of the Eddy Correlation microelectrode system (ECE1) in Tweed River seagrass beds.

Moreton Bay

The 2011 Queensland floods were caused by strong La Niña conditions combined with an uncharacteristically heavy monsoon period during late 2010 and early 2011. These conditions resulted in record rainfall throughout Queensland. In 2013, floods were caused by ex-tropical Cyclone Oswald and an associated monsoon trough passed over parts of southern Queensland and northern New South Wales, causing widespread damage including severe storms and flooding All of these events led to large volumes of sediment-laden freshwater being released into Moreton Bay (Queensland).

The second generation of the Eddy Correlation microelectrode system (ECE2; Unisense A/S, Denmark; Figure 4.5) and the MiniProfiler MP4 system (Unisense A/S, Denmark; Figure 4.8) were deployed in October 2012 and February 2013 in order to quantify benthic O_2 flux in Moreton Bay. The MP4 system was deployed to investigate O_2 flux in sediment at MB48 (GPS location: -27.166615º, 153.09881º; Figure 4.4) on 21st October 2012 and at MB27 (GPS location: -27.22810333º, 153.1854433º; Figure 4.4) on 22nd October 2012. The MP4 system was also deployed in seagrass beds (MBSG9 location: -27.1931 º, 153.076 º; Figure 4.4) on 12th Febuary 2013. The ECE2 was deployed at MB48 on 21st October 2012 and at MBSG9 on 13th February 2013. In May 2013, two deployments of the first generation of the Eddy Correlation system (ECE1) were performed in seagrass beds at DWN (GPS location: -27.45824444º, 153.4001333; Figure 4.4; Table 4.1).

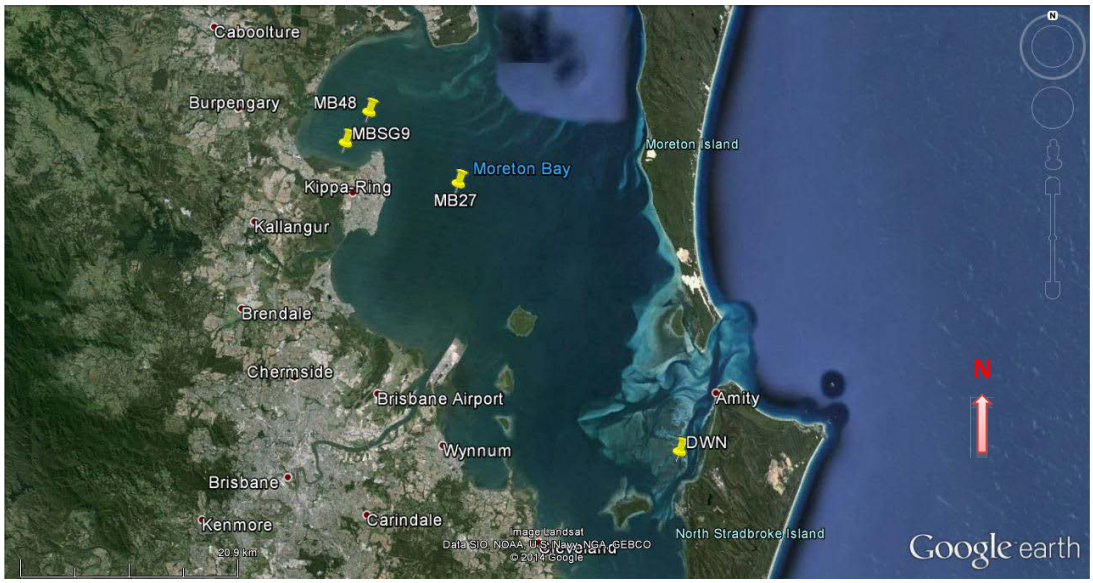

Figure 4.4: Location of deployment sites in Moreton Bay, Queensland.

Figure 4.5: The second generation of the Eddy Correlation microelectrode system (ECE2) in Moreton Bay.

Heron Island

The study of O_2 flux in an open water ecosystem was conducted in Heron Island, Queensland (Figure 4.6; Table 7.1) in order to investigate oxygen dynamics in Heron Island lagoon. The first generation of the Eddy Correlation optode system (ECO1; Unisense A/S, Denmark; Figure 4.7) was deployed over benthic microalgae (BMA) in Heron Island lagoon (GPS location: -23.6988889º, 152.1436111º). The water depth in the lagoon was approximately 4 meters. Three deployments occurred during the period 9th – 14th April, 2013.

Figure 4.6: Location of deployment sites in Heron Island, Queensland.

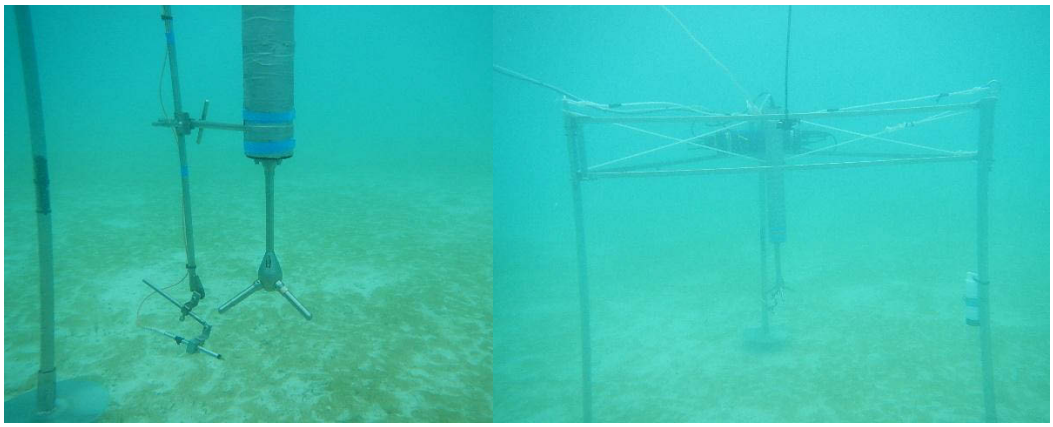

Figure 4.7: The first generation of the Eddy Correlation optode system (ECO1) was deployed over benthic microalgae on Heron Island lagoon.

4.2.2 Eddy Correlation O_2 flux measurements in the Tweed River, Moreton Bay, and Heron Island

The first generation of the Eddy Correlation microelectrode system (ECE1; Figure 7.2) included an acoustic Doppler velocimeter (ADV; Nortek A/S, Norway) modified to interface with a Clark-type oxygen microelectrode (Unisense A/S, Denmark) through a custom-built pico-amplifier (Max Planck Institute for Marine Microbiology, Germany). The custom-built pico-amplifier was replaced with a Unisense O_2 amplifier in the second generation of the Eddy Correlation microelectrode system (ECE2; Figure 4.5) in order to reduce noisy data during measurement. In the first generation of the Eddy Correlation optode system (ECO1; Figure 7.7), the microelectrode and its amplifier were replaced with an optode system (PyroScience GmbH, Germany) in order to make the ECO1 more robust. These sensors were mounted on a frame with the ADV aligned vertically facing the sediment surface and the microelectrode or optode positioned at an approximately 45º angle to the vertical axis of the ADV's, with a ~ 1 cm^3 measuring volume.

In the Tweed River, this measuring volume was ~ 25 cm above the sediment surface of the seagrass site. This was above the maximum canopy height of ~ 20 cm under low current conditons. Measurements were made at intervals consisting of 64 Hz data recordings for 14.5 min followed by a 0.5-min ‘‘sleep’’ period (standard protocol from manufacturer). In addition to these high-speed recordings of the three velocity components (two horizontal and one vertical) and O_2 concentration, the ADV also records temperature, water depth, and the measuring volume's position above sediment surface with a coarser temporal resolution. The duration of each deployment was approximately 18 h. Ambient DO and turbidity were determined with a handheld water quality meter (YSI Sonde 6600 V2, YSI Inc, USA). The microelectrode of YSI Sonde was calibrated at the beginning and the end of each deployment. Water surface and underwater irradiance at two depths (PAR) were measured using a 2π quantum sensor (LI-COR Biosciences, USA) measuring every 5 s. In total, three deployments were made from February 28th, 2011 to March 4th, 2011 at the Tweed River sites. Two deployments were performed at TWD1 and another one was performed at TWD2 (Figure 4.1). The water depth was approximately 2 m during deployment. The eddy correlation system was always deployed and recovered during low tide

In Moreton Bay, the second generation of the Eddy Correlation microelectrode system (ECE2; Figure 4.5) was deployed at site MB48. The measuring volume was 30 cm above sediment surface. Two deployments were performed at 64 Hz for 24 h per deployment, from 20th– 22th October 2012. In each deployment, the ECE1 was deployed along with meteorological instruments including PAR sensors (Odyssey, New Zealand). In addition, the first generation of the Eddy Correlation optode

system (ECO1) was deployed along with a weather station including PAR sensors (Odyssey, New Zealand) in Moreton Bay seagrass beds (Site DWN, Figure 4.4). The measuring height was 15 cm above the seagrass canopy. Two 24 h deployments were made from 8 – 10th May, 2013.

In Heron Island lagoon, the three deployments of the first generation of the Eddy Correlation optode system (ECO1) were performed at BMA site (Figure 6). In each deployment, the measurements were made continuously at 64 Hz for 24 h, and the ECO1 was deployed along with a weather station including Odyssey PAR recorders (Odyssey, New Zealand) and a dissolved oxygen and temperature logger (miniDot; PME, Canada) as a reference optode. The measuring height was 40 cm above lagoon floor.

During field deployments in Tweed River, Moreton Bay and Heron Island, the EC was deployed in the middle of a large patch of selected habitats (e.g. seagrass, benthic microalgae and bethic sediment) in order to eliminate interference of other habitats due to flow changes.

Data Processing

The raw oxygen and velocity data were converted into readable data using data conversion software (Unisense A/S, Denmark). The flux processing and calculation were performed using MATLAB scripts written by this PhD candidate in conjunction with EddyFlux software (Unisense A/S, Denmark). The coordinate rotation routine was applied to the data, if the mean of vertical velocity ($\bar{v}_z$) was not close to zero. Time lag adjustment was applied, if the position of the oxygen sensor was not in the measurement volume. Both coordinate rotation and time lag

adjustment was applied in order to obtain the maximum data resolution from the flux measurements.

4.2.3 Estimation of seagrass health in Tweed River

Morphometrics of seagrass site

Four key morphometric measurements were made at each study site: shoot density, percentage cover of seagrass, seagrass canopy height and above-ground and below-ground biomass. To monitor shoot density (number of plant per m^2) and percentage cover (%) of seagrasses at TWD1 and TWD2, a line transect of 20 m was placed at each site. The shoot density (shoot m^{-2}) of *Z. capricorni* and the percentage cover of *Z. capricorni* and *H. ovalis* (%) were determined in 11 quadrats (10 x 10 cm and 25 x 25 cm, respectively) placed along the transect line at 2 m interval. Canopy heights (cm) were investigated using a tape measure placed from base to tip of the plants (*n* = 3 per quadrate). Epiphyte percentage leaf cover (%) was determined in plants collected from each quadrant along the transect (*n* = 11) using image processing (Image J). Ten *Z. capricorni* plants were randomly collected for the analyses of above-ground and below-ground biomass (g dry weight), length (cm), width (mm) and area (cm^2) of leaf.

Underwater light climate

Downwelling Photosynthetically Active Radiation (PAR) was determined at each seagrass site using an underwater quantum sensor (LI-COR LI192SA) attached to a lowering frame and a photometer (LI-1400).

Effective quantum yield of seagrass health

Chlorophyll *a* fluorescence measurements were conducted using a Pulse Amplitude Modulated fluorometer (Diving-PAM; Walz GmbH, Effeltrich, Germany). Rapid light curves (RLCs) were measured using the in-built software routine utilising nine incrementing actinic illumination steps (0, 33, 72, 117, 178, 249, 375, 512, 780 µmol photons m^{-2} s^{-1}) at 10 s intervals. A specialised leaf clip was used to position the fibre optic probe at a fixed distance from the leaf blade for each measurement. All measurements were performed on the second youngest leaf blade in order to be comparable across all plants. Relative electron transport rate (rETR) was calculated as a product of effective quantum yield ($\Delta F/F_M'$) and irradiance (µmol photons m^{-2} s^{-1}). Data were fitted according to the double exponential function (Ralph and Gademann 2005) and three photosynthetic parameters; maximum rate of oxygen evolution ($rETR_{max}$), light utilisation efficiency (α) and minimum saturating irradiance (I_k) also derived from these curves (SigmaPlot version 12.5).

Data analysis

To determine any significant differences among sites in shoot density and percentage cover of seagrasses, canopy height, epiphyte percentage cover, above-ground and below-ground+ biomass, and length, width and area of leaf, one-way ANOVA tests were used (SPSS Version 17) with a significance level of 95%. Data were transformed using $\log_{10,}$ or square root if the data did not meet the assumptions of normality (Kolmogorov-Smirnov test) and equal variance (Levene's test).

4.2.4 MiniProfiler MP4 flux measurements in Moreton Bay

A MiniProfiler MP4 system (Unisense A/S, Denmark; Figure 4.8) was deployed on both field trips at 2 stations (MB27 and MB48) in order to measure changes in dissolved oxygen content through the sediment-water interface (SWI). Poor weather conditions prevented its use at the remaining sites. The MiniProfiler MP4 system consists of a 4-channel data logger and a motor system for 1D profiling, and is mounted on a shallow water *in situ* frame (Unisense A/S, Denmark).

Each deployment profiled across the sediment diffusive boundary layer, penetrating the sediment to a depth that exceeded the depth of the diffusive boundary layer at each site. Oxygen concentration profiles were measured at a few millimetres above the sediment-water interface (SWI) using Clark-type O_2 microsensors (OX-100, Unisense) connected to an *in situ* sensor amplifier (Unisense A/S, Denmark) and mounted on the MiniProfiler platform. The microelectrode had a 100 µm outer tip diameter, a 90% response time of <8 s and stirring sensitivity of <1.5%. A two-point calibration of the microelectrode was carried out in Schott glass bottles with air-saturated seawater and O_2-free seawater, made anoxic by the addition of sodium hydrosulphite. The calibration procedure was performed before each deployment to avoid microelectrode interference.

Two profiles were conducted at each site. In each profile, the O_2 concentration was sampled every 10 seconds. The step size of the motor was controlled by manufacturer software (Lander; Unisense A/S, Denmark) at 100 µm, excepting the MB-48a oxygen profile which had 200 µm step size. The microelectrode moved every 30 seconds, in incremental steps from the water column towards the sediment.

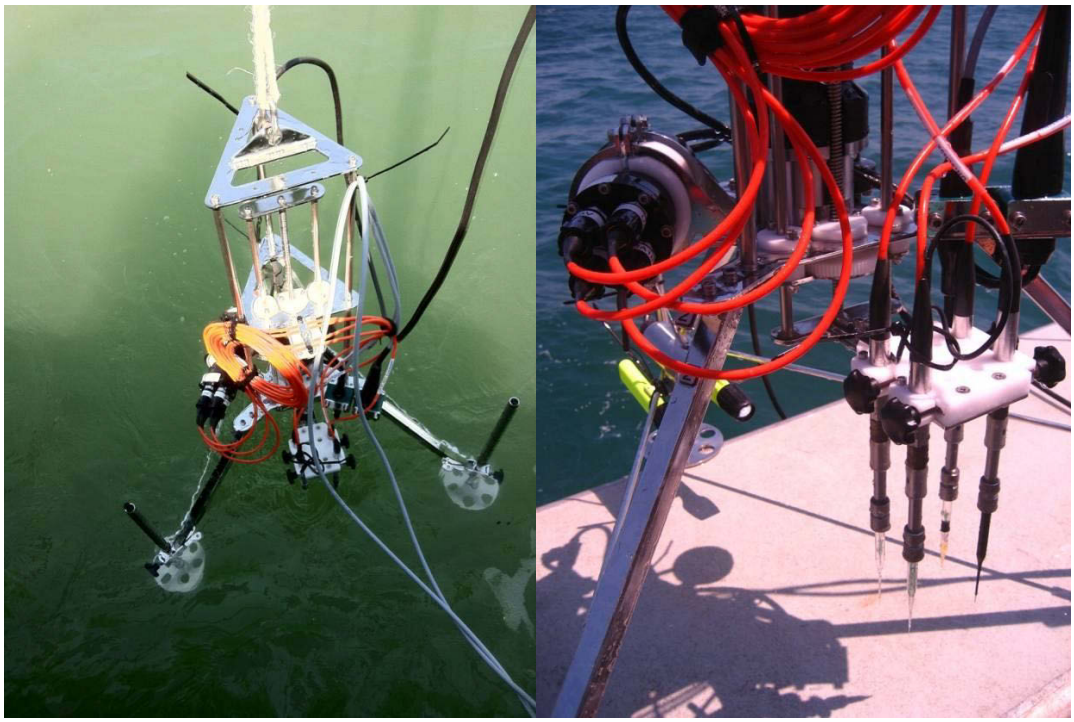

Figure 4.8: O_2, pH, H_2S and N_2O microelectrodes were mounted on MiniProfiler MP4 System.

Table 4.2: Characteristics of seafloor and MiniProfiler MP4 deployment times in Moreton Bay.

Station	Date	Time hhmm	Sediment Type	Temp (°C)	Salinity (ppt)	Depth (m)	pH
MB-48a	21 Oct 2012	0934	Mud	22.1	35	4.2	8.01
MB-48b	21 Oct 2012	0945	Mud	22.1	35	4.2	8.01
MB-48c	21 Oct 2012	0951	Mud	22.1	35	4.2	8.01
MB-27a	22 Oct 2012	1118	Mud	22.6	35	9.9	8.08
MB-27b	22 Oct 2012	1140	Mud	22.6	35	9.9	8.08
MB-27c	22 Oct 2012	1158	Mud	22.6	35	9.9	8.08
MB-27d	22 Oct 2012	1233	Mud	22.6	35	9.9	8.08
MB-SG9a	12 Feb 2013	1436	Seagrass	27.0	26	2.7	8.01
MB-SG9b	12 Feb 2013	1528	Seagrass	27.1	26	2.7	8.01

Oxygen flux analysis

Dissolved oxygen content in water was used to calculate the flux at each site as shown in Table 4.2. Benthic fluxes across the sediment-water interface were calculated by linear regression of the concentration data. Positive values represent efflux from the sediment into the water column while negative values are uptake by the sediment. For the dissolved oxygen fluxes, the initial linear portion of the curve was selected. This was to account for settlement and re-suspension of sediment into the water column, as well as water temperature stabilisation.

According to the transport of solute in the diffusion boundary layer (DBL), vertical concentration of oxygen ($\partial C/\partial Z$) is constant in the water column and oxygen concentration decreases linearly through the sediment-water interface (SWI) due to vertical molecular diffusion in the DBL (Glud et al. 1992). Therefore, DBL thickness can be determined from the linearly distributed zone in the oxygen profiles.

The diffusive O_2 flux (J; mmol m^{-2} d^{-1}), that is the sediment O_2 consumption rate, was calculated from measured steady-state O_2 concentration profiles by Fick's first law:

$$J = -D_O\left(\frac{\partial C}{\partial Z}\right)$$

where D_0 is the molecular diffusion coefficient in seawater at salinity and temperature at each deployment site, and $\partial C/\partial Z$ is the linear slope of the O_2 concentration profile within the DBL above SWI.

4.3 RESULTS

4.3.1 Dissolved oxygen flux in Tweed River using Eddy Correlation system (ECE1)

On 1st March, 2011, the first deployment of the first generation of the Eddy Correlation microelectrode system (ECE1) in seagrass meadows (TWD1) was made. The oxygen concentration decreased from midnight to 04:00, and increased from 04:00 to 08:00 (Figure 4.9a). Water velocity fluctuated over the deployment period, with water velocities lower than 1 cm s^{-1} occurring at 20:00, 01:00, and 08:00 (Figure 4.9a). The oxygen flux was negative from 16:00 to 09:00 and was positive from 09:00 to 11:00 (Figure 4.9b). After the probe was replaced and the ECE1 battery was recharged, the second deployment was performed on the 2nd March 2011 at TWD1 in order to replicate the events that occurred in the first deployment. Unfortunately, this deployment was unsuccessful due to an O_2 microelectrode failure. The microelectrode was broken within the first few minutes of the deployment; therefore, there was no O_2 data that could be used to calculate the O_2 fluxes in seagrass meadows.

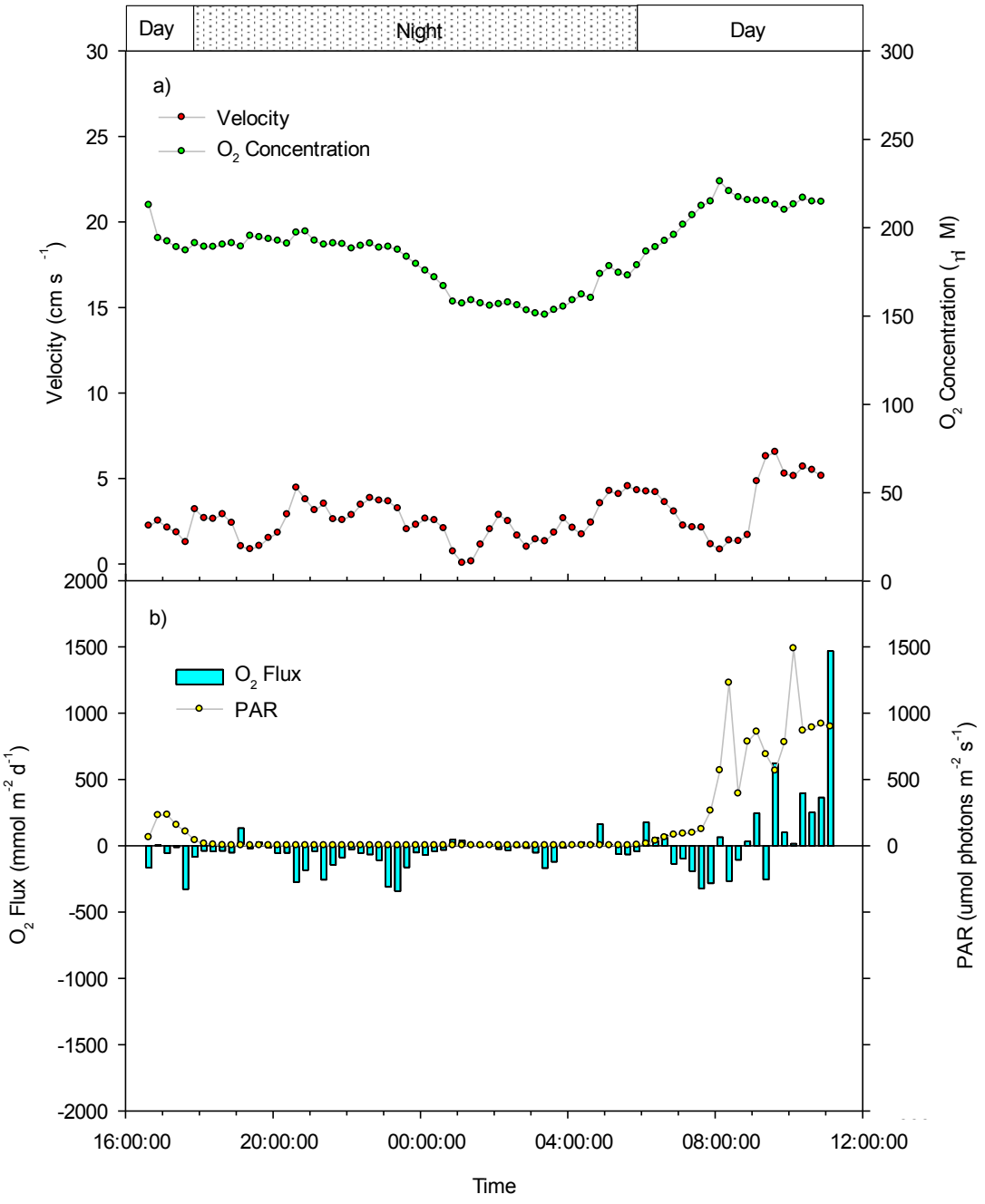

Figure 4.9: Mean water velocity, O_2 concentration (a), O_2 flux and PAR (b) every 15 min at TWD1 in Tweed River seagrass meadows measured by the first generation of the Eddy Correlation microelectrode system (ECE1).

On 3rd March, 2011, the ECE1 was deployed in a TWD2 seagrass patch for 18 h. The water velocity increased to 24 cm s^{-1} at 21:00 and 08:00 to 10:00, while it was close to zero during other periods (Figure 4.10a). The O_2 concentration, however, fluctuated from 180 to 210 μM during both daytime and nighttime (Figure 4.10a). The O_2 fluxes also varied during daytime and nighttime, with negative fluxes observed from 18:00 to 22:00 and 06:00 to 11:00. Interestingly, O_2 fluxes were positive at nighttime from 23:00 to 04:00 and negative during daytime from 05:00 to 11:00 (Figure 4.10b).

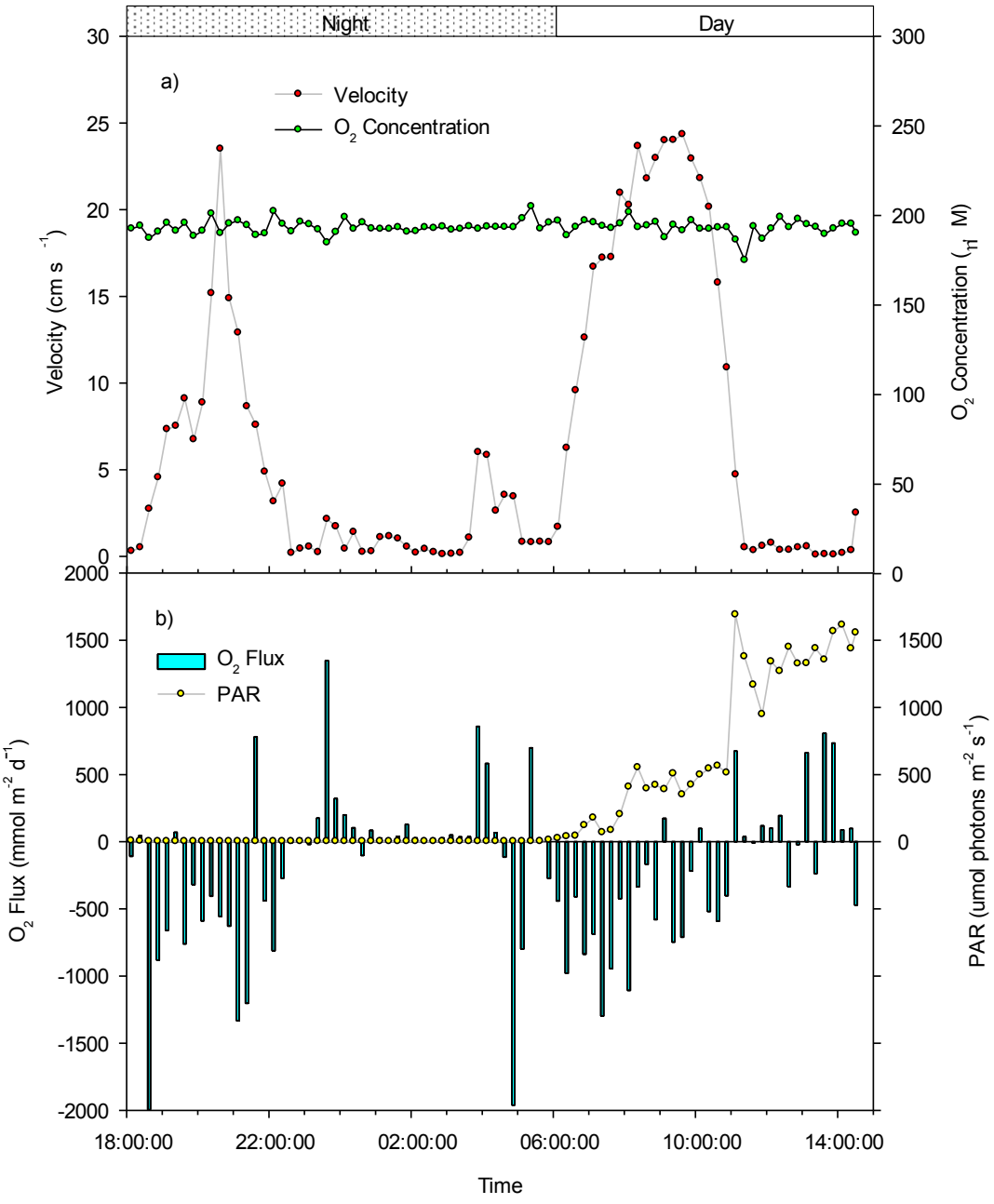

Figure 4.10: Mean water velocity, O_2 concentration (a), O_2 flux and PAR (b) every 15 min at TWD2 in Tweed River seagrass meadows measured by the first generation of the Eddy Correlation microelectrode system (ECE1).

4.3.2 Seagrass morphometrics in Tweed River

Percentage cover of seagrasses and specifically *Z. capricorni* were not significantly different between sites (p = 0.770 and 0.220, respectively; Figure 4.11). *H. ovalis* was observed only at TWD1. Epiphytic algal cover on *Z. capricorni* was significantly higher at TWD1 (p = <0.001; Figure 4.11). Shoot density of *Z. capricorni* was significantly higher from TWD2 in relation to TWD1 (p <0.001; Figure 4.12). Morphological study showed that *Z. capricorni* from TWD2 was considerably larger than in TWD1, as shown by canopy height (p < 0.001), leaf length (p < 0.001), leaf width (p = 0.001), leaf area (p < 0.001) and above-ground and below-ground biomass (p = 0.004 and 0.001, respectively; Figure 4.12).

Due to the failure of the Diving-PAM, replications of photosynthetic performance on TWD2 was not obtained (n = 1), therefore statistical analyses to determine significant difference between sites were not performed. $\Delta F/F_M$', $rETR_{max}$, I_k and α of *Z. capricorni* from TWD1 and TWD2 are shown in Table 4.3.

Table 4.3: a) Effective quantum yield of PSII ($\Delta F/F_M$'), (b) maximum relative electron transport rate ($rETR_{max}$; μmol electrons m^{-2} s^{-1}), (c) minimum saturating irradiance ($I_{k;}$ μmol photons m^{-2} s^{-1}) and (d) initial slope of rapid light curves (α) of *Z. capricorni* from TWD1 and TWD2 within Tweed River. Means ± SE, n = 5.

Parameters	Mean ± SE	
	TWD1	TWD2
$\Delta F/F_M$'	0.677±0.020	0.626
$rETR_{max}$ (μmol electrons m^{-2})	63.2±5.3	38.7
I_k (μmol photons m^{-2} s^{-1})	107.8±66.4	66.4
α	0.62±0.07	0.58

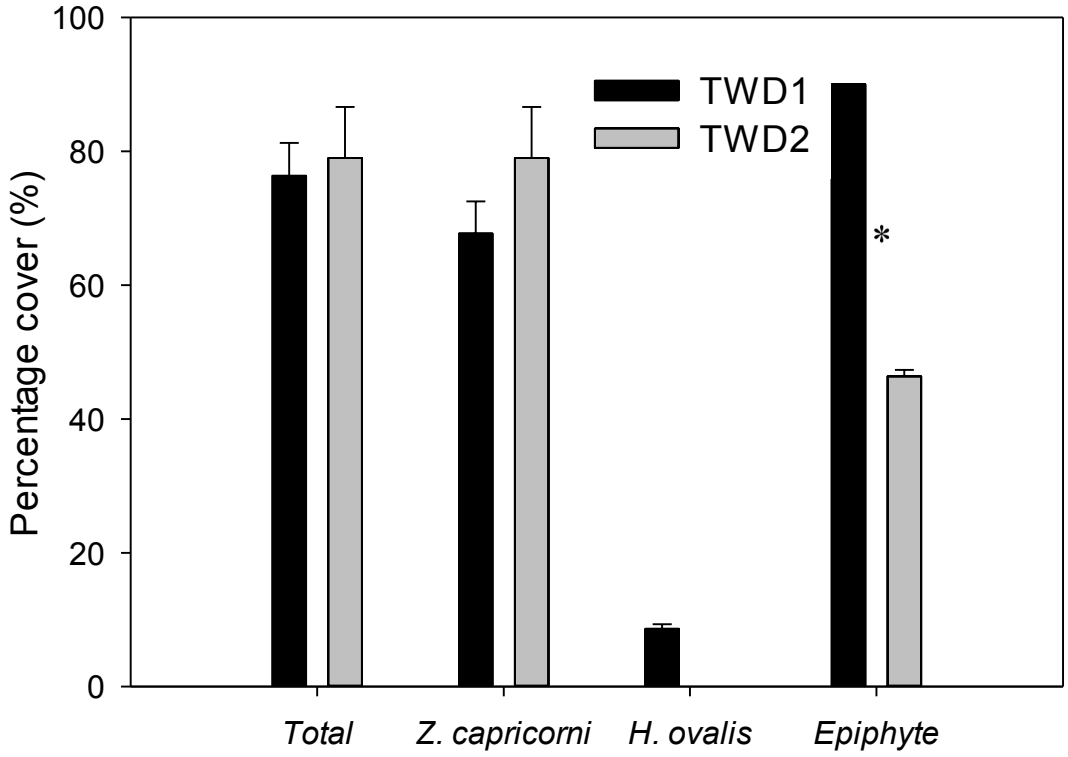

Figure 4.11: Percentage cover (%) of total seagrasses, *Z. capricorni, H. ovalis,* and epiphytic algae from TWD1 and TWD2 within Tweed River. Data represent mean + SE (*n* =11).

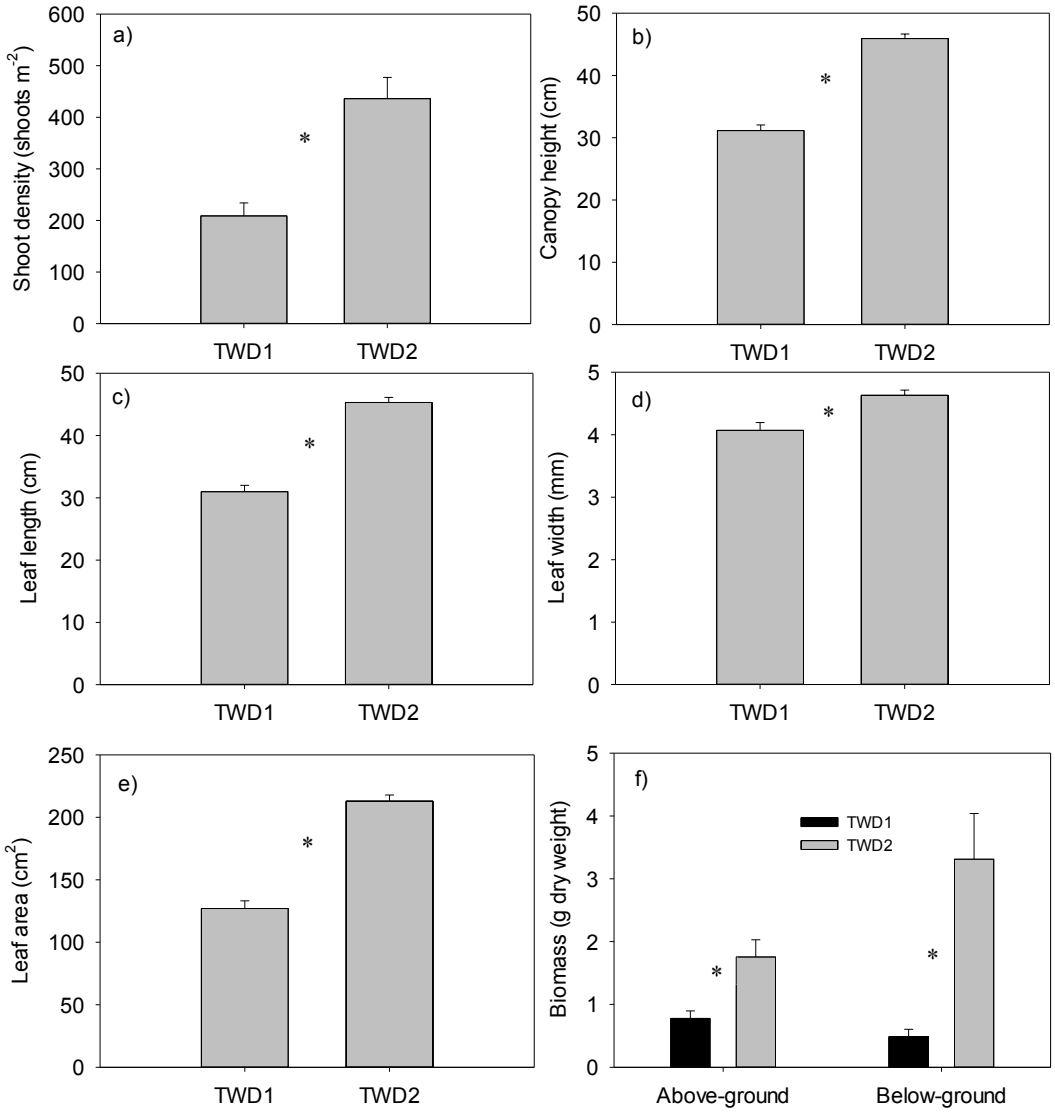

Figure 4.12: Morphological properties of *Z. capricorni* from TWD1 and TWD2 within the Tweed River. a) shoot density (shoot m^{-2}); b) canopy height (cm); c) leaf length (cm); d) leaf width (mm); e) leaf area (cm^2 per shoot); f) above-ground and below-ground biomass. Data represent mean + SE (*n* =10).

4.3.3 Dissolved oxygen flux in Moreton Bay using the Eddy Correlation system (ECE2 and ECO1)

The ECE2 was deployed in Moreton Bay in order to determine O_2 fluxes in marine sediment after the 2011 floods caused extensive sediment deposition in Moreton Bay. At site MB48, the ECE2 was deployed on 21st October 2012 at 22:30, and retrieved after 24 h of measurements. The water depth at MB48 was 24 m with no light during daylight. Unfortunately, the ECE2 microelectrode was broken by jellyfish at approximately 08:00 (see Appendix E: MB48 raw data); therefore, O_2 fluxes after 08:00 were discounted (Figure 4.13). The water velocity at MB48 was from 0 to 9 cm s^{-1}, while the oxygen concentration was 75-85 µM (Figure 4.13a). The O_2 flux was negative during nighttime, was highest at 500 mmol m^{-2} s^{-1} at 22.30 and close to zero during the rest of the deployment.

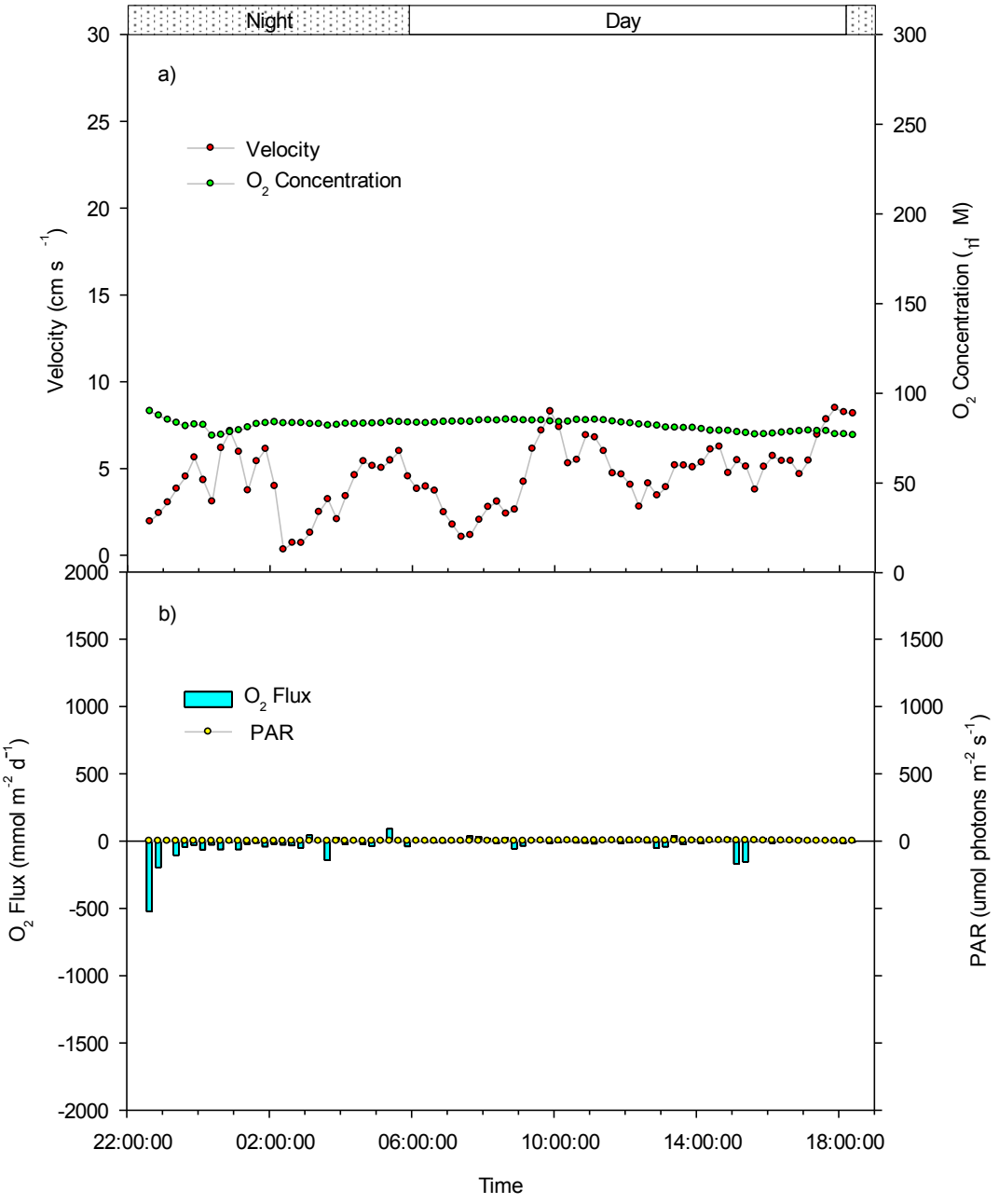

Figure 4.13: Mean water velocity and O_2 concentration (a) and O_2 fluxes and PAR every 15 min at MB48 in Moreton Bay sediment measured by the second generation of the Eddy Correlation microelectrode system (ECE2).

In May 2013, the ECO1 was deployed at site DWN (Figure 4.4) in order to determine the O_2 dynamics in open water seagrass beds. Two deployments were performed from 8th-10th May 2013. The first deployment was performed from 8th May 2013 at 09:00 to 9th May 2013 at 09:00 (DWN1, Figure 4.14). The second deployment was made at DWN from 9th May 2013 at 16:30 to 10th May 2013 at 10:00 (DWN2, Figure 4.15). Due to the failure of the PAR sensor, PAR data in DWN1 and DWN2 were not be obtained. The results from DWN1 showed an increase in O_2 concentration during daylight (09:00 to 15:00 and 06:00 to 09:00) and a decrease in O_2 concentration in the afternoon and during darkness (15:00 to 06:00) (Figure 4.14a). Water velocity ranged from 2 to 23 cm s^{-1} (Figure 4.14a) and increased from 22:00 to 23:00 and 02:00 to 04:00. Positive O_2 fluxes were found during daylight (09:00 to 16:00) and in some periods during darkness (22:00 to 23:00 and 02:00 to 04:00) (Figure 4.14b). The results from DWN2 showed a slight decrease in O_2 concentration after 16:30 to 05:30, and a slight increase in O_2 concentration from 05:30 to 10:00 (Figure 4.15a). Water velocity increased at 20:00 to 22:00, 01:00 to 04:00 and 08:00 to 10:00 (Figure 4.15a). O_2 flux fluctuated from 16:30 to 22:00, but followed the previous trend where positive flux was observed at 02:00 to 05:00 and 08:00 to 10:00 (Figure 4.15b).

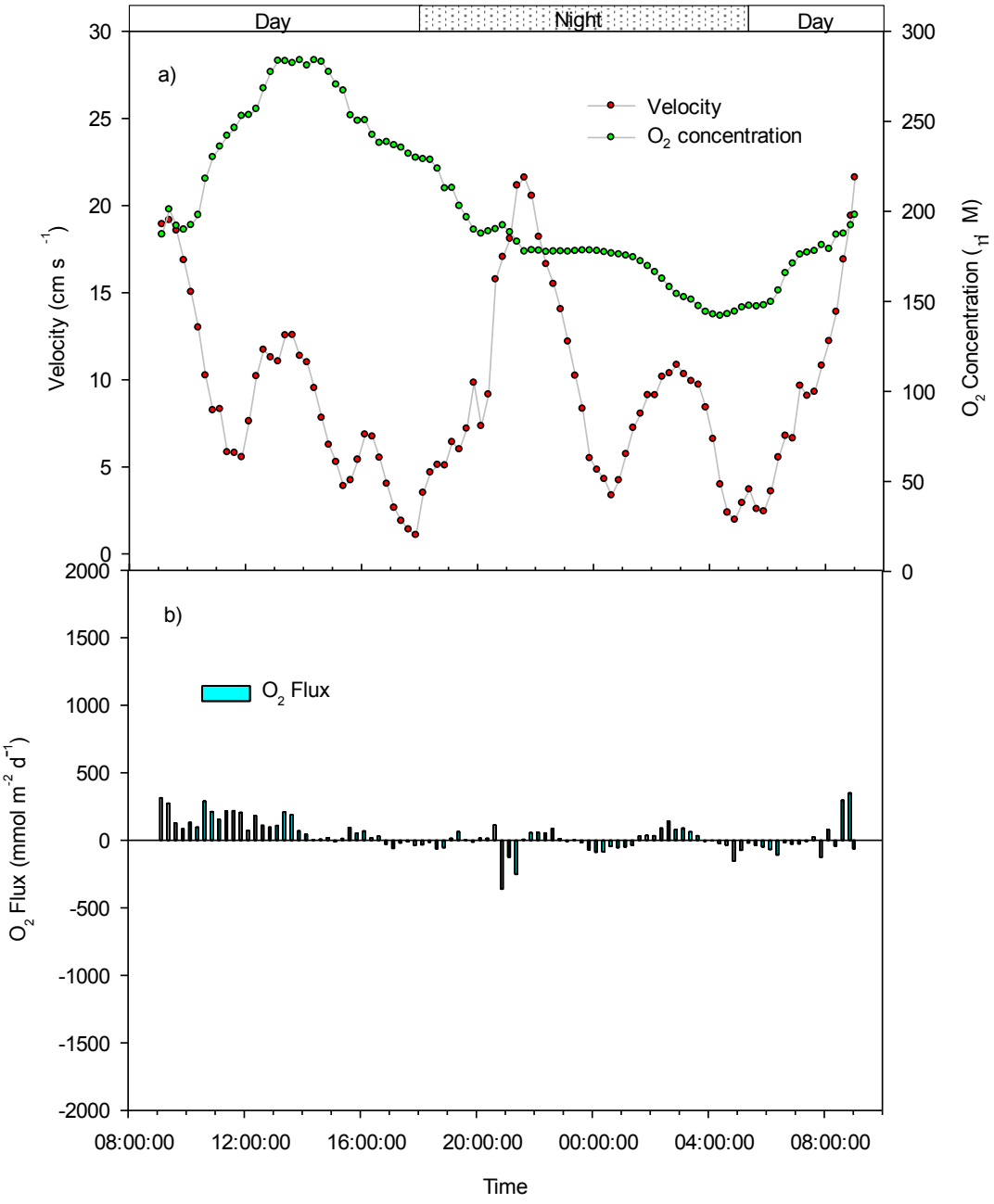

Figure 4.14: Mean water velocity, O_2 concentration (a) and O_2 fluxes every 15 min from the first deployment at DWN1 in Moreton Bay seagrass beds from 8th May 2013 at 09:00 to 9th May 2013 at 09:00 measured by the first generation of the Eddy Correlation optode system (ECO1).

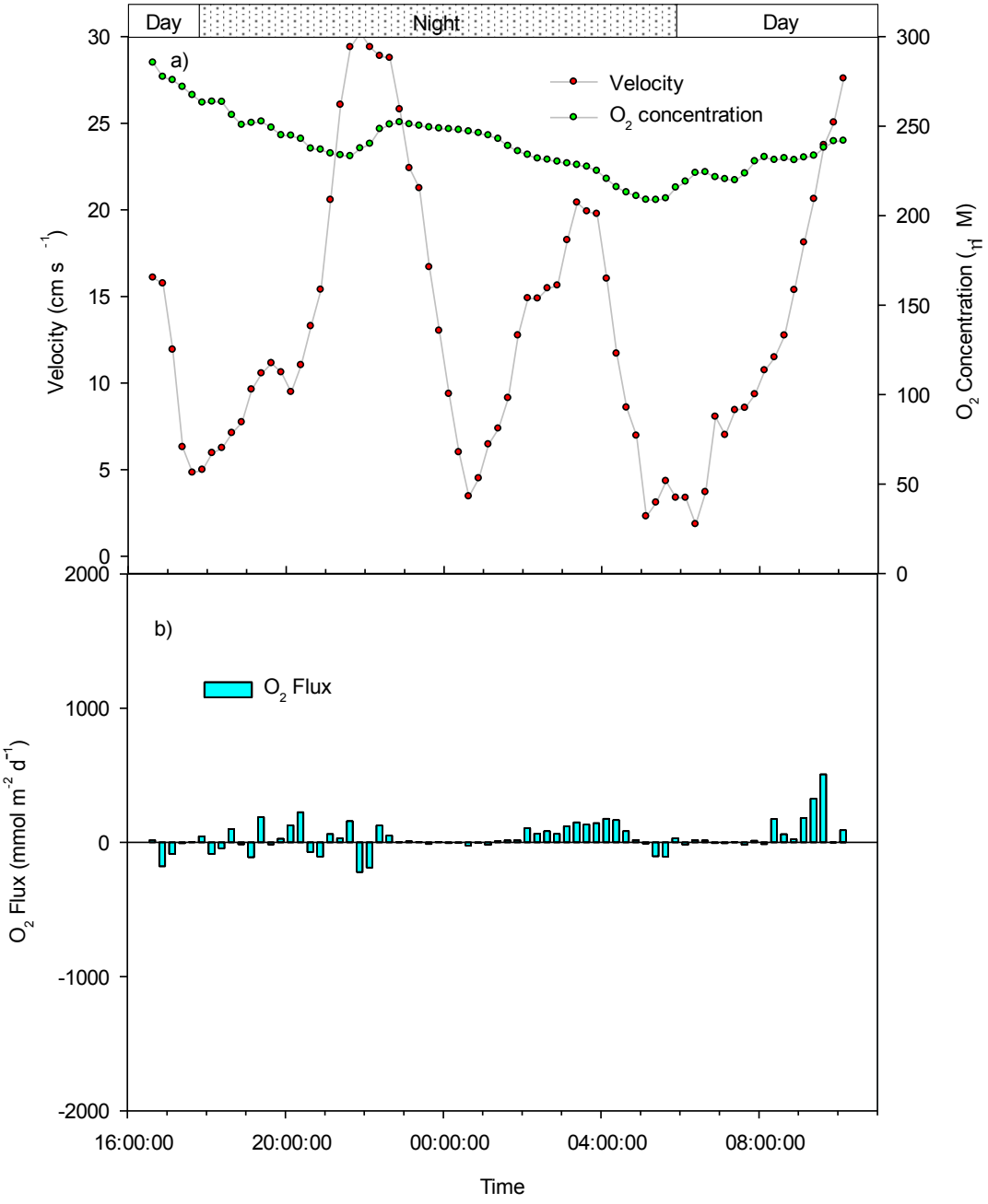

Figure 4.15: Mean water velocity, O_2 concentration (a) and O_2 fluxes every 15 min from the second deployment at DWN2 in Moreton Bay seagrass beds from 9 May 2013 at 16:30 to 10 May 2013 at 10:00 measured by the first generation of the Eddy Correlation optode system (ECO1).

4.3.4 Dissolved oxygen flux in Moreton Bay sediment with the MiniProfiler MP4 system

In October 2012, dissolved oxygen profiles at sites MB27 in central Moreton Bay and site MB48 in Deception Bay were similar and subsequently pooled (Figure 4.16). All sites showed a similar bulk-water DO concentration of ~ 230 μM (above the SWI). At MB27, in the centre of the Bay, DO concentrations decreased rapidly with depth and anoxic conditions recorded at ~0.8 mm below SWI. At MB48, in Deception Bay, DO concentrations declined less rapidly and penetrated deeper into the sediments with anoxic conditions being measured at 1.5-1.8 mm below the SWI (Figure 4.16). In February 2013, at MBSG9 in shallow seagrass beds inshore from MB48, bulk-water DO concentrations were ~270 μM and decreased rapidly below the SWI with anoxic conditions recorded at less than 0.5 mm below the sediment surface. Flux rates estimated from the MiniProfiler MP4 system are shown in Table 4.4. There were no significant differences in O_2 flux among MB27, MB48 and MBSG9.

Table 4.4: The diffusive boundary layer (DBL) thickness (mm), diffusion coefficient of seawater and O_2 flux (mmol m^{-2} d^{-1}) found at each station.

Date	Station	DBL thickness (mm)	Diffusion Coefficient (cm^2 s^{-1})	O_2 flux (mmol m^{-2} d^{-1}) (μmol m^{-2} h^{-1})
21 Oct 2012	MB-48a	0.6	2.0637×10^{-5}	- 20.64 (-1026.67)
21 Oct 2012	MB-48b	0.3	2.0637×10^{-5}	- 44.35 (-1847.92)
22 Oct 2012	MB-27a	0.1	2.1187×10^{-5}	- 169.42 (-7059.17)
22 Oct 2012	MB-27b	0.4	2.1187×10^{-5}	- 52.04 (-2168.33)
12 Feb 2013	MB-SG9a	0.4	2.3292×10^{-5}	-74.83 (-3117.92)
12 Feb 2013	MB-SG9b	0.5	2.3292×10^{-5}	-56.82 (-2367.50)

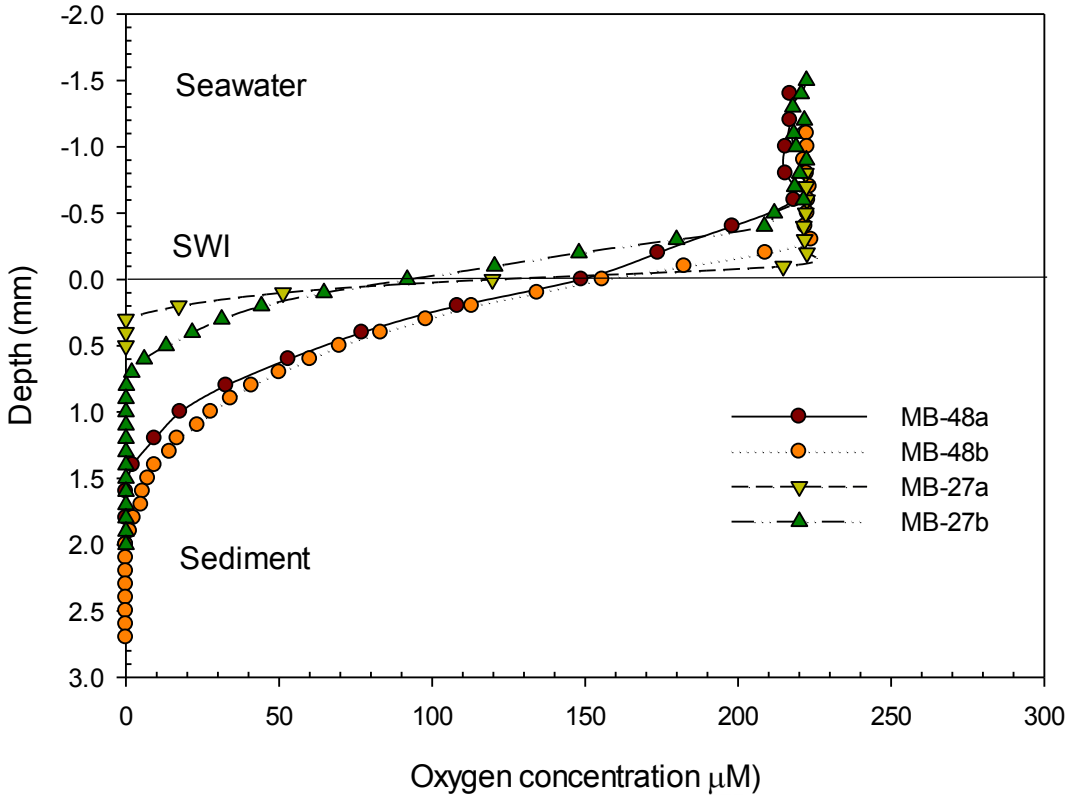

Figure 4.16: Oxygen concentration profiles obtained from the MiniProfiler MP4 system at sites MB27 and MB48.

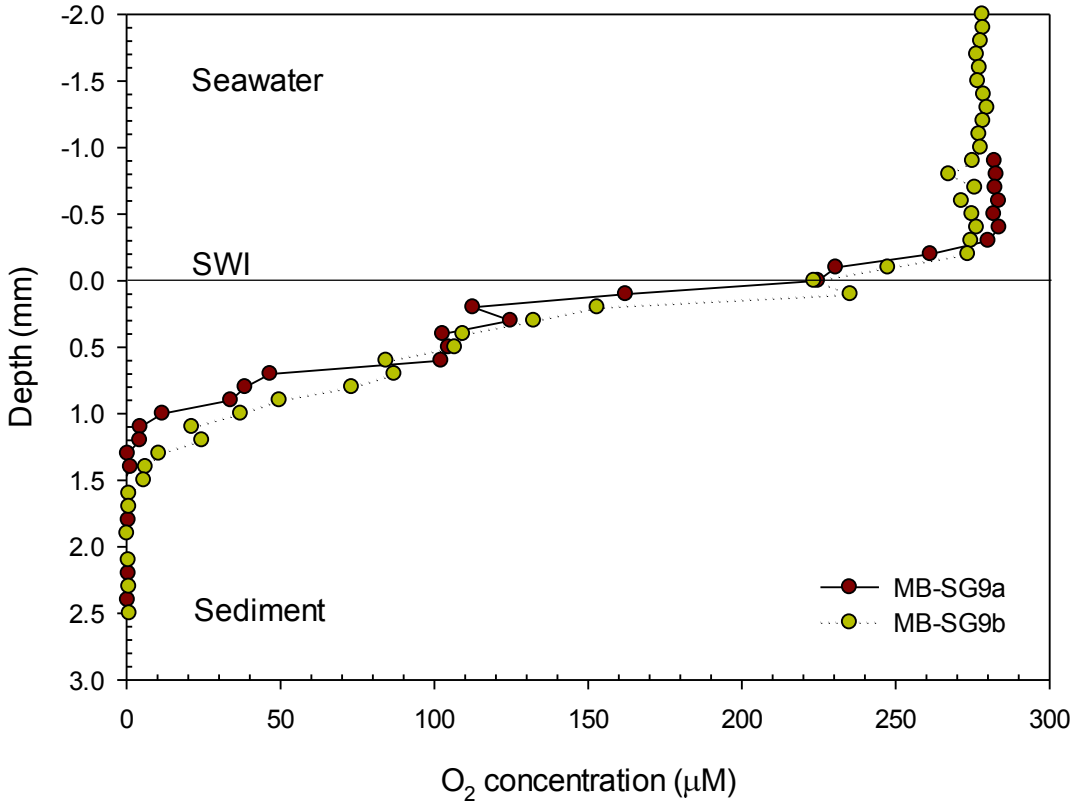

Figure 4.17: Oxygen concentration profiles obtained from the MiniProfiler MP4 at site MBSG9.

4.3.5 Dissolved oxygen flux in Heron Island lagoon using the Eddy Correlation system (ECO1)

The first generation of the Eddy Correlation optode system (ECO1) was deployed above a benthic microalgal (BMA) community in Heron Island lagoon from 10th April, 2013 at 09:00 to 11th April 2013, at 09:00. Water velocity fluctuated over the deployment period from 0 to 20 cm s^{-1} (Figure 4.18a). Low velocity (<5 cm s^{-1}) was observed from 09:00 to 10:00, 12:00 to 17:00, and 17:00 to 22:00. The O_2 concentration increased to 270 μM in daylight and decreased to 240 μM during darkness (Figure 4.18b). Positive O_2 fluxes occurred during daylight from 09:00 to 18:00. Interestingly, there were positive O_2 fluxes during darkness from 19:00 to 03:00.

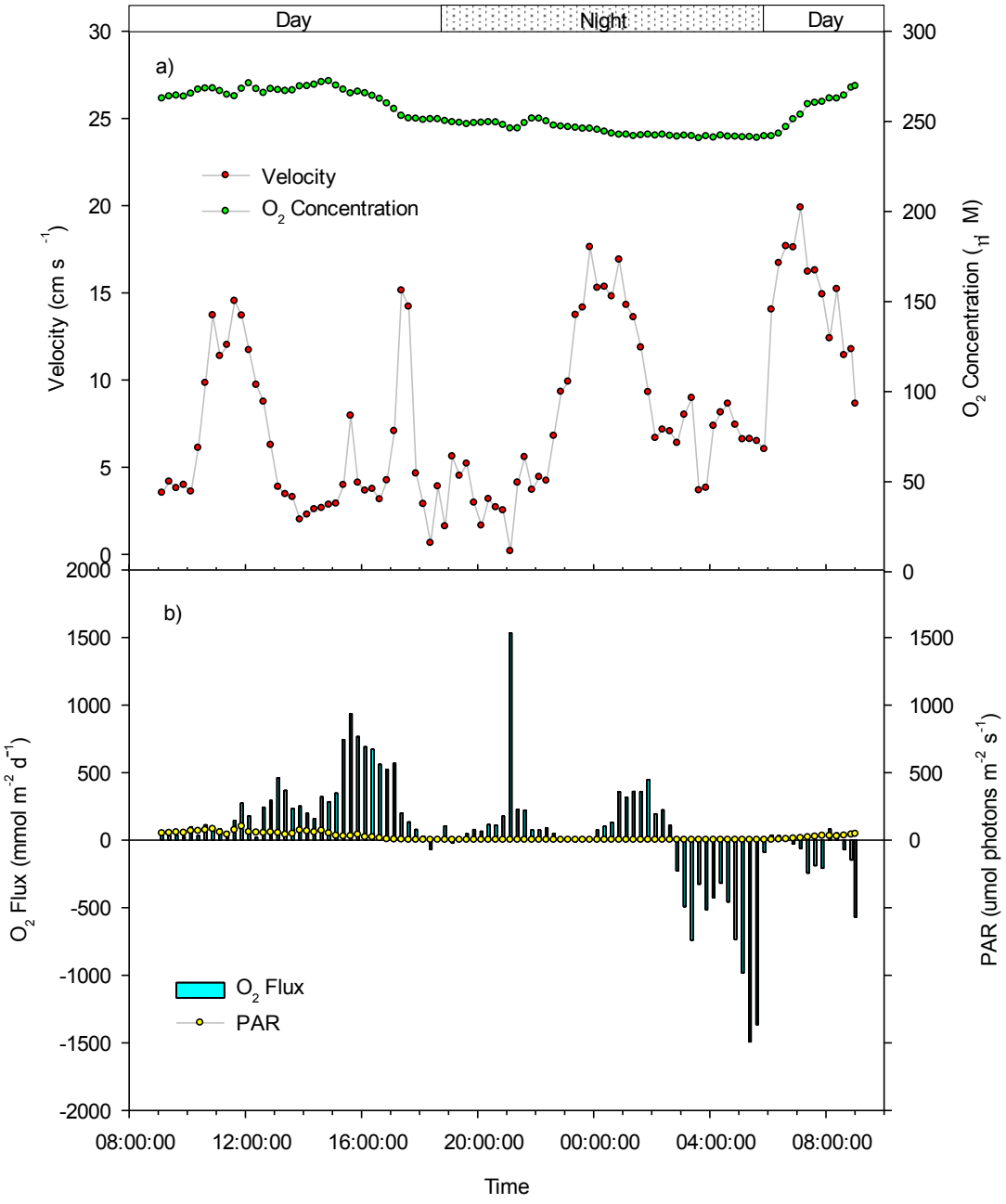

Figure 4.18: Mean water velocity, O_2 concentration (a), O_2 fluxes and PAR (b) every 15 min at BMA in Heron Island lagoon from 10th April 2013 at 09:00 to 11th April 2013 at 09:00 measured by the first generation of the Eddy Correlation optode system (ECO1).

Figure 4.19 also shows the results of O_2 flux measurements on BMA in Heron Island lagoon using the ECO1 from 13th April 2013 at 10:30 to 14th April 2013 at 10:30. Water velocity fluctuated from 2 to 15 cm s^{-1} (Figure 4.19a). O_2 concentration increased to 300 μM in daylight and decreased to 250 μM during darkness (Figure 4.19a). Positive O_2 fluxes were observed during daylight from 10:30 to 19:00; however, positive O_2 fluxes also occurred during darkness (Figure 4.19b).

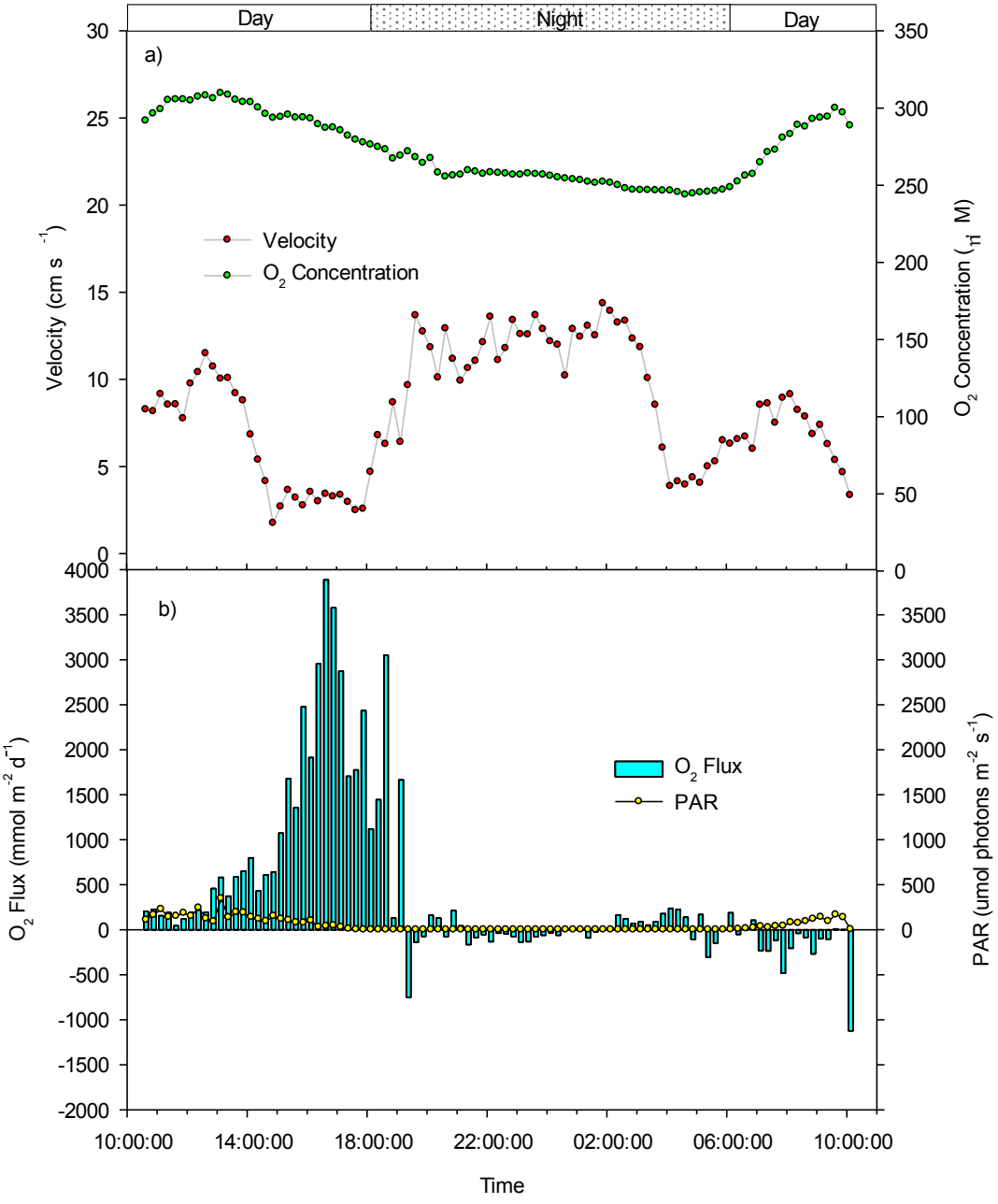

Figure 4.19: Mean water velocity, O_2 concentration (a), O_2 fluxes and PAR (b) every 15 min at BMA in Heron Island lagoon from 13 April 2013 at 10:30 to 14 April 2013 at 10:30 measured by the first generation of the Eddy Correlation optode system (ECO1).

4.4 DISCUSSION

The most significant finding of this study was that the EC system has some operational limitations when used in complex aquatic environments due to wind and current directions and tidal events.

4.4.1 Seagrass morphometrics

Distribution, abundance, as well as morphology and growth of seagrasses are influenced by several abiotic and biotic factors such as light, temperature, pH, water velocity and nutrients (Short and Neckles 1999; Ralph and Gademann 2005). An increase in water velocity reduces the diffusive boundary layer thickness, leading to a higher rate of nutrient uptake by seagrasses (Thomas et al. 2000), including nutrient-dependent process (e.g., photosynthesis) seagrass (Koch 1994). Greater water velocity in TWD2 (6.6 cm s^{-1}) compared to TWD1 (2.9 cm s^{-1}) may have therefore increased photosynthesis and nutrient uptake of seagrass in TWD2, leading to higher biomass, density and leaf size. Lower water velocity in TWD1 may promote the growth of epiphytic algae on leaves (Anderson and Martone 2014). Excessive epiphytic growth is known to reduce photosynthesis, productivity and growth, leading to mortality and a decline in seagrass abundance (Bulthuis and Woelkerling 1983; Neckles et al. 1994; Tomasko and Lapointe 1991; Frankovich and Fourqurean 1997). Therefore, a higher water velocity in TWD2, in combination with a higher epiphytic algal cover in TWD1 may result in a higher biomass, density and leaf size at TWD2.

4.4.2 An estimation of sediment O_2 flux using MiniProfiler

The MiniProfiler was deployed at Moreton Bay in order to investigate dissolved oxygen flux at the sediment interface. The biogeochemistry of marine sediments is influenced by physical, biological and chemical factors including types of fauna and flora, temperature, pH and water velocity (Risgaard-Petersen et al. 1994; Hemminga and Duarte 2000; Sundback et al. 2000; Sakamaki et al. 2006). It is suggested that seagrass can transport O_2 into sediment through their roots and rhizomes, resulting in a more O_2 flux in the sediment (Ku et al. 1999). High oxygen consumption rates were generally found in bare sediments and during macrophyte senescence, while net O_2 production was observed in vegetated areas (Pinardi et al. 2009). Our study, however, found a net O_2 consumption in both bare sediment sites (MB27, MB48) and the seagrass site (MBSG9) and the difference in net O_2 consumptions were insignificant between sites. This may be a result of the fact that the seagrass in MBSG9 experienced high turbidity due to an extensive re-suspension of sediment from ex-tropical cyclone Oswald, resulting in lower productivity (Hauxwell and Valiela 2004). The oxygen profiles in MB-SG9 were not linear; this is possibly due to seagrass roots and rhizomes within the sediment (Figure 4.17).

4.4.3 O_2 flux measurements using the Eddy Correlation system

O_2 flux results from TWD1 were unexpected, as shown in Figure 4.9. Positive fluxes were expected to occur during daylight due to the fact that the photosynthetic activity in seagrass meadows was greater than the respiration rate (Hume et al. 2011; Long et al. 2012). During darkness, negative fluxes should have occurred due to respiration of the seagrass meadow (Hume et al. 2011; Long et al. 2012). In this deployment, the negative fluxes still appeared during daylight, especially from 06:00

(Figure 4.9b) although the O_2 concentration increased linearly during the same period (Figure 4.9a). In addition, the large fluctuation in water velocity (especially at low mean velocity) may alter the flux measurements (Lorrai et al. 2010; Long et al. 2012). Reduced water velocity at 20:00, 22:00 and 01:00 may have resulted in no measures of sediment respiration; therefore, O_2 flux was close to zero during these periods. Even though O_2 concentration increased from 06:00 to 09:00, reduced water velocity may limit mixing and allow sediment respiration; therefore the diffusion boundary layer was increased and caused a negative flux. It should be noted that there was a limitation in monitoring data real-time as the battery of the ECE1 needed regular recharging.

At TWD2, results showed that O_2 fluxes were fluctuating during both daylight and darkness (Figure 4.10b). The result demonstrated that positive fluxes occurred during darkness from 23:00 to 04:00. These positive fluxes may have appeared due to the fact that there was no movement of bulk water (velocity close to 0; Figure 4.10a) during this period. However, the largest amount of negative fluxes occurred from 05:00 to 11:00 (Figure 4.10b) which may have been due to rapid changes in tidal flushing from 05:00 to 11:00 even though this event appeared in daylight. This suggested tidal event may have interfered with the O_2 flux measurement when using the ECE1. Subsequent instrumental improvements are needed to enhance their reliability, in order to allow data to be checked real-time and prevent operation time loss. After further investigation in the laboratory flume and in consultation with the manufacturer (Unisense A/S, Denmark), the ECE1 was replaced with the second generation of Eddy Correlation microelectrode system (ECE2) which was used in

Moreton Bay. Unisense A/S claimed the replacement system would provide better O_2 measurement and performance (see Chapter 3).

At Moreton Bay (MB48), the O_2 flux in the marine sediment was examined using ECE2. Due to the depth of water and sediment re-suspension at MB48, there was low PAR (Figure 4.13b) at the seafloor resulting in low O_2 concentration (Figure 4.13a). When comparing the O_2 flux data in MB48 among ECE1 (-1741 μmol m^{-2} h^{-1}), MiniProfiler MP4 system (Table 4.4), Geoscience Australia benthic chamber and CSIRO benthic chamber (~1800 μmol m^{-2} h^{-1}; Steven et al. 2013; see Appendix D and E), the ECE1 showed O_2 flux in the same range as the MiniProfiler and benthic chambers suggesting the ECE1 may provide a good estimation of flux. However, the O_2 microelectrode was broken after 9 hours of deployment. O_2 concentration at MB48 was much lower than TWD1 and TWD2 due to the fact that MB48 was bare sediment and has lower PAR, leading to higher respiration from microbial activities (e.g., respiration, decomposition, remineralisation) (Murray and Wetzel 1987; Berg et al. 2013). The fluctuation of O_2 fluxes, which was unexpected, occurred when the ECE2 was deployed above benthic sediment with no light. We expected to obtain a negative flux during the deployment time due to the fact that respiration is greater than photosynthetic activity in darkness (Berg et al 2003; Berg et al 2008). Therefore, second and third attempts to deploy the ECE2 were made in order to replicate these usual O_2 fluxes. However, due to massive schools of jellyfish and severe weather, these attempts were unsuccessful. This suggested that the ECE was not suitable for use in the field due to the fragility of the O_2 microelectrode. Due to the unexpected results and non-robust EC system, the ECE2 was re-examined in the laboratory flume to assess whether the ECE2 was working properly or not. After

consulting with Unisense A/S, the ECE2 was replaced with the first generation of the Eddy Correlation optode system (ECO1) in order to obtain more robust data and provide a better flux measurement system.

At DWN in Moreton Bay, O_2 flux was investigated using ECO1. The positive and negative O_2 occurred randomly where there were positive fluxes during darkness and negative fluxes during daylight; this was not expected (Figure 4.14 and 4.15). However, there were positive fluxes during darkness, following the same trend of increased water velocity. This indicates a non-consistency and unreliability of the measurements. There may be many parameters that alter the measurements (e.g. complex circulation, mixing, and viscosity of water), resulting in poor flux estimation. First of all, there was rough weather and strong wind during this deployment which may alter flux measurement (see velocity in Figure 4.14a and 4.15a). Secondly, the study site was located in the current channel in Moreton Bay; however, the current and wind direction kept changing over time so this may have interfered with flux measurement (Figure 4.14a and 4.15a). This supports the previous finding from the Tweed River deployments, that the complexity of the environment (e.g., wind and current directions) plays a major role in flux measurement.

The ECO1 was also used to measure O_2 flux in benthic microalgae (BMA) from Heron Island lagoon. Surprisingly, positive O_2 fluxes were observed despite it being nighttime and decreasing in O_2 concentration in both deployments (Figure 4.18 and 4.19). This event occurred during a very low flow velocity (<5 cm s^{-1}) which might result in O_2 accumulation on the seafloor or at a gradient under the measurement point. Therefore, when the eddies (the circulation of water) occurred, the O_2

concentration was released from the seafloor, and then the optode would detect the O_2 fluctuation resulting in the appearance of positive O_2 fluxes during darkness. Then the negative O_2 occurred after the O_2 concentration was well-mixed in water column as shown in Figure 4.18 and 4.19. Furthermore, the tide on Heron Island also played an important role in O_2 dynamics because tidal currents influence water velocity which in turn controls O_2 flux measurements. Last but not least, due to the inconsistency in ECO1 in the field, which may be from other environmental factors (e.g. wave, current, tide), the ECO1 was then examined in the laboratory flume under controlled flow conditions in order to verify the limitation and reliability of the ECO1 in O_2 flux measurement (see Chapter 3).

4.5 CONCLUSION

Water velocity has an effect on the density of seagrasses (*Zostera capricorni* and *Halophila ovalis*), epiphytic algal cover and morphology of *Z. capricorni* from the Tweed River, Queensland. The Eddy Correlation system was deployed in three marine environments and has the potential to measure O_2 flux; however, there were some situations where the EC was not able to measure O_2 flux correctly. For example, if the environmental conditions of the study site were complex due to changing wind and current directions, the EC was not able to capture all fluxes. In addition, if the study site had large amounts of mobile fauna this could cause breakages to the EC system, especially to the EC microelectrode which is fragile. However, the Eddy Correlation system can be used to measure O_2 fluxes if it is deployed in a non-complex environment, such as a narrow canals or deep sea habitats. Therefore, the accuracy and precision of the EC depends upon water flow, tide and current conditions. There is a limitation in monitoring data real-time and

recharging the battery of the ECE1, however, this issue has been improved in the ECO1 where the raw data can be monitored in real-time. It is not possible to have a replication from both ECE and ECO but the data processing and data interpretation for ECE and ECO are similar. The ECO is more robust than ECE; therefore the ECO is more suitable for using in the field environment. However, there were some logistic difficulties in deploying the EC system in exposed coastal environment (e.g., Heron Island) due to the large size of the system, which will require significant manpower for field deployment.

CHAPTER 5:

GENERAL DISCUSSION

5. GENERAL DISCUSSION

5.1 SUMMARY OF EXPERIMENTS TO DETERMINE O_2 FLUX, RELIABILITY AND LIMITATIONS OF EDDY CORRELATION SYSTEM

This thesis represents the first research to provide insight into the reliability and limitations of the Eddy Correlation (EC) technique in measuring O_2 flux in marine and estuarine benthic communities. Dissolved oxygen flux was investigated both in the field studies of seagrass meadows, benthic microalgal community, and bare sediment, and in the laboratory flume using both EC and O_2 microprofiling techniques. The O_2 microprofiling technique was used to validate the data taken from the EC system.

5.2 RELIABILITY AND LIMITATIONS OF EDDY CORRELATION SYSTEM

The reliability and limitations of EC were assessed under these criteria: accuracy and precision, ranges of environmental conditions, sensor technology requirements, data processing and data interpretation, ease of operation and replication. The Eddy Correlation technique has several theoretical advantages over other flux measurement methods because it can measure over vegetated, permeable sediments, hard surfaces and coral reefs without disturbing natural light and hydrodynamic conditions (Kuwae et al. 2006; Glud et al. 2010; Hume et al. 2011) and the measurements can cover relativeley large areas (>100 m^2) (Berg et al. 2007). However, the validation of the EC technique in the field and laboratory were only

partially completed. Our study is the first study to determine the limitations and reliability of the EC technique when deployed in the field and laboratory.

5.2.1 Accuracy, precision and range of environmental conditions

5.2.1.1 Field study (natural habitat)

O_2 flux was investigated in the field at Tweed River (TWD1, TWD2), Moreton Bay (MB48, DWN) and Heron Island lagoon (BMA) using a series of EC systems (ECE1, ECE2 and ECO1) (Chapter 4). At vegetated sites (e.g. TWD1, TWD2, BMA), the positive O_2 fluxes were expected during daylight because photosynthetic activity is greater than respiration, while negative O_2 fluxes were expected during darkness due to the respiration of seagrass and other microbial activities (Hume et al. 2011; Long et al. 2012). At an unvegetated site (e.g., MB48, DWN), a negative O_2 flux is expected due to microbial activities (e.g., respiration, decomposition, remineralisation) (Murray and Wetzel; Berg et al. 2013). However, our study showed unexpected results e.g., positive O_2 flux during darkness and negative O_2 flux during daylight. This may have resulted from a large fluctuation in water velocity which may have been caused by tidal change (TWD; BMA), rough water, strong wind and current (DWN, BMA).

Under low water velocity, an inconsistency of O_2 flux (close to zero, or positive flux or negative flux) was found. Low water velocity may result in limiting mixing and no measure of sediment respiration. However, low water velocity may also limit mixing and allow sediment respiration, therefore, the DBL increased and caused negative flux. On the other hand, low water velocity may allow O_2 accumulation on the seafloor or gradient under the measurement point. When the eddies (the circulation of water) occurred, the O_2 accumulated on the seafloor was released into

the water column, and then was detected by the optode, leading to positive O_2 flux measurement. These unexpected results from the field study indicated an inconsistency and inaccuracy of the EC technique when used in a complex environment (tidal change, rough water, strong wind and current) and in a low flow environment.

5.2.1.2 Laboratory study (racetrack flume)

ECE1, ECO1 and ECO2 were used to investigate the O_2 flux in seagrass and sediment in the laboratory racetrack flume (Chapter 2, 3). In the seagrass experiments, positive O_2 fluxes occurred during light conditions and negative O_2 flux occurred during darkness and this is consistent with other field-studies (Hume et al. 2011; Long et al. 2013; Rheuban et al. 2014). In addition, net metabolism of seagrass should be influenced by light and temperature, and follow the same trend as chlorophyll *a* fluorescence measurement (Franklin and Badger 2001; Longstaff et al. 2002) due to the fact that photosynthesis and O_2 flux would be highest at the optimum temperature and light. However, this study showed a random fluctuation of O_2 fluxes during light and dark conditions in both temperature and light treatments (measured using ECE1; Chapter 3) and the results were not consistent with other studies (Marsh et al. 1986; Bulthuis 1987; Perez and Romero 1992; Lee et al. 2007; Massa et al. 2009; Marba and Duarte 2010; Hume et al. 2011). These inconsistencies may be due to the footprint of the laboratory racetrack flume (Berg et al. 2007), along with the low density of the seagrass patch. The positive flux during darkness may be due to electrical noises from nearby electrical equipment, which we were unable to control (McGinnis et al. 2011). In addition, low flow velocity (7 cm^{-1}) used

in this study may lead to low turbulence in the racetrack flume, therefore, inaccuracy of O_2 flux measurement was found.

When comparing sediment O_2 fluxes between ECO1 and O_2 microprofiling techniques, there was no significant difference in sediment O_2 uptake at middle and high flow (Chapter 3). However, an underestimation of O_2 flux was found when using ECO1 at low flow velocity due to the fact that there was a small flux at low flow (Chapter 3; Berg et al. 2003; Berg et al. 2009). These results indicated the limitation of ECE1 and ECO1 in capturing small flux under low flow velocity (Chapter 3).

Later, the ECO1 was replaced with the ECO2 in order to improve O_2 flux measurement (Chapter 2). The ECO2 was used to investigate the sediment O_2 flux in the laboratory racetrack flume and the data were validated using the O_2 microprofiling technique (Chapter 3). This study showed that there was no significant difference between O_2 fluxes measured by ECO2 and O_2 microprofiling. This indicates that the ECO2 is more reliable in measuring O_2 flux in the laboratory racetrack flume; however, it should be noted that strong light (e.g., in shallow water or exposure to direct sunlight), may interfere with O_2 flux measurement, and it may not be able to be used for long-term deployment due to photo-bleaching of indicator dyes.

5.2.2 Scale of measurement

EC allows measurement of O_2 flux under natural conditions, as it does not disturb the hydrodynamic conditions or light field and it can be used in complex topographic substrates (e.g., seagrass, infauna, not just bare sediment). More importantly, it can

be used *in situ* for long-term data collection and allows a much larger area of habitat to be sampled (100's m^2), providing a much more integrated sample of the habitat. On the other hand, benthic chambers and the microprofiling method are limited in measuring the whole community or whole plant metabolism as the benthic chamber and microprofiling method can be used to measure the flux at only 0.5 m^2 and at the microscale (Borum et al. 2006; Silva et al. 2009). Therefore, the EC application removes the sample bias towards small-scale heterogeneity as can occur with smaller sample techniques (Silva et al. 2009).

5.2.3 Sensor technology requirement and ease of operation

Both optodes and microelectrodes can be used for underwater eddy covariance (EC) measurements. The O_2 optode is also not very invasive, especially if a thin, very sensitive optical sensor is used (such as a microoptode). It can measure very low O_2 concentrations and is more robust compared to a microelectrode; however, the O_2 optode has a slightly slower response than microelectrode and new approaches are currently being tested to improve the speed of optode (Chipman et al. 2012). The fragility of the ECE indicates that it is not suitable for use in fields which have large amounts of mobile fauna (e.g., jelly fish, fish) or are experiencing severe weather condition (long-term data collection). This study showed that the accuracy and precision of the ECE depends on flow condition and surrounding environment (e.g., electrical instrument), while the accuracy and precision of the ECO depends only on flow condition. Even though the ECE has more sensitivity than the ECO (lower sensor response time) and higher sensor resolution (64 Hz for ECE and 16 Hz for ECO), the ECO provides more robustness than the ECE which will allow the ECO to be used in more extreme environments with greater ease of use.

5.2.4 Data processing, data interpretation and replication

For the ECO, two types of conversion methods (phase shifted (PS) and fluorescence intensity signal (IT)) have been used for O_2 conversion (Klimant et al. 1995; Holst et al. 1997). The phase-shifted method is based on the luminescence lifetimes or decays (Holst et al. 1997) and is the most common method for O_2 conversion (Lakowicz 1983; Berndt and Lakowicz 1992; Wolfbeis 1991; Holst et al. 1997; Kühl 2005; Rickelt et al. 2013). On the other hand, the intensity signal method, which is less popular, can be vulnerable to interference from the fluctuation of light sources or the bleaching effect of indicator dyes (Holst et al. 1995; Klimant et al. 1995). Interestingly, this study showed that O_2 conversion based on intensity signal (IT) provided better results due to the lower fluctuation of O_2 concentration, which led to steadier O_2 consumption rate in sediment (Chapter 2). O_2 flux from the phase-shifted (PS) method, however, provided an inconsistent flux due to higher noise. This indicates that the intensity signal (IT) method is more reliable for applications of the EC system that need high frequency measurement (>16 Hz) of O_2 (Berg et al. 2007; Chipman et al. 2012).

In the EC method, the fluctuation of vertical velocity and O_2 concentration can be calculated by subtracting the mean value of the measurement from its instantaneous value (Kabat 2004; Hume et al. 2011; Reimer et al. 2012; Long et al. 2013). The mean can be calculated by various methods, such as linear detrending (LD) and running mean (RM). This study compared the O_2 flux calculated by linear detrending (LD) and running mean (RM) and found no significant difference between the two methods (Chapter 2), indicating that both are acceptable to use for O_2 flux calculation. However, it has been suggested that the linear detrending (LD) was

preferable due to its 15 minute block calculations. In addition, Lorrai et al. (2010) found no difference in some situations, but the running mean was not appropriate where there were shifts in the direction of water velocity.

The data from ECO1 has also been validated with the O_2 microprofiling technique, where O_2 fluxes from intensity signal conversion (IT-LD and IT-RM) were not significantly different from O_2 fluxes from O_2 microprofiling technique. This result is consistent with previous studies that used EC to measure O_2 flux in sediment (Lorrai et al. 2010; Reimers et al. 2012; Berg et al. 2013; Holtappels et al. 2013; Long et al. 2013). This study suggested that the intensity method in the EC system can be used to convert the O_2.

Due to the problem in accessing data real-time, which may lead to time-wasting in deployment if some difficulties occur (e.g., sensor is broken), software development is needed to monitor real-time data collection real-time. Data processing and data interpretation for the ECE and ECO are similar and it is not possible to have a replication from both the ECE and ECO. The lack of replication is one of the weakest points of EC compared to other methods (e.g., benthic chamber, O_2 microprofiler).

5.3 METABOLISM OF MARINE AND ESTUARINE ECOSYSTEMS

5.3.1 Seagrass: effects of light, temperature and water velocity

Photosynthetic efficiency and metabolism of seagrass *Zostera muelleri* under different temperatures and light conditions were investigated using chlorophyll *a* fluorescence and the EC technique in order to understand how light and temperature affect primary production of this species. Photosynthesis of *Z. muelleri* was

investigated at both the organism scale (PAM fluorometry and community scale (EC)). PAM fluorometry allows the measurement of PSII photochemical efficiency and determination of stress in photosynthetic organisms (Silva et al. 2009). Effective quantum yield ($\Delta F/F_m'$) and non-regulated heat dissipation (Y(NO)) at 28 and 31°C and 400 and 600 µmol photons m^{-2} s^{-1} were significantly lower and higher, respectively (Chapter 3). These results indicate a decrease in the number of PSII reaction centres, a loss of functional PSII units, a down-regulation of photochemistry and/or photoinhibition leading to less capacity for light absorption and photosynthesis (Campbell et al. 2006; Allakhverdiev et al. 2008). Temperature and light stress are likely to damage PSII reaction centres possibly by damaging the D1 protein and disrupting thylakoid membrane stability (Allakhverdiev et al. 2008). These results are consistent with other studies that demonstrated damage in seagrass photosynthesis under temperature and light stress (Ralph 1998; Ralph 1999; Campbell et al. 2006; York et al. 2013). $\Delta F/F_m'$ was highest at 25°C and 150-250 µmol photons m^{-2} s^{-1}, suggesting these conditions are the optimal temperature and irradiance for photosynthesis of *Z. muelleri* from Lake Macquarie.

At a community scale, average O_2 flux was highest at 25°C under 400 µmol photons m^{-2} s^{-1} and at 21°C and 600 µmol photons m^{-2} s^{-1}. The lowest O_2 flux was observed at 21°C under 400 µmol photons m^{-2} s^{-1} and at 21°C and 150 µmol photons m^{-2} s^{-1} (Chapter 3). Previous studies suggest that optimal temperature and light may be related due to their need to maintain a positive carbon balance, indicating that seagrass at higher temperature needs more light for photosynthesis than seagrass at lower temperature (Masini et al. 1995; Lee et al. 2007; Collier et al. 2011). On the other hand, seagrass living at higher light intensity may be less tolerant to higher

temperatures due to thermal stress and photoinhibition (Ralph 1999). Therefore, further studies of the combined effect of light and temperature on seagrass photosynthesis and metabolism should be considered.

This study showed that in darkness, oxygen production rapidly decreased. This suggested that post-illumination enhanced respiration (PIER) occurred (Beardall et al. 1994), resulting in substantial removal of O_2 and a rapid switch in microbial activity from aerobic to anaerobic condition (Chapter 3). This result is consistent with a previous study showing that the level of PIER (or O_2 consumption) increased with increasing light intensity (Chapter 3; Beardall et al. 1994).

Percentage cover and density of seagrasses (*Zostera capricorni* and *Halophila ovalis*), epiphytic algal cover and morphology of *Z. capricorni* were investigated at two sites with different water velocites in the Tweed River, Queensland (Chapter 4). Higher seagrass biomass, shoot density and leaf size were observed at the high water velocity site (TWD2), while greater epiphytic algal cover was found at the lower water velocity site (TWD1). These results indicate that higher water velocity may reduce the diffusive boundary layer thickness, resulting in higher nutrient uptake and photosynthesis of seagrass (Koch 1994; Thomas et al. 2000). In euthrophic conditions, lower water velocities may also allow excessive epiphytic algal growth which will reduce light and nutrient availability for seagrasses, and therefore, photosynthesis, productivity and growth of seagrasses will be inhibited (Bulthuis and Woelkerling 1983; Tomasko and Lapointe 1991; Neckles et al. 1994; Frankovich and Fourqurean 1997; Anderson and Martone 2014).

5.3.2 Seagrass and benthic microalgal communities vs bare sediment

Seagrass metabolism, benthic microalgae communities and bare sediment were investigated in the field and laboratory (Chapter 3, 4) using the EC and O_2 microprofiling techniques. Sediment O_2 uptake was observed in both field and laboratory (Chapter 3, 4) and the laboratory experiment found that sediment O_2 uptake varied in relation to temperature and water velocity (Chapter 3). These results may be due to the fact that increased temperature leads to higher microbial activity and microbial population, and lower viscosity and higher diffusive coefficient of water (Iannotti et al. 1993; Liang et al. 2003), whilst increased water velocity leads to the lowering of diffusive boundary layer thickness and increases in the rate of sediment O_2 uptake (Jorgensen and Marais 1990). In the field, this study found net sediment O_2 uptake in both sediment sites (MB27, MB48) and the seagrass site (MGSG9) in Moreton Bay (Chapter 4). Generally, seagrass can transport O_2 into sediment through their roots and rhizomes, which results in increasing positive O_2 flux into the sediment (Ku et al. 1999). The negative O_2 flux found at the seagrass site may be due to low productivity from high turbidity and extensive resuspension of sediment (Hauxwell and Valiera 2004).

There was positive O_2 flux during daylight and negative O_2 flux during darkness in benthic microalgae communities (BMA) in Heron Island lagoon (Chapter 4). However, some positive O_2 flux occurred during darkness at this site under very low flow velocity (<5 cm s^{-1}). Under very low flow conditions, there may be an O_2 accumulation on the seafloor or gradient under the measurement point. However, when eddies (the circulation of water) occurred, the O_2 accumulated at the seafloor was released into the water column, and detected by the optode, leading to positive

O_2 flux measurements. After mixing of the water column occurred, the negative O_2 flux was detected.

In summary, these results (Chapter 3, 4) clearly demonstrate that O_2 flux in sediment, seagrass and benthic algal community is dependent on several environmental parameters including water temperature, light and water velocity and that EC is capable of distinguishing these factors. In particular, insight into the BBL dynamic conditions provided by EC and the subsequent effect on O_2 flux offers a richer understanding of the factors affecting flux rates.

5.4 SUMMARY OF KEY FINDINGS

This study showed that the Eddy Correlation technique has potential to determine net ecosystem metabolism in sediment, seagrass and benthic microalgae, and may be applied to other ecosystems (e.g., coral reefs, sea ice). However, the deployment of the Eddy Correlation system should be conducted with care and with the validation of other methods (e.g., benthic chamber, microprofiling).

5.4.1 Flow velocity and temperature play an important role in sediment O_2 flux and flow velocity has more influence than temperature.

5.4.2 Temperature and light have an effect on the photosynthetic capacity of *Zostera mulleri.* The optimal temperature and light for photosynthesis for *Z. mulleri* from Lake Macquarie, New South Wales is 25°C and 150-250 μmol photons m^{-2} s^{-1}.

5.4.3 Limitations of Eddy Correlation in the field are: 1) the ECO is more suitable than the ECE for use in the field for long-term data collection due to the fragility of microelectrode, 2) O_2 flux measured by EC were inconsistent due

to a large fluctuation in water velocity which may be caused by tidal change (TWD; BMA), rough water, strong wind and current, 3) O_2 flux may be under or overestimated when used under low flow velocity conditions due to non-mixing water, and 4) strong light may have an effect on EC systems that utlilise optodes.

5.4.4 The limitations of Eddy Correlation used in the laboratory are: 1) O_2 flux may be underestimated in low flow environments, 2) electrical noise from nearby equipment may interfere with EC measurement, 3) flux footprint may play an important role in EC measurement in a laboratory flume, and 4) high-speed sampling of the ECO (>10 Hz) may also increase noise in the O_2 signal.

5.5 PERSPECTIVE FOR FUTURE RESEARCH

This research has provided a better understanding of the Eddy Correlation technique in O_2 flux measurement in seagrass, benthic microalgae and sediment. However, the limitations and reliability of O_2 flux measurement when using EC in other ecosystems (e.g., coral reef, sea ice, macroalgae) require further investigation. The optode technology should be further developed in order to improve its response time, sampling frequency, sensor resolution, time synchronisation with ADV and robustness. In addition, temperature compensation of optodes should be developed in order to achieve high sampling rates. The microelectrode technology should also be further developed to improve its robustness. The development of software is needed to monitor the real-time data collection. The installation of LED light on the EC system to show the electrode status (working or broken) should be helpful.

Assuming we have homogenous habitat, steady conditions (flow, temperature) and flat terrain which are basic assumptions that has been used in terrestrial EC in order to obtain the most accurate flux, we expect to see positive O_2 flux from benthic communities during daylight and negative flux during night time. These fluxes should have a similar trend when compared to EC applications in terrestrial habitats. It is very difficult to find the large scale homogenous habitat in aquatic systems, therefore it is difficult to meet these assumptions, EC in aquatic systems still has potential to measure the O_2 flux due to the smaller footprint in aquatic systems, comparing to terrestrial systems as linked to difference in fluid viscosity between air and water. Due to the technical issues associated with EC which have led to unreliable results, this thesis was unable to focus on issue of scale, heterogeneity and flow.

The lack of replication is one of the weakest points of EC compared to other methods; therefore, hardware technology should be developed to allow data collection with replications. This requires multiple instruments and cheaper systems. At this stage, the EC should mainly be applied in steady and less complex environmental and hydrodynamic conditions (e.g. narrow river, estuary, and deep water). I would recommend the Eddy Correlation optode system over the Eddy correlation microelectode system to be used for investigating the fluxes for field deployment due to the optode robustness. Furthermore, the characterization of boundary layers in the water column and indirect and direct measurements of other fluxes (e.g., CH_4, CO_2, pH, temperature) using the Eddy Correlation system requires further development and investigation. However, nitrate flux has been measured by Eddy correation technique in order to quantify the sediment-fixed nitrogen loss

(Johnson et al 2011). To quantify CH_4 flux would be really interesting due to the role of CH_4 in climate change and ocean acidification scenarios. Additionally, it will be important to investigate the combined effect of light, temperature, pH and water velocity on photosynthesis and metabolism of seagrass, benthic microalgae and sediment in the future. Real-time temperature correction would be useful for O_2 flux measured by ECO.

REFERENCES

REFERENCES

Referencing format consistent with the Journal of Marine Biology

Allakhverdiev SI, Kreslavski VD, Klimov VV, Los DA, Carpentier R, Mohanty P (2008) Heat stress: an overview of molecular responses in photosynthesis. Photosynthetic Research 98: 541-550

Alongi DM, Boto KG, Tirendi F (1989) Effect of exported mangrove litter on bacterial productivity and dissolved organic carbon fluxes in adjacent tropical nearshore sediments. Marine Ecology Progress Series 56: 133-144

Anderson L, Martone PT (2014) Biomechanical consequences of epiphytism in intertidal macroalgae. Journal of Experimental Biology 217: 1167-1174

Arnosti C, Jorgensen BB, Sagemann J, Thamdrup B (1998) Temperature dependent of microbial degradation of organic matter in marine sediments: polysaccharide hydrolysis, oxygen consumption, and sulfate reduction. Marine Ecology Progress Series 165: 59-70

Aro EM, McCaffery S, Anderson JM (1993) Photoinhibition and D1 protein degradation in peas acclimated to different growth irradiances. Plant Physiology 103: 835-843

Atkinson MJ, Kotler E, Newton P (1994) Effects of water velocity on respiration, calcification, and ammonium uptake of a *Porites compressa* community. Pacific Science 48: 296-303

Atkinson MJ, Smith SV (1983) C:N:P ratios of benthic marine plants. Limnology and Oceanography. 28: 568-574

Atwell BJ, Kriedemann PE, Turnbull CGN (1999) Plants in action: adaptation in nature, performance in cultivation. Macmillan publisher Australia

Aubinet M (2008) Eddy covariance CO_2-flux measurements in nocturnal conditions: An analysis of the problem. Ecological Applications 18: 1368-1378

Backman TW, Barilotti DC (1976) Irradiance reduction: Effects on standing crops of the eelgrass *Zostera marina* in a coastal lagoon. Marine Biology 34: 33-40

Baird D, Asmus H, Asmus R (2011) Carbon, nitrogen and phosphorus dynamics in nine sub-systems of the Sylt-Rømø Bight ecosystem, German Wadden Sea. Estuarine, Coastal and Shelf Science 91: 51-68

Baird ME (2001) Technical description of the CSIRO SERM ecological model. CSIRO Land and Water, Canberra ACT, Australia

Baldocchi DD (2003). Assessing the eddy covariance technique for evaluating carbon dioxide exchange rates of ecosystem: past, present and future. Global Change Biology 9: 479-492

Barnes DJ (1983) Profiling coral reef productivity and calcification using pH and oxygen electrodes. Journal of Experimental Marine Biology and Ecology 66: 149-161

Barr JG, Engel V, Fuentes JD, Zieman JC, O'Halloran TL, Smith TJ, Anderson GH (2010) Controls on mangrove forest-atmosphere carbon dioxide exchanges in western Everglades National Park. Journal of Geophysical Research: Biogeosciences (2005–2012) 115

Beardall J, Burger-Wiersma T, Rijkeboer M, Sukenik A, Lemoalle J, Dubinsky Z, Fontvielle D (1994) Studies on enhanced post-illumination respiration in microalgae. Journal of Plankton Research 16: 1401-1410

Beardall J, Sobrino C, Stojkovic S (2009) Interactions between the impacts of ultraviolet radiation, elevated CO_2, and nutrient limitation on marine primary producers. Photochemical and Photobiological Sciences 8(9): 1257-1265

Bender M, Grande K, Johnson K, Marra J, Williams PJlB, Sieburth J, Pilson M, Langdon C, Hitchcock G, Orchado J, Ilunt C, Donaghay P, Heinemann K (1987) A comparison of four methods for determining planktonic community production. Limnology and Oceanography 32: 1085-1098

Bender M, Orchado J, Dickson M-L, Barber R, Lindley S (1999) In vitro O_2 fluxes compared with ^{14}C production and other rate terms during the JGOFS Equatorial Pacific experiment. Deep Sea Research 46: 637-654

Berg P, Glud RN, Hume A, Stahl H, Oguri K, Meyer V, Kitazato H (2009) Eddy correlation measurements of oxygen uptake in deep ocean sediments. Limnology and Oceanography: Methods 7: 576-584

Berg P, Huettel M (2008) Monitoring the seafloor using the non-invasive eddy correlation technique: Integrated benthic exchange dynamics. Oceanography 21: 164-167

Berg P, Long MH, Huettel M, Rheuban JE, McGlathery KJ, Howarth RW, Foreman KH, Giblin AE, Marino R (2013) Eddy correlation measurements of oxygen fluxes in permeable sediments exposed to varying current flow and light. Limnology and Oceanography 58: 1329-1343

Berg P, Roy H, Janssen F, Meyer V, Jorgensen BB, Huettel M, De Beer D (2003) Oxygen uptake by aquatic sediments measured with a novel non-invasive eddy-correlation technique. Marine Ecology Progress Series 261: 75-83

Berg P, Roy H, Wiberg PL (2007) Eddy correlation flux measurements : The sediment surface area that contributes to the flux. Limnology and Oceanography A 52: 1672-1684

Berndt KW, Lakowics JR (1992) Electroluminescent lamp-based phase fluorometer and oxygen sensor. Analytical Biochemistry 201: 319-325

Berner RA (1980) Early diagenesis: A theoretical approach. Princeton University Press, NJ

Berninger U-G, Huettel M (1997) Impact of flow on oxygen dynamics in photosynthetically active sediments. Aquatic microbial ecology 12: 291-302

Binzer T, Borum J, Pedersen O (2005) Flow velocity affects internal oxygen conditions in the seagrass *Cymodocea nodosa*. Aquatic Botany 83: 239-247

Borum J, Sand-Jensen K, Binzer T, Pedersen O, Greve TM (2006) Oxygen movement in seagrasses. In: Larkum AWD, Orth RJ, Duarte C (eds) Seagrasses: Biology, Ecology and Conservation. Springer, Dordrecht, Netherlands, pp 255-270

Bottom DL (1981) A flow-through system for field measurements of production by marine macroalgae. Marine Biology 64: 251-257

Boudreau BP (2001) Solute transport above the sediment-water interface. In: Boudreau BP, Jørgensen BB (eds) The Benthic Boundary Layer: Transport Processes and Biogeochemistry. Oxford University Press, Oxford, pp 104-126

Boudreau BP, Paul B (1997) Diagenetic models and their implementation: modelling transport and reactions in aquatic sediments. Springer New York

Brand A, McGinnis DF, Wehrli B, Wuest A (2008) Intermittent oxygen flux from the interior into the bottom boundary of lakes as observed by eddy correlation. Limnology and Oceanography 53: 10

Bulthuis DA (1983) Effect of in situ light reduction on density and growth of the seagrass *Heterozoster tasmanica* (Martens Ex Aschers) Den Hartog in Western Port, Victoria, Australia. Journal of Experimental Marine Biology and Ecology 67: 91-103

Bulthuis DA (1987) Effects of temperature on photosynthesis and growth of seagrasses. Aquatic Botany 27: 27-40

Bulthuis DA, Woelkerling WJ (1983) Biomass accumulation and shading effects of epiphytes on leaves of the seagrass, *Heterozoster tasmanica* in Victoria, Australia. Aquatic Botany 16: 137-148

Burba G (2013) Eddy covariance method for scientific, industrial, agricultural and regulatory applications: a field book on measuring ecosystem gas exchange and areal emission rates. LI-COR Bioscience, Lincoln, USA, 331 pp

Burba GG, Anderson DJ (2010) A brief practical guide to eddy covariance flux measurements: Principles and workflow examples for scientific and industrial applications. LI-COR Biosciences, Lincoln, Nebraska, USA

Cahoon LB (1988) Use of whirling cup rotor to stir benthic chambers. Hydrobiologia 160: 193-198

Campbell SJ, McKenzie LJ, Kerville SP (2006) Photosynthetic responses of seven tropical seagrasses to elevated seawater temperature. Journal of Experimental Marine Biology and Ecology 330: 455-468

Carvalho MC, Eyre BD (2012) Measurement of planktonic CO_2 respiration in the light. Limnology and Oceanography: Methods 10: 167-178

Chipman L, Huettel M, Berg P, Meyer V, Klimant I, Glud R, Wenzhoefer F (2012) Oxygen optodes as fast sensors for eddy correlation measurements in aquatic systems. Limnology and Oceanography: Methods 10: 304-316

Collier CJ, Lavery PS, Masini RJ, Ralph PJ (2009) Shade-induced response and recovery of the seagrass *Posidonia sinuosa*. J Journal of Experimental Marine Biology and Ecology 370: 89–103

Connell EL, Colmer TD, Walker DI (1999) Radial oxygen loss from intact roots of Halophila ovalis as a function of distance behind the root tip and shoot illumination. Aquatic Botany 63: 219-228

Cornelisen CD, Thomas FIM (2002) Ammonium uptake by seagrass epiphytes: Isolation of the effects of water velocity using an isotope label. Limnology and Oceanography 47: 1223-1229

Cornelisen CD, Thomas FIM (2004) Ammonium and nitrate uptake by leaves of the seagrass *Thalassia testudinum*: impact of hydrodynamic regime and epiphyte cover on uptake rates. Journal of Marine Systems 49: 177-194

Costanza R, dArge R, de Groot R, Farber S, Grasso M, Hannon B, Limburg K, Naeem S, Oniell RV, Paruelo J, Raskin RG, Sutton P, van den Belt M (1997) The value of the world's ecosystem services and natural capital. Nature 387: 253-260

Crusius J, Berg P, Koopmans DJ, Erban L (2008) Eddy correlation measurements of submarine groundwater discharge. Marine Chemistry 109: 77-85

De Beer D, Larkum AWD (2001) Photosynthesis and calcification in the calcifying algae *Halimeda discoidea* studied with microsensors. Plant Cell and Environment 24: 1209-1217

Diaz-Pulido G (2008) Macroalgae. In: Patricia Hutchings MJK, Ove Hoegh-Guldberg (ed) The Great Barrier Reef: Biology, environment and management. CSIRO Publishing, Collingwood, pp 145-155

Drew EA (1979) Physiological aspects of primary production in seagrasses. Aquatic Botany 7: 139-150

Duarte C, Dennison W, Orth R, Carruthers T (2008) The charisma of coastal ecosystems: Addressing the imbalance. Estuaries and Coasts 31: 233-238

Duarte CM (2009) Global loss of coastal habitats – rates, cause and consequences. Fundacion BBVA, Bilbao, Spain 184 pp

Duarte CM, Cebrian J (1996) The fate of marine autotrophic production. Limnology and Oceanography 41: 1758-1766

Eyre BD, Ferguson AJP (2005) Benthic metabolism and nitrogen cycling in a subtropical east Australian estuary (Brunswick): Temporal variability and controlling factors. Limnology and Oceanography 50: 81-96

Eyre BD, Ferguson AJP, Webb A, Maher D, Oakes JM (2011) Metabolism of different benthic habitats and their contribution to the carbon budget of a shallow oligotrophic sub-tropical coastal system (southern Moreton Bay, Australia). Biogeochemistry 102: 87-110

Ferguson A, Eyre B (2013) Interaction of benthic microalgae and macrofauna in the control of benthic metabolism, nutrient fluxes and denitrification in a shallow sub-tropical coastal embayment (western Moreton Bay, Australia). Biogeochemistry 112: 423-440

Ferguson AJP, Eyre BD, Gay JM (2003) Organic matter and benthic metabolism in euphotic sediments along shallow sub-tropical estuaries, northern New South Wales, Australia. Aquatic Microbial Ecology 33: 137-154

Ferguson AP, Eyre B (2010) Carbon and nitrogen cycling in a shallow productive sub-tropical coastal embayment (Western Moreton Bay, Australia): The importance of pelagic–benthic coupling. Ecosystems 13: 1127-1144

Finnigan J (1999) A comment on the paper (1998): ‘‘On micrometeorological observations of surface–air exchange over tall vegetation’’. Boundary-Layer Meteorology 97: 55–64

Finnigan JJ, Clement R, Malhi Y, Leuning R, Cleugh HA (2003) A re-evaluation of long-term flux measurement techniques part I: Averaging and coordinate rotation. Boundary-Layer Meteorology 107: 1-48

Fitzpatrick J, Kirkman H (1995) Effects of prolonged shading stress on growth and survival of seagrass *Posidonia australis* in Jervis Bay, New South Wales, Australia. Marine Ecology Progress Series 127: 279-289

Foken T (2008) Experimental methods for estimating the fluxes of energy and matter. micrometeorology Micrometeorology. Springer Berlin Heidelberg, pp 105-151

Fonseca MS, Kenworthy WJ (1987) Effects of current on photosynthesis and distribution of seagrasses. Aquatic Botany 27: 59-78

Fonseca MS, Zieman JC, Thayer GW, Fisher JS (1983) The role of current velocity in structuring eelgrass (*Zostera marina L.*) meadows. Estuarine, Coastal and Shelf Science 17: 367-380

Forster S, Huettel M, Ziebis W (1996) Impact of boundary layer flow velocity on oxygen utilisation in coastal sediments. Marine Ecology Progress Series 13: 173-185

Fourqurean JW, Duarte CM, Kennedy H, Marbà N, Holmer M, Mateo MA, Apostolaki ET, Kendrick GA, Krause-Jensen D, McGlathery KJ, Serrano O (2012) Seagrass ecosystems as a globally significant carbon stock. Nature Geoscience 5: 505-509

Franklin L, Badger MR (2001) A comparison of photosynthetic electron transport rates in macroalgae measured by pulse amplitude chlorophyll fluorescence and mass spectrometry. Journal of Phycology 37: 756-767

Frankovich TA, Fourqurean JW (1997) Seagrass epiphyte loads along a nutrient availability gradient, Florida Bay, USA. Marine Ecology Progress Series 159: 37-50

Gao F, Yates SR (1998) Laboratory study of closed and dynamic flux chambers: Experimental results and implications for field application. Journal of Geophysical Research: Atmospheres 103: 26115-26125

Gattuso J-P, Frankignoulle M, Smith SV (1999) Measurement of community metabolism and significance of coral reefs in the CO_2 source-sink debate. Proceedings of the National Academy of Science U.S.A. 96:13017-13022

Gattuso J-P, Pichon M, Delesalle B, Canon C, Frankignoulle M (1996) Carbon fluxes in coral reefs. 1. Lagrangian measurement of community metabolism and resulting air-sea CO_2 disequilibrium. Marine Ecology Progress Series 145:109-121

Gattuso J-P, Pichon M, Delesalle B, Frankignoulle M (1993) Community metabolism and air-sea CO_2 fluxes in a coral reef ecosystem (Moorea, French Polynesia). Marine Ecology Progress Series 96:259-267

Gevaert F, Delebecq G, Menu D, Brutier L (2011) A fully automated system for measurements of photosynthetic oxygen exchange under immersed conditions: an example of its use in *Laminaria digitata* (Heterokontophyta: Phaeophyceae). Limnology and Oceanography: Methods 9: 361-379

Glud RN, Berg P, Hume A, Batty P, Blicher ME, Lennert K, Rysgaard S (2010) Benthic O_2 exchange across hard bottom substrates quantified by eddy correlation in a sub-Arctic fjord. Marine Ecology Progress Series 417:1-12

Glud RN, Ramsing B, Revsbech NP (1992) Photosynthesis and photosynthesis coupled respiration in natural biofilms quantified with oxygen microsensors. Journal of Phycology 28: 51-60

Gordon DM, Grey KA, Chase SC, Simpson CJ (1994) Changes to the structure and productivity of a *Posidonia sinuosa* meadow during and after imposed shading. Aquatic Botany 47: 265-275

Goring DG, Nikora VI (2002) Despiking acoustic doppler velocimeter data. Journal of Hydraulic Engineering 128: 117-126

Grande KD, Marra J, Langdon C, Heinemann K, Bender ML (1989) Rates of respiration in the light measured in marine phytoplankton using a ^{18}O isotope-labelling technique. Journal of Experimental Marine Biology and Ecology 129: 95-120

Greiner JT, McGlathery KJ, Gunnell J, McKee BA (2013) Seagrass restoration enhances "Blue Carbon" sequestration in coastal waters. Plos One 8: e72469

Gribsholt B, Boschker HT, Struyf E, Andersson M, Tramper A, De Brabandere L, Van Damme S, Brion N, Meire P, Dehairs F (2005) Nitrogen processing in a tidal freshwater marsh: A whole ecosystem ^{15}N labeling study. Limnology and Oceanography 50: 1945

Gruber RK, Kemp WM (2010) Feedback effects in a coastal canopy-forming submersed plant bed. Limnology and Oceanography 55: 2285-2298

Häder D-P, Porst M, Herrmann H, Schafer J, Regas S (1996) Photoinhibition in the Mediterranean green alga *Halimeda tuna* Ellis et Sol measured *in situ*. Photochemistry and Photobiology 64: 428-434

Hama T, Miyazaki T, Ogawa Y, Iwakuma T, Takahashi M, Otsuki A, Ichimura S (1983) Measurement of photosynthetic production of a marine phytoplankton population using a stable 13C isotope. Marine Biology 73: 31-36

Hanelt D, Huppertz K, Nultsch W (1993) Daily course of photosynthesis and photoinhibition in marine macroalgae investigated in the laboratory and field. Marine Ecology Progress Series 97: 31-37

Hargrave BT (1969) Similarity of oxygen uptake by benthic communities. Limnology and Oceanography 14: 801-805

Harrison P, Booth DJ (2007) Coral Reefs: naturally dynamic and increasingly disturbed ecosystems. In: S. D. Connell BMG (ed) Marine ecology: an Australian perspective. Oxford University Press, pp 316-377

Hauxwell J, Valiela I (2004) Effects of nutrient loading on shallow seagrass-dominated coastal systems: patterns and processes. In: Nielsen SL, Banta GT, Pedersen MF (eds) Estuarine nutrient cycling: the influence of primary producers. Kluwer Academic Publishers, Dordrecht, pp 59−92

Hemminga MA (1998) The root/rhizome system of seagrasses: an asset and a burden. Journal of Sea Research 39: 183-196

Hemminga MA, Duarte CM (2000) Seagrass ecology. Cambridge University Press

Hermand JP, Nascetti P, Cinelli F (1998) Inversion of acoustic waveguide propagation features to measure oxygen synthesis by *Posidonia oceanica*. OCEANS '98 Conference Proceedings 912: 919-926

Holst G, Glud RN, Kühl M, Klimant I (1997) A microoptode array for fine-scale measurement of oxygen distribution. Sensors and Actuators B: Chemical 38: 122-129

Holst G, Kohls O, Klimant I, König B, Richter T, Kühl M (1998) A modular luminescence lifetime imaging system for mapping oxygen distribution in biological samples. Sensors and Actuators B 51: 163-170

Holst GA, Kühl M, Klimant I (1995) Novel measuring system for oxygen microoptodes based on a phase modulation technique. Proc. SPIE 2508, Chemical, Biochemical, and Environmental Fiber Sensors VII 387

Holtappels M, Glud RN, Donis D, Liu B, Hume A, Wenzhöfer F, Kuypers MMM (2013) Effects of transient bottom water currents and oxygen concentrations on benthic exchange rates as assessed by eddy correlation measurements. Journal of Geophysical Research: Oceans 118: 1157-1169

Holtappels M, Noss C, Hancke K, Cathalot C, McGinnis DF, Lorke A (2015) Aquatic eddy correlation: Quantifying the artificial flux caused by Stirring-Sensitive O_2 Sensors. PLoS ONE 10(1): e0116564

Hooper JNA, Soest RWMV, Debrenne F (2002) Phylum Porifera Grant 1836. In: J. N. A. Hooper RWMVS (ed) Systema Porifera: a guide to the classification of sponges. Kluwer Academic/Plenum Publishers, New York, pp 9-13

Hopkinson CS, Fallon RD, Jansson B-O, Schubauer JP (1991) Community metabolism and nutrient cycling at Gray's Reef, a hard bottom habitat in the Georgia Bight. Marine Ecology Progress Series 73: 105-120

Houghton J (2009) Global warming: the complete briefing. Cambridge University Press, United Kingdom

Hubas C, Davoult D, Cariou T, Artigas LF (2006) Factors controlling benthic metabolism during low tide along a granulometric gradient in an intertidal bay (Roscoff Aber Bay, France). Marine Ecology Progress Series 316: 53-68

Hughes TP (2008) Human impact on coral reefs. In: Patricia Hutchings MJK, Ove Hoegh-Guldberg (ed) The Great Barrier Reef: Biology, environment and management. CSIRO Publishing, Collingwood, pp 85-94

Hume AC, Berg P, McGlathery KJ (2011) Dissolved oxygen fluxes and ecosystem metabolism in an eelgrass (*Zostera marina*) meadow measured with the eddy correlation technique. Limnology and Oceanography 56: 86-96

Iannotti DA, Pang T, Toth BL, Elwell DL, Keener HM, Hoitink HAJ, (1993) A quantitative respirometric method for monitoring composting stability. Compost Science and Utilization 1: 52–56.

Ibarra-Obando SE, Heck KL, Spitzer PM (2004) Effects of simultaneous changes in light, nutrients, and herbivory levels, on the structure and function of a subtropical turtlegrass meadow. Journal of Experimental Marine Biology and Ecology 301: 193-224

Johnson JE, Marshall PA (2007) Climate change and the Great Barrier Reef: A vulnerability assessment. Great Barrier Reef Marine Park Authority and Australian Greenhouse Office, Australia

Johnson KS, Barry JP, Coletti LJ, Fitzwater SE, Jannasch HW, Love CF (2011) Nitrate and oxygen flux across the sediment-water interface observed by eddy correlation measurements on the open continental shelf. Limnology and Oceanography Methods 9: 543-553

Jørgensen BB, Marais DJ (1990) The diffusive boundary layer of sediments: Oxygen microgradients over a microbial mat. Limnology and Oceanography 35: 1343-1355

Jørgensen BB, Revsbech NP (1985) Diffusive boundary layers and the oxygen uptake of sediments and detritus. Limnology and Oceanography 30: 111-122

Jørgensen CB, Møhlenberg F, Sten-Knudsen O (1986) Nature of relation between ventilation and oxygen consumption in filter feeders. Compost Sci. Util. 29: 73-88

Juranek LW, Quay PD (2013) Using triple isotopes of dissolved oxygen to evaluate global marine productivity. Annual Review of Marine Science 5

Kabat P (2004) Vegetation, water, humans and the climate: A new perspective on an interactive system. Springer

Kaldy JE, Brown CA, Andersen CP (2013) In situ ^{13}C tracer experiments elucidate carbon translocation rates and allocation patterns in eelgrass *Zostera marina*. Compost Sci. Util. 487: 27-39

Karande TS (2007) Effect of scaffold architecture on diffusion of oxygen in tissue engineering constructs. PhD Dissertation. University of Texas at Austin

Kemp WM, Boynton WR, Sampou P (1987) Relative roles of benthic vs. pelagic processes in establishing and maintaining anoxia in Chesapeake Bay. In Mackiernan GB (ed): Dissolved oxygen in the Chesapeake Bay: Processes and effects. Marland Sea Grant Publiation Number UM-SG-TS-87-03

Klimant I (2003) Method and device for referencing fluorescence intensity signals. U.S. Patent No. 6,602,716. 5 August 2003

Klimant I, Meyer V, Kühl M (1995) Fiber-optic oxygen microsensors, a new tool in aquatic biology. Limnology and Oceanography 40: 1159-1165

Koch EW (1994) Hydrodynamics, diffusion-boundary layers and photosynthesis of the seagrass *Thalassia testudinum* and *Cymodocea nodosa*. Marine Biology 118: 767-776

Köhler-Rink S, Kühl M (2000) Microsensor studies of photosynthesis and respiration in larger symbiotic foraminifera. The physico-chemical microenvironment of *Marginopora vertebralis, Amphistegina lobifera* and *Amphisorus hemprichii*. Marine Biology 137: 473-486

Koopmans M, Martens D, Wijffels RH (2010) Growth efficiency and carbon balance for the sponge *Haliclona oculata*. Marine Biotechnology 12: 340-349

Kramer DM, Johnson G, Kiirats O, Edwards GE (2004) New fluorescence parameters for the determination of QA redox state and excitation energy fluxes. Photosynthesis Research 79: 209–218

Ku TCW, Walter LM, Coleman ML, Blake RE, Martini AM (1999). Coupling between sulfur recycling and syndepositional carbonate dissolution: Evidence from oxygen and sulfur isotope compositions of pore water sulfate, South Florida Platform, USA. Geochimica et Cosmochimica Acta 63: 2529–2546

Kühl M (2005) Optical microsensors for analysis of microbial communities. Methods in Enzymology 397: 166-199

Kuwae T, Kamio K, Inoue T, Miyoshi E, Uchiyama Y (2006) Oxygen exchange flux between sediment and water in an intertidal sandflat, measured *in situ* by the eddy-correlation method. Geochim. Cosmochim. Act307: 59-68

Lagauzére S, Moreira S, Koschorreck M (2011) Influence of bioturbation on the biogeochemistry of littoral sediments of an acidic post-mining pit lake. Biogeosciences 8: 339-352

Lakowicz JR (1983) Measurement of fluorescence lifetimes. Principles of fluorescence spectroscopy. Springer US, pp 51-93

Langdon C, Gattuso J-P, Andersson A (2013) Measurements of calcification and dissolution of benthic organisms and communities. In: Riebesell U, Fabry VJ, Hansson L, Gattuso J-P (Eds) Guide to best practices for ocean acidification research and data reporting. Publications Office of the European Union, Luxembourg, 260 pp

Larkum A, Roberts G, Kuo J, Strother S (1989) Gaseous movement in seagrasses. In: Larkum A, McComb A, Shepherd S (eds) Biology of seagrasses A treatise on the biology of seagrasses with special reference to the Australian region. Elsevier, Amsterdam, pp 686–722

Larned ST, Atkinson M (1997) Effects of water velocity on NH_4 and PO_4 uptake and nutrient-limited growth in the macroalga *Dictyosphaeria cavernosa*. Geochim. Cosmochim. Act157: 295-302

Lavery PS, Mateo M-A, Serrano O, Rozaimi M (2013) Variability in the carbon storage of seagrass habitats and its complications for global estimates of blue carbon ecosystem service. Plos One 8: e73748

Law BE, Turner D, Campbell J, Sun OJ, Tuyl SV, Ritts WD, Cohen WB (2004) Disturbance and climate effects on carbon stocks and fluxes across Western Oregon USA. Global Change Biology 2004: 1429-1444

Leclerc MY, Thurtell GW (1990) Footprint prediction of scarlar fluxes using a Markovian analysis. Bounrary Layer Meterorology 53: 247-258

Lee K-S, Dunton KH (1997) Effect of *in situ* light reduction on the maintenance, growth and partitioning of carbon resources in *Thalassia testudinum* banks ex König. Journal of Experimental Marine Biology and Ecology 210: 53-73

Lee K-S, Park SR, Kim YK (2007) Effects of irradiance, temperature, and nutrients on growth dynamics of seagrasses: A review. Journal of Experimental Marine Biology and Ecology 350: 144-175

Lee X, Massman W, Law BE (2004) Handbook of micrometeorology: a guide for surface flux measurement and analysis. Kluwer Academic Publishers

Lesser MP, Weis VM, Patterson MR, Jokiel PL (1994) Effects of morphology and water motion on carbon delivery and productivity in the reef coral, *Pocillopora damicornis* (Linnaeus): Diffusion barriers, inorganic carbon limitation, and biochemical plasticity. Journal of Experimental Marine Biology and Ecology 178: 153-179

Levy O, Achituv Y, Yacobi YZ, Dubinsky Z, Stambler N (2006) Diel "tuning" of coral metabolism: physiological responses to light cues. Journal of Experimental Biology 209: 273-283

Liang N, Inoue G, Fujinuma Y (2003) A multichannel automated chamber system for continuous measurement of forest soil CO_2 efflux. Tree Physiology 23: 825-832

Lobban C, Harrison PJ (1994) Seaweed ecology and physiology. Cambridge University Press, Cambridge

Long MH, Berg P, de Beer D, Zieman JC (2013) In situ coral reef oxygen metabolism: An eddy correlation study. PLoS ONE 8: e58581

Long MH, Koopmans D, Berg P, Rysgaard S, Glud RN, and Sogaard DH (2012) Oxygen exchange and ice melt measured at the ice-water interface by eddy correlation. Biogeosciences 9(6): 1957-1967

Longstaff BJ, Kildea T, Runcie JW, Cheshire A, Dennison WC, Hurd C, Kana T, Raven JA, Larkum AWD (2002) An in situ study of photosynthetic oxygen exchange and electron transport rate in the marine macroalga *Ulva lactuca* (Chlorophyta). Photosynthesis Research 74: 281-293

Lorrai C, McGinnis DF, Berg P, Brand A, Wüest A (2010) Application of oxygen eddy correlation in aquatic systems. Journal of Atmospheric and Oceanic Technology 27: 1553-1546

Lowe RJ, Koseff JR, Monismith SG, Falter JL (2005) Oscillatory flow through submerged canopies: 2. Canopy mass transfer, Journal of Geophysical Research: Oceans 110: C10017

Luz B, Barkan E (2000) Assessment of oceanic productivity with the triple-isotope composition of dissolved oxygen. Science 288: 2028-2031

Macreadie PI, Ross DJ, Longmore AR, Keough MJ (2006) Denitrification measurements of sediments using cores and chambers. Marine Ecology Progress Series 326: 49-59

Madsen JD, Chambers PA, James WF, Koch EW, Westlake DF (2001) The interaction between water movement, sediment dynamics and submersed macrophytes. Hydrobiologia 444: 71-84

Maher D, Eyre BD (2011) Benthic carbon metabolism in southeast Australian estuaries: habitat importance, driving forces, and application of artificial neural network models. Marine Ecology Progress Series 439: 97-115

Maher DT, Santos IR, Leuven JRFW, Oakes JM, Erler DV, Carvalho MC, Eyre BD (2013) Novel use of cavity ring-down spectroscopy to investigate aquatic carbon cycling from microbial to ecosystem scales. Environmental Science and Technology 47: 12938-12945

Maljanen M, Hytönen J, Martikainen P (2001) Fluxes of N_2O, CH_4 and CO_2 on afforested boreal agricultural soils. Plant and Soil 231: 113-121

Marbà N, Duarte CM (2010) Mediterranean warming triggers seagrass (*Posidonia oceanica*) shoot mortality. Global Change Biology 16: 2366-2375

Marbà N, Hemminga M, Duarte C (2006) Resource translocation within seagrass clones: allometric scaling to plant size and productivity. Oecologia 150: 362-372

Marin-Guirao L, Ruiz JM, Sandoval-Gil JM, Bernardeau-Esteller J, Stinco CM, Melendez-Martinez A (2013) Xanthophyll cycle-related photoprotective mechanism in the Mediterranean seagrasses *Posidonia ceanica* and *Cymodocea nodosa* under normal and stressful hypersaline conditions. Aquatic Botany 109: 14-24

Marra J (2009) Net and gross productivity: weighing in with ^{14}C. Aquatic Microbial Ecology 56: 123-131

Marsh JA, Smith SV (1978) Productivity measurements of coral reefs in flowing water. In: Stoddart DR, Johannes RE (Eds.) Coral reefs research methods. Unesco, Paris, pp. 361-377

Marsh Jr JA, Dennison WC, Alberte RS (1986) Effects of temperature on photosynthesis and respiration in eelgrass (*Zostera marina* L.). Journal of Experimental Marine Biology and Ecology 101: 257-267

Masini RJ, Cary JL, Simpson CJ, McComb AJ (1995) Effects of light and temperature on the photosynthesis of temperate meadow-forming seagrasses in Western Australia. Aquatic Botany 46: 239-254

Masini RJ, Manning CR (1997) The photosynthetic responses to irradiance and temperature of four meadow-forming seagrasses. Aquatic Botany 58: 21–36

Mass T, Genin A, Shavit U, Grinstein M, Tchernov D (2010) Flow enhances photosynthesis in marine benthic autotrophs by increasing the efflux of oxygen from the organism to the water. Proceedings of the National Academy of Sciences 107: 2527-2531

Massa S, Arnaud-Haond S, Pearson G, Serrão E (2009) Temperature tolerance and survival of intertidal populations of the seagrass *Zostera noltii* (Hornemann) in Southern Europe (Ria Formosa, Portugal). Hydrobiologia 619: 195-201

Mateo MA, Renom P, Hemminga MA, Peene J (2001) Measurement of seagrass production using the ^{13}C stable isotope compared with classical O_2 and ^{14}C methods. Marine Ecology Progress Series 223: 157-165

Mateo MA, Romero J, Pérez M, Littler MM, Littler DS (1997) Dynamics of millenary organic deposits resulting from the growth of the Mediterranean seagrass *Posidonia oceanica*. Estuarine, Coastal and Shelf Science 44: 103-110

McCann-Grosvenor K (2010) Eddy correlation benthic O_2 exchange rates and characterization of sediment properties from the Central Oregon Shelf at 30 meters. In partial fulfillment of the requirements for the degree of Master of Science. College of Oceanic and Atmospheric Sciences, Corvallis, Oregon

McGinnis DF, Berg P, Brand A, Lorrai C, Edmonds TJ, Wüest A (2008) Measurements of eddy correlation oxygen fluxes in shallow freshwaters: Towards routine applications and analysis. Geophysical Research Letter 35: L04403

McGinnis DF, Cherednichenko S, Sommer S, Berg P, Rovelli L, Schwarz R, Glud RN, Linke P (2011) Simple, robust eddy correlation amplifier for aquatic dissolved oxygen and hydrogen sulfide flux measurements. Limnology and Oceanography: Methods 9: 340-347

Miller HL, Dunton KH (2007) Stable isotope (^{13}C) and O_2 micro-optode alternatives for measuring photosythesis in seaweeds. Marine Ecology Progress Series 329: 85-97

Miller RJ, Reed DC, Brzezinski MA (2009) Community structure and productivity of subtidal turf and foliose algal assemblages. Marine Ecology Progress Series 388: 1-11

Moncrieff J (2006) EdiRe http://www.geos.ed.ac.uk/abs/research/micromet/EdiRe/ [Accessed 2014]

Monismith SG (2007) Hydrodynamics of coral reefs. Annual Review of Fluid Mechanics 39: 37-55

Moore K, Short F (2006) *Zostera*: Biology, ecology, and management. In: Larkum AWD, Orth RJ, Duarte C (eds) Seagrasses: Biology, Ecology and Conservation. Springer Netherlands, pp 361-386

Moore KA, Wetzel RL, Orth RJ (1997) Seasonal pulses of turbidity and their relations to eelgrass (*Zostera marina* L.) survival in an estuary. Journal of Experimental Marine Biology and Ecology. 215: 115-134.

Murray L, Wetzel RL (1987) Oxygen production and consumption associated with the major autotrophic components in two temperate seagrass communities. Marine Ecology Progress Series 38: 231-239

Nayar S, Collings GJ, Miller DJ, Bryars S, Cheshire AC (2009) Uptake and resource allocation of inorganic carbon by the temperate seagrasses *Posidonia* and *Amphibolis*. Journal of Experimental Marine Biology and Ecology 373: 87-95

Neckles H, Koepfler E, Haas L, Wetzel R, Orth R (1994) Dynamics of epiphytic photoautotrophs and heterotrophs *Zostera marina* (eelgrass) microcosms: Responses to nutrient enrichment and grazing. Estuaries and Coasts 17: 597-605

Oakes JM, Connolly RMR, Andrew T. (2010) Isotope enrichment in mangrove forests separates microphytobenthos and detritus as carbon sources for animals. Limnology and Oceanography 55: 393-402

Oakes JM, Eyre BD (2013) Transformation and fate of microphytobenthos carbon in subtropical, intertidal sediments: long-term carbon retention revealed by ^{13}C-labeling. Biogeosciences Discussion 10: 19773-19809

Oakes JM, Eyre BD, Middelburg JJ, Boschker HTS (2010) Composition, production, and loss of carbohydrates in subtropical shallow subtidal sandy sediments: rapid processing and long-term retention revealed by ^{13}C-labeling. Limnology and Oceanography 55: 2126–2138

Odum HT (1956) Primary production in flowing waters. Limnology and Oceanography 1:102-117

Okimoto Y, Nose A, Katsuta Y, Tateda Y, Agarie S, Ikeda K (2007) Gas exchange analysis for estimating net CO_2 fixation capacity of mangrove (*Rhizophora stylosa)* forest in the mouth of river Fukido, Ishigaki Island, Japan. Plant Production Science 10: 303-313

Osburn CL, St-Jean G (2007) The use of wet chemical oxidation with high-amplification isotope ratio mass spectrometry (WCO-IRMS) to measure stable isotope values of dissolved organic carbon in seawater. Limnology and Oceanography: Methods 5: 296-308

Ostrom NE, Carrick HJ, Twiss MR, Piwinski L (2005) Evaluation of primary production in Lake Erie by multiple proxies. Oecologia 144: 115-124

Paling EI, van Keulen M, Wheeler KD, Phillips J, Dyhrberg R (2003) Influence of spacing on mechanically transplanted seagrass survival in a high wave energy regime. Restoration Ecology 11: 56-61

Patterson MR, Sebens KP, Olson RR (1991) In situ measurements of flow effects on primary production and dark respiration in reef corals. Limnology and Oceanography 36: 936-948

Pérez M, Romero J (1992) Photosynthetic response to light and temperature of the seagrass *Cymodocea nodosa* and the prediction of its seasonality. Aquatic Botany 43: 51-62

Peterson BJ (1980) Aquatic primary productivity and the ^{14}C-CO_2 method: A history of the productivity problem. Annual Review of Ecology and Systematics 11: 359-385

Pinardi M, Bartoli M, Longhi D, Marzocchi U, Laini A, Ribaudo C, Viaroli P (2009) Benthic metabolism and denitrification in a river reach: a comparison between vegetated and bare sediments. Journal of Limnology 68: 133-145

Pischedda L, Poggiale JC, Cuny P, Gilbert F (2008) Imaging oxygen distribution in marine sediments. The importance of bioturbation and sediment heterogeneity. Acta Biotheoretica 56: 123-135

Plante-Cuny M-R, Plante R, MazouniI N, Fontaine M-F, Souchu P, Dedlous-Paoli J-M, Grenz C (1998) Oxygen fluxes involving the benthic micro- and macrophytic components in the Thau Lagoon under pre-anoxic conditions. Oceanologica Arca 21: 819-829

Polsenaere P, Lamaud E, Lafon V, Bonnefond JM, Bretel P, Delille B, Deborde J, Loustau D, Abril G (2012) Spatial and temporal CO_2 exchanges measured by Eddy Covariance over a temperate intertidal flat and their relationships to net ecosystem production. Biogeosciences 9: 249-268

Quay PD, Peacock C, Björkman K, Karl DM (2010) Measuring primary production rates in the ocean: Enigmatic results between incubation and non-incubation methods at Station ALOHA. Global Biogeochemistry Cycles 24: GB3014

Ralph PJ (1998) Photosynthetic response of laboratory-cultured *Halophila ovalis* to thermal stress. Marine Ecology Progress Series 171: 123-130

Ralph PJ (1999) Light-Induced Photoinhibitory Stress Responses of Laboratory-Cultured *Halophila ovalis*. Botanica Marina 42: 11-2

Ralph PJ (2000) Herbicide toxicity of *Halophila ovalis* assessed by chlorophyll a fluorescence. Aquatic Botany 66: 141-152

Ralph PJ, Gademann R (2005) Rapid light curves: A powerful tool to assess photosynthetic activity. Aquatic Botany 82: 222-237

Ralph PJ, Tomasko D, Moore K, Seddon S, Macinnis-Ng CMO (2006) Human Impacts on Seagrasses: Eutrophication, Sedimentation, and Contamination. In: Larkum AWD, Orth RJ, Duarte CM (eds) Seagrasses: Biology, Ecology and Conservation. Springer Netherlands, pp 567-593

Rannik U, Vesala T (1999) Autoregressive filtering versus linear detrending in estimation of fluxes by the eddy covariance method. Boundary-Layer Meteorology 91: 259-280

Rasmussen H, Jørgensen BB (1992) Microelectrode studies of seasonal oxygen uptake in a coastal sediment: role of molecular diffusion. Marine Ecology Progress Series 81: 289-303

Regaudie-de-Gioux A, Lasternas S, Agusti S, Duarte CM (2014) Comparing marine primary production estimates through different methods and development of conversion equations. Frontiers of Marine Science 1:19

Reimers CE, Özkan-Haller HT, Berg P, Devol A, McCann-Grosvenor K, Sanders RD (2012) Benthic oxygen consumption rates during hypoxic conditions on the Oregon continental shelf: Evaluation of the eddy correlation method. Journal of Geophysical Research 117: C02021

Revsbech NP, Sorensen J, Blackburn TH, Lomholt JP (1980) Distribution of oxygen in marine sediments measured with microelectrodes. Limnology and Oceanography 25: 403-411

Reynolds O (1895) On the dynamical theory of incompressible viscous fluids and the determination of the criterion. Philosophical Transactions of the Royal Society of London: Mathematical, Physical and Engineering Sciences 186: 123-164

Rheuban JE, Berg P, McGlathery KJ (2014) Multiple timescale processes drive ecosystem metabolism in eelgrass (*Zostera marina*) meadows 507: 1-13

Rickelt LF, Askaer L, Walpersdorf E, Elberling B, Glud RN, Kühl M (2013) An optode sensor array for long term in situ measurements of O_2 in soil and sediment. Journal of Environmental Quality 42: 1267-1273

Risgaard-Petersen N, Nielsen LP, Revsbech NP (1994) Diurnal variation of denitrification and nitrification in sediments colonized by benthic microphytes. Limnology and Oceanography 39: 573-579

Roberts M, Reiss M, Monger G (2000) Advanced biology. Nelson Thornes, Cheltenham

Robinson C, Tilstone GH, Rees AP, Smyth TJ, Fishwick JR, Tarran GA, Luz B, Barkan E, David E (2009) Comparison of *in vitro* and *in situ* plankton production determinations. Aquatic Microbial Ecology 54: 13-34

Ruiz JM, Romero J (2001) Effects of *in situ* experimental shading on the Mediterranean seagrass *Posidonia oceanica*. Marine Ecology Progress Series 215: 107-120

Sakamaki T, Nishimura O, Sudo R, 2006. Tidal time-scale variation in nutrient flux across the sediment-water interface of an estuarine tidal flat. Estuarine Coastal and Shelf Science 67: 653e663

Sand-Jensen K, Nielsen SL (2004) Estuarine primary producers. In: Søren Laurentius Nielsen GTB, Morten Foldager Pedersen (ed) Estuarine nutrient cycling: The influence of primary producers. Kluwer Academic Publishers, Dordreche, pp 303

Sarma VVSS, Abe O, Hashimoto S, Hinuma A, Saino T (2005) Seasonal variations in triple oxygen isotopes and gross oxygen production in the Sagami Bay, central Japan. Limnology and Oceanography 50: 544-552

Schanz A, Polte P, Asmus H (2002) Cascading effects of hydrodynamics on an epiphyte-grazer system in intertidal seagrass beds of the Wadden Sea. Marine Biology 141: 287-297

Schmid HP (2002) Footprint modeling for vegetation atmosphere exchange studies: a review and perspective. Agricultural and Forest Meteorology 113: 159-183

Schuepp PH, Leclerc MY, MacPherson Ji, Desjardins RL (1990) Footprint prediction of scalar fluxes from analytical solutions of the diffusion equation. Boundary-Layer Meteorology 50: 355-373

Schwarz AM, Matheson F, Mathieson T (2004) The role of sediment in keeping seagrass beds healthy. Water & Atmosphere 12: 18–19

Seiki T, Izawa H, Date E, Sunahara H (1994) Sediment oxygen demand in Hiroshima Bay. Water Research 28: 385-393

Shaw EC, Phinn SR, Tilbrook B, Steven A (2014) Comparability of slack Water and Lagrangian flow respirometry methods for community metabolic measurements. PLoS ONE 9(11): e112161

Short FT, Burdick DM, Kaldy III JE (1995) Mesocosm experiments quantify the effects of eutrophication on eelgrass, *Zostera marina*. Limnology and Oceanography 40: 740-749

Short FT, Neckles HA (1999) The effects of global climate change on seagrasses. Aquatic Botany 63: 169-196

Silva J, Sharon Y, Santos R, Beer S (2009) Measuring seagrass photosynthesis: methods and applications. Aquatic Biology 7: 127-141

Slawyck G, Collos Y, Auclair JC (1977). The use of the ^{13}C and ^{15}N isotopes for the simultaneous measurement of carbon and nitrogen turnover rates in marine phytoplankton. Limnology and Oceanography 22: 925-932

Smith JE, Price NN, Hass A (2013) Coupled changes in dissolved oxygen and pH associated with metabolism of benthic reef organisms. Marine Biology 160(9): 2437-2447

Staniši MM (1985) The mathematical theory of turbulence. Springer, New York

Stern O, Volmer M (1919) Uber die Abklingzeit der Fluoreszenz. Phys. Z 20: 183-188

Steven A, Carlin G, Revill A, McLaughlin J, Chotikarn P, Fry G, Moeseneder C, Franklin H (2013) Distribution, volume and impact of sediment deposited by 2011 and 2013 floods on marine and estuarine habitats in Moreton Bay. Final Report 21 June 2013, Healthy Waterways Partnership and the Queensland Department of Environment and Heritage, 36 pp

Sundbäck K, Enoksson V, Granéli W, Pettersson K (1991) Influence of sublittoral microphytobenthos on the oxygen and nutrient flux between sediment and water. A laboratory continuous-flow study. Marine Ecology Progress Series 74: 263-279

Sundbäck K, Miles A, Göransson E (2000) Nitrogen fluxes, denitrification and the role of microphytobenthos in microtidal shallow-water sediments: an annual study. Marine Ecology Progress Series 200: 59-76.

Swett MP (2010) Assessment of bentic flux of dissolved organic carbon in estuaries using the eddy correlation technique. M. Sc. (in Civil Engineering). Civil & Environmental Engineering, Orono, Maine, USA

Tait LW, Schiel DR (2013) Impacts of temperature on primary productivity and respiration in naturally structured macroalgal assemblages. Plos One 8: e744413

Tengberg A, Hall POJ, Andersson U, Lindén B, Styrenius O, Boland G, de Bovee F, Carlsson B, Ceradini S, Devol A, Duineveld G, Friemann JU, Glud RN, Khripounoff A, Leather J, Linke P, Lund-Hansen L, Rowe G, Santschi P, de Wilde P, Witte U (2005) Intercalibration of benthic flux chambers: II. Hydrodynamic characterization and flux comparisons of 14 different designs. Marine Chemistry 94: 147-173

Thomas FIM, Cornelisen CD (2003) Ammonium uptake by seagrass communities: effects of oscillatory versus unidirectional flow. Marine Ecology Progress Series 247: 51-57

Thomas FIM, Cornelisen CD, Zande JM (2000) Effects of water velocity and canopy morphology on ammonium uptake by seagrass communities. Ecology 81: 2704-2713

Tomasko DA, Lapointe BE (1991) Productivity and biomass of *Thalassia testudinum* as related to water column nutrient availability and epiphyte levels: field observations and experimental studies. Marine Ecology Progress Series 75: 9-16

Valdes-Lozano DS, Chumacero M, Real E (2006) Sediment oxygen consumption in a developed coastal lagoon of the Mexican Caribbean. Indian Journal of Marine Science 35: 227-234

Vogel S (1994) Life in moving fluids: The physical biology of flow. Princeton University Press, Princeton

Wangpraseurt D, Weber M, Røy H, Polerecky L, Beer Dd, Suharsono, Nugues MM (2012) In situ oxygen dynamics in coral-algal interactions. Plos One 7: e31192

Watson RT, Noble IR, Bolin B, Ravindranath NH, Verardo DJ, Dokken DJ (2000) Land use, land-use change and forestry. Cambridge University Press, Cambridge

Webb AP, Eyre BD (2004a) The effects of two benthic chamber stirring systems: a conventional rotor and a two dimensional flow system, over the diffusive boundary layer, solute efflux and passive flow through a macrofauna borrow. Estuaries 27: 353-362

Webb AP, Eyre BD (2004b) Effect of natural populations of burrowing thalassinidean shrimp on sediment irrigation, benthic metabolism, nutrient fluxes and denitrification. Marine Ecology Progress Series 268: 205-220

Wieland A, Kühl M (2000) Irradiance and temperature regulation of oxygenic photosynthesis and O_2 consumption in a hypersaline cyanobacterial mat (Solar Lake, Egypt). Marine Biology 137: 71-85

Wildish D, Kristmanson D (1997) Benthic suspension feeders and flow. Cambridge University Press, Cambridge

Wilkinson CR (2002) Status of coral reefs of the world: 2002. Global Coral Reef Monitoring Network and Australian Institute of Marine Science, Townsville

Wolfbies OS (1991) Fiber optic chemical sensors and biosensors. CRC Press, Boston, London

Yacobi YZ, Perel N, Barkan E, Luz B (2007) Unexpected underestimation of primary productivity by ^{18}O and ^{14}C methods in a lake: Implications for slow diffusion of isotope tracers in and out of cells. Limnology and Oceanography 52: 329-337

Yates KK, Halley RB (2003) Measuring coral reef community metabolism using new benthic chamber technology. Coral Reefs 22: 247-255

York PH, Gruber RK, Hill R, Ralph PJ, Booth DJ, Macreadie PI (2013) Physiological and morphological responses of the temperate seagrass *Zostera muelleri* to multiple stressors: Investigating the interactive effects of light and temperature. Plos One 8: e76377

APPENDICES

APPENDICES

Appendix A: Eddy correlation system firmware during this research

Firmware No.	Descriptions	EC model
fw223	Initial firmware of ECE1	ECE1
fw229	Added a rewiring of COMM cable to improve data downloaded	ECE1
uwm_updatedelta_1.0.5	Initail firmware of ECE2	ECE2
uwm_updatedelta_1.0.6	Support new optotode protocols from AADI, uptadated and redesigned the web interface	ECE2
uwm_updatedelta_1.0.7	Support new optotode protocols from AADI, uptadated and redesigned the web interface	ECE2
uwm_updatedelta_1.0.8	Support new optotode protocols from AADI, uptadated and redesigned the web interface	ECE2
uwm_updatedelta_1.0.9	Support new optotode protocols from AADI, uptadated and redesigned the web interface	ECE2
uwm_updatedelta_1.1.0	Support new optotode protocols from AADI, uptadated and redesigned the web interface	ECE2
uwm_updatedelta_1.1.1	Support new optotode protocols from AADI, uptadated and redesigned the web interface	ECE2
uwm_updatedelta_1.1.2	Support new optotode protocols from AADI, uptadated and redesigned the web interface	ECE2
uwm_updatedelta_1.1.3	Added submodule optodeLib to support new optode devices, Updated PowerSupply	ECE2
uwm_updatedeltadebug_1.1.3	Fixed bugs	ECE2
uwm_updatedeltadebug2_1.1.3	Fixed bugs	ECE2
uwm_updatedelta_1.1.4	Minor OptodeManager correction	ECE2
uwm_updatedelta_1.1.5	Updated to last hwlib	ECE2
uwm_updatedelta_1.1.6	Updated inherited EC powersupply	ECE2
uwm_updatedelta_1.1.7	Support of deployment field ‘optode salinity’	ECE2
uwm_updatedelta_1.1.8	Updated to lastest version of OptodeLib	ECO1
uwm_updatedelta_1.1.9	Added support for FireStingII SUBPORT (UW MicroOotode)	ECO1
uwm_updatedelta_1.1.9-r2	Fixed bugs	ECO1
uwm_updatedelta_1.2.0	Updated active state	ECO1
uwm_updatedelta_1.2.0-r2	Fixed bugs	ECO1
uwm_updatedelta_1.2.0-r3	Fixed bugs	ECO1

Appendix A (cont): Eddy correlation system firmware during this research

Firmware No.	Descriptions	EC model
uwm_updatedelta_1.2.0-r4	Fixed bugs	ECO1
uwm_updatedelta_1.2.1	Updated class OptodeManager	ECO1
uwm_updatedelta_1.2.2	Updated logging state	ECO1
uwm_updatedelta_1.2.3	Added FireSting ClientLib as a submodule	ECO1
uwm_updatedelta_1.2.3-r2	Fixed Bugs	ECO1
uwm_updatedelta_1.2.4	Added digital ouput for FireStingII	ECO2
uwm_updatedelta_1.2.5	Added extra webpage for FireSting setting	ECO2

Appendix B: The Eddy Correlation microelectrode system workflow

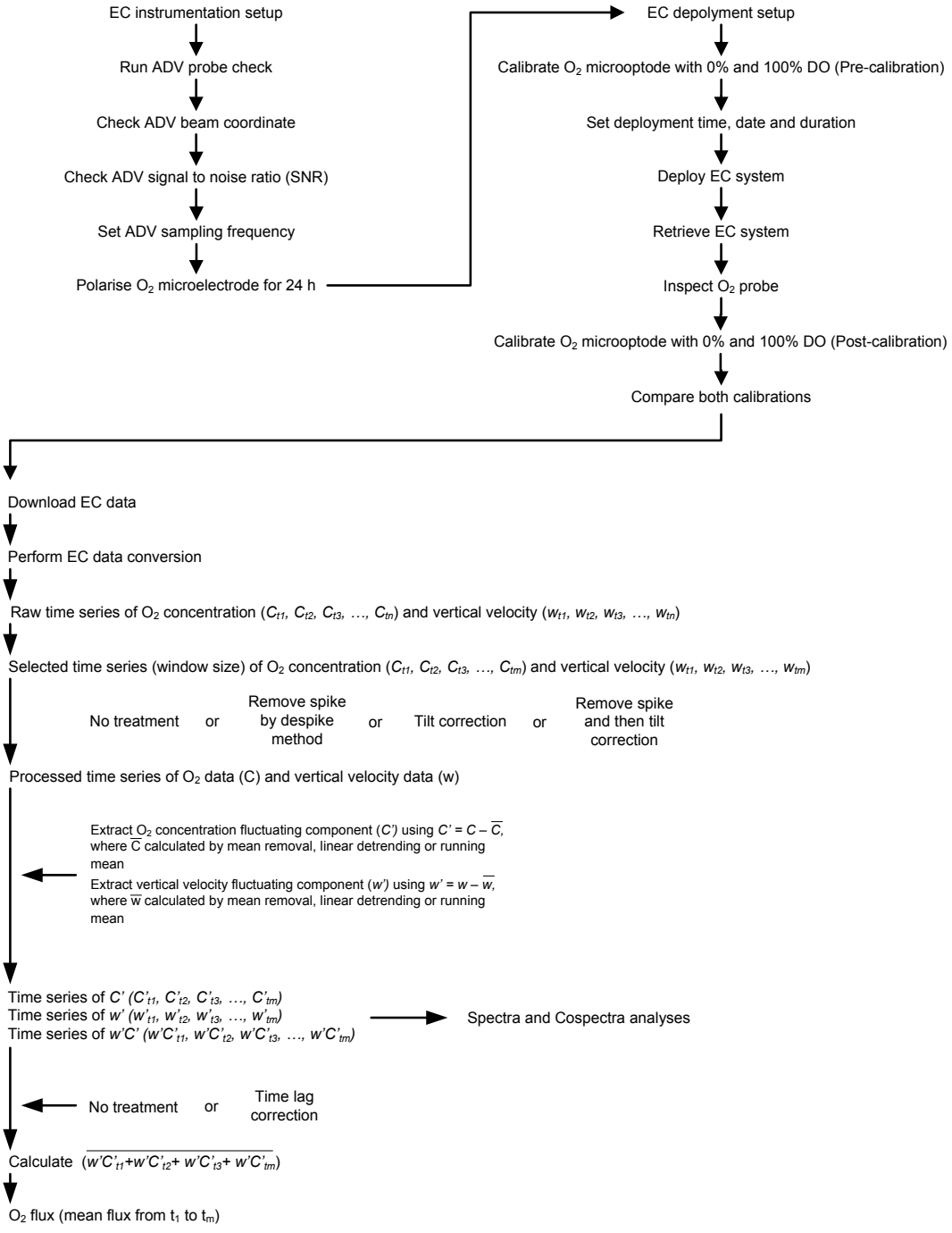

Appendix C: The Eddy Correlation optode system workflow

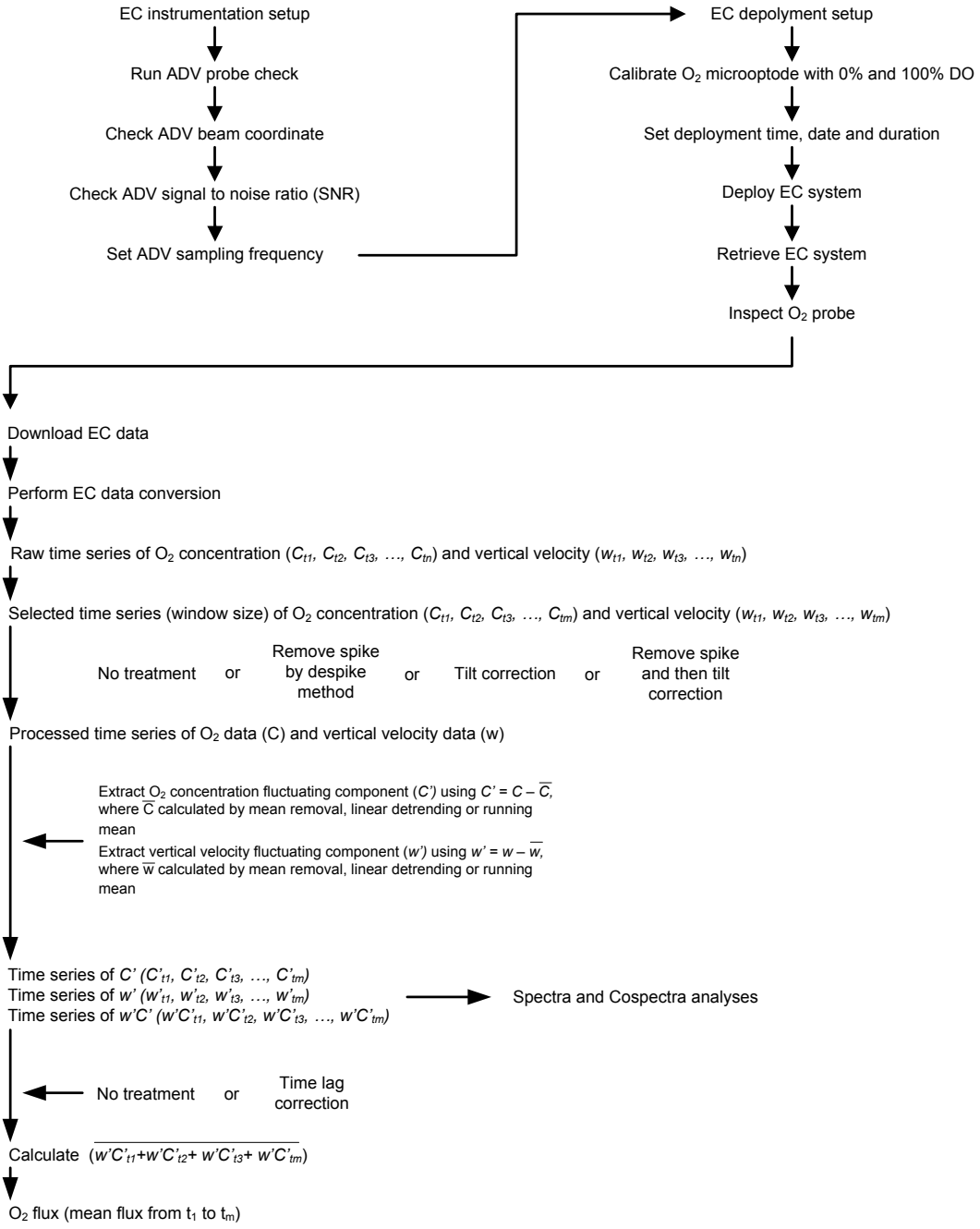

Appendix D: Dissolved oxygen fluxes measured in October 2012 and February 2013 using CMAR and GA chamber and the Miniprofiler (Steven et al. 2013)

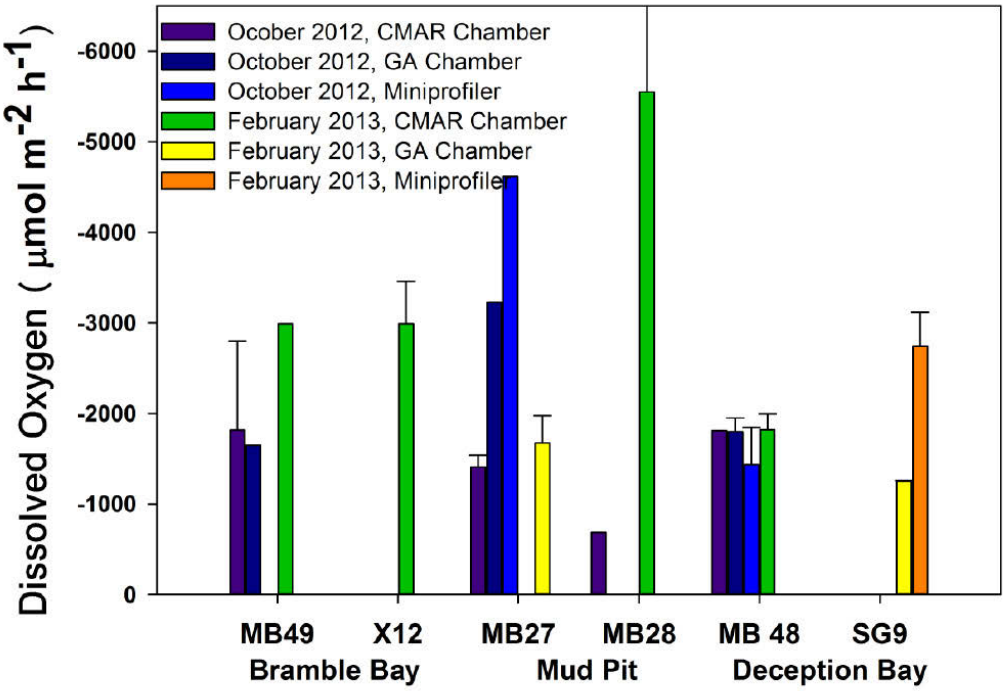

Figure D.1 Dissolved oxygen fluxes measured in October 2012 and February 2013 using CMAR and GA chamber and the Miniprofiler (Steven et al. 2013).

Appendix E: MB48 data

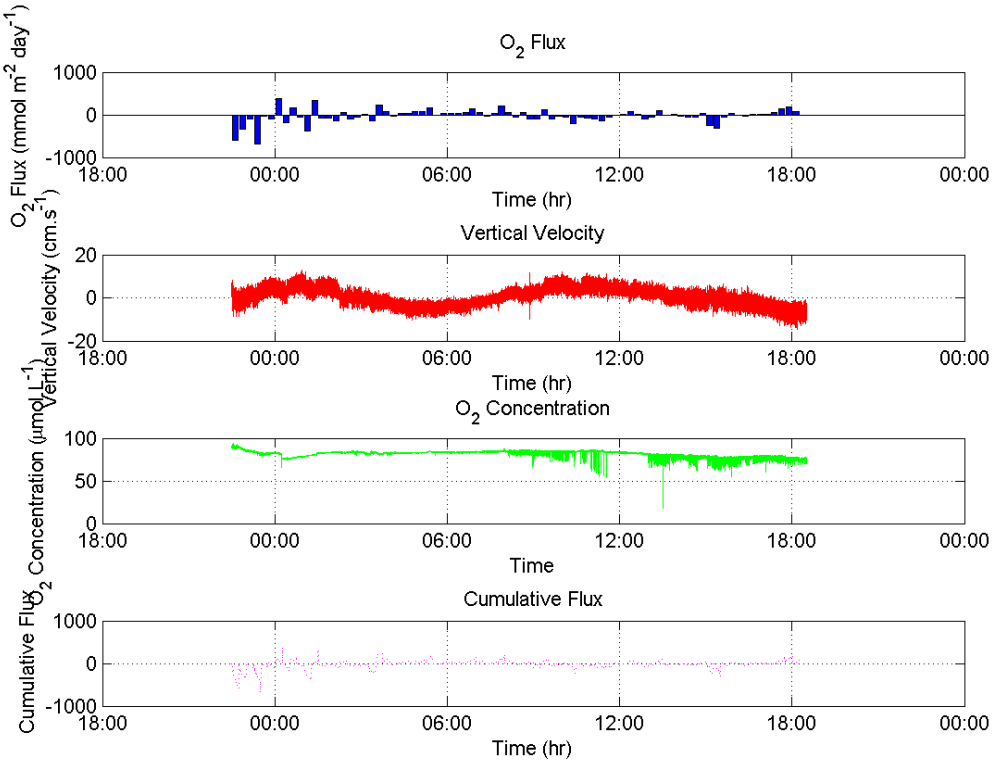

Fig E.1: Dissolved O_2 fluxes, vertical velocity, O_2 concentration and cumulative O_2 flux measured in October 2012 at MB48 using ECE2.

Appendix F: Examples of spectra and cospectra in EC laboratory flume studies

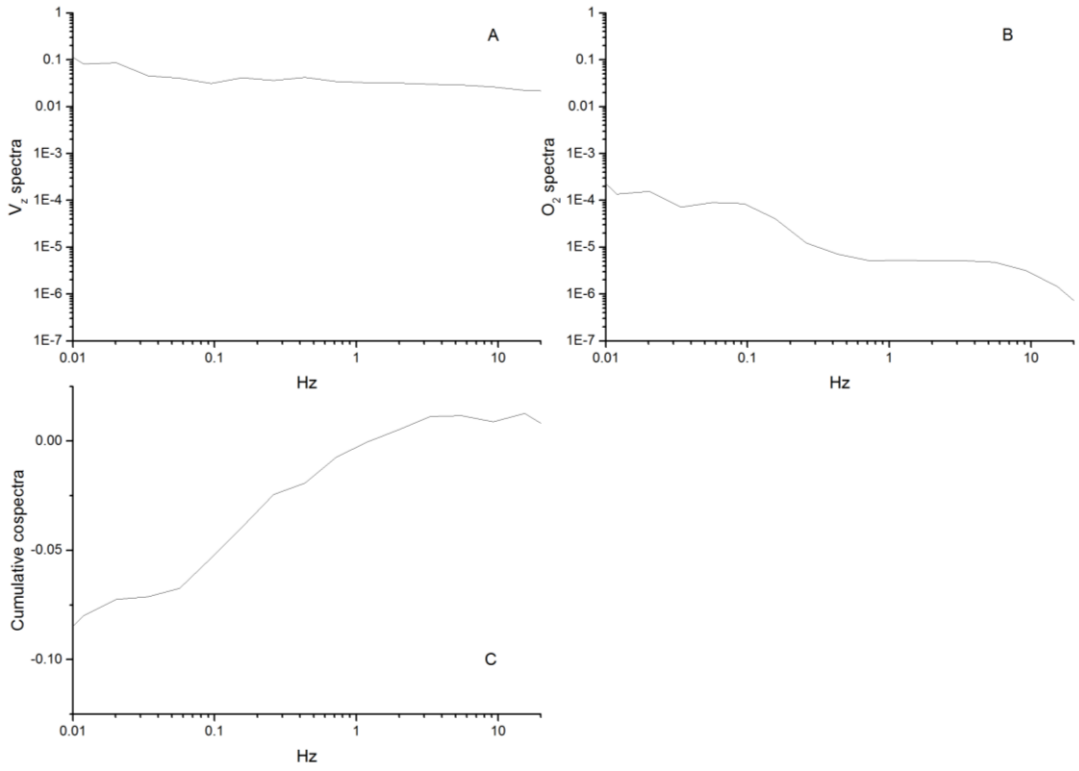

Figure F.1: Example of spectra and cospectra at tempurature = 21°C, irradiance = 400 μmol photon m^{-2} s^{-1} in seagrass experiments; Vertical velocity spectra (A), O_2 spectra (B) and Culmulative cospectra (C).

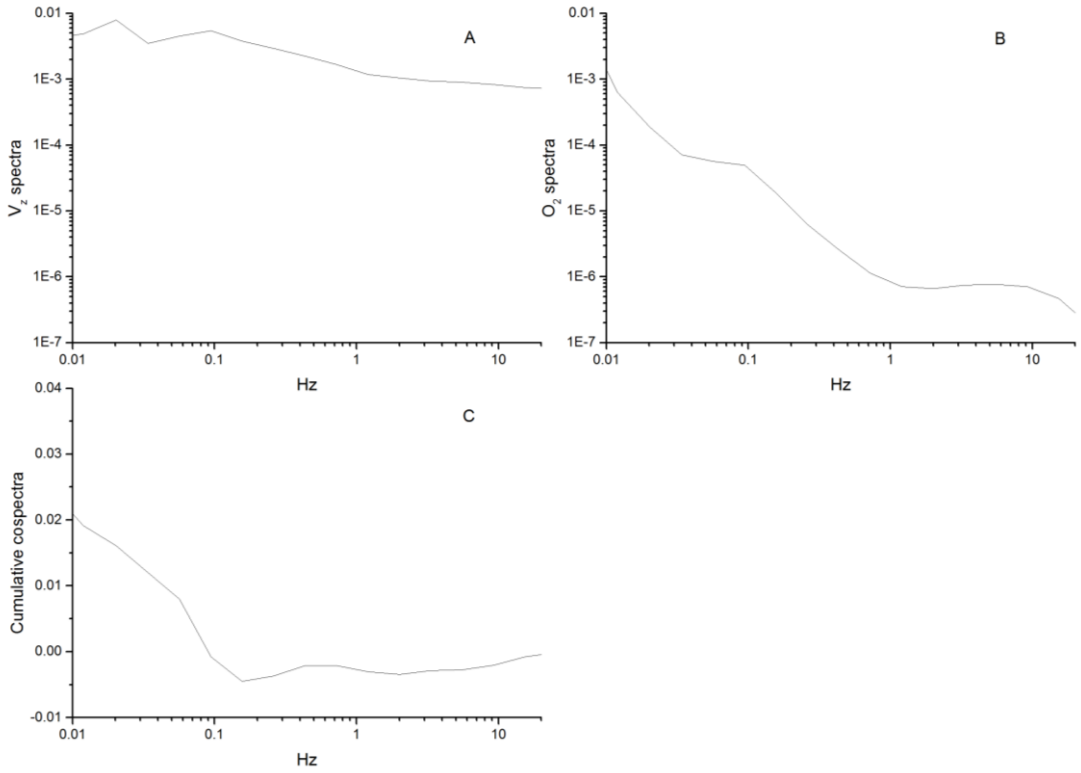

Figure F.2: Example of spectra and cospectra at tempurature = 25°C, irradiance = 400 µmol photon m^{-2} s^{-1} in seagrass experiments; Vertical velocity spectra (A), O_2 spectra (B) and Culmulative cospectra (C).

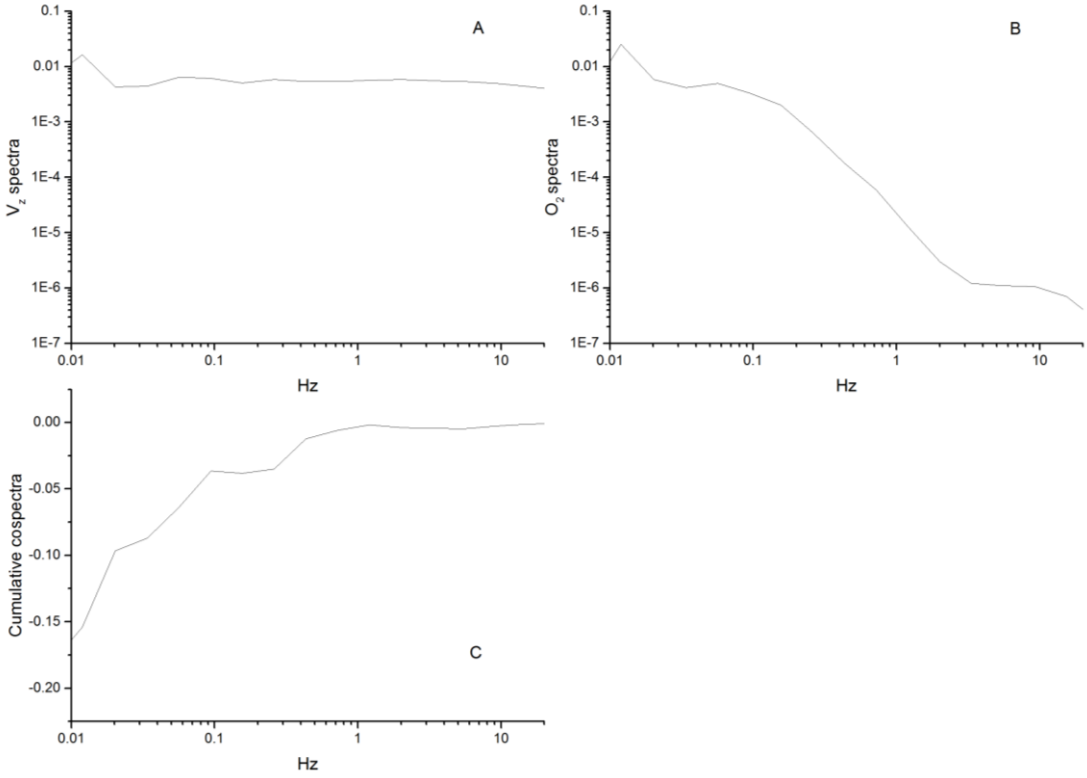

Figure F.3: Example of spectra and cospectra at tempurature = 28°C, irradiance = 400 µmol photon m^{-2} s^{-1} in seagrass experiments; Vertical velocity spectra (A), O_2 spectra (B) and Culmulative cospectra (C).

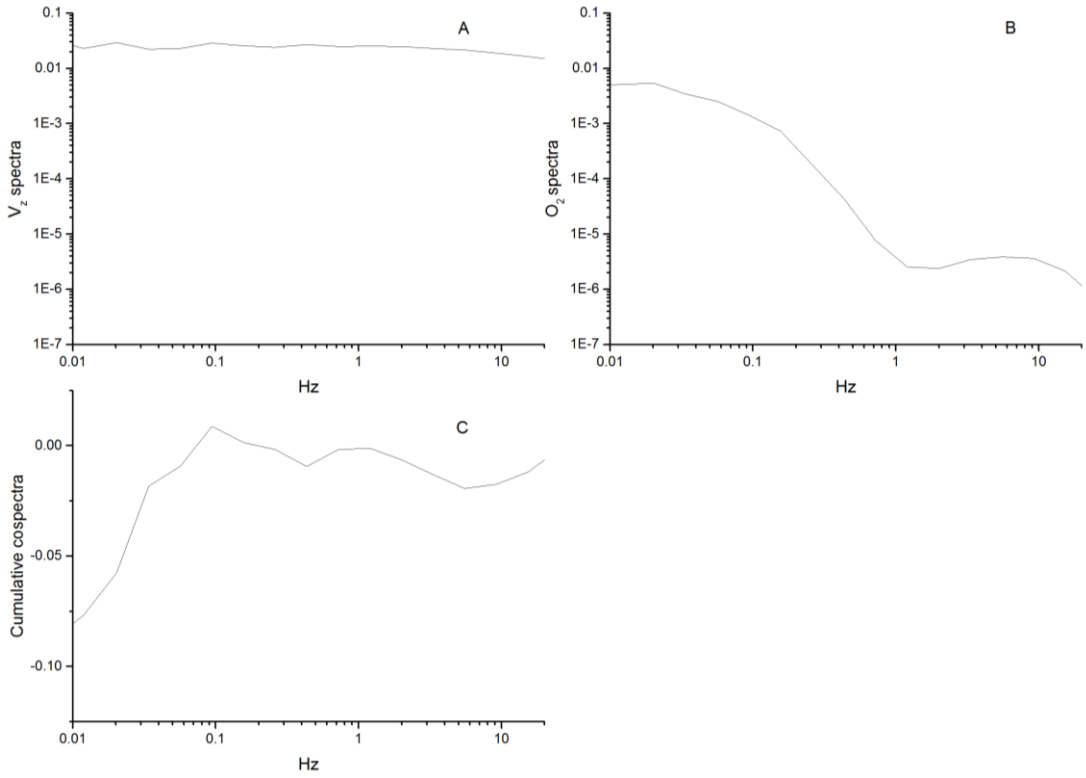

Figure F.4: Example of spectra and cospectra at tempurature = 31°C, irradiance = 400 µmol photon m^{-2} s^{-1} in seagrass experiments; Vertical velocity spectra (A), O_2 spectra (B) and Culmulative cospectra (C).

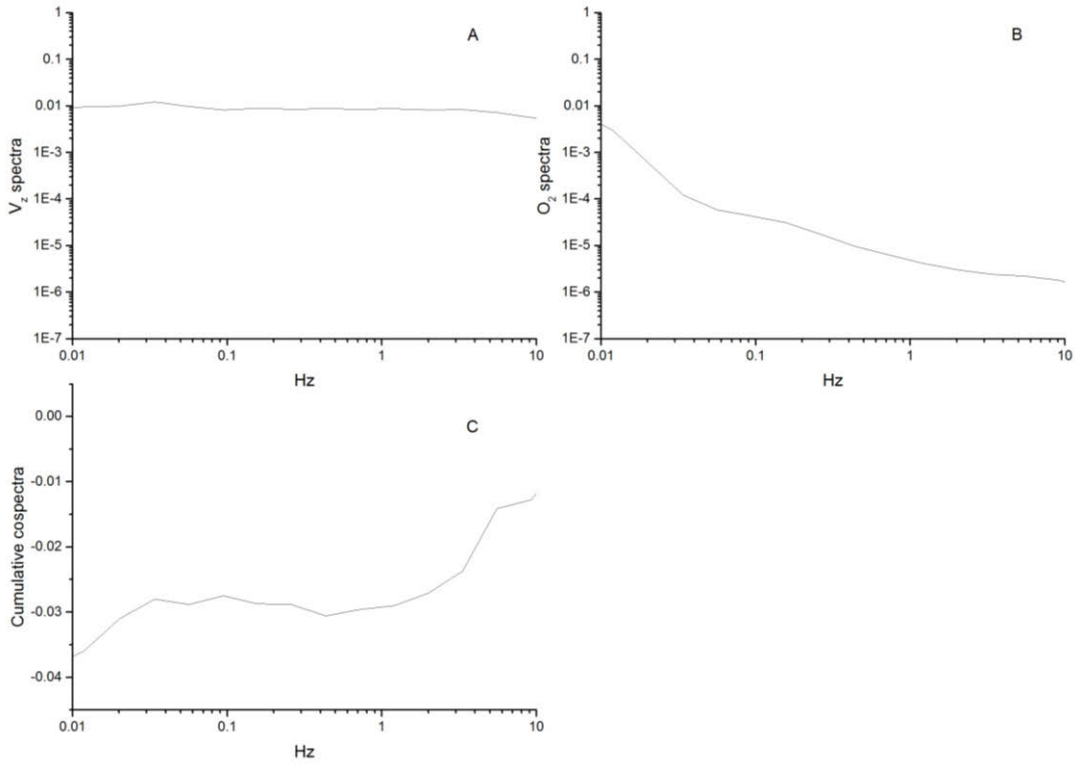

Figure F.5: Example of spectra and cospectra at irradiance = 150 µmol photon m^{-2} s^{-1}, tempurature = 25°C in seagrass experiments; Vertical velocity spectra (A), O_2 spectra (B) and Culmulative cospectra (C).

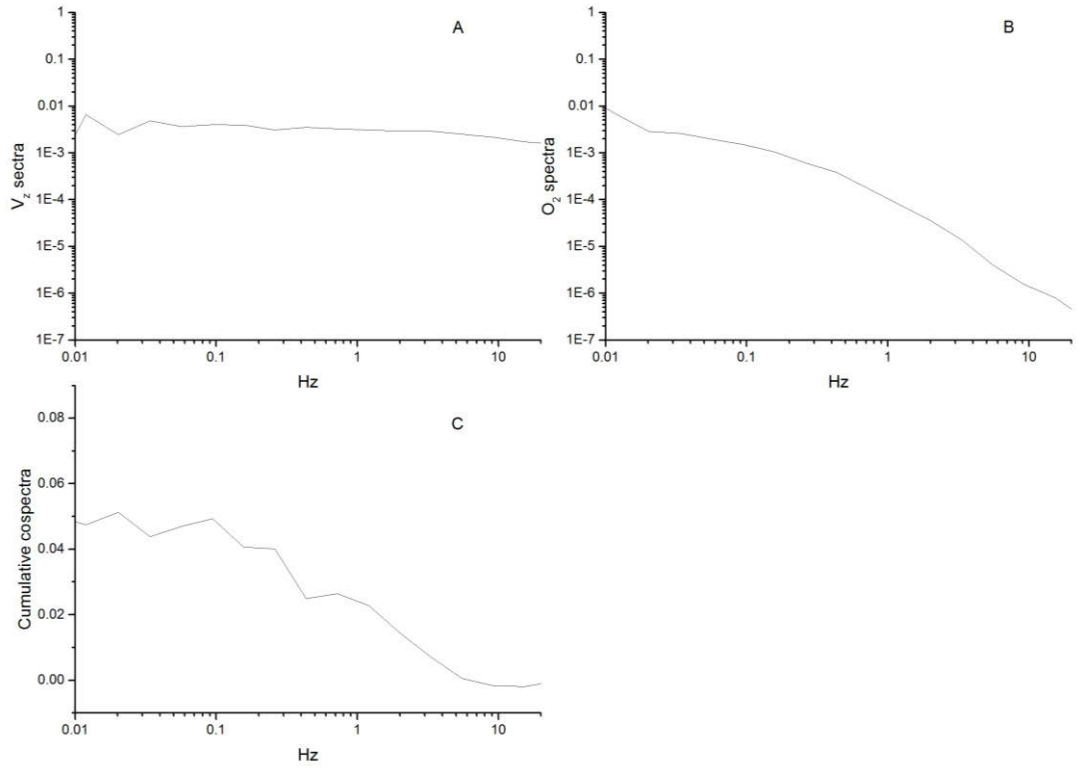

Figure F.5: Example of spectra and cospectra at irradiance = 250 μmol photon m^{-2} s^{-1}, tempurature = 25°C in seagrass experiments; Vertical velocity spectra (A), O_2 spectra (B) and Culmulative cospectra (C).

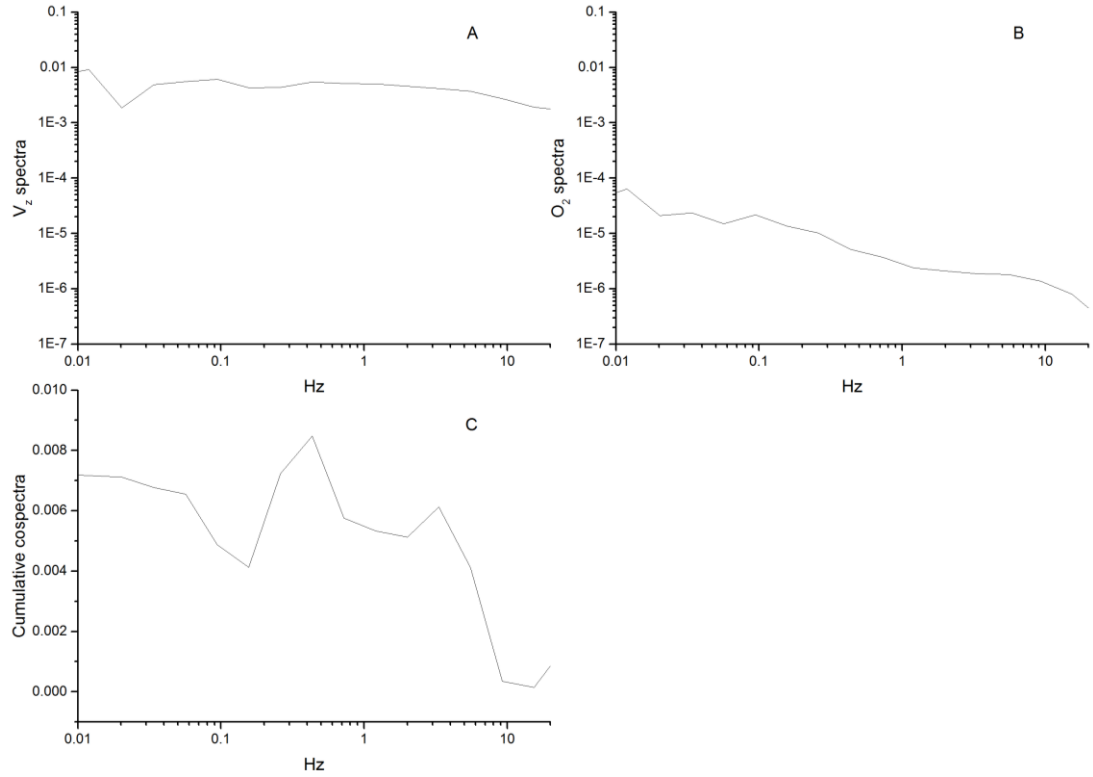

Figure F.6: Example of spectra and cospectra at irradiance = 600 µmol photon m^{-2} s^{-1}, tempurature = 25°C in seagrass experiments; Vertical velocity spectra (A), O_2 spectra (B) and Culmulative cospectra (C).

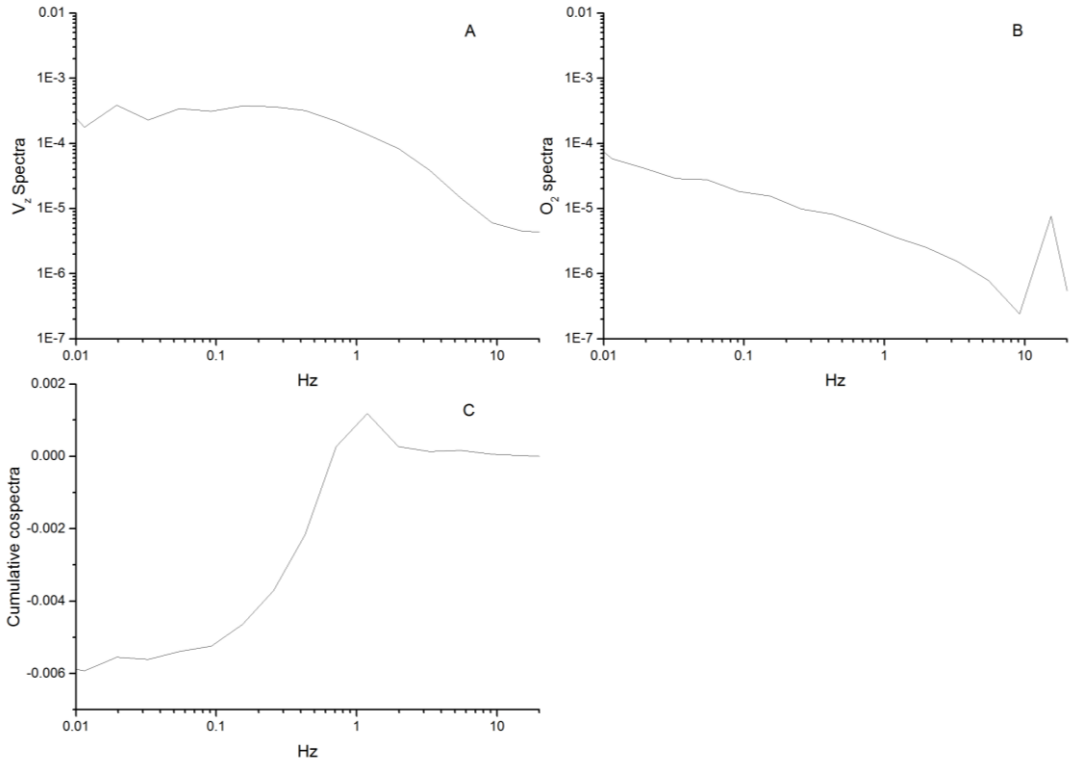

Figure F.8: Example of spectra and cospectra at flow = 17 cm s^{-1}, temperature = 18°C in sediment experiments; Vertical velocity spectra (A), O_2 spectra (B) and Culmulative cospectra (C).

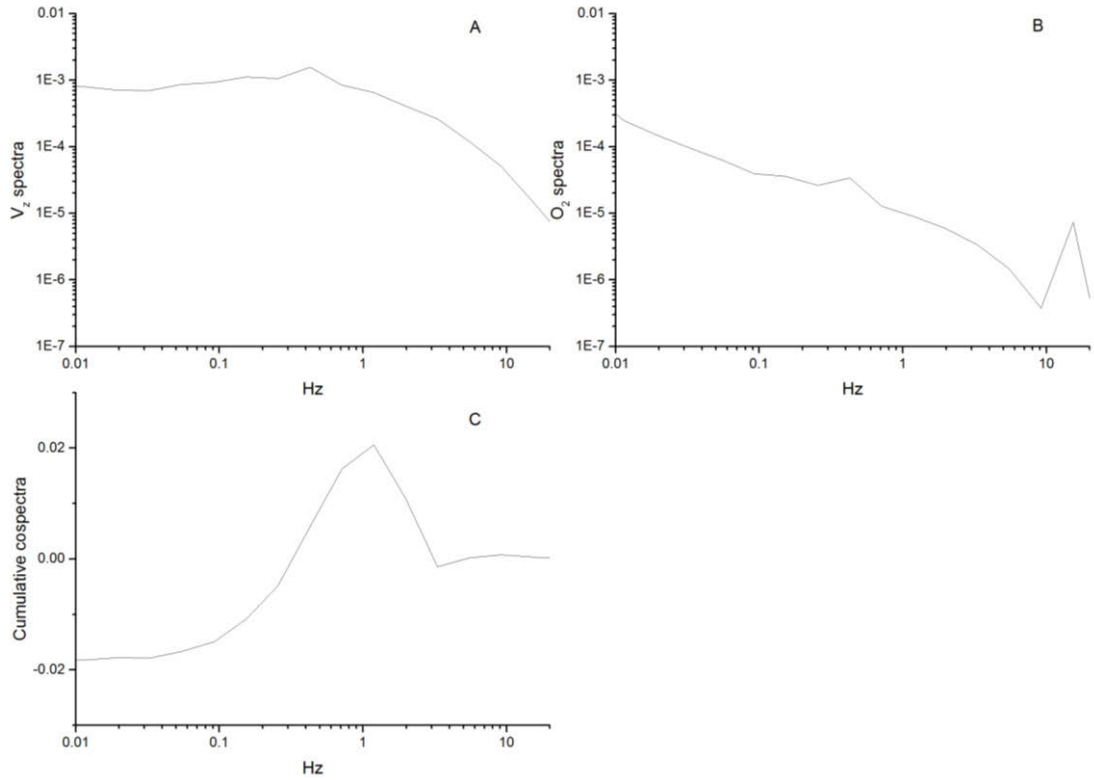

Figure F.9: Example of spectra and cospectra at flow = 34 cm s^{-1}, temperature = 18°C in sediment experiments; Vertical velocity spectra (A), O_2 spectra (B) and Culmulative cospectra (C).

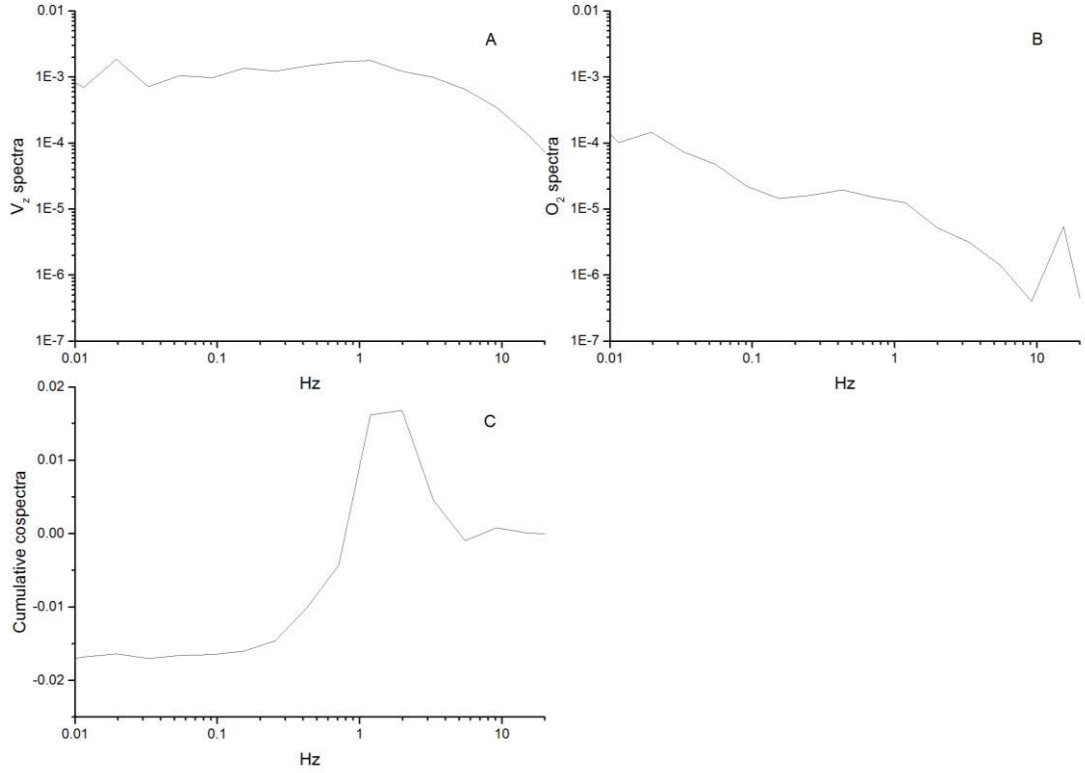

Figure F.10: Example of spectra and cospectra at flow = 51 cm s^{-1}, temperature = 18°C in sediment experiments; Vertical velocity spectra (A), O_2 spectra (B) and Culmulative cospectra (C).

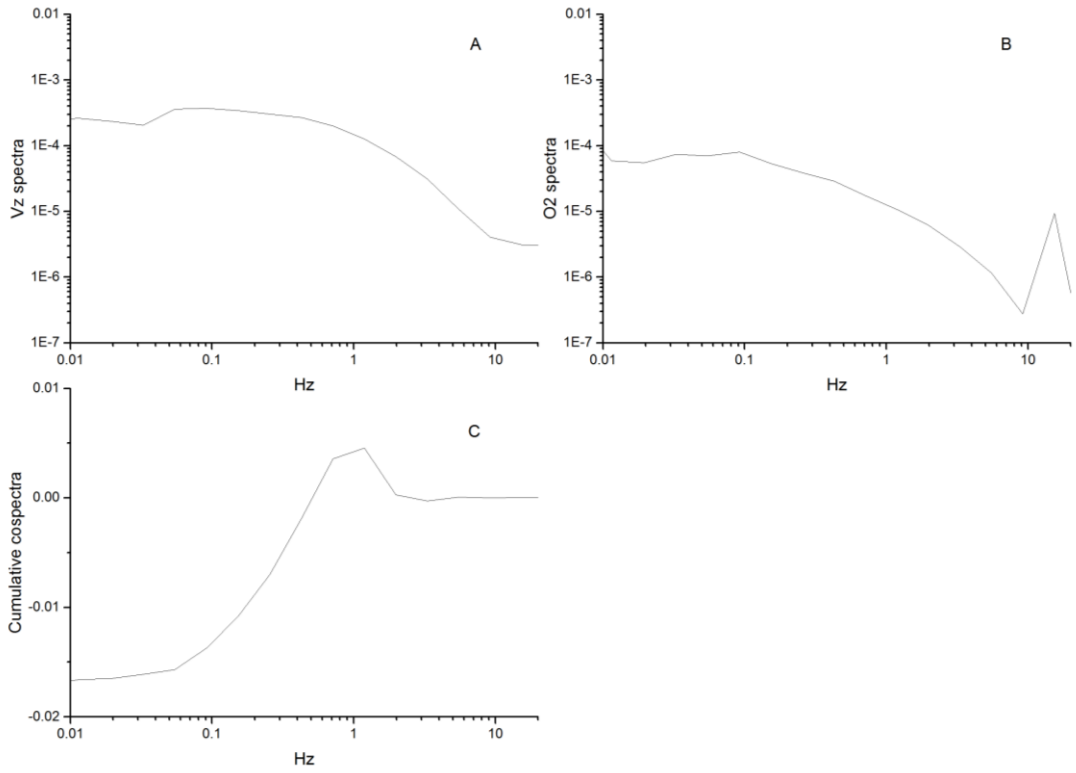

Figure F.11: Example of spectra and cospectra at temperature = 23°C, flow = 17 cm s^{-1} in sediment experiments; Vertical velocity spectra (A), O_2 spectra (B) and Culmulative cospectra (C).

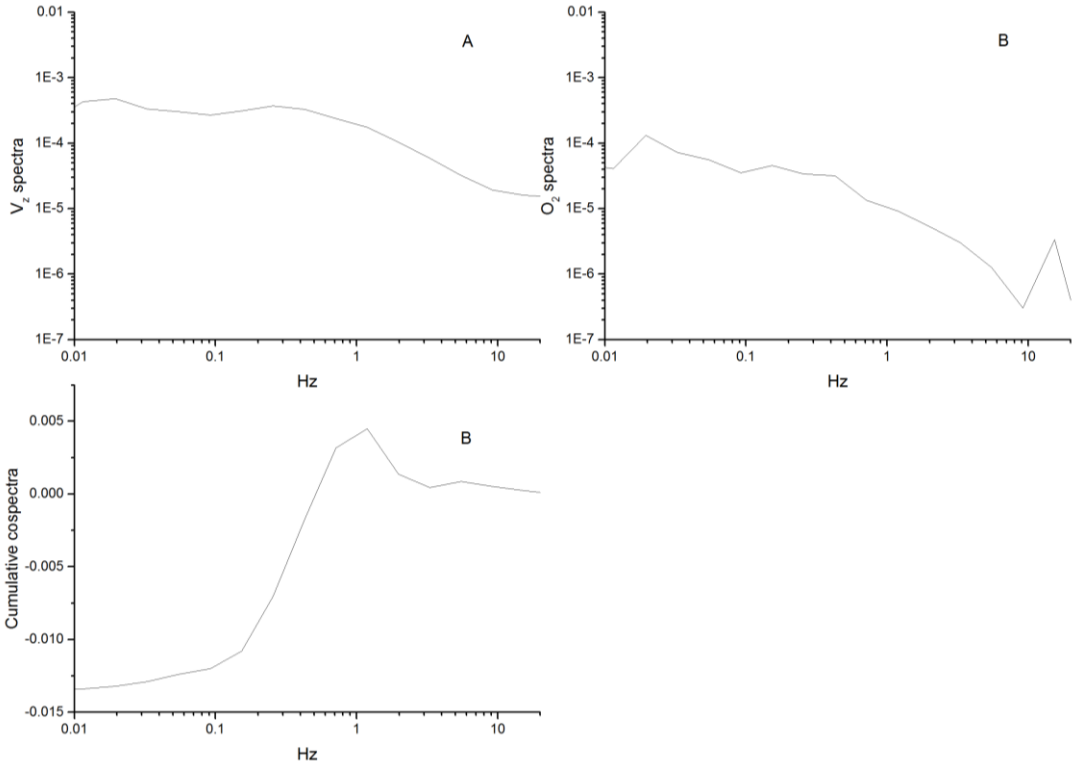

Figure F.12: Example of spectra and cospectra at temperature = 28°C, flow = 17 cm s^{-1} in sediment experiments; Vertical velocity spectra (A), O_2 spectra (B) and Culmulative cospectra (C).

Appendix G: Example of spectra and cospectra in EC field studies

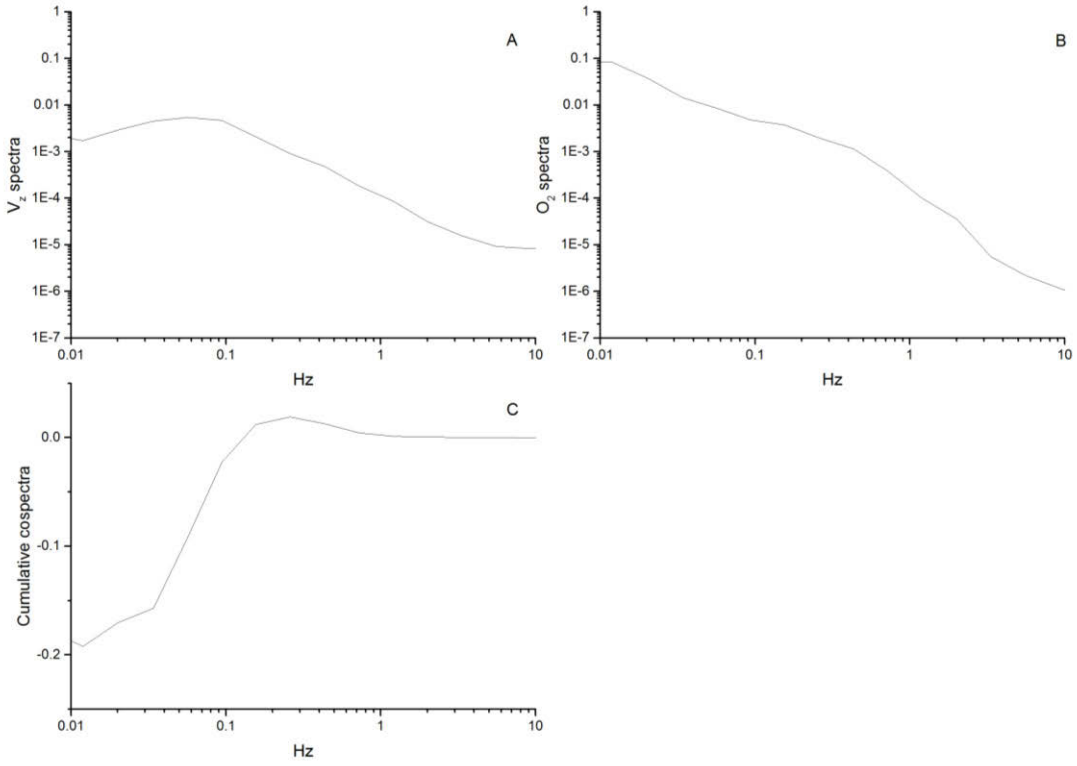

Figure G.1: Example of spectra and cospectra at TWD1; Vertical velocity spectra (A), O_2 spectra (B) and Culmulative cospectra (C).

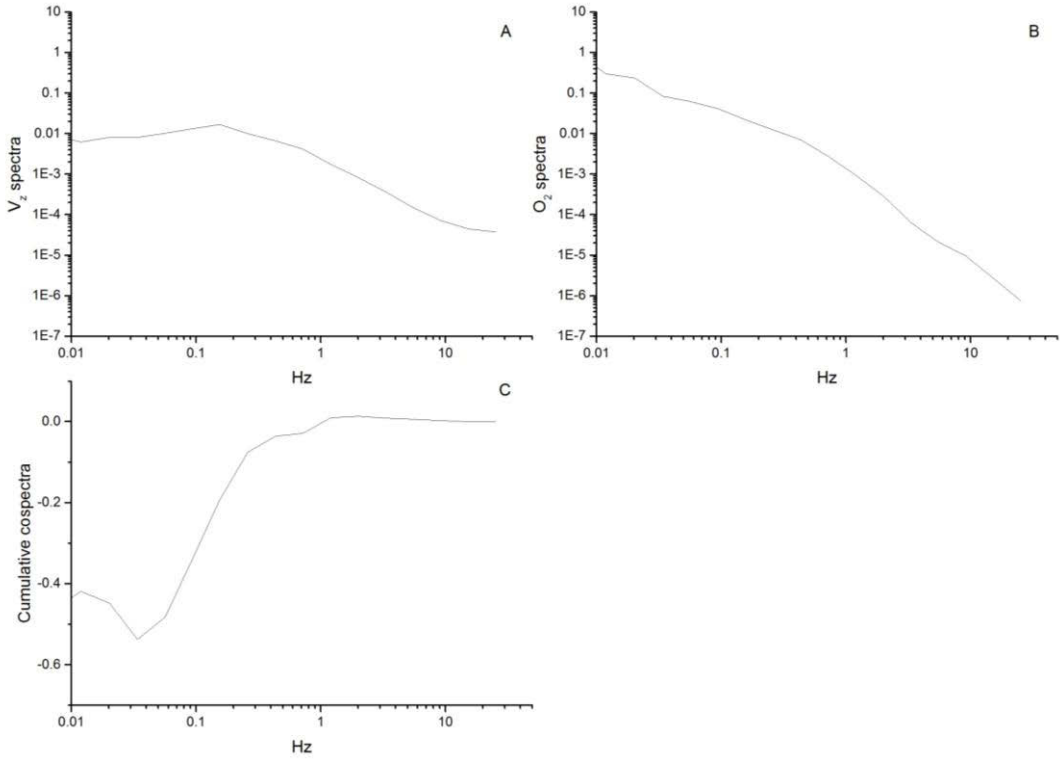

Figure G.2: Example of spectra and cospectra at TWD1; Vertical velocity spectra (A), O_2 spectra (B) and Culmulative cospectra (C).

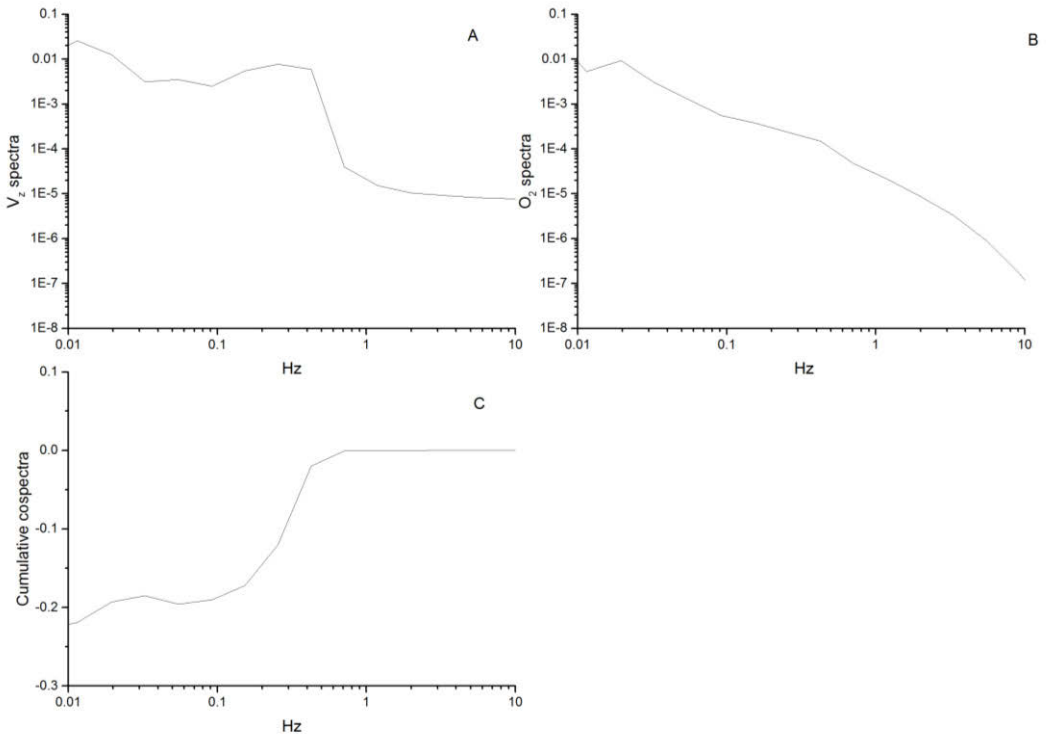

Figure G.3: Example of spectra and cospectra at MB48; Vertical velocity spectra (A), O_2 spectra (B) and Culmulative cospectra (C).

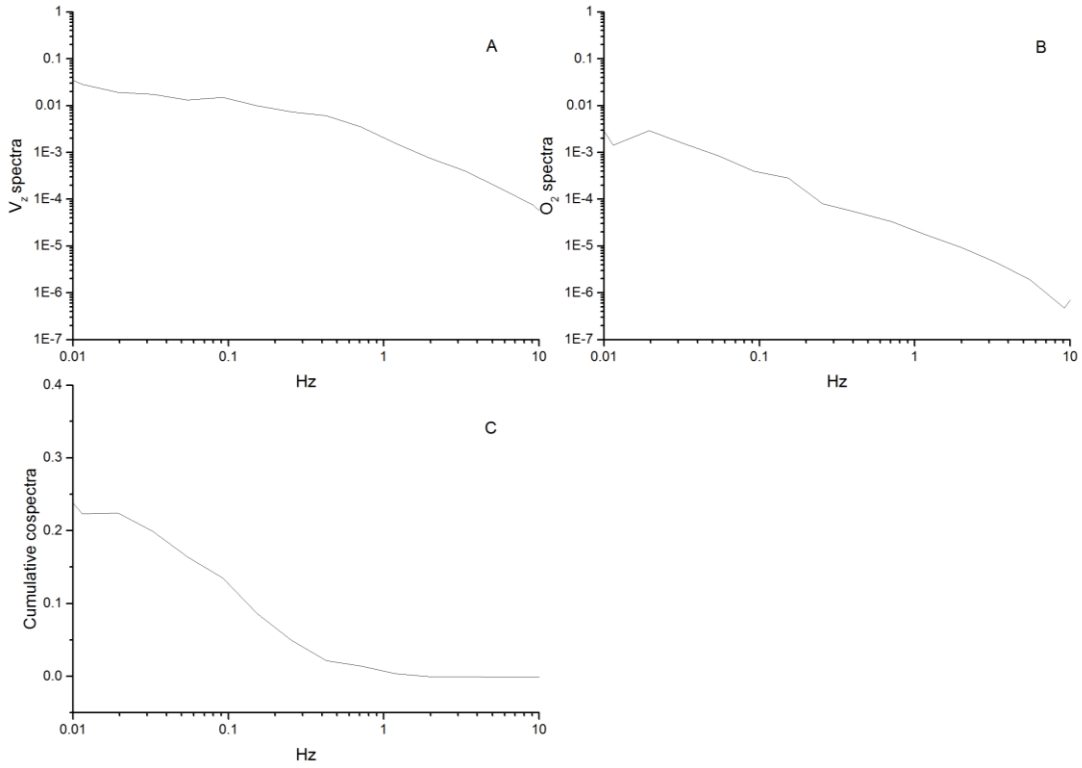

Figure G.4: Example of spectra and cospectra at DWN1; Vertical velocity spectra (A), O_2 spectra (B) and Culmulative cospectra (C).

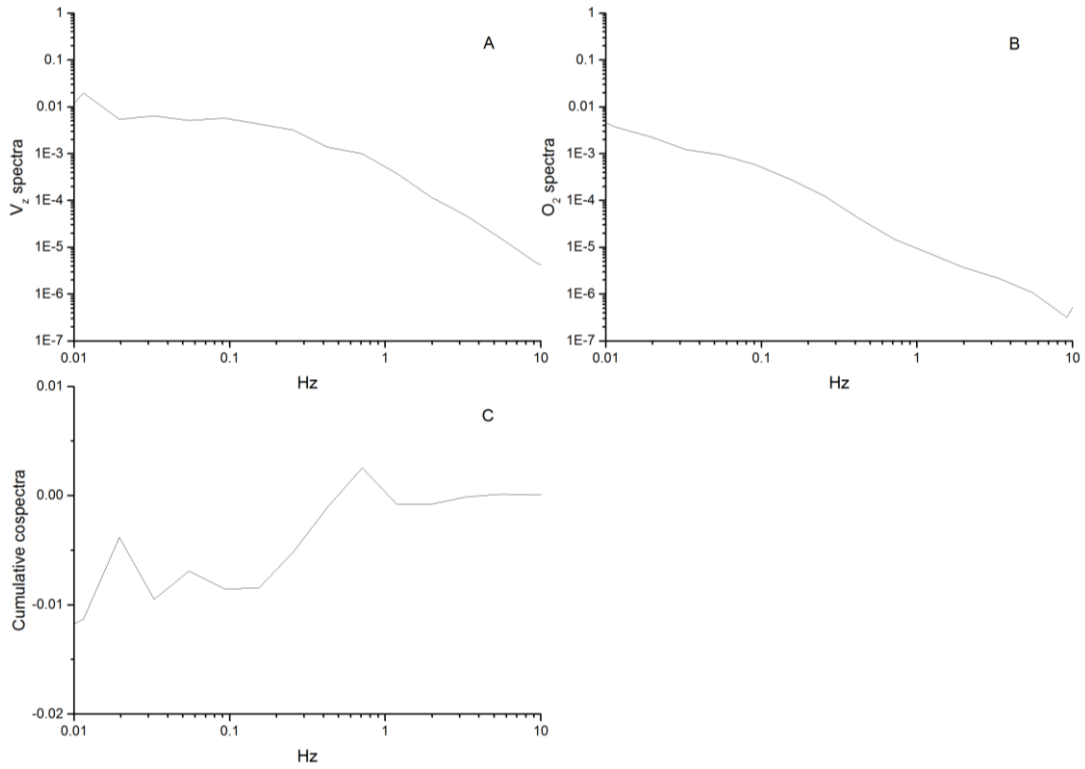

Figure G.5: Example of spectra and cospectra at DWN2; Vertical velocity spectra (A), O_2 spectra (B) and Culmulative cospectra (C).

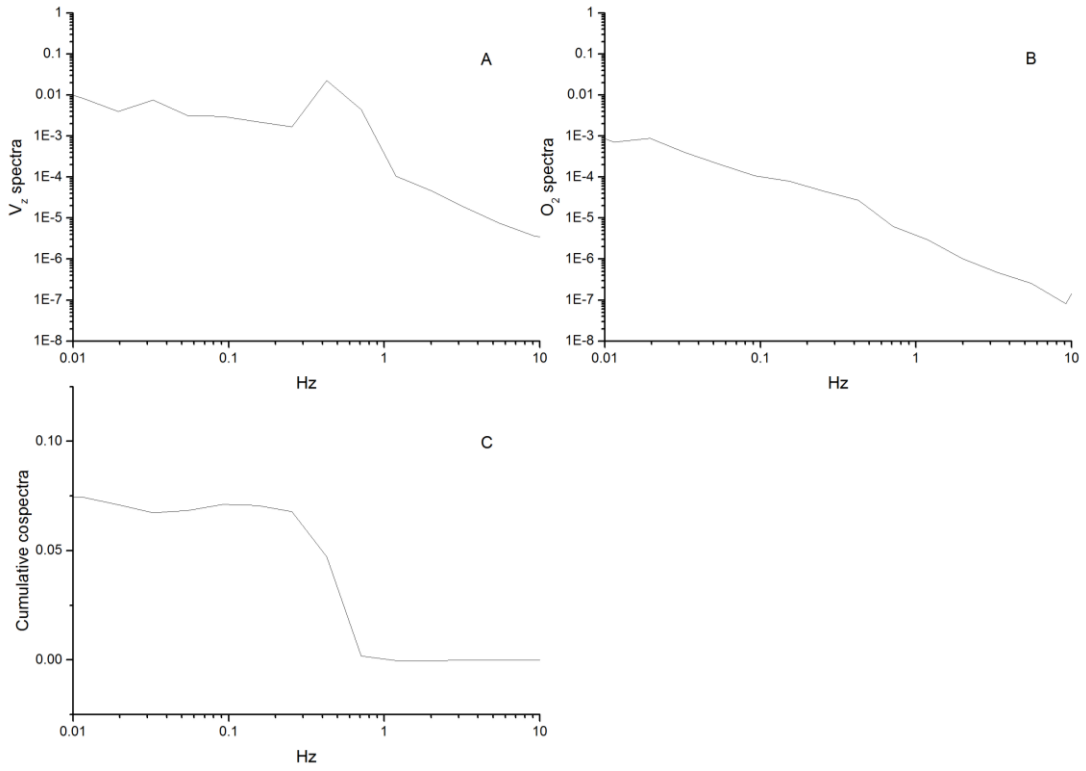

Figure G.6: Example of spectra and cospectra of the first EC deployment at BMA; Vertical velocity spectra (A), O_2 spectra (B) and Culmulative cospectra (C).

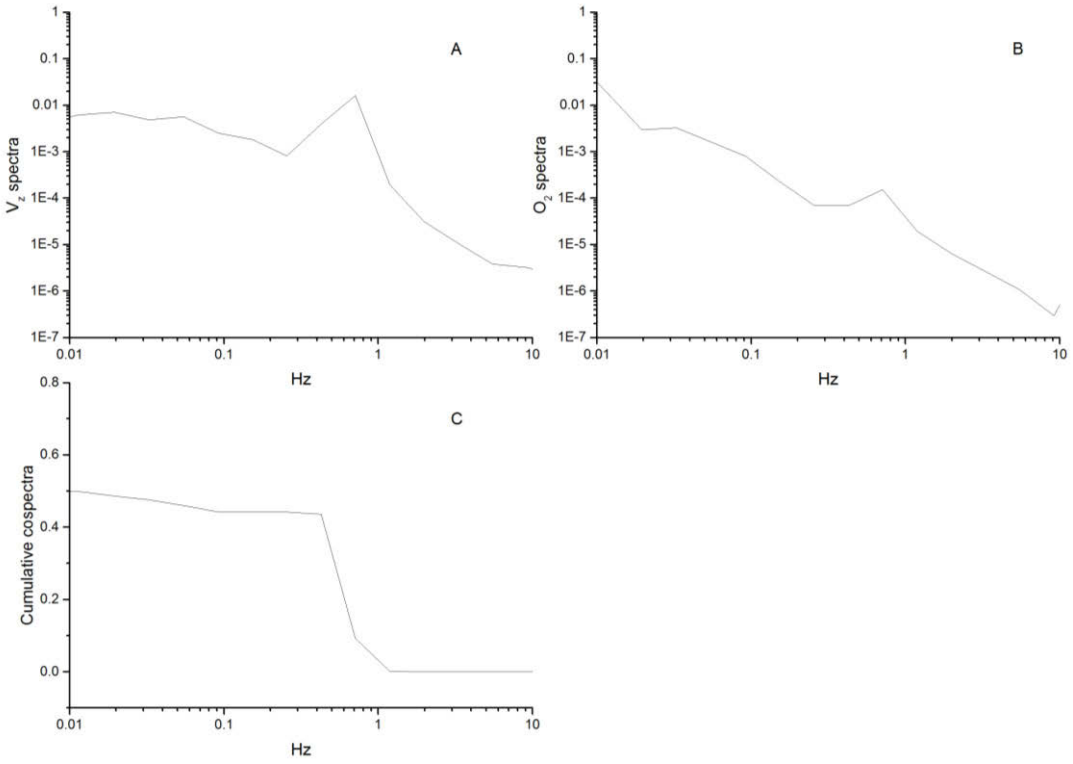

Figure G.7: Example of spectra and cospectra of the second EC deployment at BMA; Vertical velocity spectra (A), O_2 spectra (B) and Culmulative cospectra (C).

Appendix H: Cumulative O_2 flux and cumulative cospectra on BMA measured by ECO1 after reducing data frequency from 64 Hz in 4x steps to 16 Hz.

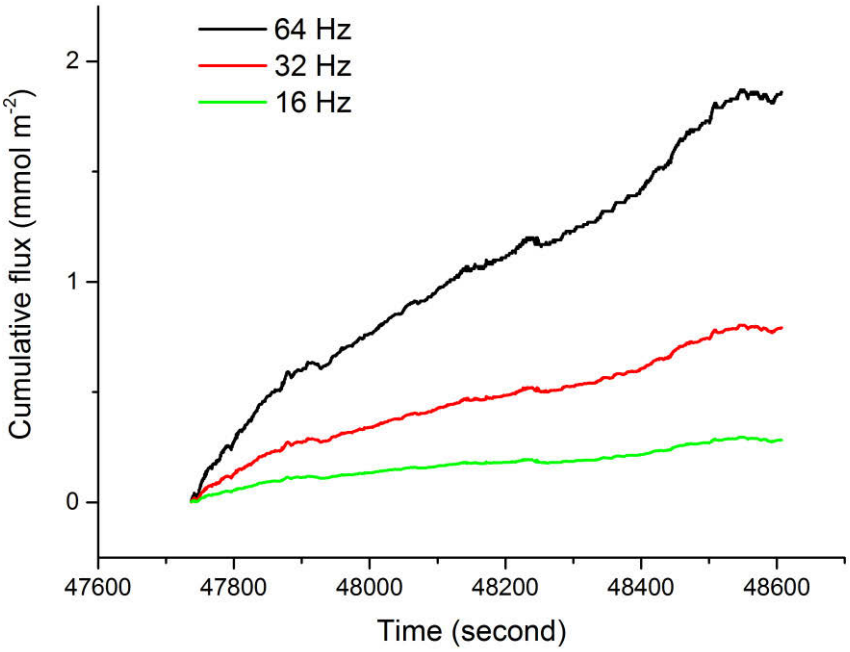

Figure H.1 Cumulative O_2 flux at different frequency (data from the first deployment at BMA measured by ECO1). Each data point was compute as an average of raw data.

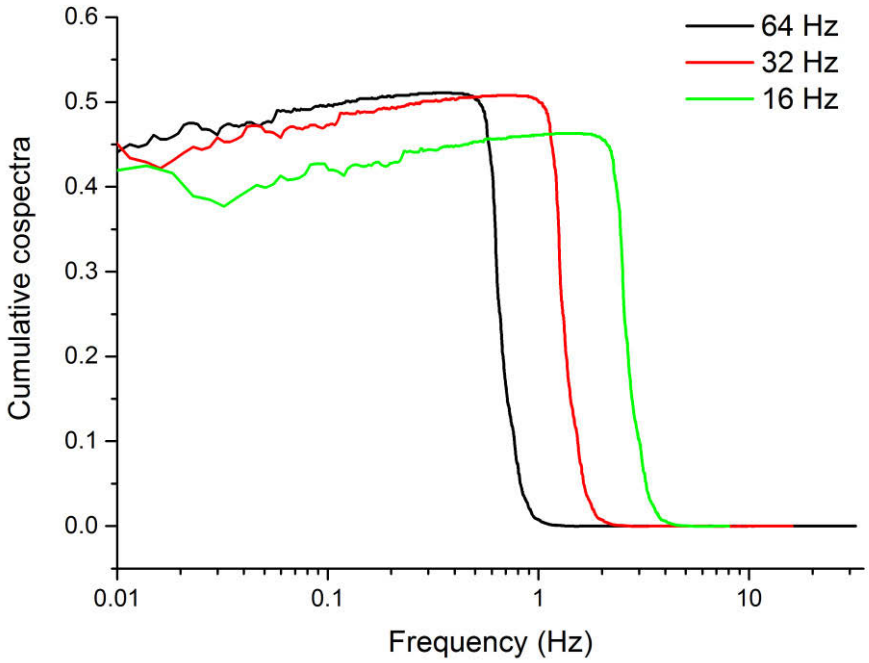

Figure H.2 Cumulative cospectra at different frequency (data from the first deployment at BMA measured by ECO1). Each data point was compute as an average of raw data.